EVALUATION OF THE CAUSATIVE FACTORS FOR SLOPE FAILURES IN NORTH DAKOTA

A Thesis
Submitted to the Graduate Faculty
of the
North Dakota State University
of Agriculture and Applied Science

By

Kamal Raj Upadhaya

In Partial Fulfillment of the Requirements
for the Degree of
MASTER OF SCIENCE

Major Department:
Civil and Environmental Engineering

July 2021

Fargo, North Dakota

North Dakota State University
Graduate School

Title

EVALUATION OF THE CAUSATIVE FACTORS FOR SLOPE FAILURES IN NORTH DAKOTA

By

Kamal Raj Upadhaya

The Supervisory Committee certifies that this ***disquisition*** complies with North Dakota State University's regulations and meets the accepted standards for the degree of

MASTER OF SCIENCE

SUPERVISORY COMMITTEE:

Beena Ajmera, PhD., PE, M.ASCE (Chair)

Aaron Lee M. Daigh, PhD. (Co-chair)

Wenjie Xia, PhD.

Approved:

08/13/2021	Kalpana S. Katti, PhD., F. AIMBE
Date	Department Chair

ABSTRACT

A large number of landslides with damage to roads and utilities, destruction of property, and flood risks were encountered in North Dakota (ND). Using a correlation matrix, causative factors such as soil salinity, land cover, geology, average rainfall, and average snowfall were studied. With areas ranging from 103 to 6,977,692 m^2, a total of 24,098 landslides were observed. Among these landslides, there were 1,497 large-scale landslides that had areas greater than 100,000 m^2. When examining the influence of different parameters using a correlation matrix, more landslides were observed in the northern and western regions of North Dakota, which corresponded to areas with steep slope inclinations, absence of dissolved salt concentrations, and high groundwater tables. Similarly, the correlation matrix for large-scale landslides suggest that the steep slope, leaching of dissolved salts, presence of herbaceous vegetation, and/or presence of rainfall with wetlands was the likely causes for the occurrence of large-scale landslides.

ACKNOWLEDGMENTS

I would like to extend my sincere and heartfelt obligation towards every individual who helped me with this endeavor. Without their continuous guidance, support, cooperation, and encouragement, I would not have made progress in this research work.

I am ineffably indebted to my supervisor, Dr. Beena Ajmera, for her intellectual input, insightful suggestions, and valuable feedback throughout my research. Without her persistent help and guidance, this thesis would not have been possible. I also offer my sincere gratitude to my co-adviser, Dr. Aaron Daigh, for his guidance, comprehensive advice, and unwavering support until this work came to completion. I am also thankful to my supervisory committee member, Dr. Wenjie Xia, for his assistance with this research project.

I am particularly indebted to Braun Intertec Corporation for providing me with the opportunity to work with them. The help by this firm in getting the readings and providing the equipment, laptop and inclinometers needed for the completion of this study is highly appreciated. I would like to express my appreciation to the faculty members of the Civil and Environmental Engineering Department at North Dakota State University for their guidance and lectures, which were influential in shaping my knowledge about the engineering profession and research endeavors.

Finally, I would like to express my profound gratitude to my parents, brothers, sister, and my girlfriend for being my source of motivation and for providing me with constant support and encouragement throughout my studies and research. This accomplishment would not have been possible without them.

DEDICATION

This thesis is dedicated to my parents: Mr. Ganesh Raj Upadhaya and Ms. Bishnamati Upadhaya.

TABLE OF CONTENTS

ABSTRACT iii

ACKNOWLEDGMENTS iv

DEDICATION v

LIST OF TABLES x

LIST OF FIGURES xi

LIST OF APPENDIX TABLES xiv

LIST OF APPENDIX FIGURES xv

CHAPTER 1: INTRODUCTION 1

Background 1

Objectives of the Research 4

Organization of Thesis 4

CHAPTER 2: LITERATURE REVIEW 6

Introduction 6

Earthquake-Induced Landslides 9

Rainfall-Induced Landslides 11

Summary 13

CHAPTER 3: MATERIALS AND METHODS 15

Introduction 15

Study Area 15

Mapping Landslide Hazard Zones with Geographic Information System (GIS) 17

ArcGIS 18

Rainfall, Snowfall, and Land Cover Data 20

Soil Salinity and Sodium Adsorption Ratio (SAR) Data 21

Calculations 22

Dissolved Salt Concentration Calculations 22
Correlation Matrix Calculation 27
Laboratory Testing 28
Sample Preparation 29
Fieldwork 34
CHAPTER 4: SLOPE FAILURES IN NORTH DAKOTA AND THE ROLE OF POTENTIAL FACTORS 36
Abstract 36
Introduction 37
Study Area 38
Geology of North Dakota 38
Climate of North Dakota 41
Topography of North Dakota 41
Data Collection and Analysis 42
Land Cover, Rainfall, and Snowfall at Landslide Sites 44
Calculation of Dissolved Salts at the Landslide Locations 45
Statistical Calculations 47
Distribution of Landslides 49
Size Distribution of the Landslides 49
Landslides and Their Concentration in Geological Formations 49
Landslides and Their Concentration in Counties 51
Distribution of Landslides based upon Slope Inclination 52
Types of Land Cover at Landslide Locations 53
Rainfall and Snowfall Distribution for the Landslide Areas 55
Distribution of Landslides Based on the Concentration of Dissolved Salts 57
Landslide Susceptibility 62

Conclusions 67

References 68

CHAPTER 5: LARGE-SCALE LANDSLIDES IN NORTH DAKOTA: THE INFLUENCE OF CAUSATIVE FACTORS 74

Abstract 74

Introduction 75

Study Area 76

Data Collection and Analysis Methods 76

Statistical Calculations 79

Distribution of Landslides 81

Size Distribution of the Landslides 81

Large-Scale Landslides and Their Concentration in Geological Formations 82

Slope Inclination of Large-Scale Landslides 84

Large-Scale Landslides and Their Concentration in Counties 86

Types of Land Cover at Large-Scale Landslide Locations 87

Rainfall and Snowfall Distribution for the Large-Scale Landslide Areas 88

Distribution of Large-Scale Landslides Based on the Concentration of Dissolved Salts 90

Discussion for Large-Scale Landslides 93

Comparison of All Landslides with Large-Scale Landslides 99

Conclusions 102

References 103

CHAPTER 6: RESULTS FROM LABORATORY TESTING AND FIELDWORK 107

Results from the Laboratory Testing 107

Results from Fieldwork 113

CHAPTER 7: CONCLUSIONS 117

REFERENCES 119

APPENDIX A: GEOLOGICAL COMPOSITIONS WITH THEIR LITHOLOGY AND DEPOSITIONAL ENVIRONMENT IN NORTH DAKOTA ADAPTED FROM MURPHY ET AL. (2009)..... 131

APPENDIX B: ARCGIS PROCEDURES 134

APPENDIX C: CALCULATIONS IN EXCEL 144

APPENDIX D: VBA CODE 150

APPENDIX E: GRAPHS FROM STATISTICAL CALCULATIONS 151

APPENDIX F: COMPLETE CORRELATION MATRIX FROM DRAFT PAPER IN CHAPTER 4 160

APPENDIX G: COMPLETE CORRELATION MATRIX FROM DRAFT PAPER IN CHAPTER 5 165

APPENDIX H: LIQUID LIMIT AND PLASTIC LIMIT RESULTS..... 170

LIST OF TABLES

Table — Page

3.1. Mass Concentration and Molecular Weight of Na^{+}, Ca^{2+}, Mg^{2+} and SO_4^{2-} Ions along with the Solubility of Na_2SO_4, $CaSO_4$, and $MgSO_4$. Data from ACS (2006)..... 23

3.2. Percentage of Minerals Based on the Dry Weight of Samples Tested (M Represents the Percentage of Montmorillonite, K Represents the Percentage of Kaolinite, Q Represents the Percentage of Quartz, SN Represents Sample Number and LL Represents Liquid Limit with Distilled Water, and PI Represents Plasticity Index with Distilled Water.)..... 29

4.1. Mass Concentration and Molecular Weight of Na^{+}, Ca^{2+}, Mg^{2+} and SO_4^{2-} Ions along with the Solubility of Na_2SO_4, $CaSO_4$, and $MgSO_4$. Data from ACS (2006)..... 46

4.2. Partial Correlation Matrix Results 64

5.1. Large-Scale Landslides where Field Reconnaissance was Performed 79

5.2. Thresholds for the Correlation Coefficients 94

5.3. Partial Correlation Matrix Results for Large-Scale Landslides..... 95

6.1. LL and PI of Mixtures of Different Proportions of Clay Minerals with Sodium Sulfate Solution and Distilled Water as the Pore Fluids..... 108

LIST OF FIGURES

Figure		Page
1.1.	Annual Number of Deaths Globally Due to Landslides (2000 to 2019). Data from EMDAT (2020).	2
1.2.	Annual Global Economic Damages from 2000 to 2019. Data from EMDAT (2020).	3
3.1.	Topographical Map of North Dakota Adapted from Bluemle and Biek (2007).	17
3.2.	Map Showing Landslide Polygons.	19
3.3.	Map Showing Centroids of Landslide Areas.	20
3.4.	Calculation of [Na^+], [Ca^{2+}], and [Mg^{2+}] Ions and [Na_2SO_4], [$CaSO_4$], and [$MgSO_4$].	25
3.5.	Sample Placed in the Casagrande Device for the Liquid Limit Test.	32
3.6.	Liquid Limit Test in the Casagrande Device.	33
3.7.	Slope Failure at Kathryn in Barnes County, ND (Source: Google Earth).	35
4.1.	Geological Map of North Dakota Showing the Landslides. Base Map was Obtained from USGS (2020b).	39
4.2.	Slope Map for North Dakota Showing the Centroids of the Identified Landslides.	44
4.3.	Distribution of Landslide Areas.	49
4.4.	Distribution of Landslides across the Geological Formations.	50
4.5.	Distribution of Landslides in the North Dakota Counties.	52
4.6.	Distribution of Landslides with Their Slope Inclination.	53
4.7.	Types of Land Cover Available at the Landslide Sites	54
4.8.	Distribution of Landslides based upon the Average Rainfall Data from 2016 to 2019	56
4.9.	Distribution of Landslides based upon Average Snowfall Data from 2010 to 2019.	57
4.10.	Distribution of Landslides based upon SAR at the Landslide Locations.	58
4.11.	Distribution of Landslides based upon the Availability of EC at the Landslide Locations.	59

4.12. Landslide Distribution with the Sodium, Calcium, and Magnesium Sulfate Concentrations. 60

4.13. Comparison of Dissolved Salts Concentration. 62

5.1. Distribution of Large-Scale Landslides by Area. 82

5.2. Geological Map of North Dakota with the Location of Large-Scale Landslides. The Geological Base Map was Obtained from USGS (2020). 83

5.3. Distribution of Large-Scale Landslides in the Geological Formations. 84

5.4. Slope Map for North Dakota with Locations of the Large-Scale Landslides. 85

5.5. Distribution of the Large-Scale Landslides with Slope Inclination. 86

5.6. Distribution of Large-Scale Landslides in Counties of North Dakota. 87

5.7. Distribution of Large-Scale Landslides based upon the Available Land Cover. 88

5.8. Distribution of Large-Scale Landslide based upon Average Rainfall from 2016 to 2019 89

5.9. Distribution of Large-Scale Landslide based upon Average Snowfall from 2009 to 2019 90

5.10. Distribution of Large-Scale Landslides based upon the Availability of SAR at the Landslide Locations. 91

5.11. Distribution of Large-Scale Landslides based upon the Availability of EC (dS/m) at the Landslide Locations. 92

5.12. Landslide Distribution with the Sodium, Calcium, and Magnesium Sulfate Concentrations. 93

5.13. Picture Showing Leached Salt at the Toe of the Landslide. 97

5.14. Another Example of Leached Salt at Landslide Toe. 97

6.1. Plasticity Chart for the Montmorillonite-Quartz Mixtures Tested in this Study. 109

6.2. Plasticity Chart for the Kaolinite-Quartz Mixtures Tested in this Study. 110

6.3. Liquid Limit of Kaolinite Mixed with Quartz in Different Ratios with Sodium Sulfate Solution and Distilled Water as the Pore Fluids. 111

6.4. Plasticity Index of Kaolinite Mixed with Quartz in Different Ratios with Sodium Sulfate Solution and Distilled Water as the Pore Fluids. 111

6.5. Liquid Limit of Montmorillonite Mixed with Quartz in Different Ratios with Sodium Sulfate Solution and Distilled Water as the Pore Fluids. 112

6.6. Plasticity Index of Montmorillonite Mixed with Quartz in Different Ratios with Sodium Sulfate Solution and Distilled Water as the Pore Fluids. 112

6.7. Cumulative Displacement Observed for Inclinometer 6. 115

6.8. Cumulative Displacement Observed for Inclinometer 7. 116

LIST OF APPENDIX TABLES

Table		Page
H.1.	Measurement of LL for K100	170
H.2.	Measurement of PL for K100	170
H.3.	Measurement of LL for K70Q30	171
H.4.	Measurement of PL for K70Q30	171
H.5.	Measurement of LL for K50Q50	172
H.6.	Measurement of PL for K50Q50	172
H.7.	Measurement of LL for K30Q70	173
H.8.	Measurement of PL for K30Q70	173
H.9.	Measurement of LL for K10Q90	174
H.10.	Measurement of PL for K10Q90	174
H.11.	Measurement of LL for M100	175
H.12.	Measurement of PL for M100	175
H.13.	Measurement of LL for M70Q30	176
H.14.	Measurement of PL for M70Q30	176
H.15.	Measurement of LL for M50Q50	177
H.16.	Measurement of PL for M50Q50	177
H.17.	Measurement of LL for M30Q70	178
H.18.	Measurement of PL for M30Q70	178
H.19.	Measurement of LL for M10Q90	179
H.20.	Measurement of PL for M10Q90	179

LIST OF APPENDIX FIGURES

Figure Page

B.1. Searching for Feature to Point in the Geoprocessing Toolbar. 134

B.2. Input and Output Feature Selection to Calculate the Centroid of Each Landslide. 135

B.3. Searching for Spatial Join in the Geoprocessing Toolbar. 136

B.4. Target and Join Features to Calculate the Number of Slope Failures within Each Geological Composition. 137

B.5. Searching for Slope in the Geoprocessing Toolbar. 138

B.6. Input and Output Feature Selection to Calculate the Slope Map. 139

B.7. Searching for Extract Multi Value to Point in the Geoprocessing Toolbar. 140

B.8. Input and Output Feature Selection to Calculate the Slope Inclination. 140

B.9. Searching for Zonal Statistics in the Geoprocessing Toolbar. 142

B.10. Input and Output Feature Calculation for the Land Cover. 143

C.1. Selecting Data and Solver Function in Excel Spreadsheet. 145

C.2. Solver Parameter Dialogue Box. 146

C.3. Constraint Dialogue Box. 147

C.4. Data Tab for Correlation Calculation. 148

C.5. Data Analysis Ribbon for Correlation Calculation. 148

C.6. Data Analysis Dialogue Box with Correlation Option. 149

C.7. Correlation Dialogue Box. 149

E.1. Q-Q Plot for Logarithm of Area of all Landslides. 151

E.2. Q-Q Plot for Slope Inclination of all Landslides. 151

E.3. Q-Q Plot for Distribution of Rainfall at all Landslides. 152

E.4. Q-Q Plot for Distribution of Snowfall at all Landslides. 152

E.5. Q-Q Plot for SAR at all Landslides. 153

E.6. Q-Q Plot for EC at all Landslides. 153
E.7. Q-Q Plot for Calcium Sulfate Concentration at all Landslides. 154
E.8. Q-Q Plot for Magnesium Sulfate Concentration at all Landslides. 154
E.9. Q-Q Plot for Sodium Sulfate Concentration at all Landslides. 155
E.10. Q-Q Plot for Logarithm of Area of Large-Scale Landslides. 155
E.11. Q-Q Plot for Slope Inclination of Large-Scale Landslides. 156
E.12. Q-Q Plot for Distribution of Rainfall at Large-Scale Landslides. 156
E.13. Q-Q Plot for Distribution of Snowfall at Large-Scale Landslides. 157
E.14. Q-Q Plot for Distribution of SAR at Large-Scale Landslides. 157
E.15. Q-Q Plot for Distribution of EC at Large-Scale Landslides. 158
E.16. Q-Q Plot for Distribution of Calcium Sulfate Concentration at Large-Scale Landslides. 158
E.17. Q-Q Plot for Distribution of Magnesium Sulfate Concentration at Large-Scale Landslides. 159
E.18. Q-Q Plot for Distribution of Sodium Sulfate Concentration at Large-Scale Landslides. 159
H.1. Moisture Content versus Number of Blows for K100. 171
H.2. Moisture Content versus Number of Blows for K70Q30. 172
H.3. Moisture Content versus Number of Blows for K50Q50. 173
H.4. Moisture Content versus Number of Blows for K30Q70. 174
H.5. Moisture Content versus Number of Blows for K10Q90. 175
H.6. Moisture Content versus Number of Blows for M100. 176
H.7. Moisture Content versus Number of Blows for M70Q30. 177
H.8. Moisture Content versus Number of Blows for M50Q50. 178
H.9. Moisture Content versus Number of Blows for M30Q70. 179
H.10. Moisture Content versus Number of Blows for M10Q90. 180

CHAPTER 1: INTRODUCTION

Background

According to the United States Geological Survey (USGS), landslides are defined as a mass of rock, debris, or earth moving down a slope under the influence of gravity (USGS 2020a). Landslides can occur anywhere and at any time, and they may have adverse effects on the environment. Per Emergency Events Database (EMDAT), in the last two decades, 892 people on average lost their lives annually due to landslides (EMDAT 2020) as shown in Figure 1.1. This figure shows the total deaths, including people who lost their lives and people missing after a landslide. The number of deaths from landslides varies from year to year, with 3,427 in 2010 being the highest death toll in the last two decades (Figure 1.1). In 2010, the Port-au-Prince earthquake in Haiti was one of the devastating events that pushed up the death rate (Ritchie and Roser 2014). The total number of landslides triggered by this magnitude 7 earthquake was 30,828 (Xu et al. 2014).

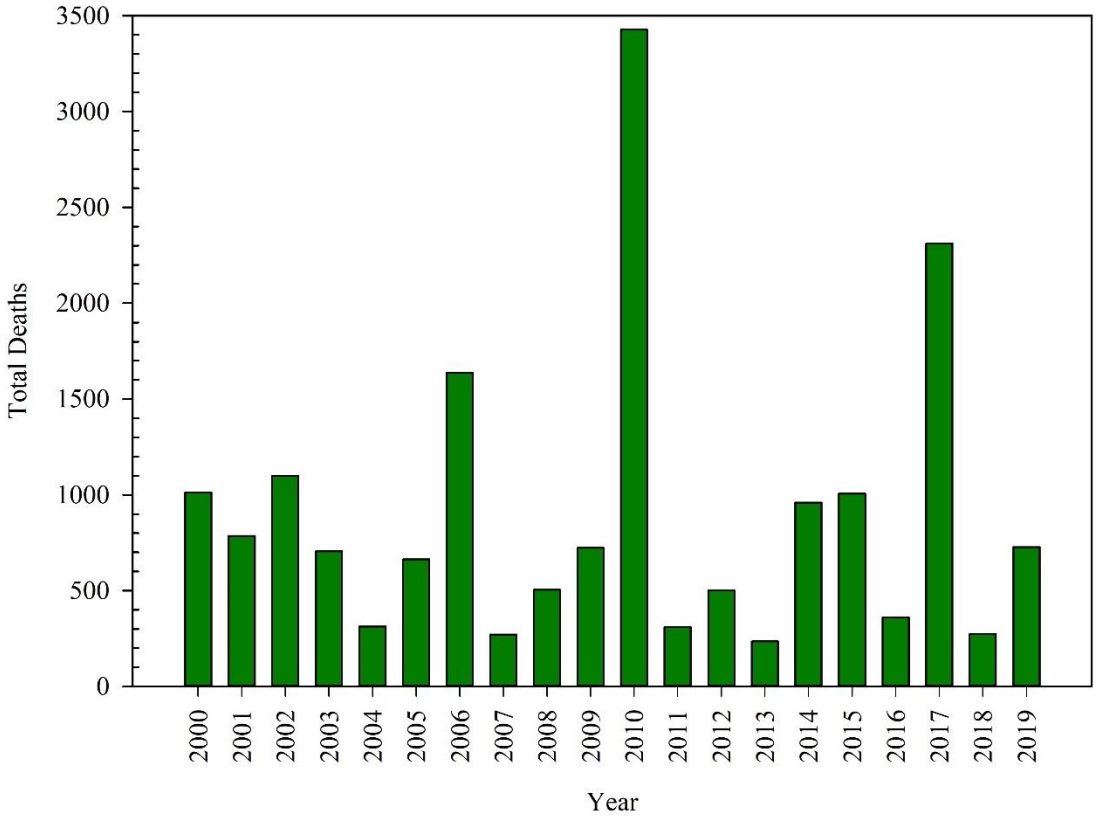

Figure 1.1. Annual Number of Deaths Globally Due to Landslides (2000 to 2019). Data from EMDAT (2020).

As shown in Figure 1.2, on average, the total estimated damages, directly or indirectly related to the landslides, was about $310 million per year for the last two decades (EMDAT 2020). The total estimated damages include social, environmental, and infrastructural damages due to landslides. The damages presented in the figure are the cost at the moment of the event. For example, although 25 landslide events were recorded in 2019, the total damage of $200 million depicted in the figure was for a single landslide event in China. For the other 24 landslide events, the total economic damages were unknown, therefore, the total estimated damages from those 24 landslide events were not considered.

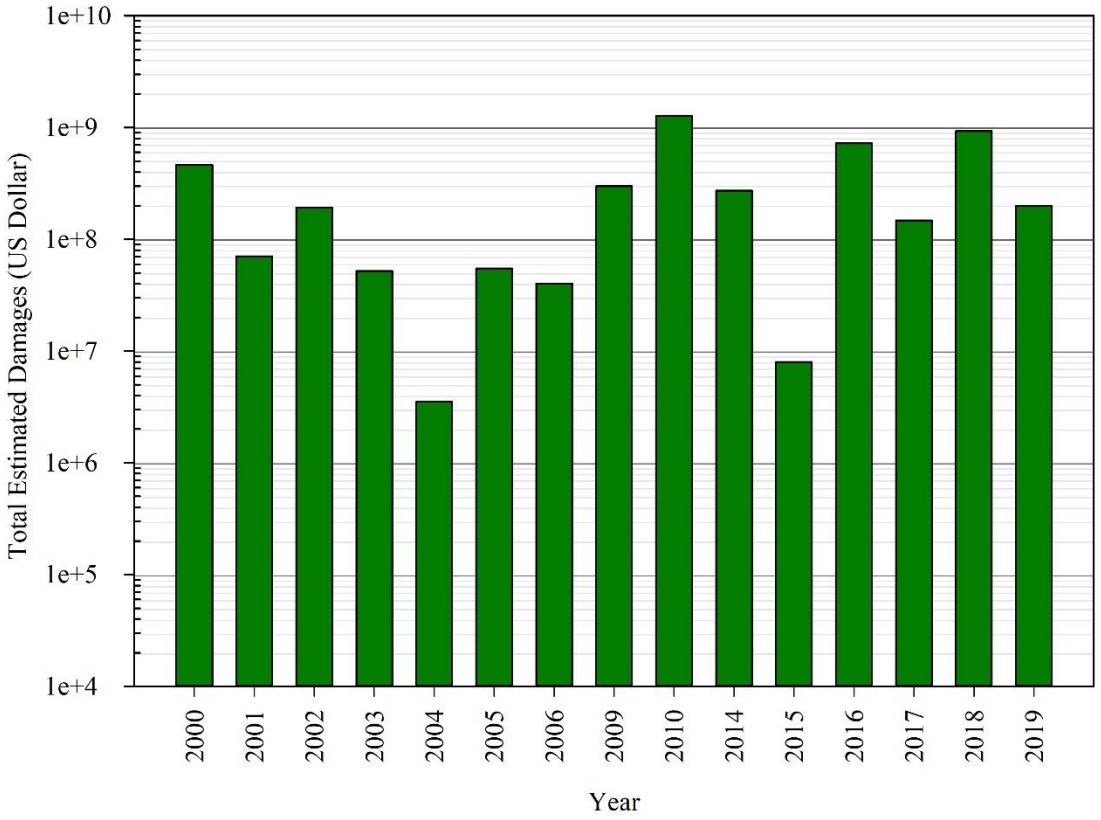

Figure 1.2. Annual Global Economic Damages from 2000 to 2019. Data from EMDAT (2020).

The annual losses from landslides in the United States (US) were estimated to exceed $1 billion in 1980 (USGS 1980). More recent USGS studies showed that the yearly loss from landslides exceeds $2 billion, with 25 to 50 people losing their lives (USGS 2003). The USGS method of recording damage is different than the EMDAT approach. USGS considers direct and indirect costs when calculating the losses from landslides. Direct loss includes physical damage to structures, buildings, and property. Indirect costs involve the money required for the relocation of buildings, roadways and railways; mitigation measures applied to prevent future landslide damage; the disruption and pollution of water sources; adverse effects for irrigation; and implications on public safety (Fleming and Taylor 1980). This estimated $1 billion loss from landslides resulted from considering both the direct and indirect costs at four US locations (Fleming and Taylor 1980). Considering damages at all other places, the loss from landslide in

US would be more than the $1 billion. Landslides can occur in all fifty states, but in this study, North Dakota serves as the study area because the state has thousands of landslides on shallow slopes, which was not expected. The annual loss in North Dakota from landslides can reach millions of dollars (Murphy 2017). Loss of property, damage to roads and infrastructure, flood risks, and loss of lives are some of the consequences of landslides within the state. Therefore, a study of the factors responsible is needed in order to minimize the damage due to these landslides. Knowing the causative factors for the occurrence of landslides will help to prepare a landslide susceptibility map.

Objectives of the Research

The main objectives of this research are as follows:

1. This study will help to prepare the distribution map of all the landslides and large-scale landslides within the state and will highlight information about past slope failures in North Dakota.
2. This study will perform statistical analyses to find correlations between different causative factors, such as geology, land cover, average rainfall, average snowfall, slope inclination, and dissolved salt concentrations.
3. The study will highlight the differences between occurrence of all landslides and large-scale landslides.
4. This study will determine the displacement for an existing slope failure.

Organization of Thesis

Following this introductory chapter, Chapter 2 focuses on landslide databases throughout the world and the need for this study. The chapter also highlights the relative importance of the study in the region where landslides are not expected. Chapter 3 discusses ArcGIS methods

utilized to collect useful information to calculate a correlation matrix for different causative factors that are responsible for landslides. The chapter also discusses the experimental work and fieldwork performed in the study. The experimental work focuses on performing Atterberg's Limit tests for different samples prepared in the laboratory, whereas the fieldwork section discusses the movement at one particular landslide location. Chapters 4 and 5 contain two draft journal papers that arose from this research work. The first paper focuses on the distribution of all landslides in North Dakota and the correlation between different causative factors. The second paper details the distribution of large-scale landslides in North Dakota. As the causative factors for the occurrence of landslides at a particular place are not generic, the article focuses on different causative factors and their correlations with each other. This paper also provides a comparison between all landslides observed in the study area and the large-scale landslides. Chapter 6 discusses the results obtained from the experimental work and the fieldwork. Chapter 7 provides the conclusions drawn from this study with limitations. Finally, there are eight appendices included within this thesis. Appendix A contains the details about the geological compositions in North Dakota. Appendices B, C, and D discuss the steps followed in ArcGIS, the calculations performed, and the Visual Basic for Applications (VBA) codes used during the calculation process, respectively. Appendix E includes the graphs for quantile-quantile (q-q) plot which were performed in the study to test the normality of the data. Appendices F and G include the correlation matrices from this study. Finally, appendix H includes figures and associated calculation tables for the Liquid Limit (LL) and Plastic Limit (PL).

CHAPTER 2: LITERATURE REVIEW

Introduction

Landslide inventories can be divided into event-based and historical inventories (Klose et al. 2015). Landslides triggered by single triggering events, such as earthquakes, rainstorms, volcanoes, rapid snowmelt, etc., that initiate the movement of slope can be placed into event-based databases. Historical databases, which are more common, include a pool of landslides in areas during a particular time and can be divided into local, regional, national, or even global scales (Guzzetti et al. 2012; Klose et al. 2015; Wood et al. 2015). These event-based and historical databases can be compiled in different ways. Automated landslide mapping of historical databases for regional or local scales may be undertaken using aerial photography or high-resolution topographic data through light detection and ranging (LiDAR) (Booth et al. 2009; Guzzetti et al. 2012). On the other hand, event-based databases can be compiled using satellite imagery and ground-based surveying techniques to determine the area, size, and volume of the triggered landslides (Tiwari et al. 2017; Xu et al. 2013).

Kirschbaum et al. (2015) identified 5,471 landslides around the world using online databases, media reports, disaster databases, scientific reports, blog entries, and other sources. To investigate spatial and temporal patterns of rainfall that triggered landslides over the world, the landslide events in the database were compared with satellite-based precipitation estimates. For each landslide, the precipitation recorded at the time of the landslide was compared with the rainfall distribution that was documented over the past fourteen years. When computing the rainfall percentiles for each landslide location for the fourteen year period, the daily precipitation for more than half of the landslides exceeded the 95^{th} percentile. The results also showed a strong correlation between the 95^{th} percentile of rainfall and landslide occurrence.

A national landslide database for Great Britain with more than 15,000 landsides on inland, coastal, and artificial slopes was available (Foster et al. 2012). These landslides are displayed in Geographic Information System (GIS) and contain over 35 attributes, including the date for the occurrence, triggering mechanisms, location, size, area, type, impacts, age, land cover, and a reference to the source. This landslide information was collected utilizing scientific literature, fieldwork, journals, reports, mapping technologies, and other online resources. Studies were conducted using the landslide databases for southwest England and south Wales in order to find the effect of antecedent precipitation on landslides (Pennington et al. 2014). The authors highlighted two significant trends to determine the threshold of precipitation required for widespread of landslides. When landslides occurred after seven days of antecedent rainfall, the rainfall event had a high intensity. However, for landslide triggered after seven to ninety days of antecedent rainfall, the rainfall event was not intense leading to a gradual accumulation of rainfall. A correlation between the type of landslide and the antecedent rainfall period was calculated for landslides triggered by antecedent rainfall from November 2012 until January 2013. For landslides which were triggered by antecedent rainfall from 2006 to 2013, a generalized linear model (GLM) was fitted to the precipitation data. The fitted precipitation data gave the expected number of landslides, which helps to determine the probabilities of landslide occurrence. The authors concluded that, based on the statistical analyses and plotting the calculated probabilities against the observed landslides for the available landslide database, it was possible to assess the likelihood of at least one landslide being triggered by antecedent rainfall of a particular duration.

Damm and Klose (2015) collected information about more than 4,200 landslides across Germany in the past 150 to 200 years. The records were obtained from field data, agency

archives, scientific publications, geospatial data products, etc. The results showed that natural and anthropogenic activities were responsible for causing these landslides. The key factors that the authors examined were soil properties, slope inclination, and soil moisture content. Case studies of landslides in Central Upland and Lower Saxony were performed. Performing statistical analyses, authors concluded that majority of the landslides in the Central Uplands were triggered by rainfall, rapid snowmelt, erosion at the slope toe, and ground shaking. Bivariate statistical analyses indicated that slope inclination was a major controlling factor for the landslides in Lower Saxony.

Using aerial color orthophotos and a field survey for northeast Sicily, Italy, a detailed inventory map for the landslides was developed (Trigila et al. 2015). The frequency-ratio method was adopted to determine the correlation between the factors that cause landslides and the shallow landslides. Controlling factors considered in the study were slope inclination, lithology, land cover, agricultural terraces, wildfires, distance to streams, etc. Multivariate, statistical landslide-susceptibility models were created and compared. The authors concluded that land use and wildfires had a strong influence on landslide occurrence.

A landslide inventory with 1,221 historical landslides in China from 1949 to 2011 was prepared (Li et al. 2016). The database was divided into six zones based on the geological environment. The authors concluded that Zone 5, composed of highlands and plateaus, had the highest percentage of landslides. Rainfall was the triggering factor, whereas land cover and geology were the main causative factors, factors that makes the slope susceptible to move. Similarly, an inventory containing 1,944 landslides of fatal Chinese landslides from 1950 to 2016, was compiled by Lin and Wang (2018). Based on the geographical detector method, possible causative factors were determined. The authors concluded that the concentration of

landslides in fourteen different provinces of China was governed by the interaction among precipitation, lithology, and land cover.

Havenith et al. (2015a) reviewed 1,600 previously mapped historical landslides (Burette 2012; Schlögel 2009; Strom and Korup 2006) and added 1,800 new landslides to make a total of 3,400 landslides in central Asia. The authors presented a landslide database due to historical earthquakes with magnitudes greater than 6.5 until 2014 and described the relation between seismicity and the presence of rock slides in the study area. Landslide densities were calculated based upon the geological composition, rainfall data, river networks, earthquake, and road networks by Havenith et al. (2015b). Correlations among scarp location, slope inclination, distance from river, and curvature of terrains were calculated in Havenith et al. (2015b). Such correlations suggested that the concentrations of landslides were strong on steep slopes with convex terrain. The authors also concluded that the susceptibility of slopes to landslides was governed by the distance from rivers, faults, and previous earthquakes.

Earthquake-Induced Landslides

Strong ground shaking during an earthquake has caused landslides in several topographical and geological environments. Keefer (1984) examined landslide databases for forty earthquake events and later Rodriguez et al. (1999) added landslide databases for 36 earthquake events that occurred throughout the world. Keefer (1984) observed correlations between earthquake magnitude and intensity with landslide distance, area, and coverage, suggesting the area that can be affected by a particular earthquake. As the study done by Rodriguez et al.(1999) was the extension of databases to Keefer (1984), Rodriguez et al.(1999) support the results drawn except in some exceptional cases where small earthquakes can also cause landslides.

The relationship among landslide characteristics, including the landslide type, area, and thickness, and the different landslide-affecting mechanisms, such as topography, geology, geomorphology, human activities, earthquake magnitude, distance from the fault plane, and distance from the epicenter helped to determine the reasons for earthquake-induced landslides (Khazai and Sitar 2004; Mahdavifar et al. 2006; Meunier et al. 2007; Yagi et al. 2009). The number of landslides concentrated in an area were high in the zone associated with lithology, geomorphology, topography, and human presence in Murree, Muzaffarabad, Abbottabad, and Patala Formations (Harp and Crone 2006; Owen et al. 2008). These associated areas were in Neelum Valley, Lamnian Valley, Jhelum Valley, Muhra Sadiq Spur, and Kaghan Valley near two cities Muzafarrabad and Balakot in Pakistan. Several thousand shallow landslides were induced by magnitude 7.6, 2005 Kashmir earthquake. Harp and Crone (2006) and Owen et al. (2008) concluded that the presence of highly fractured carbonate rocks, tertiary siliciclastic rocks, sandstone, mudstones, shale, limestone, steep slopes ($>50^{o}$), and road-construction activities were the causative factors for landslide occurrence.

Lee et al. (2008) concluded that the multivariate statistical approach has a better prediction rate for the occurrence of landslides than deterministic methods. The authors also determined that this approach does not require depth, material strength, and groundwater data to predict landslide susceptibility. Lee (2014) performed additional analyses using a statistical approach after updating the dataset from Lee et al. (2008). The updated dataset had 5 m digital elevation models and 1:50,000 scale geographic maps as compared to the previously used low resolution satellite images. The authors computed the probability of landslide occurrence by considering slope inclination, geology, terrain roughness, total curvature, total slope height, and slope roughness as the causative factors of the landslides. They concluded that it was possible to

predict earthquake-induced landslides using a statistical approach for any region if the earthquake intensity where the model was developed was similar to the earthquake intensity of the region of interest.

Tiwari et al. (2017) studied the characteristics and the correlation between different potential factors for the occurrence of moderate-to large-scale landslides that were induced by the magnitude 7.8, 2015 Gorkha earthquake. The dominant factors considered for landslide occurrence were slope inclination, distance from the epicenter, peak ground acceleration, and geology. Adopting a statistical approach, Pearson's correlation matrix, which describes the linear correlation between each pair of potential factors, was calculated. The authors concluded that there was a strong correlation between the number of landslides and slope inclination as well as peak ground acceleration. From the correlation matrix, the three major controlling factors for the occurrence of landslides were found to be: distance from the epicenter, peak ground acceleration, and slope inclination. The authors also concluded that landslides were concentrated in areas deposited with quartz, phyllite, gritstones and conglomerates, alluvium boulders, gravel, and sand.

Rainfall-Induced Landslides

Rainfall is another major triggering mechanism for landslides. Due to the interaction between soil and water, unsaturated soil loses its apparent cohesion, resulting in landslides (Kawagoe et al. 2009). Additional factors, such as antecedent rainfall, rainfall duration, and rainfall intensity, need to be considered for rainfall-induced landslides (Wieczorek 1996). Each factor has different threshold values which, when exceeded, can result in landslides. Marjanović et al. (2018) modeled large rainfall-induced landslides in western Serbia from 2001 to 2014 in order to determine the threshold value of rainfall duration for landslides. The correlation between

landslides and cumulative rainfall was determined by Marjanović et al. (2018). The authors concluded that rainfall that lasts for two to three days and exceeds 30 mm was responsible for the landslides in western Serbia because pore water pressure due to the antecedent rainfall causes the slopes to mobilize.

Numerical modeling of one of the more than twenty slope failures in Singapore for five day antecedent rainfall events demonstrated that antecedent rainfall plays an essential role in slope stability (Rahardjo et al. 2001). In the past, rainfall of the same magnitude did not produce any landslides, but the rainfall considered in the study, where the cumulative antecedent rainfall for the last five days before the landslide was almost twice the other times, triggered landslides. The authors found that rapid increases in the groundwater table with a rainfall event increases the pore water pressure and decreases the matric suction leading to slope failure. Rahardjo et al. (2008) instrumented four slope failures to study the effect of rainfall. The authors concluded that higher antecedent rainfall was required for low-permeability soils than for soils with high permeability in order to produce high pore water pressures. The researchers also found that the pore water pressure variation was greater in high-permeability soils than in low-permeability soils. Therefore, the factor of safety of high-permeability soils was more significantly affected by high pore water pressures.

Mukhlisin and Taha (2012) performed numerical modeling to determine the effect of antecedent rainfall on slope stability. The authors used the Hougawachi rainstorm that triggered large-scale debris flows, as the antecedent rainfall conditions, in which the total rainfall, peak rate of rainfall, and duration of rainfall were 379 mm, 91 mm/h, and 10 h, respectively. They concluded that the factor of safety and the pore water pressure depend on the drainage period. The authors concluded that the pore water pressure generated from a 24 h rainfall event was

greater than that from 48 h as well as 96 h rainfall events and results in a low factor of safety due to short period of antecedent rainfall drainage for 24 h. These results were consistent with Rahardjo et al. (2001; 2008). Guzzetti et al. (2008) found that antecedent rainfall is an essential factor for the occurrence of landslides when they observed and analyzed landslides that were caused by rainfall events which exceeded 48 h in duration. This result was also supported by Tiwari and Upadhyaya (2014).

Ng and Shi (1998) measured the pore water pressure in unsaturated soils and concluded that the factor of safety decreases with an increase in rainfall duration until the critical duration (the duration when the factor of safety was the lowest). This finding was also supported by Dhakal and Sidle (2004), who examined the effects of different rainstorm characteristics, such as mean and maximum hourly intensity, duration, and the amount of rainfall, on slope stability. Xue et al. (2016) found that long duration rainfall results in a high degree of saturation for the slope-forming material. Due to the dissipation of matric suction, there is an increase in the pore water pressure and a decrease in the cohesion, resulting in slope failures.

Summary

Even though the North Dakota Geological Survey (NDGS) maintains a record of historical landslides for the state (NDGS 2020), a study about the causative factors that lead to the instabilities is lacking. The literature notes that some landslides are induced by subsidence due to mining activities (Andrews 1939; Trimble 1979), but it is clear that work to find the causative factors for the occurrence of the landslides is needed. To bridge this gap, different potential factors (geology, slope inclination, land cover, electrical conductivity, sodium adsorption ratio, total dissolved salts, average rainfall, and average snowfall) for the occurrence of landslides were studied. Following the statistical approach and determining the correlations

between the landslides causative factors will help to identify their influence. Understanding the potential sources and causes of these failures will help North Dakota in many ways:

1. This study will give the knowledge about the causative factors for landslides along with the distribution of those failure areas which is required to prepare a susceptibility map.
2. This study will allow both the private sector and the government to implement different environmental restoration projects by taking effective mitigation measures in hazardous landslide areas.
3. This study will help planners and developers to select favorable locations for development activities, such as housing, roads, railroads, and transmission lines. Detecting and avoiding unstable areas in the preliminary phase will reduce the potential future economic losses.

The contributions from this study to the geotechnical literature are as follows:

1. The gap about the causative factors for the occurrence of historical landslides at the regional level in North Dakota will be closed.
2. This study will act as a base to create the inventory lists and perform probability analyses. Records for the locations of each past landslide act as a clue about future landslide activity.

CHAPTER 3: MATERIALS AND METHODS

Introduction

This chapter contains details about the methods used to analyze landslides within the study area. First, the study area is described, followed by the mapping process and the calculations performed. Next, this chapter discusses the laboratory experimental procedures and the fieldwork. The study was divided into four parts. First, the total number of landslides within the study area were determined, and the potential factors (salt concentration, slope inclination, geology, land cover, average rainfall, and average snowfall) responsible for the landslides were determined. The process of finding these landslides and calculating the potential factors for those landslide areas was completed using ArcGIS software. Second, the correlation between the causative factors was calculated by using a correlation matrix. Third, montmorillonite, kaolinite, and quartz were combined, and Atterberg's Limits for these mixtures, using the concentration of sodium sulfate obtained from previous calculations, were determined. Finally, the fieldwork completed for this study was described. This fieldwork was used to calculate the displacement of landslide using an inclinometer.

Study Area

North Dakota, located in the north-central United States, extends from 45º56′ N to 49º00′ N and from 96º33′ W to 104º03′ W. The state has an area of 183,121 km^2 (City-Data 2020). The state is roughly rectangular in size, with Minnesota to the east, Saskatchewan and Manitoba (Canadian provinces) to the north, Montana to the west, and South Dakota to the south. North Dakota has 53 counties, with McKenzie County being the largest and Eddy County as the smallest by area. The minimum and maximum elevation of the study area is 229 m along the

eastern border of the Red River Valley and 1,069 m in Slope County along the southwest border, respectively (City-Data 2020).

North Dakota has significant temperature variations with irregular precipitation, low humidity, and continuous wind. The negative temperature in winter can reach as low as -46ºC while extreme, positive summer temperatures can be as high as 48ºC (ACIS 2020). The annual rainfall in the state ranged from 33 to 50 cm while the snowfall ranges from 63 to 114 cm (NOAA 2017).

North Dakota is divided into four topographic regions: the Great Plains, the Missouri Coteau, the Glaciated Plains, and the Red River Valley (Figure 3.1) (NOAA 2017). The land in the southwestern section of the state, part of the Great Plains, has hilly to rolling plains. The Missouri Coteau has steep, rolling topography, and extends from northwest corner to the southcentral border of the state. The Glaciated Plains have gently rolling, glaciated topography. The Red River Valley in the eastern part of the state has a flat, plain topography. North Dakota has 23 different lithological compositions (Clayton 1980a). The three largest geological formations by area are the Pierre, Sentinel Butte, and Bullion Creek Formations. The characteristics for these lithological compositions are provided in Appendix A.

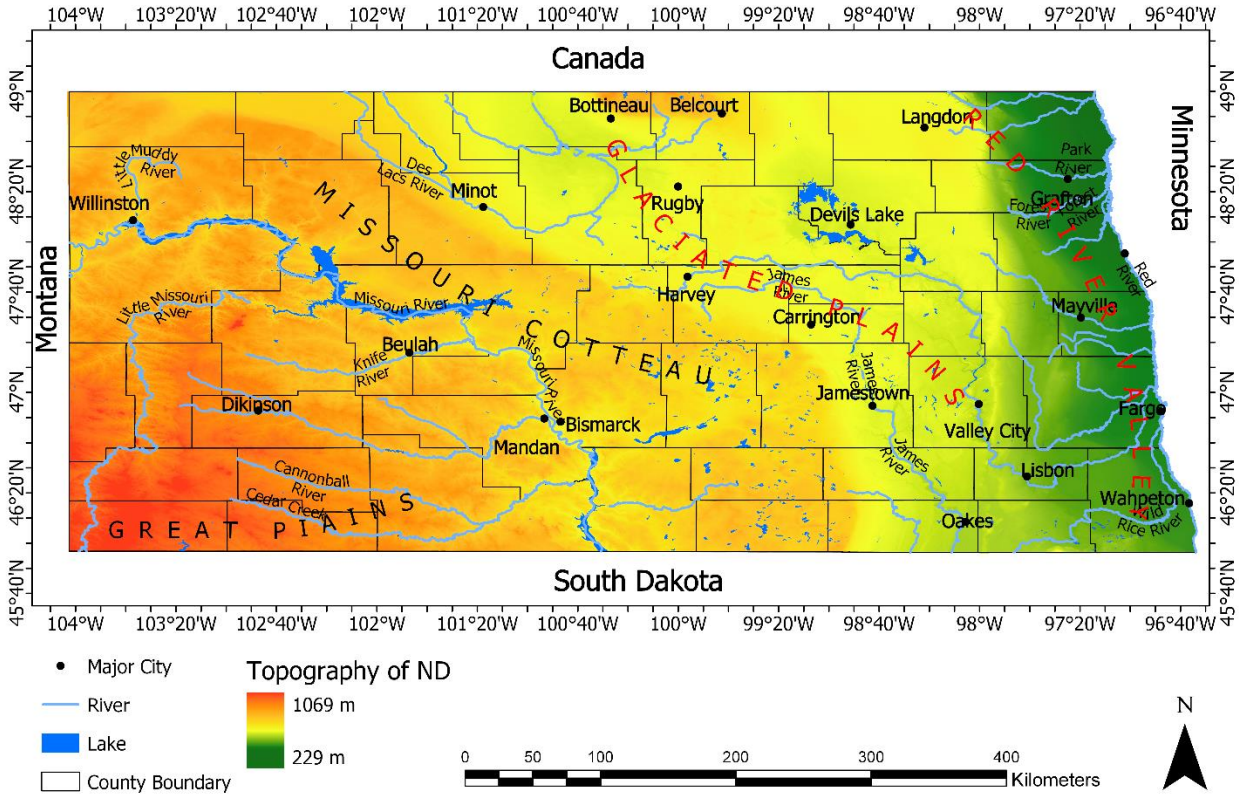

Figure 3.1. Topographical Map of North Dakota Adapted from Bluemle and Biek (2007).

Mapping Landslide Hazard Zones with Geographic Information System (GIS)

Mapping or delineating areas that are vulnerable to landslides is important for several purposes, such as managing land use activities, planning emergency management activities, and reducing the risk to residential areas and transportation. Mapping of surface geology and identification of geohazards, such as landslides, throughout the state was completed by the NDGS. NDGS started mapping these landslides in 2003 and completed eleven million acres, which is about 25% of the state, by 2017 (Murphy 2017). As of 2020, there were 24,123 landslides identified in North Dakota, and many more landslides are expected to be mapped (NDGS 2020). Mapping of landslides within the state increased rapidly from 2017 to 2019, with about 22 million acres completed by 2019 (Moxness 2019).

The primary dataset to identify these landslides was 1:20,000-scale aerial photographs that were viewed in stereopairs. These photos, taken by the United States Department of Agriculture (USDA), were captured from low-flying aircraft as early as the 1930s. The resolution of digital aerial photography to map these landslides increased from 2 m in 2003 to 60 cm in 2016 to 2018 (Moxness 2019). Updates in satellite imagery and platforms such as Google Earth made mapping these landslides quick, easy, and more reliable.

In 2017, NDGS started mapping these landslides using an unmanned aerial vehicle (UAV) named Phantom 4 Pro Drone (Anderson and Maike 2017). This method is more effective for determining geological hazards and creates detailed 3D models through the collection of high-resolution topographic data. NDGS collected more than 4,500 photos and fifty videos of various landslide areas using drones that gave detailed information about the geology of failure areas (Maike 2018a). To map geological hazards, paleontological investigation and landform identification using LiDAR with 1 m resolution have increased extensively (Maike 2018b). LiDAR allows people to see the bare surface of earth by removing vegetation and trees. As a result, landslides that were not visible with aerial imagery can now be seen clearly.

ArcGIS

Shapefiles from NDGS provide information about the location and area of each landslide and are represented as polygons (Figure 3.2). As landslides with areas less than 100 m^2 pose small threats to the environment and bear small risks to the infrastructure, only landslides with areas greater than 100 m^2 were considered in this study. The centroids by area of the polygons for each landslide were then obtained using the point type feature class through ArcGIS as explained in Appendix B. The centroids are represented by green dots in Figure 3.3. The causative factors were studied at these centroid locations.

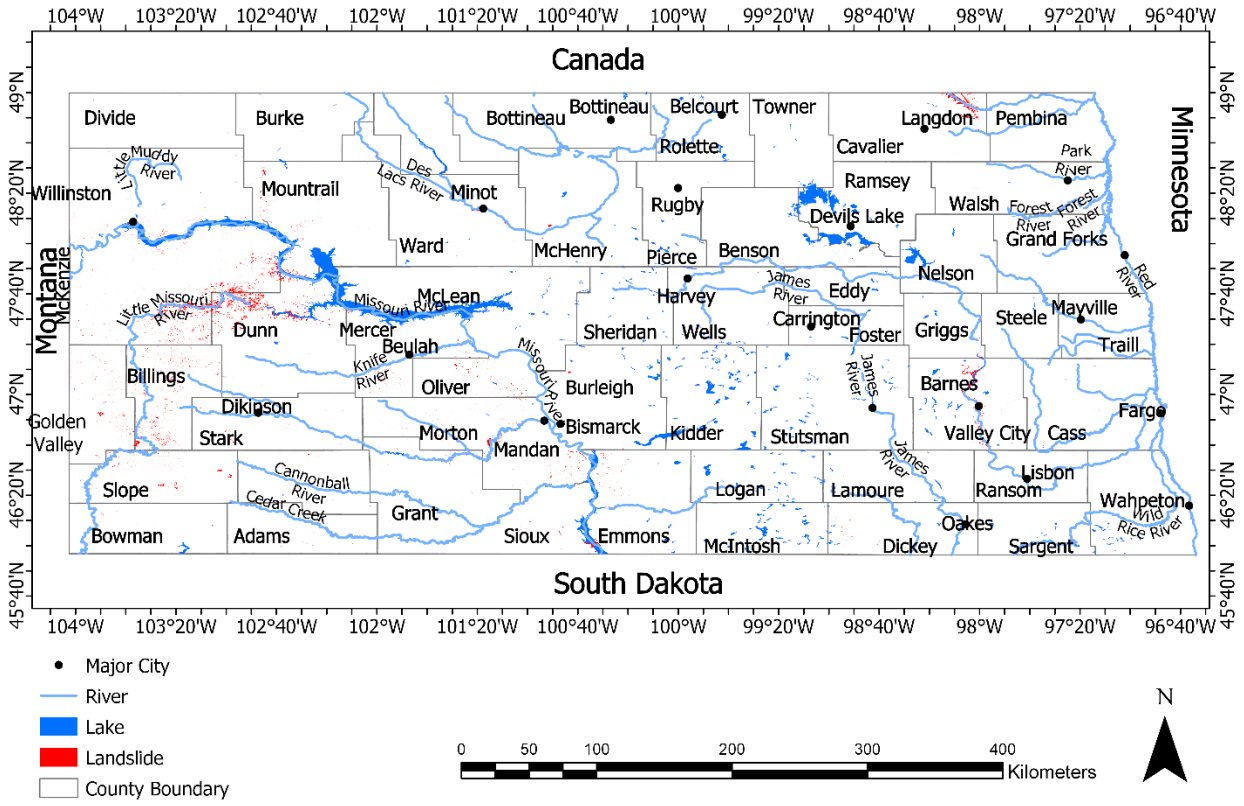

Figure 3.2. Map Showing Landslide Polygons.

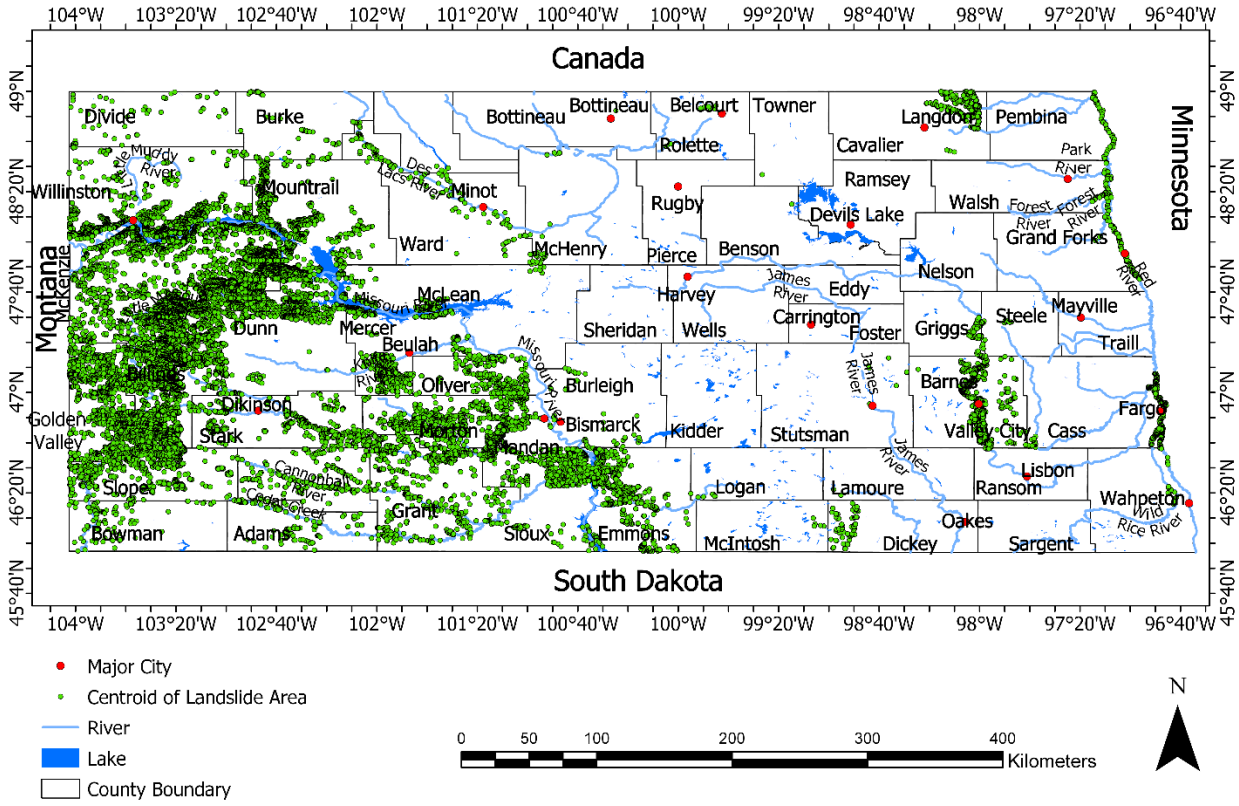

Figure 3.3. Map Showing Centroids of Landslide Areas.

The geological map of North Dakota was obtained from USGS (USGS 2020b). The number of slope failures in each geological composition were calculated using ArcGIS. The steps for this process are explained in Appendix B. The slope map for North Dakota was developed by using an elevation map obtained from the National Elevation Dataset (NED) (USGS 2019). NED is a product that is derived from USGS 10 and 30 m digital elevation models. It has a 1/3rd arc-seconds map for North Dakota. Slope inclinations at the centroid of each failure surface were calculated using the procedure outlined in Appendix B.

Rainfall, Snowfall, and Land Cover Data

Snowfall and rainfall are estimates of radar and rain gauge data collected from the National Weather Service (NWS) (NOAA 2020). Rainfall and snowfall at the landslide areas were calculated by using yearly rainfall and snowfall data for the last four and ten years,

respectively, due to limited data availability. For the correlation matrix calculations, average values of rainfall and snowfall, instead of antecedent rainfall and snowfall, were utilized due to the lack of knowledge of the triggering date. So, it is assumed that the difference between the use of four years of rainfall and ten snowfall data and the use of average rainfall and snowfall instead of antecedent rainfall and snowfall will not have any influence on calculations performed in this study.

Data from the National Land Cover Database were used to determine the land cover at the landslide locations (USGS 2016a). The most common land cover along the unstable slope was taken as the land cover for the entire slope in this study. The steps used in the study are explained in Appendix B.

Soil Salinity and Sodium Adsorption Ratio (SAR) Data

The total amount of dissolved salts present in the liquid portion (aqueous solution) of soil is called soil salinity. The major source of these dissolved salts is the geotechnical weathering of rocks (Corwin and Yemoto 2017). Soil salinity can be calculated by measuring the electrical conductivity (EC) or measuring the total dissolved salts (TDS).

EC is the electrical conductivity of an extract from a saturated soil paste (USDA 2013). It is the ability of a material to conduct or to transmit an electrical current and is a function of the chemical salt composition. High salt compositions result in high electrical conductivities. EC data from the Soil Survey Geographic Database (SSURGO) were used for this study (USDA 2020). EC values at the landslide centroids were used to find TDS.

Total dissolved salts in the soil may consist of soluble and readily dissolved salts, including charged ions such as sodium (Na^+), calcium (Ca^{2+}), magnesium ions (Mg^{2+}), potassium (K^+), chlorine (Cl^-), bicarbonate (HCO_3^-), nitrate (NO_3^-), sulfate (SO_4^{2-}), and carbon monoxide

(CO) (Corwin and Yemoto 2017). The major dominant ions present in the soil of North Dakota are Na^+, Ca^{2+}, and Mg^{2+} (Timpson and Richardson 1986). So, only these three ions were considered for the calculations. The total dissolved salts are linearly related to electrical conductivity across the range, 1 to 50 mmol/L, of salt concentrations that exist in nature (Corwin and Yemoto 2017). As more than 97% of the total landslides in this study fall within this range, EC can be multiplied by ten to obtain the TDS based on charge.

Sodium sulfate concentration can be determined by calculating the sodium concentration. Sodium concentration was computed by measuring SAR. SAR quantifies the concentration of sodium ion ($[Na^+]$) relative to concentration of calcium ($[Ca^{2+}]$) and magnesium ions ($[Mg^{2+}]$) in water extracted from a saturated soil paste (USDA 2013). SAR values at the centroid of landslides were also obtained by using data from SSURGO (USDA 2020).

Calculations

The second part of the study consists of calculating the dissolved salt concentrations and analyzing the correlation matrix. The calculation processes for each part are described in the following sections.

Dissolved Salt Concentration Calculations

The individual $[Na^+]$, $[Ca^{2+}]$, and $[Mg^{2+}]$, as well as the concentration of sodium sulfate ($[Na_2SO_4]$), calcium sulfate ($[CaSO_4]$), and magnesium sulfate ($[MgSO_4]$), present in the soil were determined using EC, SAR, and TDS. The Solver function in Excel was used. Mass concentration per milliequivalents and molecular weight of dissolved ions as indicated above were needed and are shown in Table 3.1. Mass concentration is a measure of dissolved solutes in a solvent and is the ratio of the mass of solute to the volume of the solvent. Solubility is the

ability of a solid to dissolve in a solvent. Solubilities of sodium sulfate (Na_2SO_4), calcium sulfate ($CaSO_4$), and magnesium sulfate ($MgSO_4$) are also presented in Table 3.1.

Table 3.1. Mass Concentration and Molecular Weight of Na^+, Ca^{2+}, Mg^{2+} and SO_4^{2-} Ions along with the Solubility of Na_2SO_4, $CaSO_4$, and $MgSO_4$. Data from ACS (2006)

SN	Mass concentration per milliequivalents (mg)	Molecular weight (g/mol)	Solubility (mg/L)
Ca^{2+}	20	40	
Mg^{2+}	12	24	
Na^+	23	23	
SO_4^{2-}	48	96	
$CaSO_4$			2400
$MgSO_4$			351000
Na_2SO_4			139000

EC and SAR for the landslide areas, which were obtained from SSURGO database, were exported to Excel and are represented by Columns D and E, respectively, in Figure 3.4. Columns F and G contain the TDS in milligrams per liter and millimoles of charge per liter, which were obtained by multiplying the EC by 640 and 10, respectively. Columns H, I and J represent [Ca^{2+}], [Mg^{2+}], and [Na^+] in the soil of each landslide, respectively. Random values of 3, 3, and 1 for these ions in Columns H, I, and J, respectively, were assumed to start the calculations using the Solver function. SAR in Column P was calculated using Equation 3.1 (USDA 2013). The calculated SAR for each landslide in Column P was compared with the SAR value obtained from SSURGO in Column E. The difference between these two SAR values was minimized using the sum of square errors (SSE), which was kept within a 5% error to be precise, and is represented by Column Q. If the error was not within the specified range, then the values for the assumed concentration were recalculated by the Solver function to be within the error, as shown in Column R. Columns L, M, and N are the [Ca^{2+}], [Mg^{2+}], and [Na^+] at saturation in the soil of particular landslides in milligrams per liter, respectively. These values were calculated by

multiplying Columns H, I, and J by the corresponding mass concentration per milliequivalent, as given in Table 3.1. The concentrations were then utilized to determine the total sulfate concentration ($[SO_4^{2-}]$), represented by Column O, using Equation 3.2. The constant term in the equation was obtained by dividing the molecular weight of sulfate by the molecular weight of corresponding ions, as provided in Table 3.1.

$$\text{SAR} = \frac{[\text{Na}^+]}{\sqrt{\frac{[\text{Ca}^{2+}]+[\text{Mg}^{2+}]}{2}}} \tag{3.1}$$

$$[SO_4^{2-}] = 2.39 \times [Ca^{2+}] + 3.95 \times [Mg^{2+}] + 4.18 \times [Na^+] \tag{3.2}$$

A	D	E	F	G	H	I	J	K	L	M	N	O	P	Q	R	S	T	U	V	W	X	Y	Z	AA	AB
Object ID	EC (dS/m)	SAR	TDS (mg/L)	TDS (mmolc/L)	Concentration in solution at saturation (mmolc/L)				Concentration in solution at saturation (mg/L)				Estimated	Sum of Squared Error	Sq Error Check for < 5% of Raw SAR value (0 = Pass)	Sum of ions (mg/L)	Other disolved ions (mg/L)	Overestimation Check - Dissolved ions (mg/L) (0 = Pass)	Other disolved ions in the TDS (%)	Estimated Concentration in solution at saturation (mg/L)			Over Saturation Check (mg/L) (0 = Pass)		
					$[Ca^{2+}]$	$[Mg^{2+}]$	$[Na^{+}]$	$[SO_4^{2-}]$	$[Ca^{2+}]$	$[Mg^{2+}]$	$[Na^{+}]$	$[SO_4^{2-}]$	SAR							$[CaSO_4]$	$[MgSO_4]$	$[Na_2SO_4]$	$[CaSO_4]$	$[MgSO_4]$	$[Na_2SO_4]$
1	0.400	0.100	256.0	4.0	1.3	2.0	0.1	3.4	26.0	24.4	2.3	163.6	0.08	0.000491	0	216.3	39.7	0	16	88.3	120.8	7.1	0	0	0
2	1.600	0.900	1024.0	16.0	5.5	5.8	2.1	13.4	109.3	70.2	49.0	641.9	0.90	8.01E-27	0	870.4	153.6	0	15	371.3	347.6	151.5	0	0	0
3	1.600	0.900	1024.0	16.0	5.5	5.8	2.1	13.4	109.3	70.2	49.0	641.9	0.90	8.01E-27	0	870.4	153.6	0	15	371.3	347.6	151.5	0	0	0
4	1.200	1.300	768.0	12.0	3.3	4.1	2.5	10.0	66.6	50.2	57.7	478.4	1.30	1.01E-25	0	652.8	115.2	0	15	226.2	248.4	178.2	0	0	0
5	1.200	1.300	768.0	12.0	3.3	4.1	2.5	10.0	66.6	50.2	57.7	478.4	1.30	1.01E-25	0	652.8	115.2	0	15	226.2	248.4	178.2	0	0	0
6	1.200	1.300	768.0	12.0	3.3	4.1	2.5	10.0	66.6	50.2	57.7	478.4	1.30	1.01E-25	0	652.8	115.2	0	15	226.2	248.4	178.2	0	0	0
7	0.100	0.100	64.0	1.0	0.0	0.8	0.1	0.9	0.7	10.3	1.5	45.5	0.10	2.95E-14	0	58.0	6.0	0	9	2.3	51.0	4.7	0	0	0
8	0.100	0.100	64.0	1.0	0.0	0.8	0.1	0.9	0.7	10.3	1.5	45.5	0.10	2.95E-14	0	58.0	6.0	0	9	2.3	51.0	4.7	0	0	0
9	0.100	0.100	64.0	1.0	0.0	0.8	0.1	0.9	0.7	10.3	1.5	45.5	0.10	2.95E-14	0	58.0	6.0	0	9	2.3	51.0	4.7	0	0	0
10	0.100	0.100	64.0	1.0	0.0	0.8	0.1	0.9	0.7	10.3	1.5	45.5	0.10	2.95E-14	0	58.0	6.0	0	9	2.3	51.0	4.7	0	0	0
11	2.000	1.200	1280.0	20.0	6.7	6.8	3.1	16.7	133.8	83.2	71.7	799.3	1.20	1.04E-18	0	1088.0	192.0	0	15	454.4	412.0	221.6	0	0	0
12	2.700	3.000	1728.0	27.0	8.5	5.5	7.9	21.9	169.8	66.5	182.2	1050.4	3.00	2.6E-16	0	1468.8	259.2	0	15	576.7	329.3	562.8	0	0	0
13	1.900	2.200	1216.0	19.0	5.6	4.9	5.0	15.5	111.3	60.1	115.9	746.3	2.20	1.07E-14	0	1033.6	182.4	0	15	378.0	297.6	358.0	0	0	0
14	1.900	2.200	1216.0	19.0	5.6	4.9	5.0	15.5	111.3	60.1	115.9	746.3	2.20	1.07E-14	0	1033.6	182.4	0	15	378.0	297.6	358.0	0	0	0
15	1.900	2.200	1216.0	19.0	5.6	4.9	5.0	15.5	111.3	60.1	115.9	746.3	2.20	1.07E-14	0	1033.6	182.4	0	15	378.0	297.6	358.0	0	0	0
16	1.900	2.200	1216.0	19.0	5.6	4.9	5.0	15.5	111.3	60.1	115.9	746.3	2.20	1.07E-14	0	1033.6	182.4	0	15	378.0	297.6	358.0	0	0	0
17	1.900	2.200	1216.0	19.0	5.6	4.9	5.0	15.5	111.3	60.1	115.9	746.3	2.20	1.07E-14	0	1033.6	182.4	0	15	378.0	297.6	358.0	0	0	0
18	1.900	2.200	1216.0	19.0	5.6	4.9	5.0	15.5	111.3	60.1	115.9	746.3	2.20	1.07E-14	0	1033.6	182.4	0	15	378.0	297.6	358.0	0	0	0
19	1.900	2.200	1216.0	19.0	5.6	4.9	5.0	15.5	111.3	60.1	115.9	746.3	2.20	1.07E-14	0	1033.6	182.4	0	15	378.0	297.6	358.0	0	0	0
20	1.900	2.200	1216.0	19.0	5.6	4.9	5.0	15.5	111.3	60.1	115.9	746.3	2.20	1.07E-14	0	1033.6	182.4	0	15	378.0	297.6	358.0	0	0	0

Figure 3.4. Calculation of $[Na^{+}]$, $[Ca^{2+}]$, and $[Mg^{2+}]$ Ions and $[Na_2SO_4]$, $[CaSO_4]$, and $[MgSO_4]$.

To determine if the calculated values for [Ca^{2+}], [Mg^{2+}], and [Na^{+}] ions were correct, Column S, representing the sum of ions ([Ca^{2+}], [Mg^{2+}], [Na^{+}], and [SO_4^{2-}] from Columns L, M, N, and O, respectively) was calculated and compared with the TDS in Column F. The other dissolved ions present in soil were calculated by deducting TDS (Column F) from the sum of the ions (Column S). Due to the negligible concentration of the other dissolved ions in comparison to [Ca^{2+}], [Mg^{2+}], and [Na^{+}], the constraints for the other dissolved ions were kept as positive and less than 15%. That value was chosen to obtain the correct scale for these ions. These two constraints are represented by Columns U and V. Column U was used to check for overestimation, whereas, Column V was utilized to minimize the percentage of the other dissolved ions to less than 15%. If the value of other dissolved ions in Column T is negative, it indicates that the calculated sum for the ions is greater than the TDS. In this case, Columns U and V come into play, and the Solver function recalculates the values for [Ca^{2+}], [Mg^{2+}], and [Na^{+}] to be within the constraints.

The next step was to calculate the concentrations of each salt in Columns W, X, and Y using Equations 3.3, 3.4, and 3.5, respectively. The constant term in each equation was obtained by dividing the molecular weight of the corresponding ion by the molecular weight of the sulfate, as provided in Table 3.1. Finally, the last step was to check for oversaturation or whether the amount of dissolved salts exceeds the solubility or the saturation limit for the corresponding solution. If the calculated values for each salt concentration are higher than their corresponding solubility at saturation as shown in Table 3.1, then Columns Z and AA will contain negative values, and the Solver function will recalculate the salt concentrations. The steps followed in this calculation to use Solver function are described in Appendix C. As there were many landslides in the study, it was time-consuming to manually use the Solver function at each landslide location.

This issue was eliminated by using a Visual Basic for Application (VBA) code as provided in Appendix D.

$$[CaSO_4] = [Ca^{2+}] + 2.39 \text{ ´ } [Ca^{2+}] \quad (3.3)$$

$$[\mathrm{Mg}SO_4] = [Mg^{2+}] + 3.95 \text{ ´ } [Mg^{2+}] \quad (3.4)$$

$$[Na_2SO_4] = [Na^{+}] + 4.17 \text{ ´ } [Na^{+}] \quad (3.5)$$

Correlation Matrix Calculation

A correlation matrix is a matrix that displays the correlation coefficient between variables. Correlation coefficients measure the strength of the linear relationship between two variables. Correlation coefficients are between +1 and -1, with 1 being the perfect positive correlation while -1 represents the perfect negative correlation. A correlation is a positive linear correlation if the dependent variable increases with an increase in the independent variable. In contrast, a correlation is said to be a negative linear correlation if with an increase in the independent variable results in a decrease in the dependent variable (Ratner 2009).

If the value for the correlation coefficient between these two variables ranged from 0.7 to 1, then it is said to be a strong positive correlation (Ratner 2009). This correlation means that the linear strength between the two variables is high, and an increase in the independent variable corresponds to an increase in the dependent variable. Alternatively, if the correlation coefficient is between -0.7 and -1, then it is a strong negative correlation. In this case, the linear strength is still high, but an increase in the independent variable causes a decrease in the dependent variable. Similarly, if the correlation coefficient is between 0.3 and 0.7, the correlation is positive with moderate strength. Finally, correlation coefficient between -0.3 to -0.7 indicates a negative correlation with moderate strength.

For any non-numeric parameters, a true (1) or false (0) value was assigned. Positive and negative correlation coefficients greater than 70% of the highest calculated correlation coefficient among non-numeric parameters were considered to be strong positive and negative correlations, respectively. Similarly, positive and negative correlation coefficients between 30% and 70% of the highest calculated correlation coefficient were considered to be moderate positive and negative correlations, respectively.

Each causative factor (geology, slope inclination, TDS, SAR, EC, rainfall, snowfall, and county) was correlated with every other factor in Pearson's correlation matrix. Pearson's correlation matrix was chosen due to the presence of quantitative variables. There are different correlation matrices, such as Spearman's rank-order and Kendall's Tau (Statistics 2020). These matrices are used when the data are ordinal types. Steps for calculating the correlation matrix are explained in Appendix C.

Laboratory Testing

Montmorillonite and kaolinite, which are the weakest and strongest clays, respectively, were used for the study. Ten different montmorillonite, kaolinite, and quartz mixtures, based upon their dry weights, were prepared as shown in Table 3.2. These samples were mixed with a saline solution prepared as a sodium sulfate solution with a concentration of 120 mg/L (referred to as a sodium sulfate solution in this thesis). About 70% of the landslide areas had sodium sulfate concentrations within 350 mg/L, and the average concentration in those landslide areas was 120 mg/L. The volume of sodium sulfate solution used to mix the samples corresponded to the LL of the mixture with distilled water, as obtained from Tiwari and Ajmera (2011). The steps for sample preparation are explained in the next section.

Table 3.2. Percentage of Minerals Based on the Dry Weight of Samples Tested (M Represents the Percentage of Montmorillonite, K Represents the Percentage of Kaolinite, Q Represents the Percentage of Quartz, SN Represents Sample Number and LL Represents Liquid Limit with Distilled Water, and PI Represents Plasticity Index with Distilled Water.)

SN	1	2	3	4	5	6	7	8	9	10
M	100	70	50	30	10	0	0	0	0	0
K	0	0	0	0	0	100	70	50	30	10
Q	0	30	50	70	90	0	30	50	70	90
LL	463	324	232	139	46	69	49	35	21	7
PI	409	259	172	95	29	24	17	12	7	2

Sample Preparation

The steps for preparing all the samples are identical except for the percentages of the clay minerals and corresponding liquid limits. The steps for sample preparation are as follows:

1. Ten samples, each weighing 1,000 g based on the ratios presented in Table 3.2, were prepared. For instance, to prepare Sample Number (SN) 2, a sample representing 70% montmorillonite and 30% quartz (M70Q30), 700 g of montmorillonite and 300 g quartz were weighed and mixed to make a mixture weighing a total of 1,000 g of the mixture.
2. A sodium sulfate solution with a concentration of 120 mg/L was prepared. Steps for preparing the solution are provided in a later section.
3. The sodium sulfate solution was combined with the clay mixtures. The amount of solution that needs to be mixed depends upon the LL of the mixture when distilled water is the pore fluid, as shown in Table 3.2. The LL for M70Q30 with distilled water (DW) was 304 (Tiwari and Ajmera 2011). Thus, for 1,000 g, the required weight of the sodium sulfate solution was 3,040 g.
4. The sample was left to air dry at a laboratory temperature of 25^{o}C.

5. Once the samples were completely dried, Atterberg's Limits were determined for each sample.

The steps to prepare the sodium sulfate solution are as follows:

1. Add 120 mg of sodium sulfate to one liter of distilled water, and mix the solution with a spatula to dissolve the sodium sulfate.
2. As the time required for 139 g/L of sodium sulfate to dissolve in a solution is about four hours (Jiang et al. 2000), the time allowed for the sodium sulfate to mix completely in this study was approximately ten minutes since the concentration was only 120 mg/L.

To determine the Atterberg Limits for all the mixtures, the procedures provided in American Society for Testing and Materials (ASTM) D4318-10 (2010) were followed.

The procedures for to determine the LL test are summarized here:

1. Weights of moisture tins in which the samples from the experiment were to be placed in oven (W_1) were determined.
2. About 150 g to 250 g of air-dried soil passing through a No. 40 sieve was placed in a ceramic bowl, and sodium sulfate solution was added from a plastic squeeze bottle.
3. The soil sample was mixed so that it formed a uniform paste.
4. A portion of the prepared paste was placed in the brass cup of the LL device, as shown in Figure 3.5. The maximum depth of the paste in the device was about 8 mm. The surface of soil was smoothed with a spatula.
5. Along the centerline of the soil pat in the cup, a groove was cut by using a grooving tool (Figure 3.6).

6. The crank of the LL device was rotated at a rate of 1.9 to 2.1 revolutions per second. Drop height of the brass cup was 10 mm.
7. The number of blows (N) were counted until the grove closed by a length of 13 mm.
8. If the value for the number of blows was greater than 35, paste from the brass cup was mixed with the prepared soil sample, and more sodium sulfate solution was added. A portion of the mixed sample was, again, placed in the brass cup, and the test was repeated to find the corresponding blow count. The process was repeated until the blow count was between 25 and 35.
9. A soil slice, with the approximate width of the spatula, was transferred from the brass cup to the moisture tin, and the weight (W_2) was recorded.
10. The soil paste in the brass cup was cleaned, and more sodium sulfate solution was added to the soil paste. The process was repeated until the grove was closed by a length of 13 mm with a blow count between 20 and 25. The soil was then transferred to the moisture tin, and the weight was recorded.
11. The procedure was repeated until the grove was closed with fifteen to twenty blows.
12. Five tests were conducted to obtain N values ranging from 15 to 35.
13. All the moisture tins were placed in the oven for drying. The weight of the dry soil plus the tin (W_3) was recorded after drying for 24 hours. The temperature of the oven was set to 300°F.
14. Moisture content of each sample was calculated by using Equation 3.6.

$$\text{Moisture content (w)} = \frac{W_2 - W_1}{W_3 - W_1}, 100\% \tag{3.6}$$

15. Moisture content of the each of the samples was plotted on y-axis whereas as number of blows in logarithmic scale were plotted on x-axis. The best-fit line, which is also known as flow curve and the slope of the best fit line is known as flow index, was drawn. The equation of the flow curve gives moisture content for 25 blows gives the moisture content, which is the LL.

Figure 3.5. Sample Placed in the Casagrande Device for the Liquid Limit Test.

Figure 3.6. Liquid Limit Test in the Casagrande Device.

The procedures for the PL test are summarized here:

1. The weight of the moisture tins (W_1) were recorded.
2. About 100 g of a dry soil sample that passed through the No. 40 sieve was collected in a ceramic mixing bowl.
3. Sodium sulfate solution was added to the soil sample and was mixed to form several sticky mud balls.
4. Mud balls with a weight of 1.5 to 2 g were rolled on a frosted glass plate using the palm of the hand until the mud ball changed into a thread. If the thread crumbled with a diameter of 3.18 mm, then the thread was transferred to the tin, and the

weight (W_2) was recorded. If the diameter of the thread was less than 3.18 mm, it indicates that the moisture content was more than the PL and the thread needs to be remolded into a mud ball to reduce moisture content. If the diameter of thread was greater than 3.18 mm, it indicates the moisture content was less than the PL and more sodium sulfate solution is required until the thread crumbles at 3.18 mm.

5. Five tests were conducted for each sample.
6. All the moisture tins were placed in the oven to dry for 24 hours. The weight for the mass of the dry soil sample along with the moisture tin (W_3) after 24 hours was recorded.
7. Moisture content of the soil sample can be calculated using Equation 3.6.
8. PL is the moisture content for the average value of the five samples tested. Any outliers were neglected.

Fieldwork

Pavement distress was recorded on a section of County Road 21 about a mile north of Kathryn, ND. Heavy rainfall events tended to be the sources of the distress. The east shoulder had previously drifted downward, causing damage to the northbound lane (Figure 3.7). During Summer 2019, both lanes were affected, with the northbound lane suffering the most damage.

Surface areas surrounding County Road 21 at the time of the pavement distress due to the slope failure had a sloped landscape with grass and trees to the west and farmland to the east. The west slope peaked around 412 m (1,352 ft) and descended to the east, encountering the road at an elevation of about 387 m (1,242 ft). The slope continued into an agricultural field to the east before reaching a bottom elevation of about 359 m (1,178 ft). The terrain also descended

from south to north with an elevation of about 410 m (1,345 ft) to the south and about 358 m (1,175 ft) to the north.

Based on the surface condition encountered along the slope failure area, seven standard penetration test (SPT) borings, labeled ST-01 to ST-07, were drilled. Inclinometers were installed in ST-06 and ST-07. These inclinometers were mounted to record the movements of slope failure and were tracked by the Braun Intertec Corporation for seven months. The depth of the borings ranged from 8 to 19 m (26 to 61 ft). The main objective of the geotechnical evaluation was to remediate the slope instability. The failure area, with the direction of slope movement and the location of the installed inclinometers, is shown in Figure 3.8. The primary role during the fieldwork, as presented in this study, was to take the inclinometer readings. The results obtained from those inclinometer readings are presented in Chapter 6.

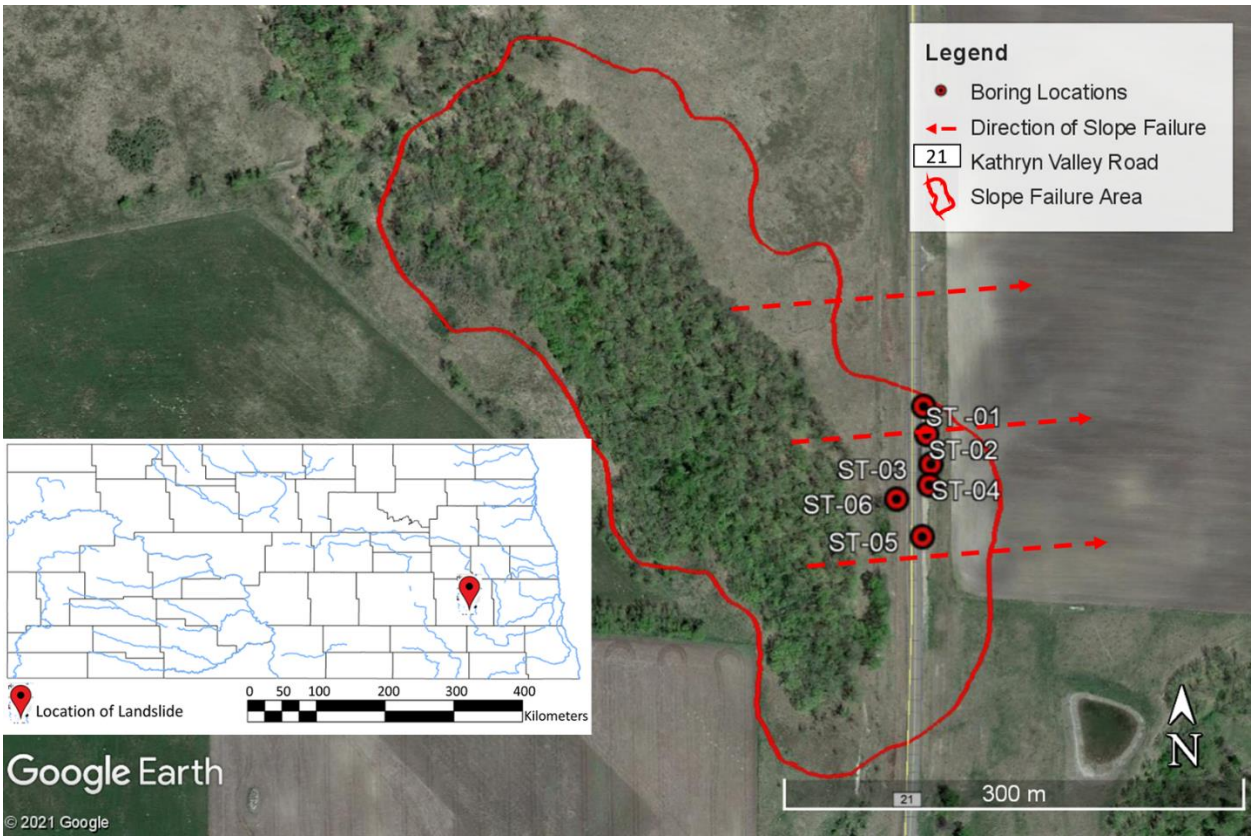

Figure 3.7. Slope Failure at Kathryn in Barnes County, ND (Source: Google Earth).

CHAPTER 4: SLOPE FAILURES IN NORTH DAKOTA AND THE ROLE OF POTENTIAL FACTORS[1]

Abstract

Although North Dakota (ND) is located on the plains, the state has a large number of slope failures. A total of 24,098 landslides, with areas ranging in size from 103 to 6,977,692 m^2, were observed. The number of landslides was log-normally distributed with area, with a mean area of 34,428 m^2 and a standard deviation (SD) of 130,563 m^2. Despite the large number of slope failures, there is little study regarding their causative factors. Therefore, a statistical approach was adopted to determine the relative importance of causative factors such as geological composition, slope inclination, sodium adsorption ratio (SAR), electrical conductivity (EC), total dissolved salts (TDS), land cover, rainfall, and snowfall, within the state. The slope inclinations for these landslides followed a normal distribution with a mean inclination of 11.9° and SD of 6.2°. About 51% of the total slope failures occurred in the Sentinel Butte Formation, and 24% of the failures were in the Bullion Creek Formation. The results showed that 21% of the total slope failures were in McKenzie County followed by Billings County with 14% of the failures. SAR, EC, and TDS at the landslide sites followed multimodal distributions. The means were 1.5, 1.8 dS/m, and 18.1 mmolc/L, respectively, and the SDs were 1.8, 1.3 dS/m, and 12.6 mmolc/L, respectively. About 80% of the total slope failures had sodium sulfate concentrations ($[Na_2SO_4]$) between 0 and 400 mg/L. Similarly, more than 65% of the landslides had calcium sulfate ($[CaSO_4]$) and magnesium sulfate concentrations ($[MgSO_4]$) between 200 and 500 mg/L. Results from the correlation matrix suggested slope failures were more likely to occur in the

[1] The material in this chapter was co-authored by Kamal Raj Upadhaya, Beena Ajmera, Ph.D., P.E., and Aaron Lee M. Daigh, Ph.D. Kamal Raj Upadhaya was primary responsible for the data collection and analyses as well as draft preparation and revisions of all versions of this chapter. Drs. Ajmera and Daigh provided oversight, verified all of the computations, and technical guidance to Kamal Raj Upadhaya.

northern and western regions of North Dakota, where slopes are steep and dissolved salt concentration in the pore fluid for majority of the landslides was absent. High groundwater table might be another potential source of landslides within the state. A large number of landslides were encountered in areas covered with herbaceous vegetation.

Introduction

Landslides are characterized by the United States Geological Survey (USGS) as a mass of rock, debris, or earth moving down a slope under the influence of gravity (USGS 2020a). In many parts of the world, landslides are common and are responsible for the loss of lives, infrastructural damages, huge monetary losses, and adverse environmental effects (Highland and Bobrowsky 2008). In the last two decades, on average, 238,000 people per year globally were affected by landslides (Ritchie and Roser 2014). The total economic cost of the damages resulting from landslides is $310 million per year for the last two decades. Similarly, around 186 people per year are injured from landslides. During these two decades, on average, 892 people lost their lives annually due to landslides, which is 1.4% of the global deaths from natural disasters (Ritchie and Roser 2014).

Natural disasters have a serious influence in the United States (US) affecting 672,000 individuals per year (Ritchie and Roser 2014). In the US, 410 people lose their lives due to natural disasters each year. Of those deaths, about 25 to 50 individuals lose their lives due to landslides. The loss from landslides in the US as per American Geosciences Institute (AGI) is between $2-4 billion each year (AGI 2021). North Dakota, despite being plain in topography, has thousands of landslides. The losses from these landslides reach millions of dollars per year (Murphy 2017). The consequences from these landslides within the state include the loss of

property, damage to roads and infrastructure, and flood risks. Hence, landslide risk management and tracking of these landslides to reduce fatalities and infrastructure damages are needed.

The main objective of this study was to understand the relative importance of causative factors for the occurrence of landslides within the state. The research was divided into two parts. The first step was to find all the landslide areas and to calculate the necessary potential factors for the landslide locations. The second step was to calculate a correlation matrix in order to identify the correlation between the potential parameters that are responsible for slope failures.

Study Area

North Dakota is located in the north-central United States. The state has 53 counties and extends from 45º56′ N to 49º00′ N and 96º33′ W to 104º03′ W. Total area of North Dakota is 183,121 km^2 (70,703 mi^2) with 179,487 km^2 (69,300 mi^2) as land and 3,634 km^2 (1,403 mi^2) as water (City-Data 2020). The state is roughly rectangular in size with three straight borders and one irregular border on the east. North Dakota is bordered by the Canadian provinces of Saskatchewan and Manitoba to the north. The east side is bordered by Minnesota, with the Red River acting as the boundary. The west and south sides are bordered by Montana and South Dakota, respectively. The maximum east-west length is about 580 km (360 mi), whereas the maximum width is about 340 km (210 mi). The total boundary length of North Dakota is 2,111 km (1,312 mi) (City-Data 2020). The study area has a minimum elevation of 229 m (750 ft) along the eastern border in Red River Valley. The maximum elevation is 1,069 m (3,506 ft) in Slope County in the southwest.

Geology of North Dakota

As shown in Figure 4.1, there are 23 different lithological compositions in North Dakota (Clayton 1980a). Pierre, Sentinel Butte, Bullion Creek, Fox Hill, and Cannonball Formations are

the most commonly encountered geological units in the state. Pierre Formation has an area of 43,550.4 km^2 (16,814.9 mi^2). It is a light to dark gray shale, generally non-calcareous, and fissile to blocky with a depth of 701 m (Murphy et al. 2009). It was deposited in an offshore environment during the Cretaceous Era (Gill and Cobban 1965). The formation is subdivided into five sections: Odanah, DeGrey, Gregory, Pembina, and Gammon, with the first four exposed in North Dakota.

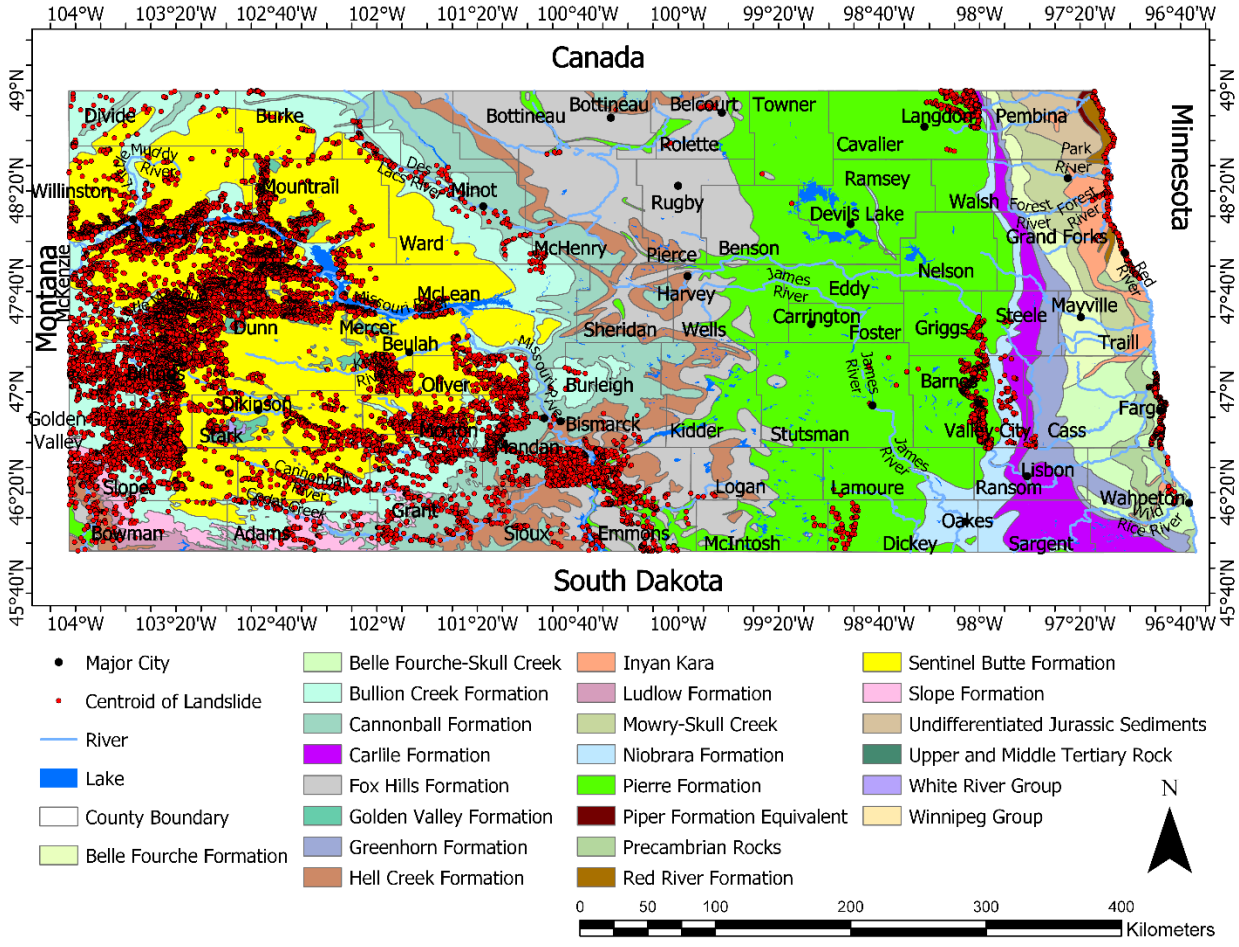

Figure 4.1. Geological Map of North Dakota Showing the Landslides. Base Map was Obtained from USGS (2020b).

Sentinel Butte Formation is the second largest geological formation of the state and has an area of 43,550 km^2 (16,814.9 mi^2). It is composed of grayish-brown silt, sand, clay, sandstone, and lignite with thicknesses up to 200 m (Clayton 1980b). It is generally somber-

colored gray, blue and brown with poorly-to-well cemented sandstone, swelling bentonites and non-swelling claystone, limestone, and iron-oxide (Murphy et al. 2009). The formation primarily consists of river, lake, and swamp sediments and belongs to the Paleocene Era (Jacob 1976). The steep slopes with badland topography in southwestern North Dakota, having petrified wood, tuffaceous beds, and Black Butte lignite, mark the base of the Sentinel Butte Formation (Murphy et al. 2009).

The third largest formation in the state with an area of 22,397.9 km^2 (8,647.9 mi^2) is the Bullion Creek Formation. It consists of yellowish-brown silt, sand, clay, sandstone, and lignite with a thickness of up to 200 m. The soils were deposited in the fluvial, lacustrine, and paludal environments of the Paleocene Era (Clayton 1980b). The formation is bright-colored yellow, brown, and gray from poorly-to-well cemented sandstone, swelling and non-swelling clay stones, limestone, and iron-oxide. The Sentinel Butte Formation has steeper and rougher topography in comparison to the Bullion Creek Formation.

The Fox Hills Formation, with an area of 20,516.9 km^2 (7,921.6 mi^2), is the fourth largest formation in the state. It consists of yellowish brown-to-gray mudstones, siltstones, and sandstone. These sandstones are poorly-to-well cemented. The Cannonball Formation is the fifth largest formation in North Dakota. It contains up to 120 m of sand, visible rock formations on the surface that are reddish olive, and shale with dark brown outcrops (Clayton 1980b). The sand in the Cannonball Formation was deposited in a marine environment, whereas the shale was deposited in an offshore environment during the Paleocene Epoch (Cvancara 1976). The deposited sandstone, which is poorly-to-well cemented, is greenish-gray to yellow, whereas the mudstone that contains lenses of siltstone and sandstone is dark gray (Murphy et al. 2009). These

five geological formations (Pierre, Sentinel Butte, Bullion Creek, Fox Hills, and Cannonball Formations) account for about 77% of the area of the state.

Climate of North Dakota

Due to the geographic location at the center of North America, North Dakota has a wide range of temperatures, with cold winters and hot summers. Irregular precipitation, abundant sunshine, low humidity, and continuous wind describe the climate (NOAA 2017). The presence of mountains in western North Dakota, which obstruct the cold, moist air movement towards the east, worsen the climate. As a result, the state receives cold and dry air from the north, with warm and humid air coming from the tropics (NOAA 2017).

Extreme negative temperature can reach -51°F (-46°C) with blizzards during the winter months, whereas the extreme positive temperature can be 118°F (48°C) with tornados in the summer (ACIS 2020). Summer spans from July to August, but sometimes, it may begin as early as April or May. The average annual rainfall throughout the state ranges from 33 cm (13 inches) to 51 cm (20 inches) (ND 2020). Snowfall usually occurs from November through March while the remaining months of the year mainly experience rainfall. The average snowfall throughout the year ranges from 63 cm (25 inches) to 114 cm (45 inches) (NOAA 2017).

Topography of North Dakota

North Dakota has two major physiographic provinces: the Central Lowlands and the Great Plains. The Central Lowlands lie to the northeast, whereas the Great Plains lie to the southwest corner of the state (Bluemle and Biek 2007). The Central Lowlands consist of the Red River Valley, which is on the eastern side of the state. The Red River Valley is generally flat and extends for about 40 to 64 km (25 to 40 mi) westward from the eastern border of the state. Due to the flatness in this area, landslides are not as common in this region as they are in the western

part of the state. Hilly to mild rolling plains with some buttes are common land features of the Great Plains. The Great Plains include the North Dakota Badlands, which were formed due to erosion and are more prone to landslides (NOAA 2017).

The Missouri Coteau extending from the northwest corner to the south-central border, can be considered as a transition zone between the Central Lowlands and Great Plains (Bluemle and Biek 2007). The topography of this region has about 91 to 152 m of elevation change with the extremely irregular and glaciated landscape. These irregular and glaciated landscapes were formed due to the collapse of super glacial sediments, and as a result, they have erosional bedrock with glacial sediments that are prone to landslides as well as plain surfaces with no landslides (Bluemle and Biek 2007).

Data Collection and Analysis

Mapping the surface geology and the identification of geohazards, such as landslides, throughout the state was completed by the North Dakota Geological Survey (NDGS). The primary dataset to identify these landslides was 1:20,000-scale aerial photographs that were viewed in stereopairs. These photos were taken from low-flying aircraft as early as the 1930s by the United States Department of Agriculture (USDA). Mapping of these landslides started in 2003 and about 25% of the state by area was completed by 2017 (Murphy 2017). The mapping increased rapidly from January 2017 to January 2019, with a total of around 49% of the state completed (Moxness 2019). The resolution of digital aerial photography for mapping increased from 2 m in 2003 to 60 cm in 2018. Starting in 2017, mapping was completed using an unnamed aerial vehicle (Anderson and Maike 2017). For North Dakota, new Light Detection and Ranging (LiDAR) data with a 1 m resolution is also available, making slope failures easy to identify.

NDGS shapefiles contain details about the location and area of landslides in the form of polygons. Red dots marking the area centroid of the polygons were obtained using ArcGIS (Figure 4.2). All the information, such as latitude, longitude, EC, SAR, average rainfall, average snowfall, and slope inclination, for the failure area was determined at the centroid of landslides. To determine the slope failures for each geological formation, a geological map of North Dakota, was obtained from the USGS (USGS 2020b). Landslide concentration (LC) was determined by using Equation 4.1.

$$\mathrm{LC} = \frac{\text{Number of landslides}}{\text{Area of geological formation}} \tag{4.1}$$

To calculate slope inclinations at the landslide locations, an elevation map from the National Elevation Dataset (NED) was used (USGS 2019). After converting the elevation map to a slope map using the Spatial Analyst tool, the slope inclinations at the centroid of the landslides were calculated in ArcGIS. Figure 4.2 represents the slope map of North Dakota, showing the distribution of landslides by county and their slope inclinations. The color from light red to dark red indicates an increase in slope inclination.

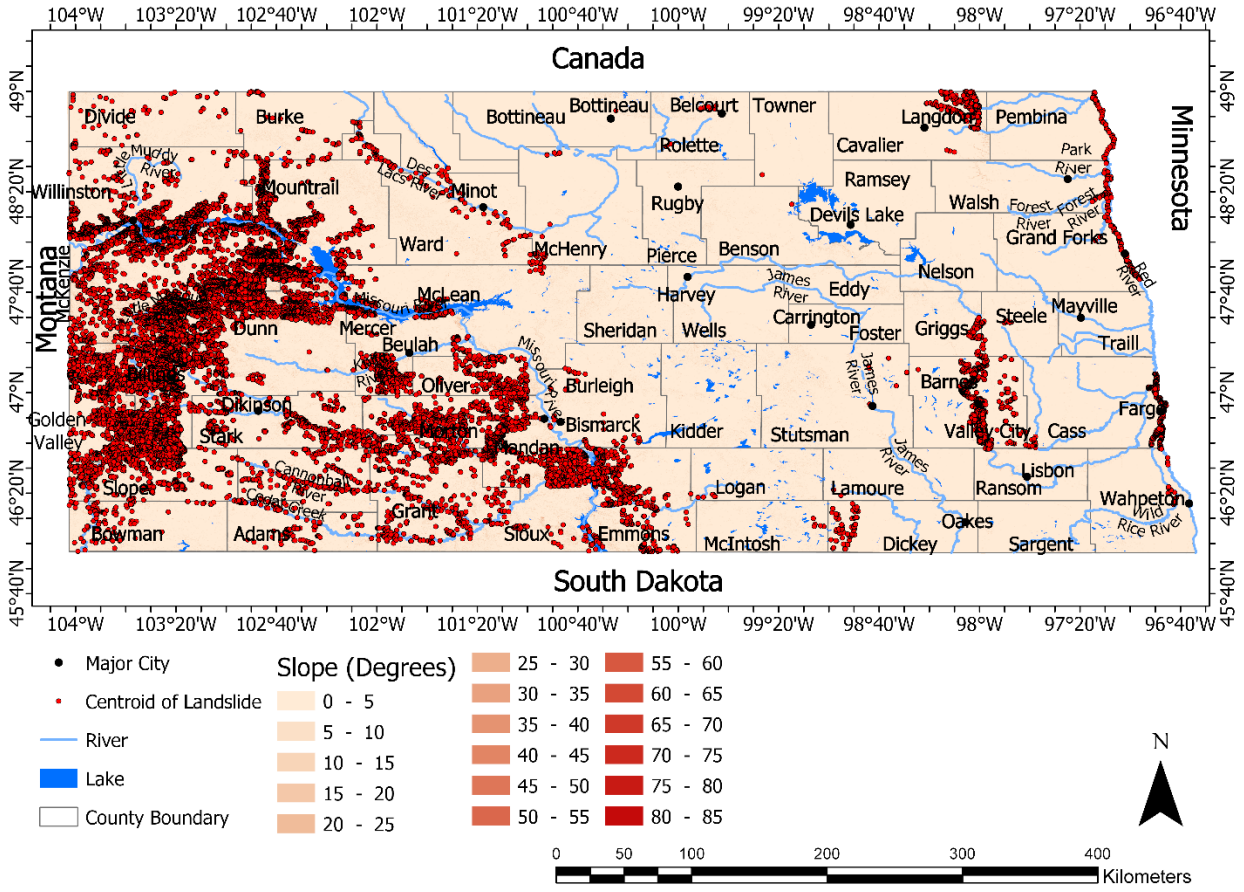

Figure 4.2. Slope Map for North Dakota Showing the Centroids of the Identified Landslides.

Land Cover, Rainfall, and Snowfall at Landslide Sites

Physical materials, vegetative or manmade constructions, on the surface of land are called land cover. Land cover data provide information about types of land cover through time at the landslide locations. Data from the National Land Cover Database (NLCD) were used to determine the land cover at the landslide locations. NLCD offers the land cover database for 2001, 2003, 2006, 2008, 2011, 2013, and 2016 (USGS 2016[2]). As the land cover was similar across these years, the data from 2016 were used to calculate the land cover at the landslide

[2] USGS (2016b) in the reference list at the end of the thesis. USGS (2016) in the reference list at the end of this paper.

locations. During the calculations, Zonal Statistics tool was used to determine the land cover that was most common in the landslide area.

Due to a lack of data, rainfall and snowfall at the landslide locations were calculated by using data from the previous four and ten years, respectively (NOAA 2020). For those years, the average rainfall and snowfall were calculated and used for the correlation matrix calculation. Given limited information related to the date of landslide occurrence, the average rather than antecedent rainfall and snowfall was used in this study.

Calculation of Dissolved Salts at the Landslide Locations

EC from the Soil Survey Geographic Database (SSURGO) for the landslide areas was determined (USDA 2020). These EC values were then used to calculate the TDS at the landslide locations by multiplying by ten (Corwin and Yemoto 2017). Similarly, for conversion based upon weight, EC is multiplied by 640 for an EC with a range of 0.1 to 5 dS/m and 800 for EC greater than 5 dS/m (Corwin and Yemoto 2017). In the study, only 640 was used because more than 97% of the landslides had ECs between 0.1 and 5 dS/m. The concentration of sodium ion ($[Na^+]$) relative to the concentration of calcium ($[Ca^{2+}]$) and magnesium ($[Mg^{2+}]$) ions in the water extracted from a saturated soil paste is called SAR (USDA 2013), which was determined from data in the SSURGO database.

Calculating the dissolved salts includes determining $[Na^+]$, $[Ca^{2+}]$, and $[Mg^{2+}]$ and concentration of sulfate ($[SO_4^{2-}]$), $[Na_2SO_4]$, $[CaSO_4]$, and $[MgSO_4]$ present in a given soil. Using EC, SAR, and TDS, the Solver function in Excel was used to calculate the concentration of each ion and each dissolved salts. The mass concentration per milliequivalents and molecular weight of the Na^+, Ca^{2+}, Mg^{2+} and SO_4^{2-} ions are shown in Table 4.1. This table also contains the solubility of Na_2SO_4, $CaSO_4$, and $MgSO_4$ at saturation.

Table 4.1. Mass Concentration and Molecular Weight of Na^+, Ca^{2+}, Mg^{2+} and SO_4^{2-} Ions along with the Solubility of Na_2SO_4, $CaSO_4$, and $MgSO_4$. Data from ACS (2006)

SN	Mass concentration per milliequivalents (mg)	Molecular weight (g/mol)	Solubility (mg/L)
Ca^{2+}	20	40	
Mg^{2+}	12	24	
Na^+	23	23	
SO_4^{2-}	48	96	
$CaSO_4$			2400
$MgSO_4$			351000
Na_2SO_4			139000

To start the Solver function, random values for the $[Na^+]$, $[Ca^{2+}]$, and $[Mg^{2+}]$ were assumed. SAR was calculated with Equation 4.2 (USDA 2013). The calculated SAR for every landslide was compared with the SAR in the SSURGO database. To minimize the difference to be within 5% error between these two compared SAR values, the sum of squared error (SSE) was utilized. $[Na^+]$, $[Ca^{2+}]$, and $[Mg^{2+}]$ were each calculated to determine $[SO_4^{2-}]$, using Equation 4.3.

$$\text{SAR} = \frac{[Na^+]}{\sqrt{\frac{[Ca^{2+}]+[Mg^{2+}]}{2}}} \tag{4.2}$$

$$[SO_4^{2-}] = 2.39 \cdot [Ca^{2+}] + 3.95 \cdot [Mg^{2+}] + 4.18 \cdot [Na^+] \tag{4.3}$$

The calculated $[Na^+]$, $[Ca^{2+}]$, $[Mg^{2+}]$, and $[SO_4^{2-}]$ were added to obtain the sum of ions, which was used to determine the amount of other dissolved ions in the soil. Constraints were introduced to obtain the correct scale for the dissolved ions. The limits were kept as positive and less than 15% due to the negligible concentrations of these other dissolved ions present in the pore fluid compared to $[Na^+]$, $[Ca^{2+}]$, and $[Mg^{2+}]$. If the difference between the TDS and the

other dissolved ions was negative, it indicated that the calculated sum for the ions was greater than the TDS and overestimated. In this case, the concentration of ions needed to be recalculated.

Finally, the last step was to calculate [$CaSO_4$], [$MgSO_4$], and [Na_2SO_4], using Equations 4.4, 4.6, and 4.6, respectively. If the calculated concentrations were greater than their corresponding solubility values, as shown in Table 4.1, an oversaturation check was set up for the Solver function to recalculate the concentrations to be within the solubility range. Solubility or saturation is the maximum capacity of an aqueous solution to dissolve a solute. Given the large number of landslides, it was time consuming to manually use the Solver function for each landslide. To eliminate this issue, a Visual Basic for Application (VBA) code was used.

$$[CaSO_4] = [Ca^{2+}] + 2.39 \text{ ´ } [Ca^{2+}] \quad (4.4)$$

$$[\mathrm{Mg}SO_4] = [Mg^{2+}] + 3.95 \text{ ´ } [Mg^{2+}] \quad (4.5)$$

$$[Na_2SO_4] = [Na^{+}] + 4.17 \text{ ´ } [Na^{+}] \quad (4.6)$$

Statistical Calculations

Histograms for all the data presented in this study were drawn and compared with different distribution types in order to fit the distribution. The distribution was fitted to predict the likelihood of occurrence of landslide within the particular interval for each of the causative factors. Normal and lognormal distributions were fitted using Equations 4.7 and 4.8, respectively, where f(x) = the probability density function, σ = standard deviation, μ = mean, and x = variable. The mean and standard deviation were calculated using Equations 4.9 and 4.10, respectively, where i = 1 is the index (lower limit of summation), $x_i = i^{th}$ value of the variable x, n = the stopping point (upper limit of summation), and N = number of data points in the population for which the calculation is required. For any parameters that follow a multimodal distribution with different local maxima, the method of moments of mixtures was adopted. The distribution

was fitted using Equation 4.11, where g_i = the probability density function of each distribution available in the dataset and p = the mixing parameter or the weight among the number of distributions within the dataset. The mixing parameter is also the probability of occurrence of distributions within the data set and was calculated by dividing the number of observed data points in each distribution by sum of total number of data points.

$$f(x) = \frac{1}{\sigma\sqrt{2\pi}}\ exp\left[\frac{-(x-m)^2}{2\sigma^2}\right] \tag{4.7}$$

$$f(x) = \frac{1}{\sigma\sqrt{2\pi}\,X}\ exp\left[\frac{-(ln\,x-m)^2}{2\sigma^2}\right] \tag{4.8}$$

$$\mathrm{m} = \frac{\sum_{i=1}^{n} x_i}{N} \tag{4.9}$$

$$\mathrm{s} = \sqrt{\frac{\sum(x_i-\mathrm{m})^2}{N}} \tag{4.10}$$

$$f(x) = pg_1(x) + (1-p)g_2(x) \tag{4.11}$$

For the statistical calculations presented in the study, the Shapiro-Wilks and Anderson-Darling tests were performed to test the normality of the data. Due to the presence of a large amount of data, the chance of the null hypothesis, (that the distribution is normal) being rejected was high, and the null hypothesis was rejected. With a large amount of data, a small deviation from normality can be detected, which leads to rejecting the null hypothesis. Quantile-quantile (q-q) plots were plotted to verify the normality; the graphs are presented in Appendix E. Some distributions, such as the q-q plot for rainfall, snowfall, and sodium sulfate concentration, were slightly skewed compared to the actual data, but as the natural phenomenon fits the normal distribution with the data being clustered around a central peak, these distributions are combinations of a normal distribution.

Distribution of Landslides

Size Distribution of the Landslides

A total of 24,123 landslides were identified in North Dakota. Of these landslides, 25 had areas less than 100 m^2 and were neglected because they possess a small risk to the environment and infrastructure. Hence, a total of 24,098 landslides, with areas ranging from 103.4 m^2 to 6,977,692.4 m^2, were considered in this study. Approximately 47% of the total landslides had areas between 100 and 10,000 m^2, as shown in Figure 4.3. There were 1,497 landslides, 6.2% of the total, had an area larger than 100,000 m^2. The landslide area followed a lognormal distribution, as shown in Figure 4.3. The average area for slope failures was 34,427.9 m^2, whereas, the standard deviation was 130,563.1 m^2.

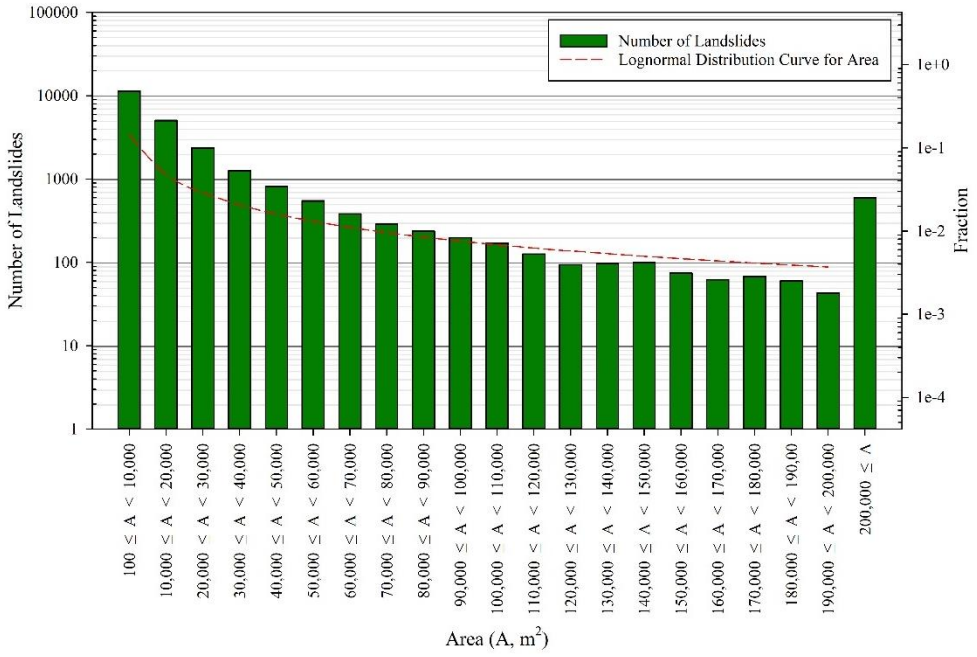

Figure 4.3. Distribution of Landslide Areas.

Landslides and Their Concentration in Geological Formations

The distribution of landslides across the geological formations of North Dakota is shown in Figure 4.4. With 12,252 landslides, the Sentinel Butte Formation had the highest number of

landslides, accounting for 50.8% of the total. The Bullion Creek Formation, with 5,829 landslides, accounted for 24.2% of the total landslides in the state. The geological formation with the third largest number of landslides is the Pierre Formation. It had 1,650, or 6.8% of the landslides.

With 0.97 landslides per km^2, the concentration of landslides was highest in the Upper and Middle Tertiary Rocks. White River Group had second highest landslide concentration with a landslide concentration of 0.8 landslides per km^2. Finally, the Sentinel Butte Formation had the third highest landslide concentration of 0.3 landslides per km^2.

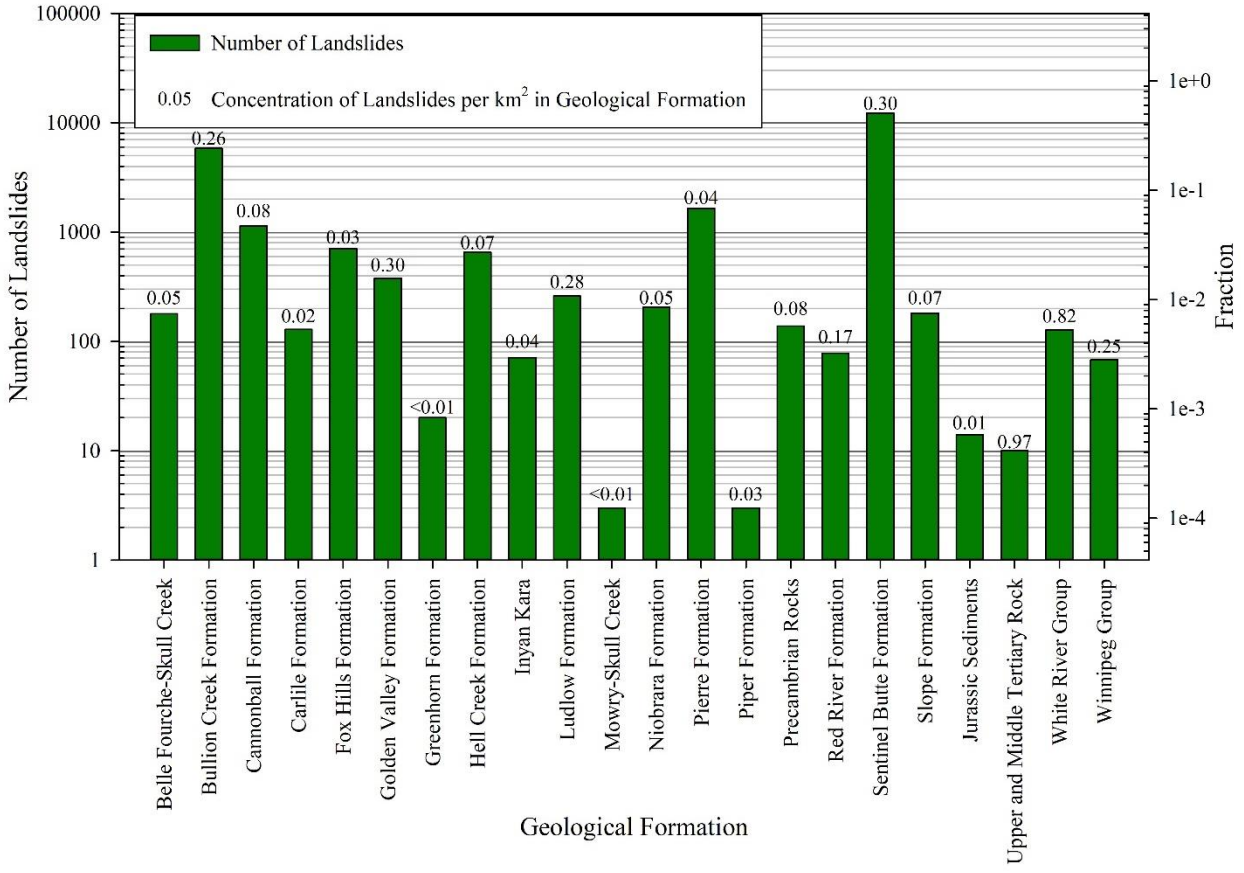

Figure 4.4. Distribution of Landslides across the Geological Formations.

Landslides and Their Concentration in Counties

The distribution of landslides by county is presented in Figure 4.5. McKenzie County, with 5,139 slope failures, had the most landslides, accounting for 21.3% of the total. Billings County, with 3,402 landslides, had the second highest number or approximately 14.1% of the landslides within the state. Finally, Morton County had 1,844 landslides, approximately 7.7% of the total landslides, with the third highest number of landslides by county.

McKenzie, Billings, Morton, Dunn, Golden Valley, Williams, Barnes, Slope, Mountrail, and Mercer Counties were the top ten counties with the most number of landslides, accounting for 78.7% of the mapped landslides. Among the 53 counties of North Dakota, four counties, Foster, Kidder, Pierce, and Wells, had no landslides. Benson, Bottineau, LaMoure, Logan, McIntosh, Renville, Stutsman, and Towner Counties had fewer than ten landslides. The concentration of landslides for Billings County was the highest, with 1.1 landslides per km^2, followed by McKenzie and Golden Valley Counties with 0.7 and 0.6 landslides per km^2, respectively.

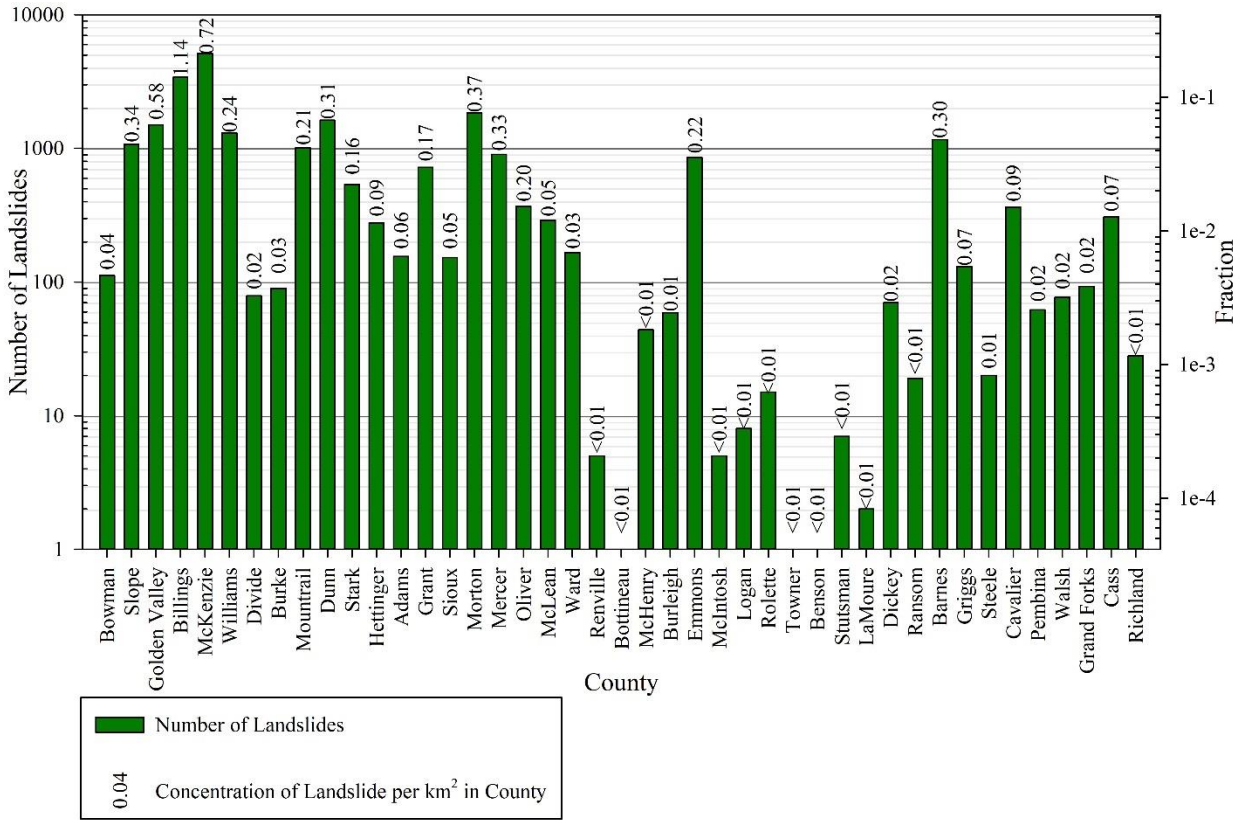

Figure 4.5. Distribution of Landslides in the North Dakota Counties.

Distribution of Landslides based upon Slope Inclination

Slope inclinations in North Dakota range from flat to 85º (Figure 4.2). About 50% of the total landslide have slope inclinations between 6º and 14º (Figure 4.6). The maximum slope inclination on which a landslide occurred was 48º. Slope inclinations on which landslides occur follow a normal distribution. The average and SD of slope inclination of the distribution was 12º and 6.2º, respectively.

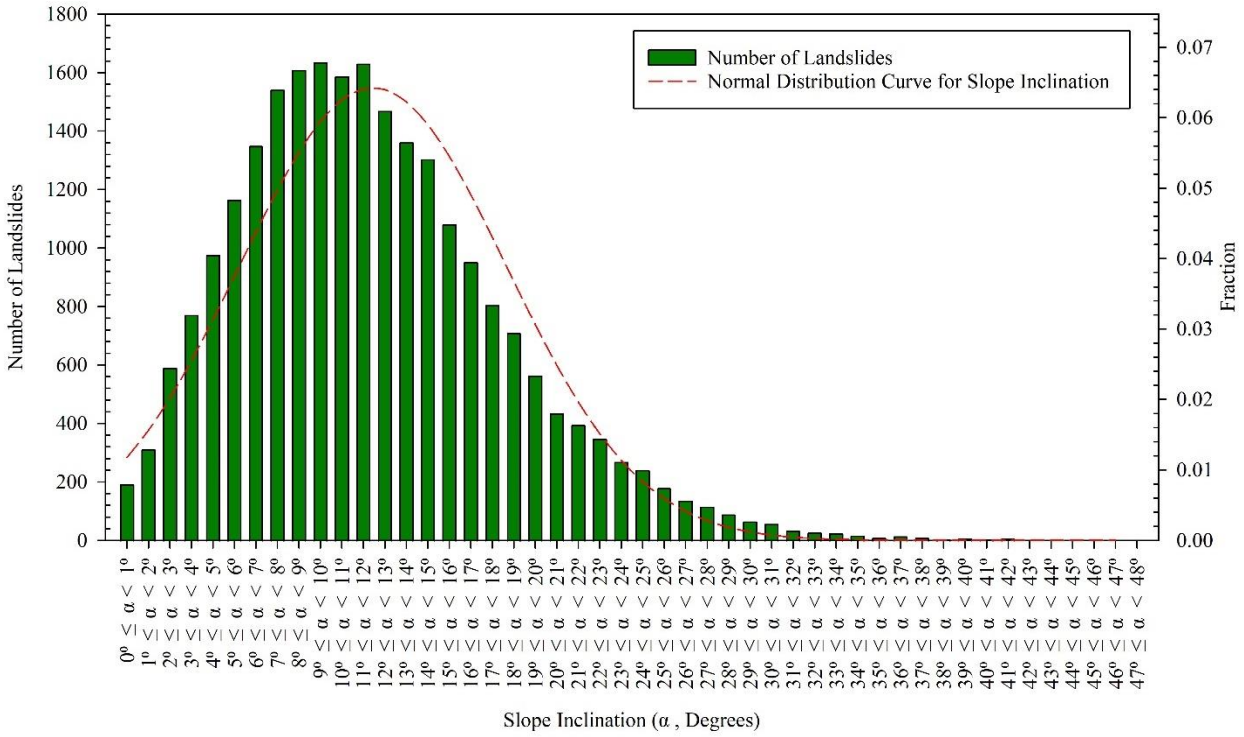

Figure 4.6. Distribution of Landslides with Their Slope Inclination.

Types of Land Cover at Landslide Locations

Figure 4.7 illustrates the distribution of landslides across the different land covers found in North Dakota. Sixty percent of the landslide locations were covered by herbaceous vegetation, which are grassland areas that are dominated by graminoid or other herbaceous vegetation, such as prairie junegrass, big bluesteam, western wheatgrass, indiangrass, little bluesteam, green needlegrass, blue grama, etc.

About 25% of the landslide areas were covered with shrubs and scrubs, such as lead plants, indigo bushes, running serviceberry, etc. These areas were dominated by shrubs, which were less than 5 m in height. The land also included young trees. Finally, about 4% of the total landslide area was covered by deciduous forest, which included trees that were greater than 5 m in height. More than 75% of these trees shed foliage. These availability of land cover at landslides indicates that landslides are common in places where herbaceous vegetation, shrubs

and scrubs were present. The landslide concentration was highest for the mixed-forest type, with 1.3 landslides per km^2. With 0.77 landslides per km^2, the woody wetlands had the second highest landslide concentration.

It can also be seen that landslides are least frequent on developed areas such as high, medium, low intensity and open space developments. Open, low, and medium developed are the areas that includes constructed materials and are distinguished by the percentage of impervious surfaces or the artificial structures such as roads, sidewalks, buildings, parks, and many more. For open, low, and medium developed areas, the percentage of impervious surfaces ranged from 0% to 20%, 20% to 49%, and 50% to 79%, respectively. Similarly, high intensity developed areas includes places with 80% to 90% of impervious surfaces.

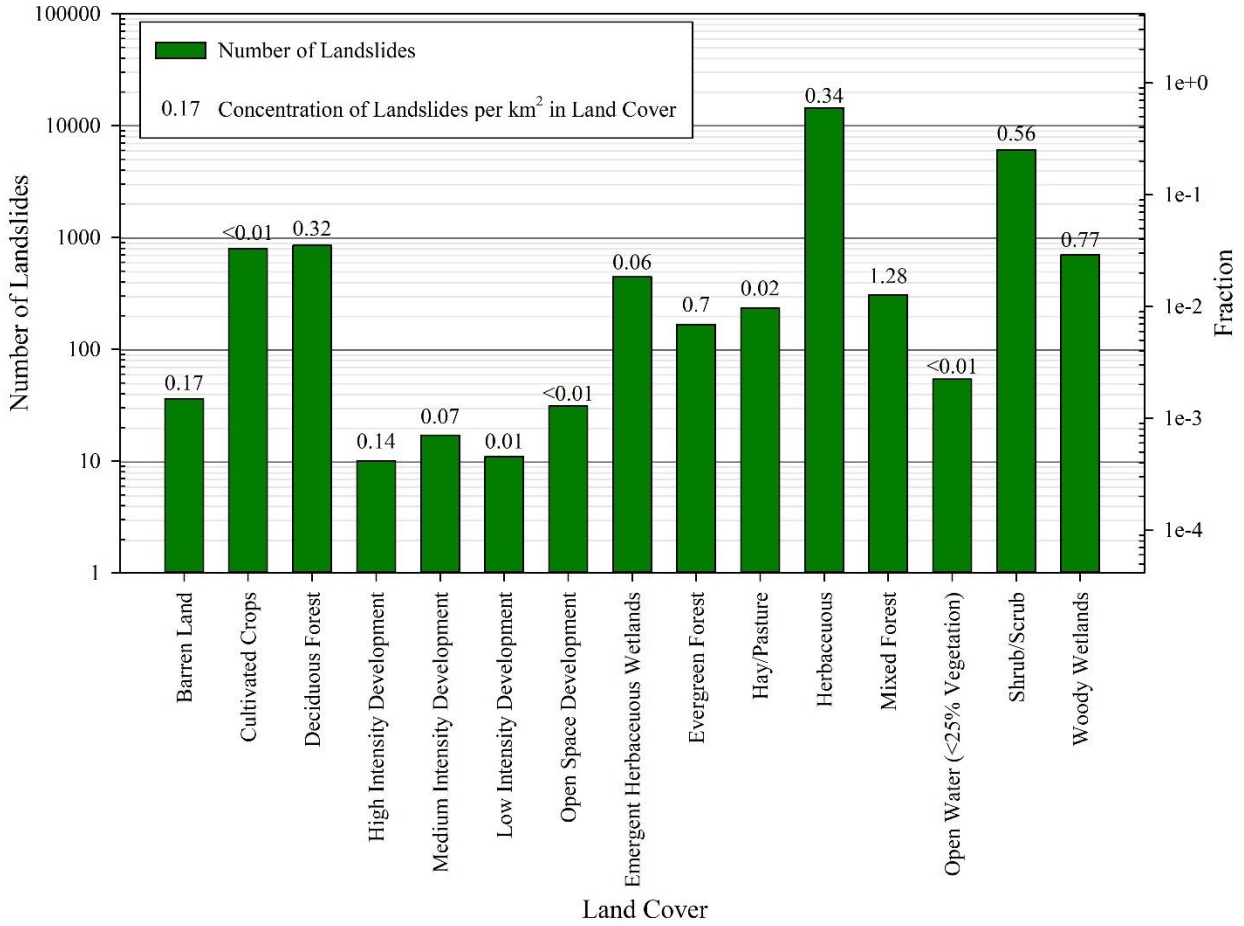

Figure 4.7. Types of Land Cover Available at the Landslide Sites.

Rainfall and Snowfall Distribution for the Landslide Areas

The distributions of rainfall and snowfall in the landslide areas were found to follow a bimodal distributions (Figures 4.8 and 4.9, respectively). From Figure 4.8, it can be seen that about 51% and 8% of landslides had rainfall ranged from 37 to 42 cm and 52 to 57 cm, respectively. Similarly, less than 1% of landslides had rainfall between 48 and 52 cm. The distribution of these landslides between the first two ranges indicates that the location for those landslides might be in a similar areas with similar causative factors that results in a high percentage of landslides. Alternatively, the distribution of landslides between the latter range indicates that the location of landslides in this range might be in different places such as in areas with low slope inclination, high salt concentration, or might be located in high intensity developed areas where low landslide tendency was found.

The minimum and maximum rainfall within the landslide areas was 34 and 61 cm, respectively. The minimum and maximum snowfall across the landslide areas was 48 and 186 cm, respectively. Almost 34% and 36% of the total landslides had snowfall between 90 and 110 cm to 125 and 145 cm, respectively. Similarly, about 17% of landslides had snowfall between 110 and 125 cm.

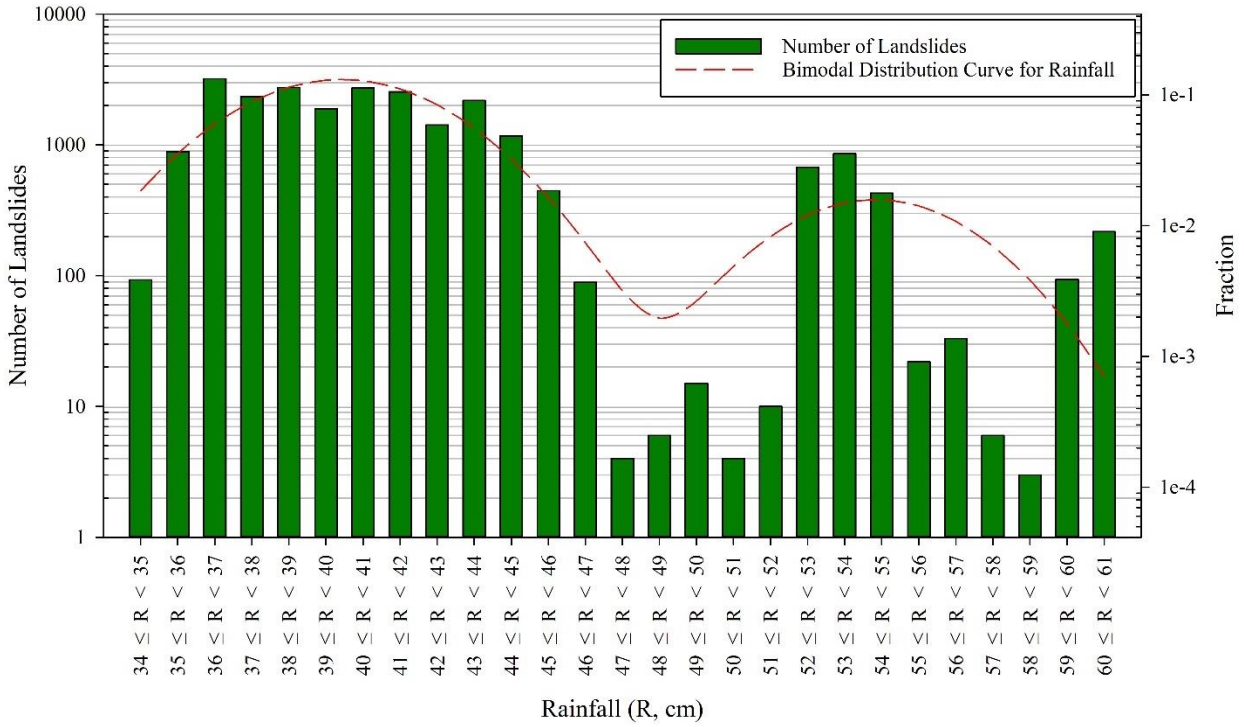

Figure 4.8. Distribution of Landslides based upon the Average Rainfall Data from 2016 to 2019.

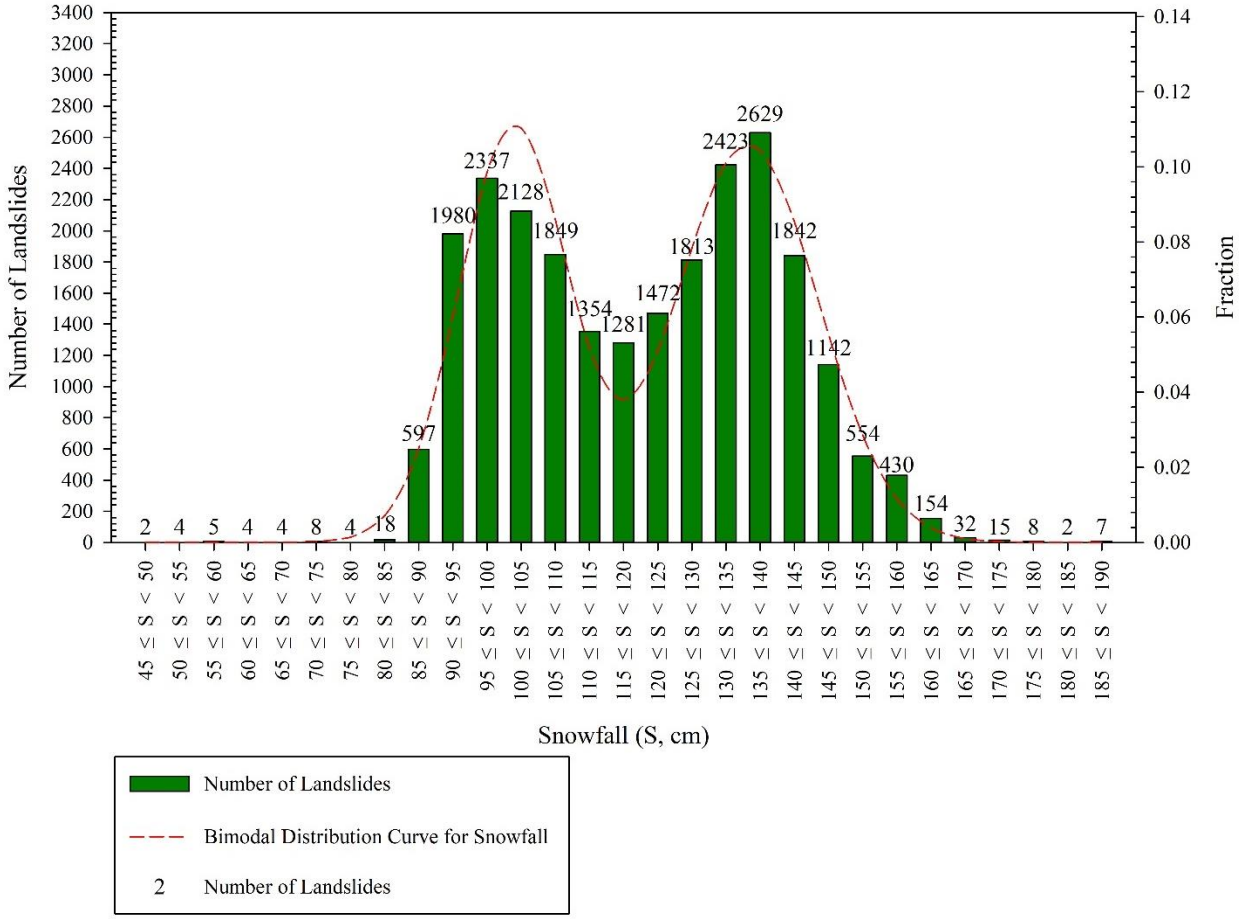

Figure 4.9. Distribution of Landslides based upon Average Snowfall Data from 2010 to 2019.

Distribution of Landslides Based on the Concentration of Dissolved Salts

A total of 11,569 landslides, 48.0% of the total, were found to have SAR values between 0 (inclusive) and 1 (non-inclusive), as shown in Figure 4.10. About 22.3% of the landslide areas had SAR values between 1 and 2. When using the SSURGO database for the calculation, 120 landslide locations did not have any SAR values. These landslide areas were along the bank of water bodies, with most of them along the bank of Missouri River. A histogram illustrated that the SAR values follow a multimodal distribution with an average value of 1.4 and a SD of 1.8. Figure 4.10 shows that the distribution is a combination of three different normal distributions with three distinct local maxima. The means of these distribution occurred at 1.3, 7.1, and 12.4, while the SD were 1.1, 1.3, and 1.6, respectively.

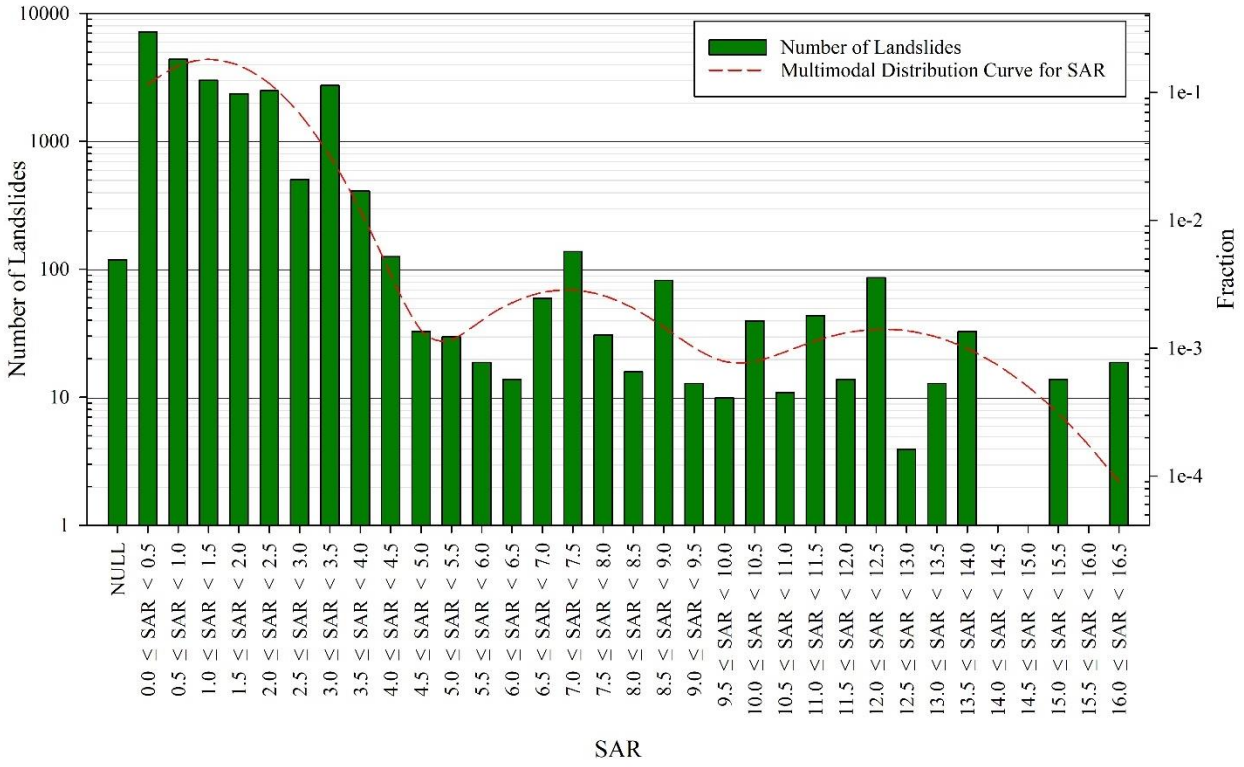

Figure 4.10. Distribution of Landslides based upon SAR at the Landslide Locations.

There were 12,497 landslides, which was about 51.8% of the total landslides, with EC between 1 and 2 dS/m (Figure 4.11). About 26.6% of the landslides (6,422 landslides) had EC between 2 and 3 dS/m. More than 95% of the total landslides had EC within 4 dS/m. Normal soils have EC less than 4 dS/m. The same 120 slope failures without SAR values also did not have EC. When plotting a histogram, the EC followed a multimodal distribution with three normal distributions, each having a distinct local maxima. The means of these distributions occurred at 1.6, 4.3, and 7.9 dS/m, while the SDs were 0.7, 0.6, and 1.4 dS/m, respectively.

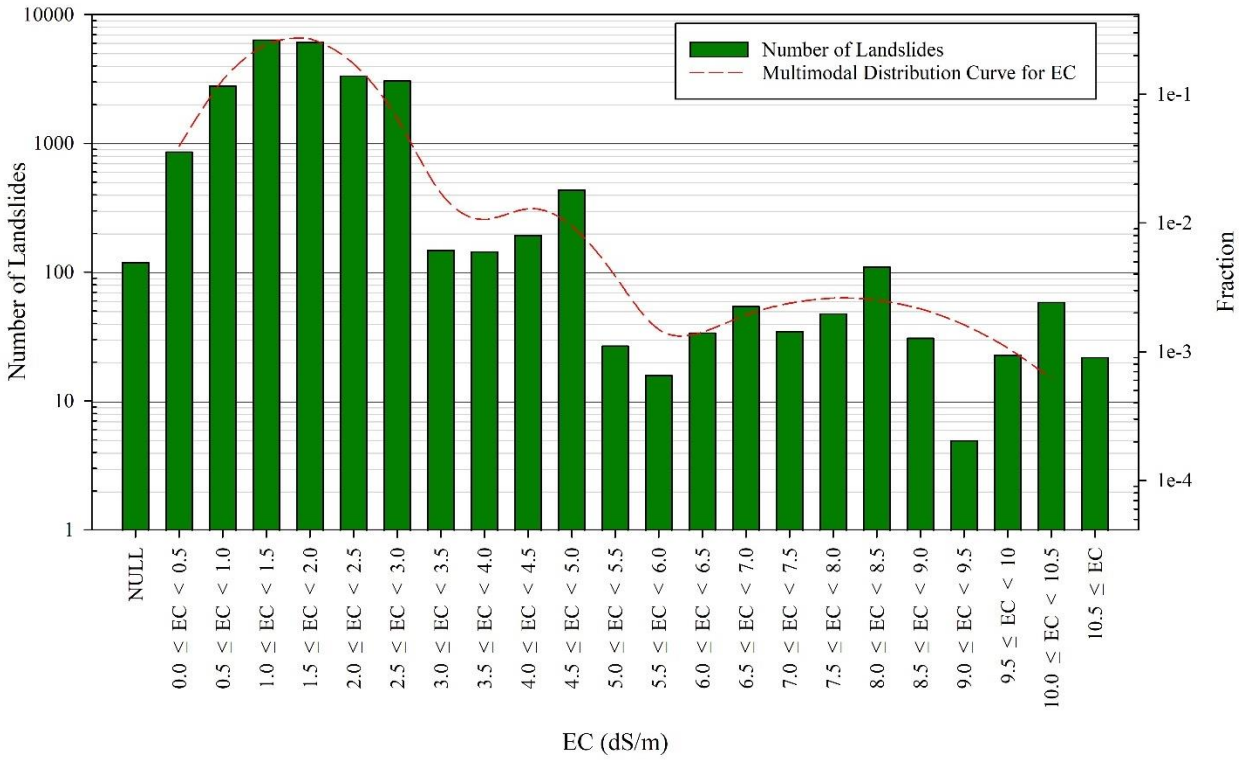

Figure 4.11. Distribution of Landslides based upon the Availability of EC at the Landslide Locations.

The sodium, calcium, and magnesium sulfate concentrations had wide ranges from 0 to 6,740 mg/L, 0 to 3,793 mg/L, and 0 to 5,055 mg/L, respectively (Figure 4.12). More than 97% of the total landslide areas had salt concentrations within 1,100 mg/L. All the concentrations for the dissolved salts follow multimodal distributions consisting of three normal distributions. The local maxima for these three salt concentrations ranged from 200 to 300 mg/L, 300 to 400 mg/L, and 300 and 400 mg/L, respectively. The means of the distributions for the sodium sulfate concentration occurred at 228, 1,554, and 2,980 mg/L, while the SDs were 217, 268, and 272 mg/L, respectively. The means of distributions for the calcium sulfate concentrations occurred at 376, 1,469, and 3,056 mg/L, while the SDs were 172, 183, and 525 mg/L, respectively. The means of distributions of the magnesium sulfate concentrations occurred at 355, 1,384, and 2,838 mg/L, while SDs were 162, 237, and 390 mg/L, respectively.

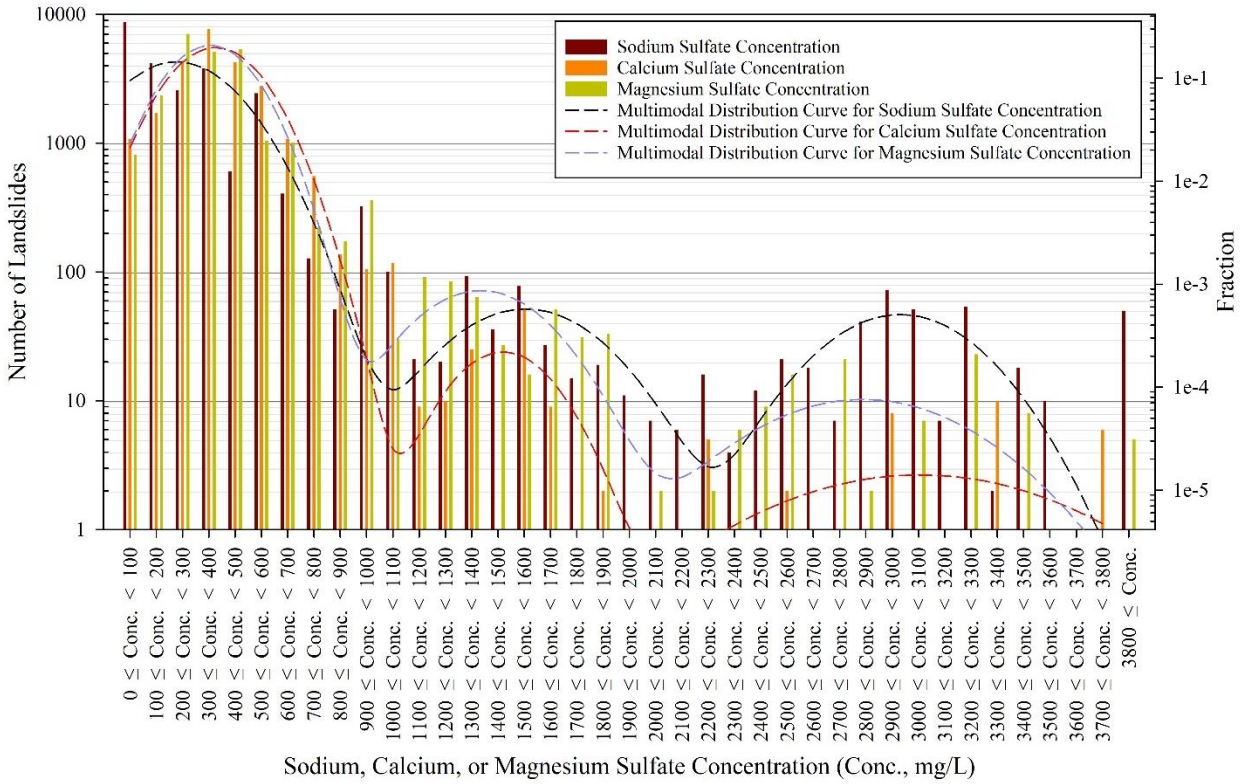

Figure 4.12. Landslide Distribution with the Sodium, Calcium, and Magnesium Sulfate Concentrations.

Soils with a high presence of salt and dominated by chlorides and sodium, calcium and magnesium sulfates are called saline soils (Abrol et al. 1988). Although the dominant soluble cation in this type of soil is Na^+, the quantities of Ca^{2+} and Mg^{2+} are also available in significant amounts. High amount of sodium concentration in saline soil can result in the dispersion of clay particles. The electrostatic forces that bind clay particles together will be destroyed when large sodium particles come between the clay particles causing separation (Pearson 2020). This separation cause clay particles to expand and cause dispersion. When calcium and magnesium concentrations in saline soil is high or available in significant amounts when compared to the sodium concentration, the effect is opposite. These ions are small in size allowing clay particles to flocculate by reducing the space created by sodium ions (Pearson 2020). These types of soils

have EC greater than 4 dS/m and SAR less than 13. The soil is said to be normal when EC and SAR are less than 4 and 13, respectively.

Soils in the study area with concentrations less than 1,100 mg/L (Figure 4.12) were found to have EC and SAR less than 4 dS/m and 13, respectively, indicating the soils were normal as per above definitions. From Figure 4.12, about 68% of the landslides where the soil was normal had sodium, calcium, and magnesium sulfate concentrations ranging from 10 to 445, 185 to 530, and 183 to 517 mg/L, respectively, and total dissolved salt concentrations less than 3 g/L. Any soils with total dissolved salt concentrations greater than 3 g/L are regarded as slightly saline soils (Brouwer et al. 1985). Low concentrations of dissolved salts in clay-rich soils indicate thick diffused double layers that have weak intermolecular bonding between clay particles which decreases the shear strength of soil, resulting in landslides (Mitchell 1993; Tiwari et al. 2005).

The distribution of landslides when EC exceeds 4 dS/m is similar to landslides when the dissolved salt concentration exceeds 1,100 mg/L, as shown in Figures 4.11 and 4.12, respectively. When the sodium sulfate concentration is between 1,100 and 1,600 mg/L or 2,100 and 3,100 mg/L, an increase in the number of landslides can be seen. The sodium sulfate concentration within these ranges is greater than the sum of the calcium and magnesium sulfate concentrations (Figure 4.13) causing dispersion of the soil (Abrol et al. 1988; Gangwar et al. 2020; Pearson 2020). Similarly, when the sodium sulfate concentration is between 1,600 and 2,100 mg/L or 3,100 and 3,800 mg/L, the sum of the calcium and magnesium sulfate concentrations may be greater than the sodium sulfate concentration to flocculate the clay (Abrol et al. 1988). This depends upon various factors such as calcium to sodium exchange efficiency, density of soil, cation exchange capacity, sodium adsorption ratio, and many more (NDSU 2019).

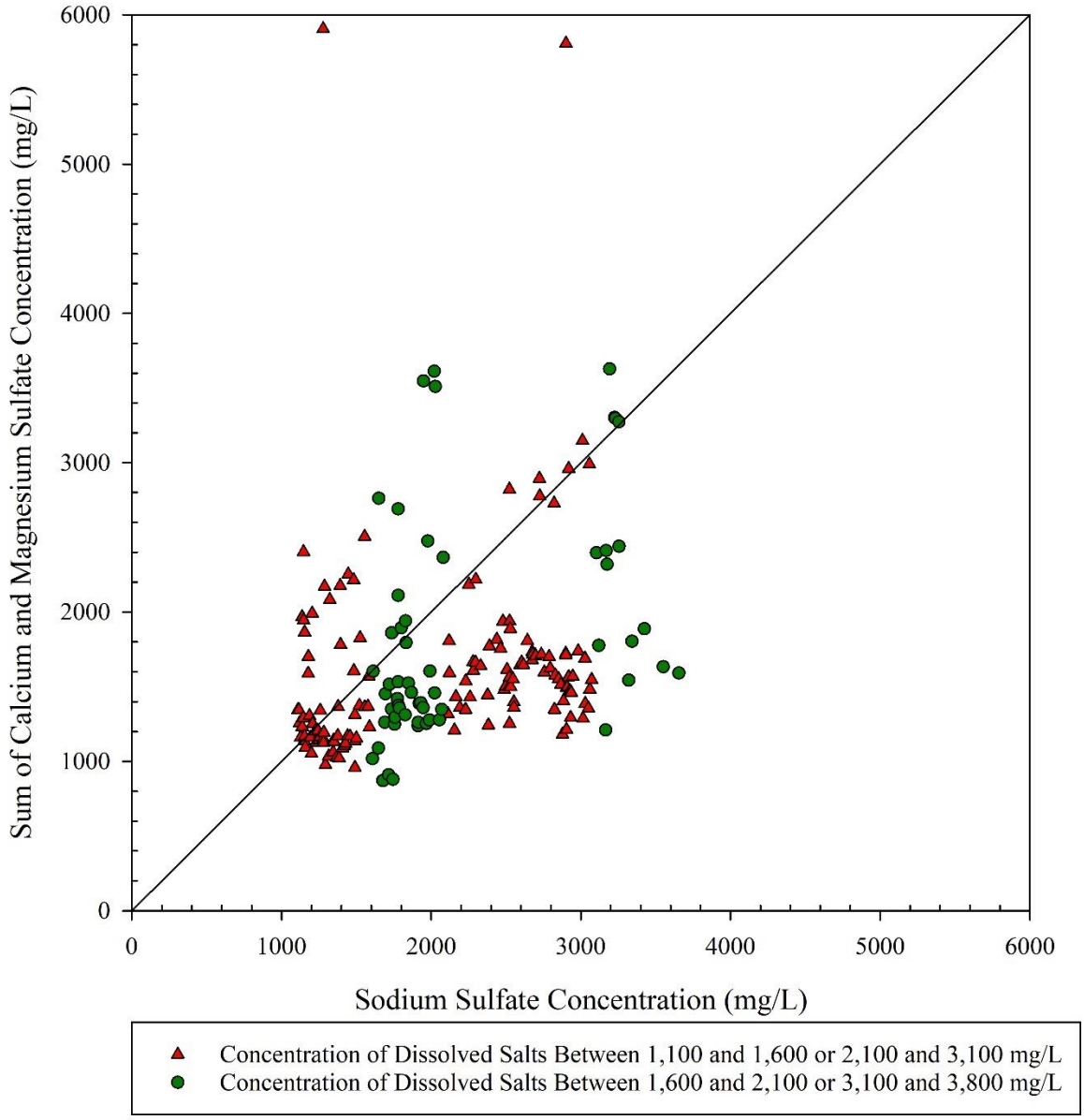

Figure 4.13. Comparison of Dissolved Salts Concentration.

Landslide Susceptibility

In this paper, a statistical approach was adopted in which Pearson's correlation matrix was calculated for all the potential factors that may contribute to the occurrence of landslides in North Dakota. Pearson's correlation matrix describes how each factor is linearly correlated with every other factor. For any factor that did not contain an associated numerical value, a true (1) or false (0) value was assigned. Assigning these values may be the reason for the small correlation

values when at least one factor was non-numeric. Any correlation coefficient between +0.70 and +1.00 is considered a strong positive correlation, whereas -0.70 to -1.00 is regarded as a strong negative correlation (Ratner 2009). Similarly, a correlation coefficient between +0.30 and +0.70 is considered a moderate positive correlation, whereas a value from -0.30 to -0.70 is regarded as a moderate negative correlation. In this study, the highest correlation coefficient observed between any of the factors with at least one non-numeric parameter was 0.60. Therefore, any values greater than 70% of 0.60, or 0.42, were taken as a strong correlation coefficients. Similarly, any values between 30% (0.18) and 70% (0.42) of the highest encountered value were taken as a moderate correlation. The partial correlation matrix results for some relevant parameters are shown in Table 4.2. The strong positive and negative as well as moderate positive and negative correlations are in bold (Table 4.2) and are discussed in Discussion section of this paper.

Table 4.2. Partial Correlation Matrix Results

Parameters	TDS	SAR	Slope Inclination	Latitude	Longitude	Bullion Creek Formation	Pierre Formation	Sentinel Butte Formation	Average Rainfall
SAR	**0.86**	1	-0.04	-0.08	**-0.20**	0.04	-0.10	0.08	**-0.19**
Slope Inclination	-0.04	-0.04	1	0.01	**-0.21**	0.06	-0.08	0.07	**-0.22**
Latitude	-0.12	-0.08	0.01	1	-0.13	-0.06	-0.11	**0.34**	-0.09
Longitude	-0.15	**-0.20**	**-0.21**	-0.13	1	**-0.25**	**0.61**	**-0.41**	**0.97**
Belle Fourche-Skull Creek	-0.09	-0.05	-0.09	-0.07	**0.27**	-	-	-	**0.319**
Bullion Creek Formation	0.06	0.04	0.06	-0.06	**-0.25**	-	-	-	**-0.28**
Fox Hills Formation	-0.03	-0.01	-0.04	**-0.24**	0.18	-	-	-	0.10
Golden Valley Formation	-0.02	-0.01	<0.01	0.03	-0.03	-	-	-	-0.01
Hell Creek Formation	0.07	0.06	-0.02	**-0.22**	0.09	-	-	-	0.06
Niobrara Formation	0.02	-0.02	-0.05	0.08	**0.23**	-	-	-	**0.22**
Pierre Formation	-0.02	-0.10	-0.08	-0.11	**0.61**	-	-	-	**059**
Precambrian Rocks	-0.08	-0.04	-0.08	-0.04	**0.24**	-	-	-	**0.28**
Sentinel Butte Formation	0.03	0.08	0.07	**0.34**	**-0.41**	-	-	-	**-0.33**
Average Rainfall	-0.16	**-0.19**	**-0.22**	-0.09	**0.97**	**-0.28**	**0.59**	**-0.33**	1
Average Snowfall	**-0.21**	**-0.21**	-0.09	<0.01	**0.36**	**-0.23**	0.07	0.02	**0.37**
Barnes County	-0.01	-0.01	-0.01	<0.01	<0.01	-0.01	-0.01	<0.01	<0.01
Dunn County	-0.01	-0.02	-0.01	-0.01	0.01	0.01	0.01	-0.02	0.01
McKenzie County	<0.01	0.01	<0.01	-0.01	0.01	-0.02	<0.01	0.02	0.01
Morton County	<0.01	<0.01	0.01	-0.01	0.01	-0.01	<0.01	<0.01	0.01
Cultivated Crops	-0.04	-0.06	-0.13	-0.02	**0.19**	-0.02	0.09	-0.08	**0.18**
Evergreen Forest	<0.01	0.02	0.07	<0.01	-0.04	0.04	-0.01	-0.01	-0.04
Herbaceous Vegetation	0.05	0.01	-0.01	-0.08	<0.01	0.08	0.05	-0.12	-0.03
Mixed Forest	-0.01	0.01	0.08	0.04	-0.05	0.02	-0.02	0.02	-0.05
Shrub/Scrub	0.03	0.07	0.07	0.04	**-0.29**	-0.05	-0.15	**0.24**	**-0.25**
Woody Wetlands	-0.11	-0.08	-0.08	0.02	**0.34**	-0.06	0.02	-0.13	**0.35**

Note: - represents parameters which do not have direct comparison.

The geological map presented in Figure 4.1 shows that Sentinel Butte Formation can be seen in the north and west parts of the state, where the slopes are steep, implying that slope failures are more likely to occur. The moderate negative correlation between longitude and SAR indicates that the majority of the area in west of the state, where landslides are encountered in Sentinel Butte Formation, also had no salt concentrations in the pore fluid. With a decrease in the total dissolved salt concentration, the thickness of the diffused double layer increases, resulting in a weakening of the intermolecular bonding between the particles and a decrease in the shear strength, which can lead to slope failures (Mitchell 1993; Tiwari and Ajmera 2015; Tiwari et al. 2005; Yong et al. 1992). Thus, the presence of steep slope inclinations with no dissolved salt concentrations for majority of the landslides caused the Sentinel Butte Formation to have the highest number of slope failures.

Location of the Bullion Creek Formation in the southwest region of the state as seen in the geological map (Figure 4.1) and the strong positive correlation of the longitude with rainfall from the correlation matrix suggest that rainfall was prominently found in the southwest regions. The Pierre Formation has the third highest number of landslides, with all of them accumulating in three places rather than being spread out across the formation. These landslides can be seen along the bank of the Pembina River towards the northeast part of the state, the bank of Lake Ashtabula and the Sheyenne River, and along the edges of the wetlands in Dickey County. Having landslides near a water source indicates that there might be a high groundwater table. Similarly, the strong positive correlation of the Pierre Formation with rainfall indicates that landslide areas within this formation also experienced rainfall. Presence of rainfall in area might fluctuate or increase in the level of ground water. A rise in the groundwater table can cause the soil to lose its cohesion due to an increase in pore water pressure and thus reduce the stability of

the slopes (Rahardjo et al. 2008; Xue et al. 2016). Thus, the presence of rainfall with high groundwater table might be the reason for landslides in both of these formations.

Several counties, namely, Foster, Kidder, Pierce, and Wells, did not have any slope failures even though they are in the Pierre Formation. These counties are in the eastern part of the state, an area that is relatively flat as compared to the rest of the state. More than 1,000 landslides were observed in McKenzie, Billings, Morton, Dunn, Golden Valley, Williams, Slope, and Mountrail Counties. These areas are in the western part of the state and underlain by the Sentinel Butte and Bullion Creek Formations. Thus, as described above, these counties will be vulnerable to slope failures.

More than half of the landslides were found to be in areas with herbaceous vegetation such as mixed-grass prairie and short-grass prairie, both of which are non-woody species and can die during the winter (ND 2021; NLCD 2016). Shear strength of soil increases due to the presence of roots especially in areas with woody species (Day 1993; Ghestem et al. 2014; Zhang et al. 2010). Thus, the absence of roots at the end of growing season and absence of tap roots might be the reasons for high slope failure in areas with herbaceous vegetation land covers. Finally, most of the landslides (more than 65%) within the state were found to have slope failures when the concentration of dissolved salt was low. Failures within areas with low salt concentrations might be due to an increase in the diffused double layer thickness that reduces the intermolecular bonding among the clay particles as described above.

The study lags the occurrence of landslides which are influenced by multiple causative factors. For instance, more than half of the landslide locations had rainfall from 37 to 42 cm, and more than 80% of the total landslide areas had dissolved salt concentrations between 300 and 600 mg/L, but the common landslides which have both the rainfall and the salt concentration

within these ranges were difficult to determine and can be considered as the limitation of the study. This is the case where only two causative factors were highlighted, but when considering all the factors together, some programming language is required. Therefore, determining common landslides that were influenced by all the considered causative factors can be overcome by using the machine learning algorithm.

Similarly, different bimodal and multimodal distributions can be seen in the study. For instance, the number of landslides seems to increase and decrease within different salt concentration ranges. Although dispersion and flocculation were the main causes explained in the study, the influence of other parameters on landslides within different ranges that lead to a multimodal distribution was missing. Landslide areas with rainfall between 37 and 42 cm were high in number and were located entirely in western North Dakota, landslide locations with rainfall between 48 and 52 cm were in eastern North Dakota. These high and low numbers of landslides at different places might be due to the effect of landcover, dissolved salt concentrations, snowfall, and slope inclination, and these factors can be considered for future study. Besides the statistical method to determine the causative factors for landslide occurrences that was adopted for this study, machine learning methods, such as neural network methods, fuzzy logic, and the kernel logistic regression model, can be used to predict the common effect of the considered causative factors (Lei et al. 2020; Wang et al. 2016). The reason for bimodality and multimodality will also be explained to determine the correlation by training and validating the data set using the logistic regression approach with machine learning.

Conclusions

A total of 24,098 landslides greater than 100 m^2 in area were observed, with most of them located in western North Dakota. Among these landslides, 1,497 had an area greater than

100,000 m^2. The Sentinel Butte Formation had the highest number of landslides (12,252), accounting for 50.8% of the total landslides of the state. The Bullion Creek Formation had 5,829 landslides and accounted for 24.2% of the total. These two formations accounted for 75% of the total landslides within the state. McKenzie and Billings Counties had 5,139 and 3,402 landslides, the highest and second highest number of landslides, respectively. These two counties accounted for 21.3% and 7.7% of the total landslides throughout the state, respectively. More than half of the slope failures occurred in topographies with inclinations between 6º and 14º. Low concentration of dissolved salts with steep slope inclinations led to a decrease in intermolecular bonding between the soil particles, presence of rainfall with high groundwater tables led to an increase in the pore water pressures and a decrease in the cohesion among soil particles. This may potentially be main reasons for landslides in North Dakota.

References

Abrol, I. P., Yadav, J. S. P., and Massoud, F. I. (1988). *Salt-Affected Soils and Their Management*, Food & Agriculture Org.

ACIS (2020). "NOAA: Regional Climate Centers." *Applied Climate Information System*, <http://scacis.rcc-acis.org/>.

ACS (2006). "Reagent Chemicals: Specifications and Procedures." *American Chemical Society*.

AGI (2021). "How Much do Landslides Cost the US in Terms of Monetary Losses?" *American Geosciences Institute*, <https://www.americangeosciences.org/critical-issues/faq/how-much-do-landslides-cost-terms-monetary-losses#:~:text=Losses%20from%20landslides%20in%20the,and%20%244%20billion%20per%20year>.

Anderson, F. J., and Maike, C. A. (2017). "Drones Rising from the Prairie: Geological Applications of Unmanned Aerial Systems." *GeoNews*, 44(2), 8-14.

Bluemle, J., and Biek, B. (2007). "No Ordinary Plain-North Dakota's Physiography and Landforms." *North Dakota Geological Survey*.

Brouwer, C., Goffeau, A., and Heibloem, M. (1985). "Irrigation Water Management: Training Manual No. 1-Introduction to Irrigation." *Food and Agriculture Organization of the United Nations, Rome, Italy*, 102-103.

Chen, X., and Chen, W. (2021). "GIS-Based Landslide Susceptibility Assessment Using Optimized Hybrid Machine Learning Methods." *Catena*, 196, 104833.

City-Data (2020). "North Dakota Location, Size and Extent." *North Dakota*, <http://www.city-data.com/states/North-Dakota-Location-size-and-extent.html>.

Clayton, L. (1980a). *Geologic Map of North Dakota*, US Geological Survey.

Clayton, L. (1980b). *Explanatory Text to Accompany the Geologic Map of North Dakota*, North Dakota Geological Survey, Grand Forks.

Corwin, D. L., and Yemoto, K. (2017). "Salinity: Electrical Conductivity and Total Dissolved Solids." *Soil Science Society of America*, 84(5), 1442-1461.

Cvancara, A. M. (1976). *Geology of the Cannonball Formation (Paleocene) in the Williston Basin, with Reference to Uranium Potential. Report of Investigation No. 57*, North Dakota University, Grand Forks.

Day, R. W. (1993). "Surficial Slope Failure: A Case Study." *Journal of Performance of Constructed Facilities*, 7(4), 264-269.

Gangwar, P., Singh, R., Trivedi, M., and Tiwari, R. K. (2020). "Sodic Soil: Management and Reclamation Strategies." *Environmental Concerns and Sustainable Development*, Springer, 175-190.

Ghestem, M., Veylon, G., Bernard, A., Vanel, Q., and Stokes, A. (2014). "Influence of Plant Root System Morphology and Architectural Traits on Soil Shear Resistance." *Plant and Soil*, 377(1), 43-61.

Gill, J. R., and Cobban, W. A. (1965). *Stratigraphy of the Pierre Shale, Valley City and Pembina Mountain Areas, North Dakota*, US Government Printing Office, Washington.

Highland, L., and Bobrowsky, P. T. (2008). *The Landslide Handbook: A Guide to Understanding Landslides*, US Geological Survey, Reston, Virginia.

Jacob, A. F. (1976). *Geology of the Upper Part of the Fort Union Group (Paleocene), Williston Basin, with Reference to Uranium*, North Dakota Geological Survey, Grand Forks.

Lei, X., Chen, W., and Pham, B. T. (2020). "Performance Evaluation of GIS-Based Artificial Intelligence Approaches for Landslide Susceptibility Modeling and Spatial Patterns Analysis." *ISPRS International Journal of Geo-Information*, 9(7), 443.

Mitchell, J. K. (1993). *Fundamentals of Soil Behavior., 2nd Edn.*, John Wiley & Sons, Inc., Wiley, New York.

Moxness, A. D. (2019). "Twenty Thousand Slides and Counting: Recent Advances in Digital Imagery Expedite Landslides Mapping in North Dakota." *GeoNews*, 17-19.

Murphy, E. C. (2017). "Landslides in North Dakota." *GeoNews*, 44(1), 1-5.

Murphy, E. C., Nordeng, S. H., Juenker, B. J., and Hoganson, J. W. (2009). "North Dakota Stratigraphic Column: North Dakota Geological Survey Miscellaneous Series 91." *North Dakota Geological Survey*.

ND (2020). "Climate." *Game and Fish*, <https://gf.nd.gov/wildlife/habitats/climate#:~:text=Annual%20precipitation%20ranges%20from%2013,to%204%20inches%20of%20rain.>.

ND (2021). "North Dakota Plants and Habitats Overview." *North Dakota Game and Fish Department*, <https://gf.nd.gov/wildlife/habitats/vegetation>.

NDSU (2019). "Sodicity and Remediation of Sodic Soils in North Dakota." *North Dakota State University*, <https://www.ag.ndsu.edu/publications/crops/sodicity-and-remediation-of-sodic-soils-in-north-dakota#section-6>.

NLCD (2016). "National Land Cover Database 2016." *Multi-Resolution Land Characteristics Consortium*, <https://www.mrlc.gov/data/legends/national-land-cover-database-2016-nlcd2016-legend#:~:text=Grassland%2FHerbaceous%2D%20areas%20dominated%20by,can%20be%20utilized%20for%20grazing.>.

NOAA (2017). "Climate of North Dakota." *National Oceanic and Atmospheric Administration*, <https://web.archive.org/web/20070926010149/http://www5.ncdc.noaa.gov/climatenormals/clim60/states/Clim_ND_01.pdf>.

NOAA (2020). "National Weather Service: National Snowfall Analysis." *National Oceanic and Atmospheric Administration*, <https://www.nohrsc.noaa.gov/snowfall_v2/index.html?season=2009-2010&date=2011060912&version=3&format=.tif>.

Pearson, K. E. (2020). "Basics of Salinity and Sodicity Effects on Soil Physical Properties." *Montana State University*, <https://waterquality.montana.edu/energy/cbm/background/soil-prop.html>.

Rahardjo, H., Leong, E. C., and Rezaur, R. B. (2008). "Effect of Antecedent Rainfall on Pore-Water Pressure Distribution Characteristics in Residual Soil Slopes under Tropical Rainfall." *Hydrological Processes: An International Journal*, 22(4), 506-523.

Ratner, B. (2009). "The Correlation Coefficient: Its Values Range Between+ 1/− 1, or Do They?" *Journal of Targeting, Measurement and Analysis for Marketing*, 17(2), 139-142.

Ritchie, H., and Roser, M. (2014). "Natural Disasters." *Our World in Data*, <https://ourworldindata.org/natural-disasters>.

Tiwari, B., and Ajmera, B. (2015). "Reduction in Fully Softened Shear Strength of Natural Clays with NaCl Leaching and its Effect on Slope Stability." *Journal of Geotechnical and Geoenvironmental Engineering*, 141(1), 04014086.

Tiwari, B., Tuladhar, G. R., and Marui, H. (2005). "Variation in Residual Shear Strength of the Soil with the Salinity of Pore Fluid." *Journal of Geotechnical and Geoenvironmental Engineering*, 131(12), 1445-1456.

USDA (2013). "National Soil Survey Handbook." *Title 430-VI*.

USDA (2020). "Web Soil Survey." *Natural Resources Conservation Service*, <https://websoilsurvey.nrcs.usda.gov/>.

USGS (2016). "NLCD Land Cover (CONUS)." *MRLC*, <https://www.mrlc.gov/data?f%5B0%5D=category%3ALand%20Cover>.

USGS (2019). "USGS National Elevation Dataset (NED)." *ND State Water Commission*, <https://catalog.data.gov/dataset/usgs-national-elevation-dataset-ned>.

USGS (2020a). "What is a Landslide and What Causes One?" *United States Geological Survey*, <https://www.usgs.gov/faqs/what-a-landslide-and-what-causes-one?qt-news_science_products=0#qt-news_science_products>.

USGS (2020b). "North Dakota Geologic Map Data." *United States Geological Survey*, <https://mrdata.usgs.gov/geology/state/state.php?state=ND>.

Wang, L.-J., Guo, M., Sawada, K., Lin, J., and Zhang, J. (2016). "A Comparative Study of Landslide Susceptibility Maps Using Logistic Regression, Frequency Ratio, Decision Tree, Weights of Evidence and Artificial Neural Network." *Geosciences Journal*, 20(1), 117-136.

Xue, K., Ajmera, B., Tiwari, B., and Hu, Y. (2016). "Effect of Long Duration Rainstorm on Stability of Red-clay Slopes." *Geoenvironmental Disasters*, 3(1), 12.

Yong, R. N., Mohamed, A.-M. O., and Warkentin, B. P. (1992). *Principles of Contaminant Transport in Soils*, Elsevier Science Publishers, Amsterdam, Netherlands.

Zhang, C.-B., Chen, L.-H., Liu, Y.-P., Ji, X.-D., and Liu, X.-P. (2010). "Triaxial Compression Test of Soil–Root Composites to Evaluate Influence of Roots on Soil Shear Strength." *Ecological Engineering*, 36(1), 19-26.

CHAPTER 5: LARGE-SCALE LANDSLIDES IN NORTH DAKOTA: THE INFLUENCE OF CAUSATIVE FACTORS[3]

Abstract

This paper focuses on landslides with areas greater than 100,000 m^2, or large-scale landslides, among the 24,098 landslides or all the landslides, identified in North Dakota (ND). With areas between 100,050 and 6,977,692 m^2, a total of 1,497 large-scale landslides were observed. The area of these large-scale landslides was log-normally distribution. More than half of the slope failures had slope inclinations between 6º and 14º with a maximum slope inclination of 39.2º. Slope inclinations on which landslides occur were normally distributed with a mean and standard deviation (SD) of 9.5º and 5.7º, respectively. Among the eighteen geological formations with large-scale landslides, the Sentinel Butte Formation, with 844 landslides, accounted for more than half of the large-scale landslides. With 376 and 369 large-scale landslides, Dunn and McKenzie Counties had the highest and second highest number of landslides, respectively. The sodium absorption ratio (SAR), electrical conductivity (EC), and total dissolved salt (TDS) at these large-scale landslide sites followed gamma distributions with means and SDs of 1.6 ± 1.7, 1.9 ± 1.1 dS/m, and 19 ± 10 mmol/L, respectively. More than 80% of the large-scale landslide locations had sodium sulfate concentrations ([Na_2SO_4]) within 400 mg/L. About 75% of those landslide areas had concentrations of both calcium sulfate ([$CaSO_4$]) and magnesium sulfate ([$MgSO_4$]) between 200 and 500 mg/L. The potential parameters for the occurrence of these large-scale landslides in the study area were as follows: a) rainfall and presence of wetlands with saturated soil act as a medium to rise the groundwater table and reduce the cohesion among soil

[3] The material in this chapter was co-authored by Kamal Raj Upadhaya, Beena Ajmera, Ph.D., P.E., and Aaron Lee M. Daigh, Ph.D. Kamal Raj Upadhaya was primary responsible for the data collection and analyses as well as draft preparation and revisions of all versions of this chapter. Drs. Ajmera and Daigh provided oversight, verified all of the computations, and technical guidance to Kamal Raj Upadhaya.

particles in the study area, b) the presence of herbaceous vegetation which die at the end of each growing season with shallow root systems to hold the soil particles, and c) steep slopes with leaching of dissolved salt concentrations that reduce the intermolecular bonding between the clay particles.

Introduction

For the past century, Asia has had the most landslides, whereas the death rate and injuries due to landslides were highest in North, Central, and South America. European landslides have been the most costly (Collins 2020). Landslides are responsible for the loss of lives and infrastructure. For the last twenty years, landslides have taken the lives of 800 to 1,000 people each year throughout the world, making landslides the seventh deadliest natural disaster (Collins 2020). For the last two decades, the overall average economic damages due to these landslides were recorded as $310 million per year (EMDAT 2020). The damages due to landslides in the United States vary from $2-4 billion, with 25-50 people losing their lives each year (AGI 2021). The analysis of landslides for mitigation or to reduce the economic damage is, therefore, significant.

The causative factors for each landslide are unique. As the reasons for their occurrence vary from place to place, the authors choose to focus on determining the causative factors of the more than 1,400 large-scale landsides in North Dakota because landslides of this scale are of large potential threat and can create huge infrastructural damages and destruction to the environment. Therefore, the main objective of this paper is to present the distribution of large-scale landslides within the state, to provide a comparison of the large-scale landslides with all the landslides mapped in the state, and to illustrate the influence of different causative factors through a statistical approach.

Study Area

North Dakota has a total area of 183,121 km^2. The state extends from 45º56′ N to 49º00′ N and from 96º33′ W to 104º03′ W. Three sides are bordered by US states: Minnesota to the east, Montana to the west, and South Dakota to the south. The north is bordered by the Canadian provinces of Saskatchewan and Manitoba. The minimum and maximum elevations of the study area are 229 m along the eastern border and 1,069 m in the southwest corner.

Wide temperature fluctuations, sporadic precipitation, abundant sunshine, low humidity, and continuous wind describe the climate of North Dakota (NOAA 2017). The extreme negative temperature during the winter can be -46ºC, whereas the summer can be as hot as 48 ºC. The average annual rainfall throughout the state ranges from 33 to 51 cm (ND 2020), and snowfall ranges from 63 to 114 cm (NOAA 2020).

The Central Lowlands and the Great Plains Provinces are the two main topographic regions in North Dakota. The Red River Valley, Missouri Escarpment, Turtle Mountains, Glaciated Plains, Pembina Escarpment, Souris Lake Plain, and Devils Lake Basin, on the eastern side of the state, lie in the Central Lowlands Province. The Great Plains Province is primarily in the southern and western parts of the state, which has hilly to rolling plains with buttes that include the steep North Dakota Badlands. The Great Plains is divided into the Missouri Plateau, the Little Missouri Badlands, the Coteau Slope, and the Missouri Coteau (Bluemle and Biek 2007).

Data Collection and Analysis Methods

The North Dakota Geological Survey (NDGS) prepared an inventory map that identifies landslides. Mapping these landslides started in 2003 using aerial photography along with Google

Earth. Starting in 2017, these landslides was mapped using a Phantom 4 Pro Drone (Anderson and Maike 2017). By 2019, about 49% of the state was mapped (Moxness 2019).

All landslide shapefiles were obtained from NDGS (NDGS 2020). The centroid of large-scale landslides was determined in ArcGIS to calculate the causative factors examined in this study. Causative factors considered were slope inclination, geological composition, soil salinity, land cover, rainfall, and snowfall. The National Elevation Dataset (NED) provides a digital elevation model for the state, that was used to estimate the slope inclination at the location of the centroid of the large-scale landslides (USGS 2019). The geological map prepared by United States Geological Survey (USGS) was utilized to estimate the geological composition at the large-scale landslide sites (USGS 2020[4]). This map gives the geological units and structural features for North Dakota. To determine land cover at the large-scale landslide sites, a map from the National Land Cover Database (NLCD), which gives the types of vegetation within the failure areas, was used (USGS 2016[5]). Data from the National Weather Service were used to estimate the rainfall and snowfall at large-scale landslide locations (NOAA 2020).

Maps prepared by the Soil Survey Geographic Database (SSURGO) were used to estimate the soil salinity for the large-scale landslide sites (USDA 2020). These maps provided information about the electrical conductivity (EC) of the pore fluid and the sodium adsorption ratio (SAR) for the large-scale landslide areas. Furthermore, EC and SAR were used to estimate [Na_2SO_4], [$CaSO_4$], and [$MgSO_4$] at the centroids of the large-scale landslide areas using the Solver function in Excel. As more than 98% of the large-scale landslide sites in this study had EC between 0.1 and 5 dS/m, EC was multiplied by 640 to obtain the total dissolved salts (TDS)

[4] USGS (2020b) in the reference list at the end of the thesis. USGS (2020) in the reference list at the end of this paper.
[5] USGS (2016b) in the reference list at the end of the thesis. USGS (2016) in the reference list at the end of this paper.

(Corwin and Yemoto 2017). This conversion was based upon weight. SAR was calculated using Equation 5.1 (USDA 2013), where [Ca^{2+}], [Mg^{2+}], and [Na^{+}] represent the concentration of the calcium, magnesium, and sodium ions, respectively. Random values for the sodium (Na^{+}), calcium (Ca^{2+}), and magnesium (Mg^{2+}) ions were assumed to calculate SAR and to start the Solver function. The calculated SAR was compared with the SAR obtained from the SSURGO database so that the calculated ions and salt concentrations were within the permissible range targeting a maximum difference of 5%. The next step was to calculate the sulfate concentration ([SO_4^{2-}]) using Equation 5.2.

$$\text{SAR} = \frac{[Na^+]}{\sqrt{\frac{[Ca^{2+}]+[Mg^{2+}]}{2}}} \tag{5.1}$$

$$[SO_4^{2-}] = 2.39 \times [Ca^{2+}] + 3.95 \times [Mg^{2+}] + 4.18 \times [Na^{+}] \tag{5.2}$$

Calculated ions were summed and deducted from TDS to determine the amount of the other dissolved ions. As the percentage of these dissolved salts was negligible compared to the salts considered in the study, two constraints, 0 and 15% of TDS, were set within the Solver function. The upper constraint was set to 15% so that the sum of the other dissolved salts was less than this percentage. Similar, the lower limit was set because the calculated values for the other dissolved ions should be positive. The dissolved salt concentrations for calcium sulfate, magnesium sulfate, and sodium sulfate were calculated using Equations 5.3, 5.4, and 5.5, respectively. Finally, the calculated concentrations were compared with their respective solubility to see if the dissolved salt concentration was within the solubility range. The solubilities of calcium sulfate ($CaSO_4$), sodium sulfate (Na_2SO_4), and magnesium sulfate ($MgSO_4$) at saturation were 2,400, 351,000, and 139,000 mg/L, respectively (ACS 2006). As there were thousands of landslides, a Visual Basic for Application (VBA) code was used.

$$[CaSO_4] = [Ca^{2+}] + 2.39 \text{ ´ } [Ca^{2+}] \quad (5.3)$$

$$[\text{Mg}SO_4] = [Mg^{2+}] + 3.95 \text{ ´ } [Mg^{2+}] \quad (5.4)$$

$$[Na_2SO_4] = [Na^{+}] + 4.17 \text{ ´ } [Na^{+}] \quad (5.5)$$

Site reconnaissance for four large-scale landslides in western North Dakota was performed as part of study. Object IDs with corresponding landslide locations are presented in Table 5.1. A couple of hand augers were performed at Landslide ID as 11505 to determine the soil composition within this formation. For the construction of well pads and roads, cutting and filling activities were undertaken at the other three landslide areas, so, visual inspection was performed to determine the soil composition at those locations. Visual inspection of landslides located along Highway 22 of Fort Berthold, North Dakota and 108th Avenue Northwest Watford City, McKenzie County, North Dakota were performed from a car. Landslide ID 5583 was located near the bank of the Missouri River whereas other three landslides were not located near any water source, as verified from Google Earth.

Table 5.1. Large-Scale Landslides where Field Reconnaissance was Performed

ID	Coordinates at Centroid	Area of Landslide (m^2)	Formation
5583	47º48’05.1” N, 102º37’46.6” W	104,641	Sentinel Butte
20017	47º40’38.4” N, 102º54’18.8” W	2,647,300	Sentinel Butte
10364	47º31’42.1” N, 102º43’04.8” W	269,387	Sentinel Butte
11505	47º33’35.4” N, 103º05’46.5” W	2,071,500	Sentinel Butte

Statistical Calculations

The distribution for each causative factor of the landslides was fitted to determine the likelihood of any causative factors on landslide occurrence. A histogram for the causative factors was plotted, and the resulting curve was compared with the distributional curve for different distributions. Equations 5.6 and 5.7 were used to fit the normal and lognormal distributions, respectively, where f(x) = the probability density function, σ = standard deviation, μ = mean, and

x = variable. The mean and standard deviation for the data were calculated using Equations 5.8 and 5.9, respectively, where i = 1 is the index (lower limit of summation), $x_i = i^{th}$ value of variable x, n = the stopping point (upper limit of summation), and N = number of data points. A distribution with two distinct maxima in a histogram indicated a bimodal distribution. If the standard deviation for the datasets contain distinct maxima and if the mean for the datasets which contain two distinct maxima differed by at least twice the common standard deviation, then a bimodal distribution fits the data. Similarly, quantile- quantile (q-q) plots were plotted to verify the normality, and the graphs are presented in Appendix E. Even though the q-q plot for some distributions, such as slope inclination, rainfall, and snowfall was slightly skewed compared to the actual data, the plots are normally distributed because the natural phenomenon fits a normal distribution.

The distribution curve for any parameter that follows a gamma distribution was fitted using Equation 5.10, where f(x) = the probability density function, x = variable, θ = scale parameter, k = shape parameter, and Γ(k) = gamma function. The scale and shape parameters were determined by using Agricultural and Meteorological Software (AgriMetSoft 2019). The shape parameter was governed by the range of the available dataset, whereas the scale parameter was determined by the rate at which the data in histogram declined towards zero.

$$f(x) = \frac{1}{\sigma\sqrt{2\pi}}\ exp\left[\frac{-(x-\mathrm{m})^2}{2\sigma^2}\right] \tag{5.6}$$

$$f(x) = \frac{1}{\sigma\sqrt{2\pi}\,X}\ exp\left[\frac{-(ln\,x-\mathrm{m})^2}{2\sigma^2}\right] \tag{5.7}$$

$$\mathrm{m} = \frac{\sum_{i=1}^{n} x_i}{N} \tag{5.8}$$

$$\mathrm{s} = \sqrt{\frac{\sum(x_i-\mathrm{m})^2}{N}} \tag{5.9}$$

$$f(x) = \frac{x^{k-1}\, e^{\frac{-x}{\theta}}}{\theta^{k}\Gamma(k)} \tag{5.10}$$

Distribution of Landslides

Size Distribution of the Landslides

With areas ranging from 100,050 to 6,977,692 m^2, a total of 1,497 large-scale landslides were observed in North Dakota, as shown in Figure 5.1. About 70% of the total large-scale landslide areas were between 100,000 and 250,000 m^2. These large-scale landslides were primarily distributed at three places, along the route of Little Missouri River in the western North Dakota, bank of Lake Ashtabula, and near the bank of Pembina River.

It was found that the area for all these large-scale landslides followed a lognormal distribution, with a mean area of 298,709 m^2 and a SD of 11,549,650 m^2. The lognormal distribution of these data indicates that there is a rapid decrease in the number of landslides with an increase in the area of landslides.

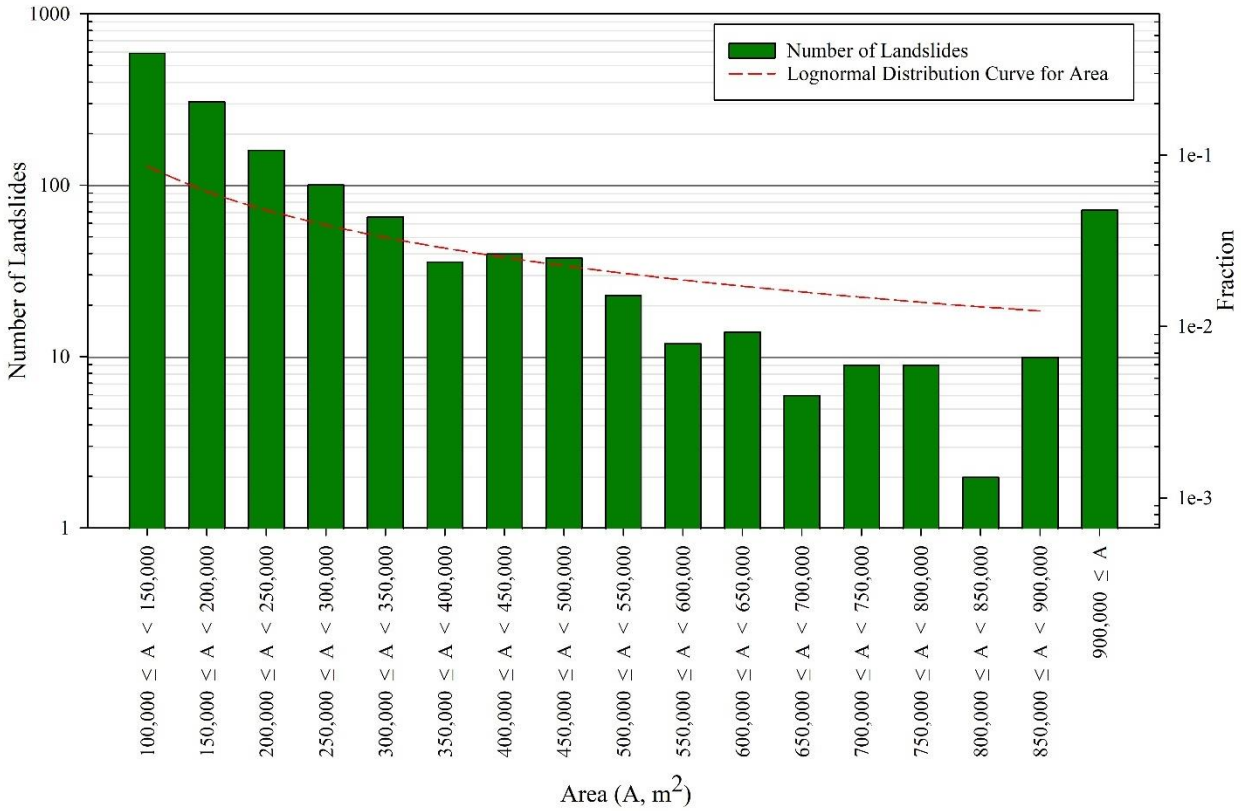

Figure 5.1. Distribution of Large-Scale Landslides by Area.

Large-Scale Landslides and Their Concentration in Geological Formations

The distribution of large-scale landslides based on geological formations is illustrated in Figures 5.2 and 5.3. The Sentinel Butte Formation, with 844 landslides, accounted for 56.4% of the large-scale landslides. Similarly, the second highest percentage of large-scale landslides were in the Pierre Formation followed by Bullion Creek Formation. These two formations had 197 and 164 large-scale landslides that accounted for 13.2% and 10.9% of the large-scale landslides, respectively. There were seven geological formations within the state that had fewer than ten large-scale landslides. Among those formations, Belle Fourche-Skull Creek, Inyan Kara, and Precambrian Rocks each had just one large-scale landslide.

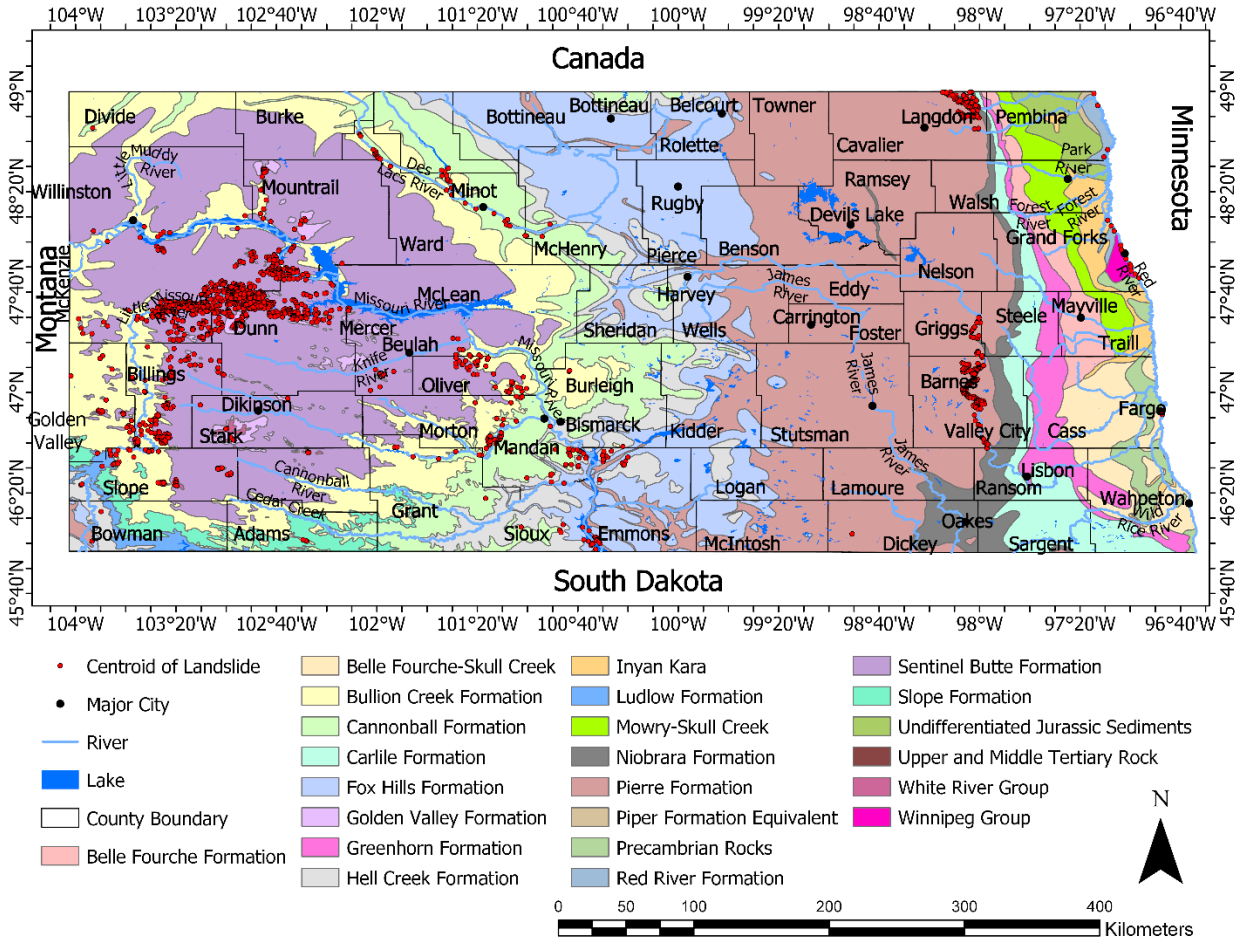

Figure 5.2. Geological Map of North Dakota with the Location of Large-Scale Landslides. The Geological Base Map was Obtained from USGS (2020).

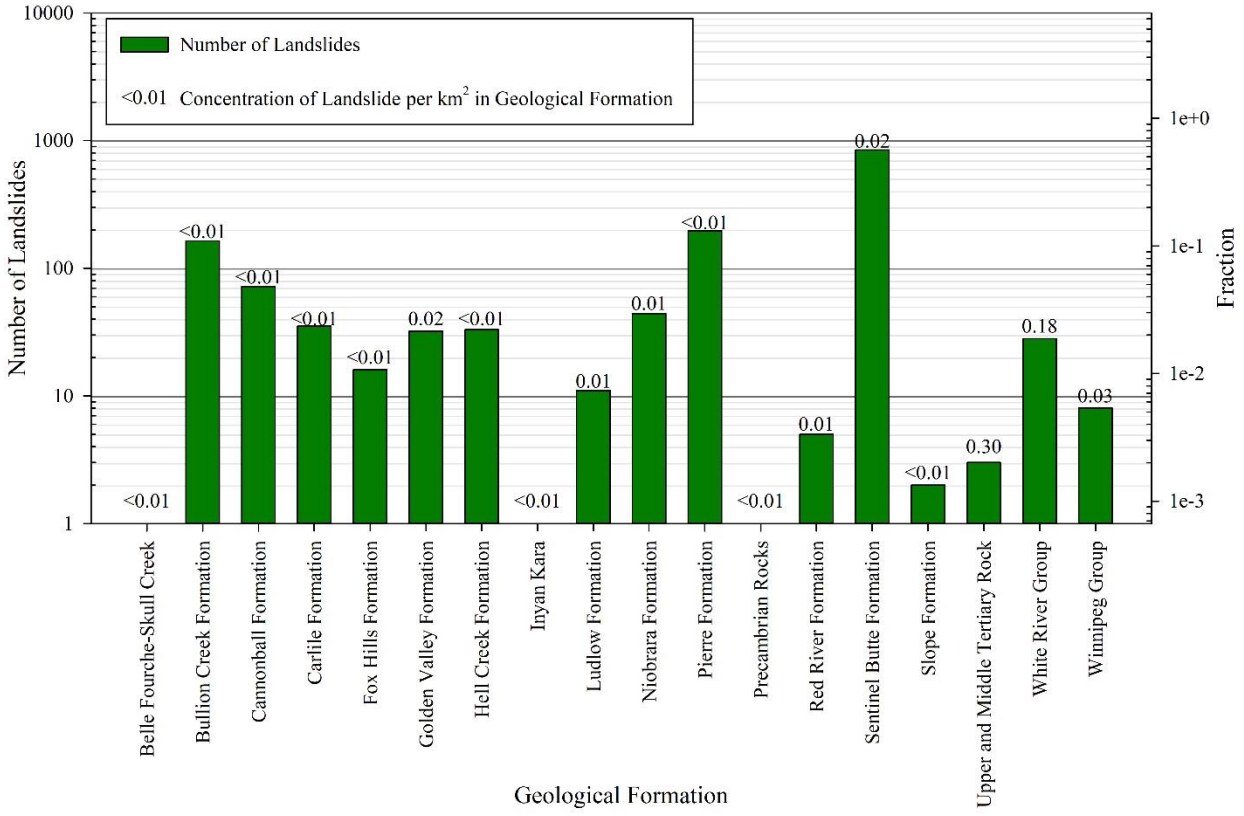

Figure 5.3. Distribution of Large-Scale Landslides in the Geological Formations.

Top three geological formations with the highest landslide concentrations were Upper and Middle Tertiary Rock, White River Group, and Winnipeg Group. Landslide concentrations in these formations were 0.30, 0.18, and 0.03 landslides per km^2 with 3, 28, and 8 large-scale landslides, respectively.

Slope Inclination of Large-Scale Landslides

Slope inclinations within the study area ranged from 0º to 85º (Figure 5.4). The distribution of large-scale landslides with slope inclination is shown in Figure 5.5. The horizontal axis in Figure 5.5 represents the slope inclination. Vertical axes in the left and right represents the number of landslides and landslide fraction, respectively. The maximum slope inclination on which a large-scale landslide occurred was 39º.

Approximately 51% of the total large-scale landslides or 771 landslides had slope inclinations between 6º and 14º (Figure 5.5). Histogram for slope followed a normal distribution. This distribution indicates that about 68% of the large-scale landslides had slope inclinations between 4º to 15º. The mean and SD for all the large-scale landslides were found to be 10º and 6º, respectively.

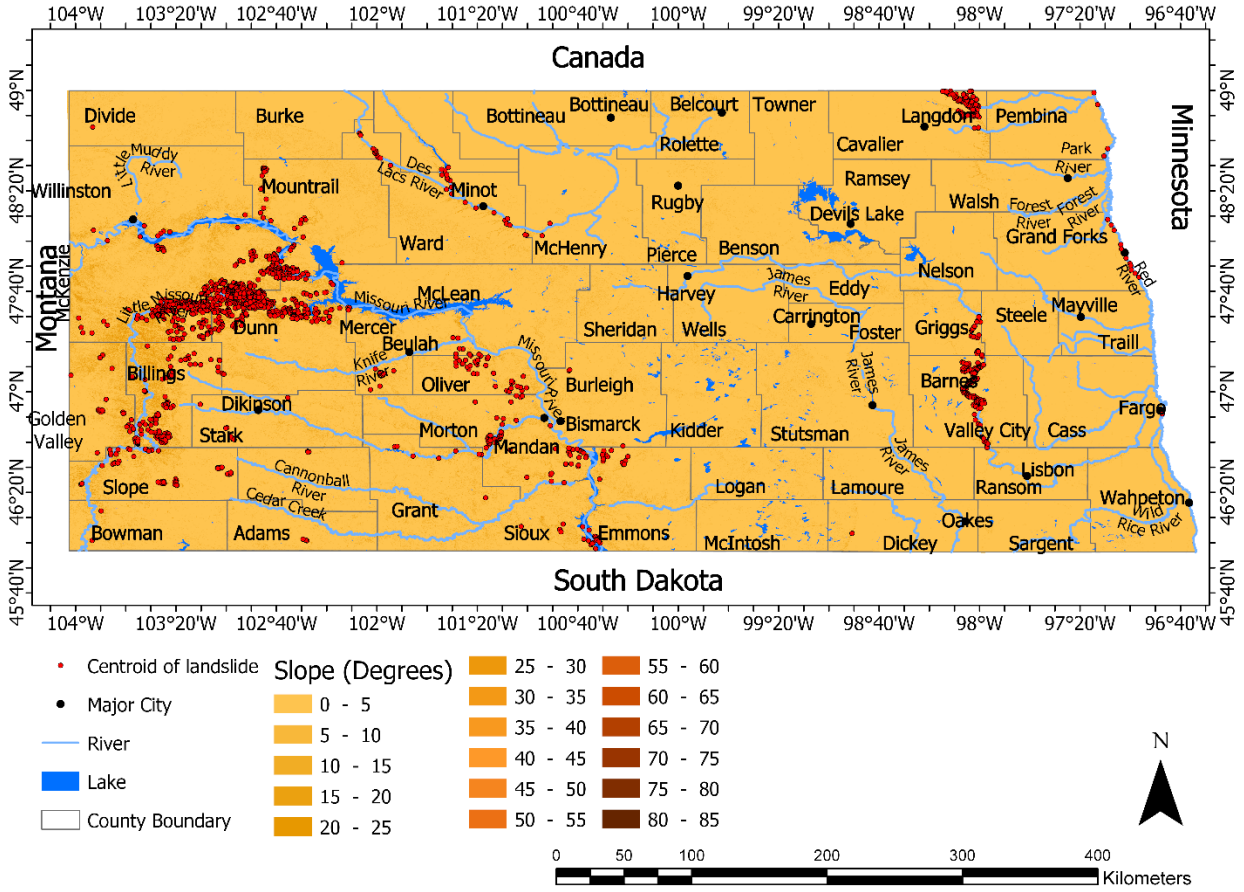

Figure 5.4. Slope Map for North Dakota with Locations of the Large-Scale Landslides.

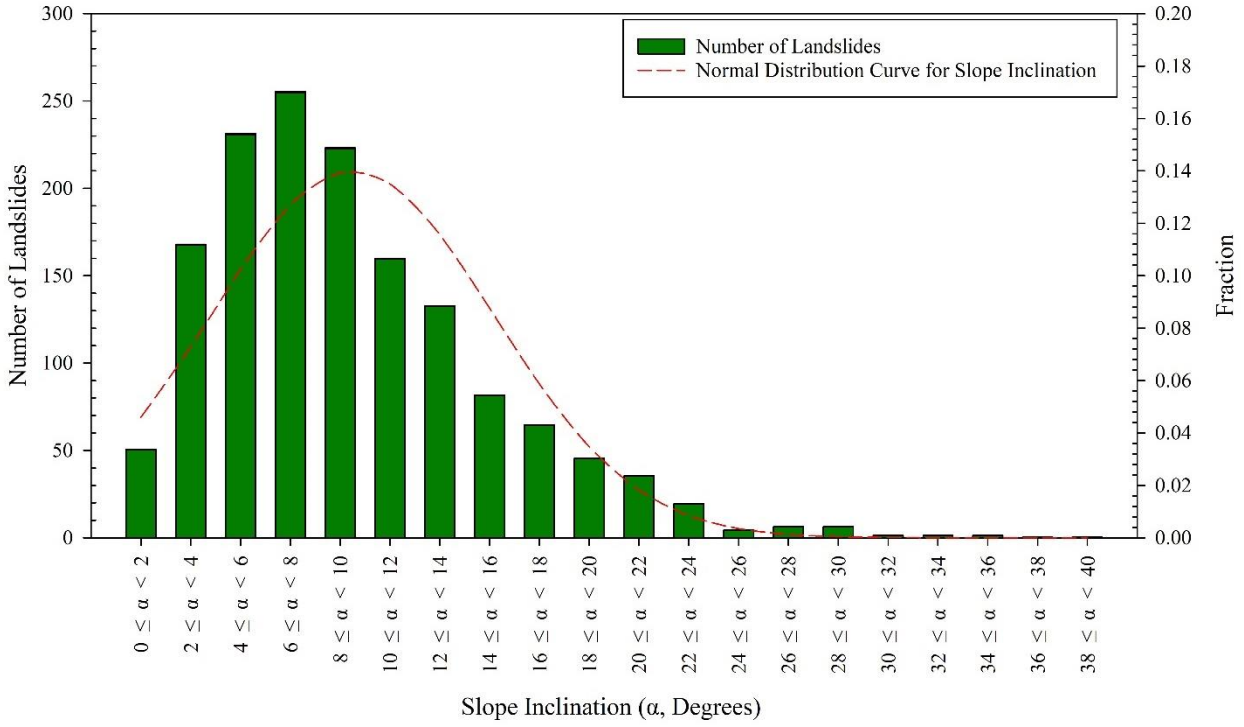

Figure 5.5. Distribution of the Large-Scale Landslides with Slope Inclination.

Large-Scale Landslides and Their Concentration in Counties

A map showing the county borders of ND along with the location of the large-scale landslides is shown in Figure 5.4. The large-scale landslide distribution, with counties arranged from west to east, and landslide concentration is shown in Figure 5.6. Twenty-three of the 53 counties did not have any large-scale landslides. Dunn and McKenzie Counties, with 376 and 369 landslides that accounted for 25.1% and 24.6% of the total landslides of the state, had the highest and second highest number of large-scale landslides, respectively. Finally, Barnes County, with 9.2% of the total large-scale landslides, had the third highest number of large-scale landslides. Figure 5.6 illustrates that four counties, Divide, Dickey, Ransom, and Cass, only had one large-scale landslide.

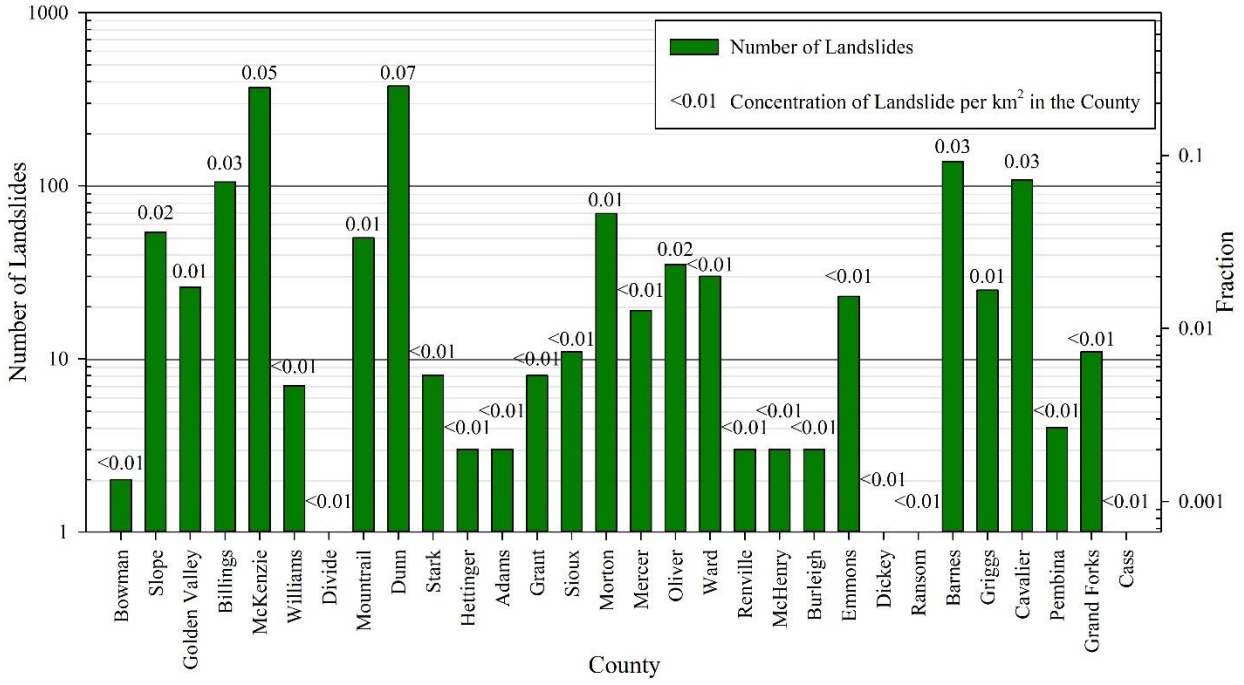

Figure 5.6. Distribution of Large-Scale Landslides in Counties of North Dakota.

The counties with the highest large-scale landslide concentrations were Dunn, McKenzie, and Barnes with 0.07, 0.05, and 0.03 landslides per km^2, respectively. These landslide concentration results were expected because they had a high number of large-scale landslides.

Types of Land Cover at Large-Scale Landslide Locations

Ten different land cover types were noted at the large-scale landslide locations, with herbaceous vegetation, shrubs, and emergent herbaceous wetlands as the top three most common land cover features, as presented by Figure 5.7. Herbaceous vegetation, dominated by graminoid, covered about 70% of the total large-scale landslide areas. About 9% and 8% of the large-scale landslide locations were covered with shrubs and emergent herbaceous wetlands, respectively. These areas included perennial herbaceous vegetation with saturated soil (NLCD 2016). The results indicated that the large-scale landslides mainly occur in areas covered with herbaceous such as big bluestem, switchgrass, prairie dropseed, bluestem, small grasses, herbs, and shrubs with saturated soil.

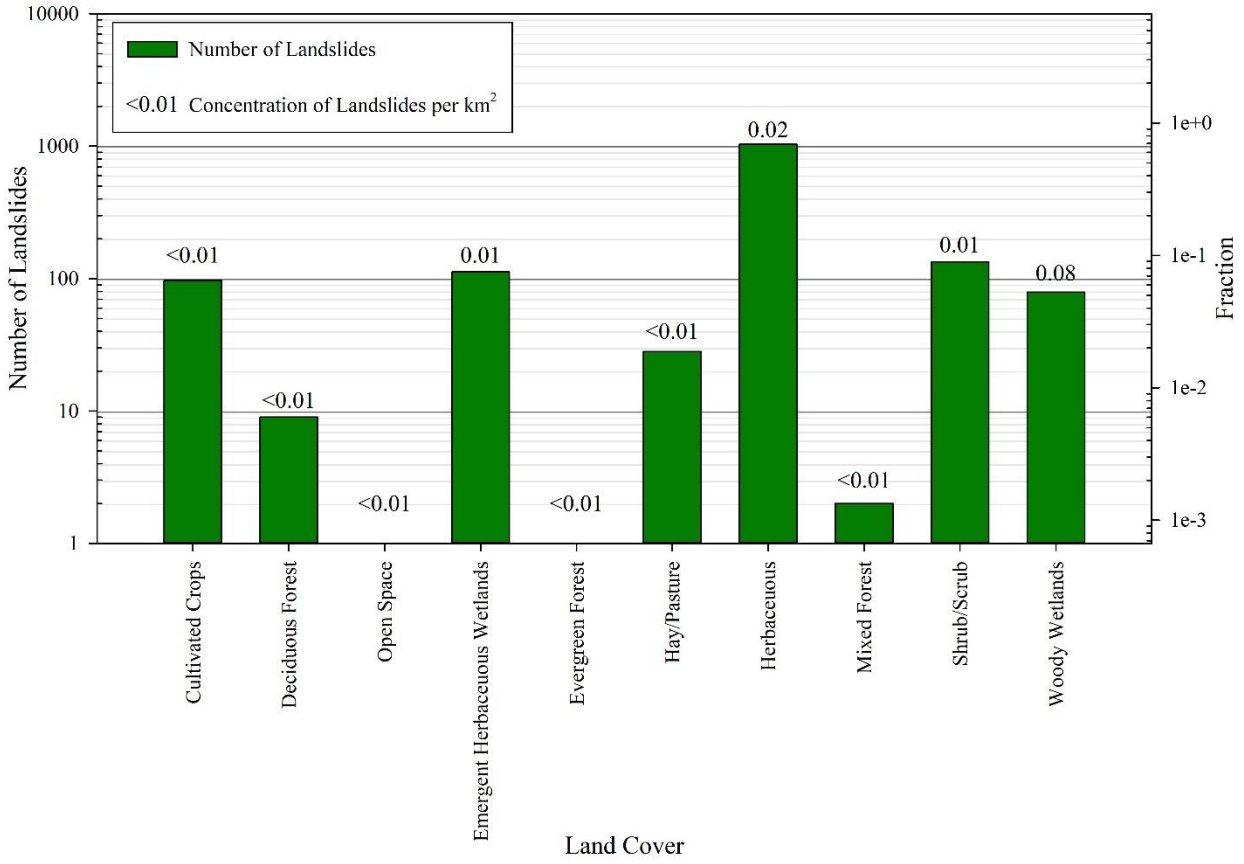

Figure 5.7. Distribution of Large-Scale Landslides based upon the Available Land Cover.

The landslide concentration was highest for woody wetlands with 0.08 landslides per km^2. With 1,034 and 112 large-scale landslides, herbaceous vegetation and emergent herbaceous wetlands had landslide concentrations of 0.02 and 0.01 landslides per km^2, respectively. These two land covers had the second and third highest landslide concentrations, respectively.

Rainfall and Snowfall Distribution for the Large-Scale Landslide Areas

The distribution of rainfall and snowfall for the large-scale landslide locations is shown in Figures 5.8 and 5.9, respectively. Rainfall at the large-scale landslide locations varied from 35 to 61 cm. About 57% of the large-scale landslide had rainfalls between 38 and 43 cm, as shown in Figure 5.8. Zero or no landslides were found in the rainfall bins between 47 and 52 cm of Figure 5.9. This indicates that there are two distinct peaks, which is an indication of bimodal

distribution. The mean and the standard deviation of first distribution for the rainfall data between 35 and 47 cm had mean and SD of 40 and 2 cm, respectively. Similarly, the second distribution between 52 and 61 cm had a mean and SD of 53 and 1 cm, respectively.

Snowfall for the large-scale landslide locations varied between 85 and 170 cm. About 29% and 57% of the total large-scale landslides occurred in the regions with snowfall between 95 and 115 cm and 125 and 145 cm, respectively. The distribution of snowfall for large-scale landslides followed a bimodal distribution with two local maxima. The first distribution for the snowfall (between 85 and 120 cm) had a mean and SD of 103 and 8 cm, respectively. Similarly, the second distribution for the data between 120 and 170 cm had a mean and SD of 134 and 8 cm, respectively.

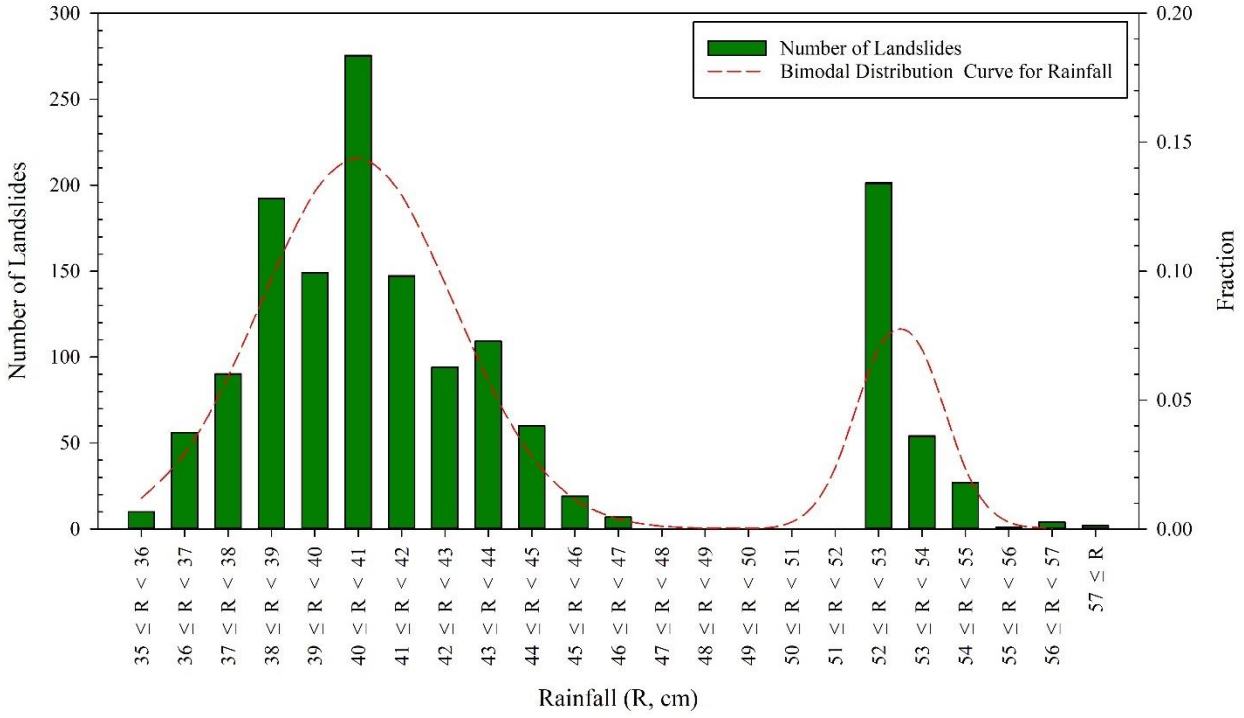

Figure 5.8. Distribution of Large-Scale Landslide based upon Average Rainfall from 2016 to 2019.

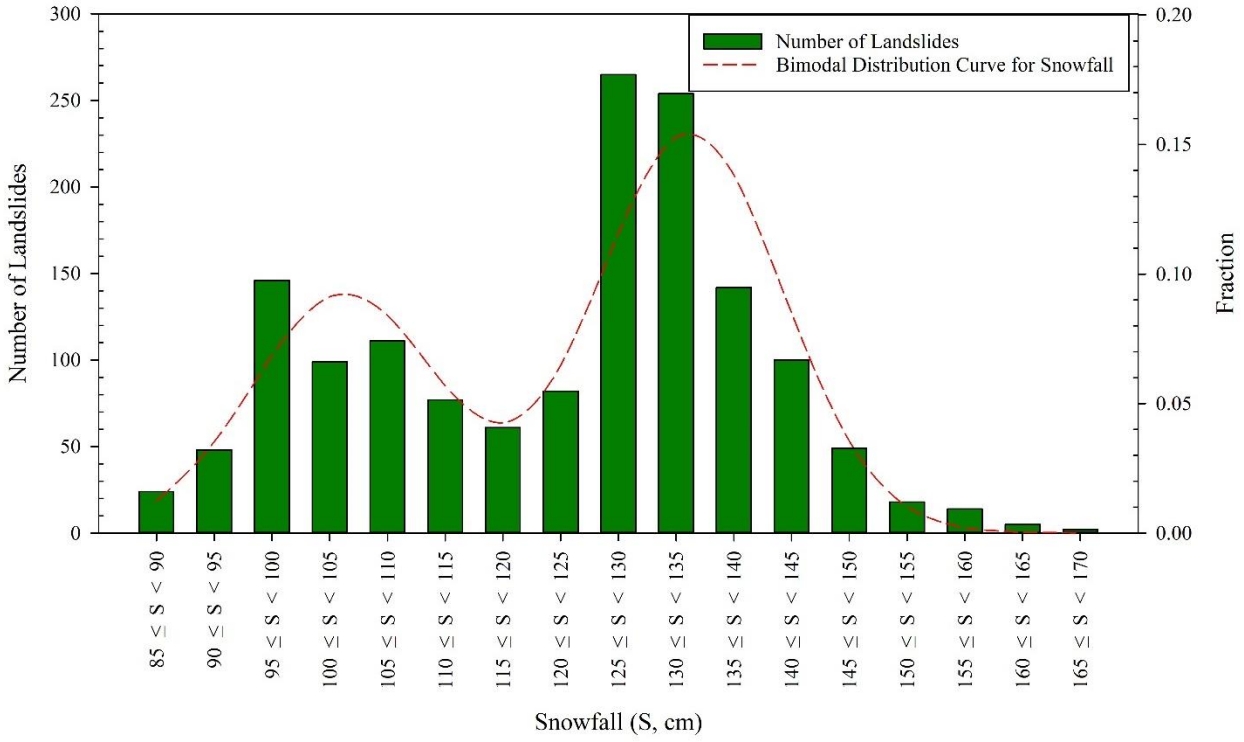

Figure 5.9. Distribution of Large-Scale Landslide based upon Average Snowfall from 2009 to 2019.

Distribution of Large-Scale Landslides Based on the Concentration of Dissolved Salts

The SAR in the large-scale landslide areas ranged from 0 to 16.4 (Figure 5.10). About 42% (628) of the total large-scale landslide areas had SARs ranging from 0 to 1. Approximately 20.4% or 306 large-scale landslide areas had SAR values between 2 and 3. SAR for 114 large-scale landslides was zero and were not considered while fitting the distribution curve. As the data for SAR was calculated from SSURGO database, the value of SAR at the centroid of these 114 large-scale landslides was zero. The plotted histogram seemed to follow a gamma distribution with shape and scale parameters as 1.6 and 1.1, respectively. The mean and SD for SAR were 1.6 and 1.7, respectively.

EC distribution in the large-scale landslide areas is presented in Figure 5.11. About 55% of the total large-scale landslides had ECs between 1 and 2 dS/m. Similarly, 35% of the total large-scale landslides had ECs between 2 and 3 dS/m. ECs for the large-scale landslides

followed a gamma distribution with shape and scale parameters as 4.4 and 0.42, respectively. The mean EC for the large-scale landslides was 1.9 dS/m and the SD was 1.1 dS/m.

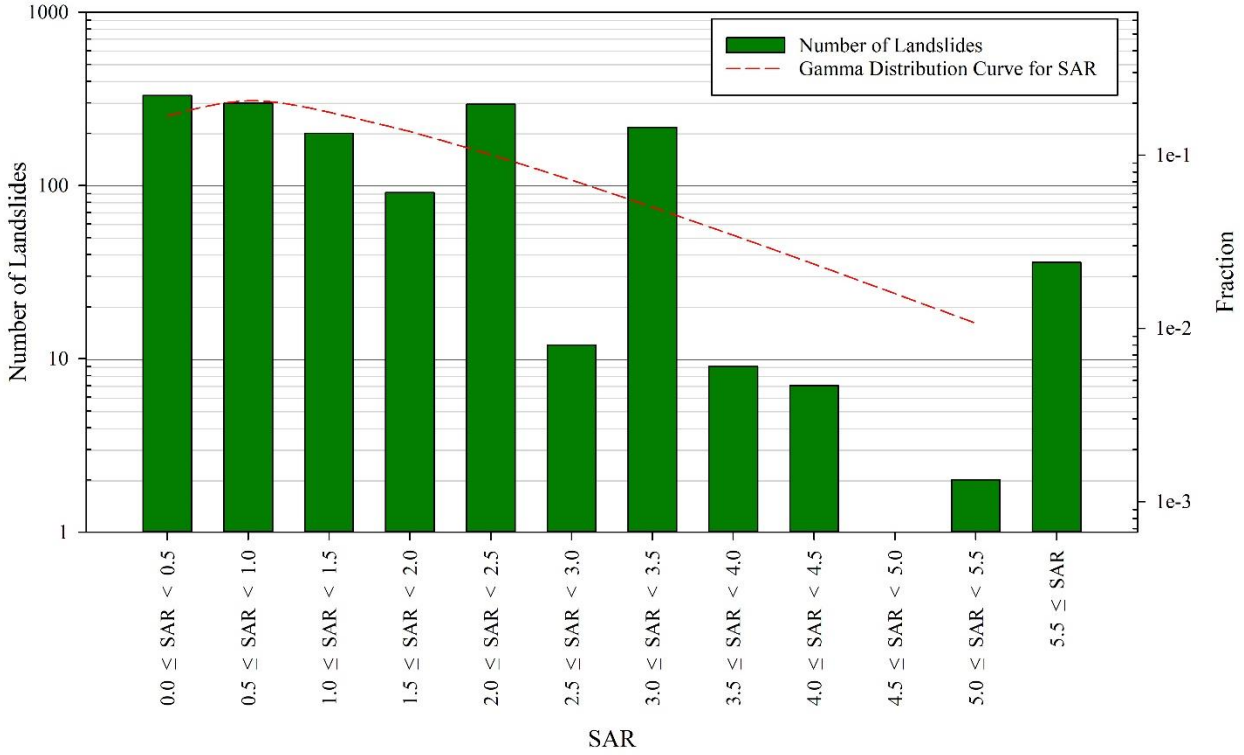

Figure 5.10. Distribution of Large-Scale Landslides based upon the Availability of SAR at the Landslide Locations.

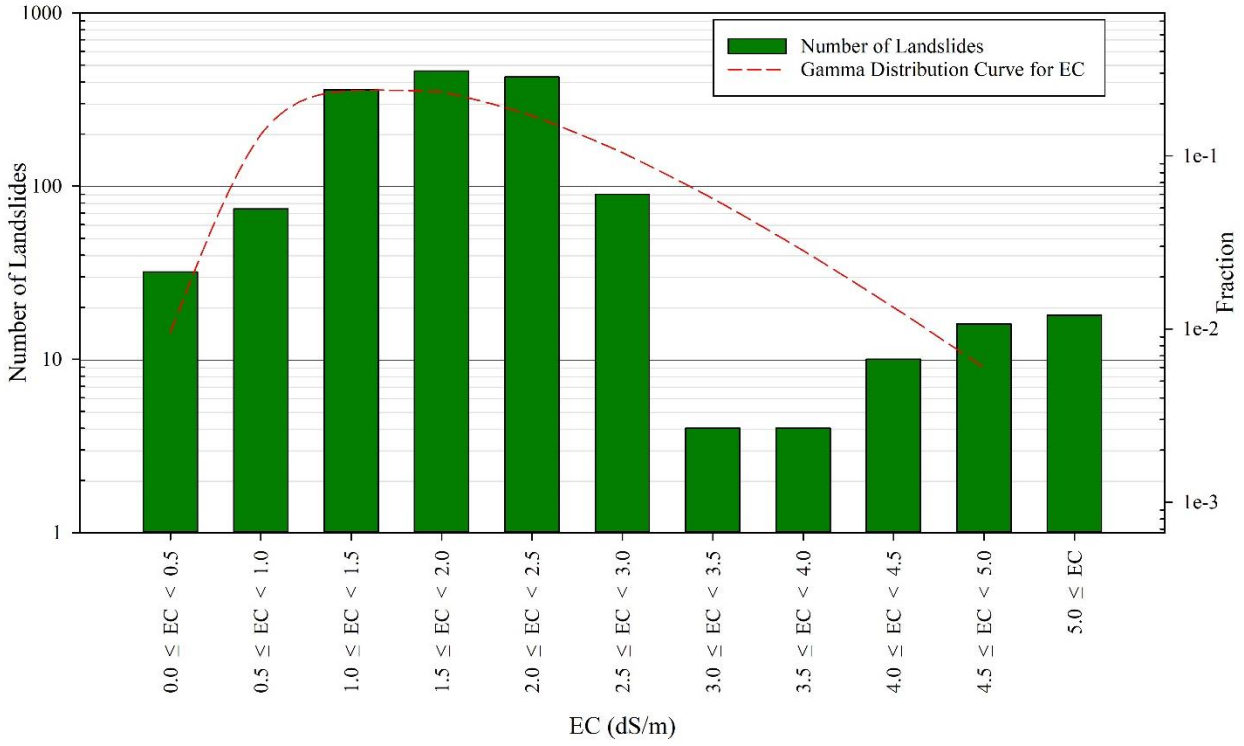

Figure 5.11. Distribution of Large-Scale Landslides based upon the Availability of EC (dS/m) at the Landslide Locations.

The distributions of slope failures with the dissolved salt concentrations is shown in Figure 5.12. More than 80% of the large-scale landslide areas had sodium sulfate concentrations within 400 mg/L, with calcium and magnesium sulfate concentrations between 200 and 600 mg/L. The salt concentration for these large-scale landslide areas followed gamma distributions, as shown in Figure 5.12. The shape parameters for each of the sodium, calcium and magnesium sulfate concentrations were 1.3, 6.5, and 5.4, whereas, the scale parameters were 257.9, 62.7, and 73.9, respectively. The mean calcium sulfate, magnesium sulfate, and sodium sulfate concentrations were 401, 393, and 308 mg/L with SDs of 176, 239, and 437 mg/L, respectively. As shown in the Figure 5.12, the concentration of more than 98% of the large-scale landslides had dissolved salt concentrations ranged between 0 and 1,100 mg/L.

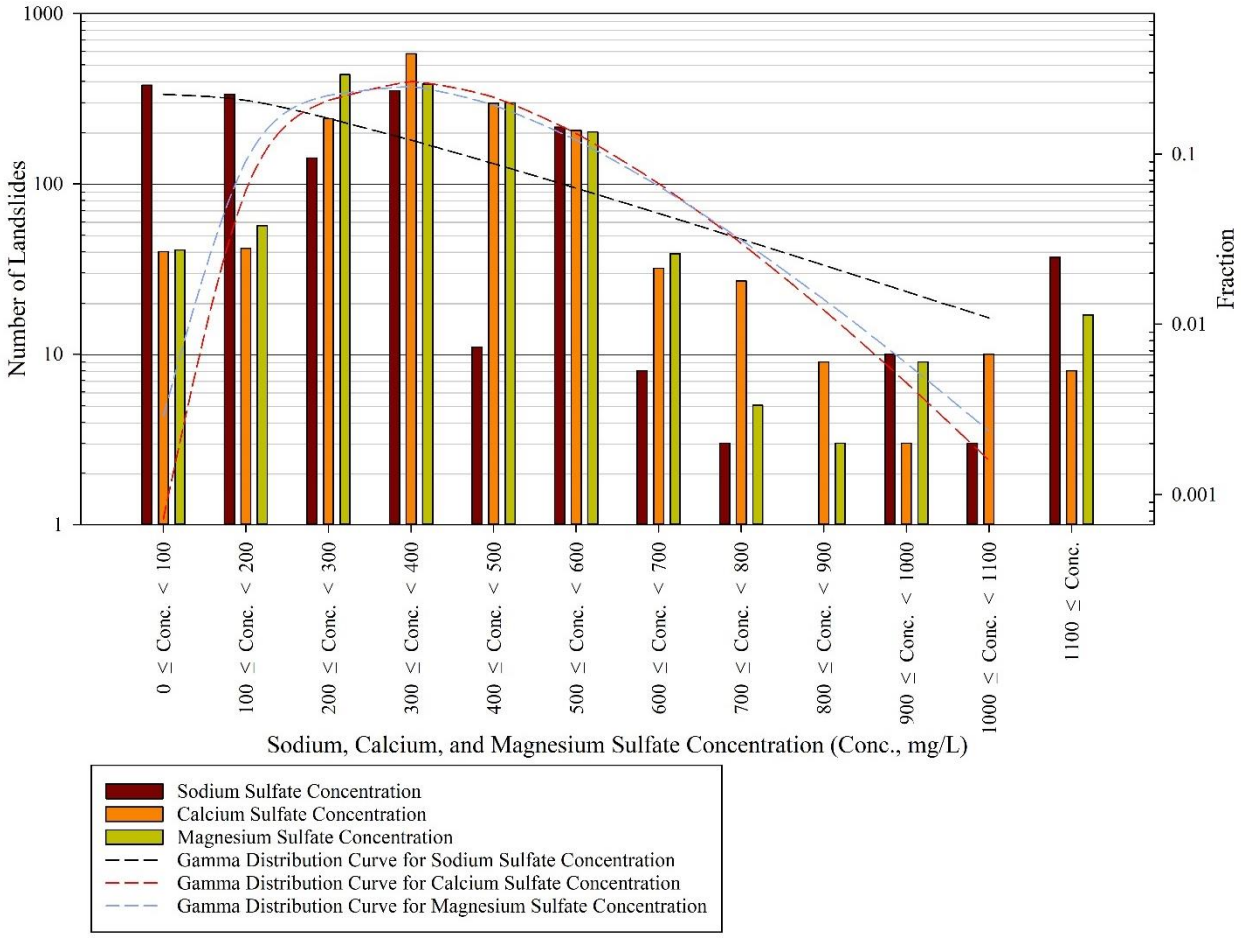

Figure 5.12. Landslide Distribution with the Sodium, Calcium, and Magnesium Sulfate Concentrations.

Discussion for Large-Scale Landslides

Different causative factors, such as geology, slope inclination, salt concentration, land cover, rainfall, and snowfall, were considered in this study. Pearson's correlation matrix was developed for the correlation between each pair of causative factors. For numeric parameters, any correlation coefficient between 0.70 and 1.00 or -0.70 and -1.00 was considered to be a strong positive and negative correlations, respectively (Ratner 2009). Similarly, correlation coefficients between 0.30 and 0.70 or -0.30 and -0.70 was considered as moderate positive and negative correlations, respectively.

The highest correlation coefficient between any of the parameters with at least one representing a non-numeric factor was 0.72. Therefore, 70% of 0.72 which is 0.50, was the threshold for strong positive correlation whereas -0.5 was considered as the threshold for a strong negative correlation (Table 5.2). Similarly, any correlation coefficient between 0.22 and 0.50 or -0.22 and -0.50 was considered to be a moderate positive and negative correlations, respectively. The thresholds for the strong and medium correlation coefficients considered in this study are shown in Table 5.2. The results from the correlation matrix are shown in Table 5.3. Due to limited space, only a partial correlation matrix result is shown in this paper. Strong positive and negative as well as moderate positive and negative correlations from the study are bold in Table 5.3 and are discussed below.

Table 5.2. Thresholds for the Correlation Coefficients

Correlation coefficient	Range
Strong Positive	0.50 to 0.72
Moderate Positive	0.21 to 0.50
Moderate Negative	-0.21 to -0.50
Strong Negative	-0.50 to -0.72

Table 5.3. Partial Correlation Matrix Results for Large-Scale Landslides

Parameters	SAR	Slope Inclination	Latitude	Longitude	Pierre Formation	Sentinel Butte Formation	Average Rainfall
Longitude	**-0.3**	**-0.21**	0.19	1	**0.72**	**-0.64**	**0.98**
Carlile Formation	-0.06	0.06	**0.36**	**0.29**	-	-	**0.29**
Fox Hills Formation	-0.07	-0.07	**-0.23**	0.06	-	-	-0.01
Hell Creek Formation	0.02	-0.01	**-0.23**	0.07	-	-	0.04
Inyan Kara	-0.02	-0.03	0.03	0.06	-	-	0.06
Ludlow Formation	0.01	<0.01	-0.13	-0.08	-	-	-0.11
Niobrara Formation	-0.07	<0.01	**0.39**	**0.32**	-	-	**0.33**
Pierre Formation	**-0.22**	-0.17	-0.09	**0.72**	-	-	**0.71**
Precambrian Rocks	-0.02	-0.02	0.06	0.06	-	-	0.06
Red River Formation	-0.04	-0.06	0.09	0.13	-	-	0.11
Sentinel Butte Formation	**0.31**	0.19	0.1	**-0.64**	-	-	**-0.58**
Slope Formation	-0.02	-0.03	-0.07	-0.02	-	-	-0.03
Upper and Middle Tertiary Rock	-0.02	0.01	-0.08	-0.04	-	-	-0.05
White River Group	-0.07	<0.01	-0.14	-0.09	-	-	-0.09
Winnipeg Group	-0.04	-0.08	0.04	0.18	-	-	0.18
Average Rainfall	**-0.28**	-0.2	**0.26**	**0.98**	**0.71**	**-0.58**	1
Average Snowfall	-0.13	-0.12	-0.09	0.1	0.05	0.03	0.13
Barnes County	-0.04	<0.01	-0.02	-0.01	-0.01	-0.01	-0.01
Billings County	0.01	-0.03	<0.01	-0.04	-0.03	0.04	-0.03
Cavalier County	-0.02	-0.03	-0.02	0.05	0.08	-0.04	0.04
Dunn County	-0.04	<0.01	-0.06	0.06	0.1	-0.06	0.05
McKenzie County	0.02	0.01	<0.01	-0.01	0.01	0.03	-0.01
Cultivated Crops	-0.11	-0.11	0.05	**0.29**	**0.28**	**-0.23**	**0.29**
Emergent Herbaceous Wetlands	-0.09	-0.12	0.08	**0.24**	**0.22**	-0.2	**0.23**
Herbaceous	0.16	0.17	-0.15	**-0.41**	**-0.28**	**0.29**	**-0.42**
Shrub/Scrub	<0.01	0.01	-0.02	-0.17	-0.12	0.14	-0.14
Woody Wetlands	-0.08	-0.05	0.18	**0.33**	0.06	**-0.2**	**0.33**

Note: - represents parameters which do not have direct comparison.

From the geological map presented in Figure 5.2, it can be seen that the Sentinel Butte Formation is in the western part of the state. Strong negative correlation of longitude with the Sentinel Butte Formation and a moderate negative correlation with slope inclination indicate the majority of the landslide areas within this formation also have steep slope inclinations. Sentinel

Butte Formation has a moderate positive correlation with herbaceous vegetation, indicating areas where landslides are encountered in the Sentinel Butte Formation, herbaceous vegetations are also encountered. These herbaceous vegetation include grasslands or graminoids, most of them are mixed-grass prairie and some are short-grass prairie, that have non-woody stems (ND 2021; NLCD 2016). These grass prairies or herbaceous vegetation die at the end of the fall and grow back in summer. Roots effectively improve soil shear strength by increasing the cohesion of soil and increasing the factor of safety (Day 1993; Ghestem et al. 2014; Xiaoming et al. 2006; Zhang et al. 2010). Similarly, woody species with taproots, numerous branches, and fines roots increase the shear resistance and the factor of safety in soil (Ghestem et al. 2014). The absence of a root structure during part of the winter season and the presence of herbaceous vegetation without tap roots in this formation lead to weak shear strengths and slope failures. Site reconnaissance for four large-scale landslides and visual inspection of several other landslides revealed exposed dissolved salts on the failure surfaces, with large amounts of salt being leached by rainfall and accumulating at the toe of the landslides, as shown in Figures 5.13 and 5.14. Results from the correlation matrix and visual inspection from site reconnaissance indicate that leaching of salt concentrations due to rainfall, presence of steep slope and lack of herbaceous vegetation to hold the exposed sand, silts, and clay surfaces might be the main reasons for large-scale landslides within these formations.

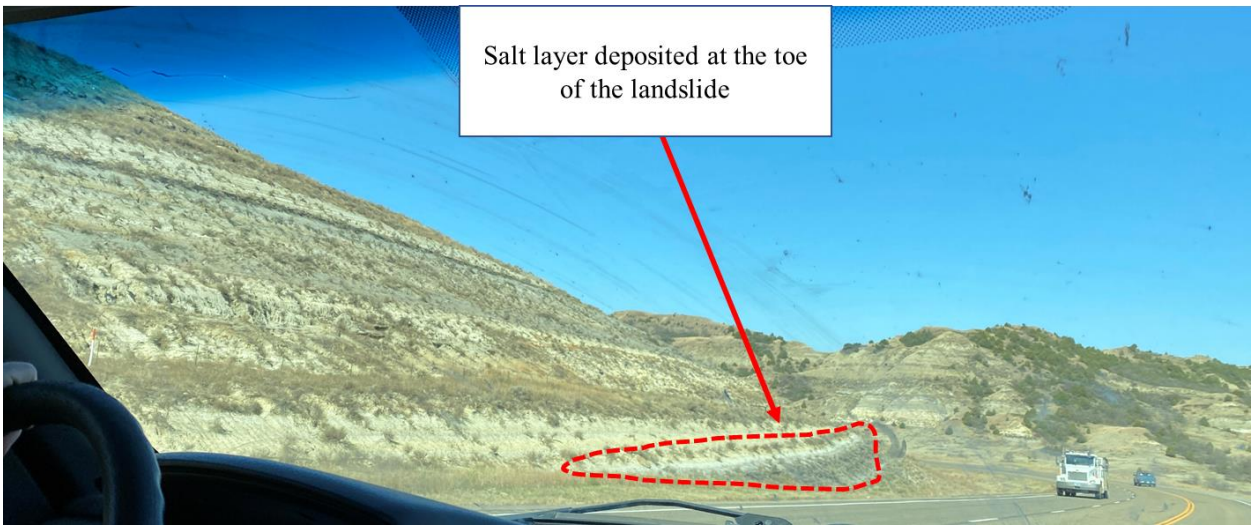

Figure 5.13. Picture Showing Leached Salt at the Toe of the Landslide.
Note: Salt concentrations were much clearer on field observations than in the picture.

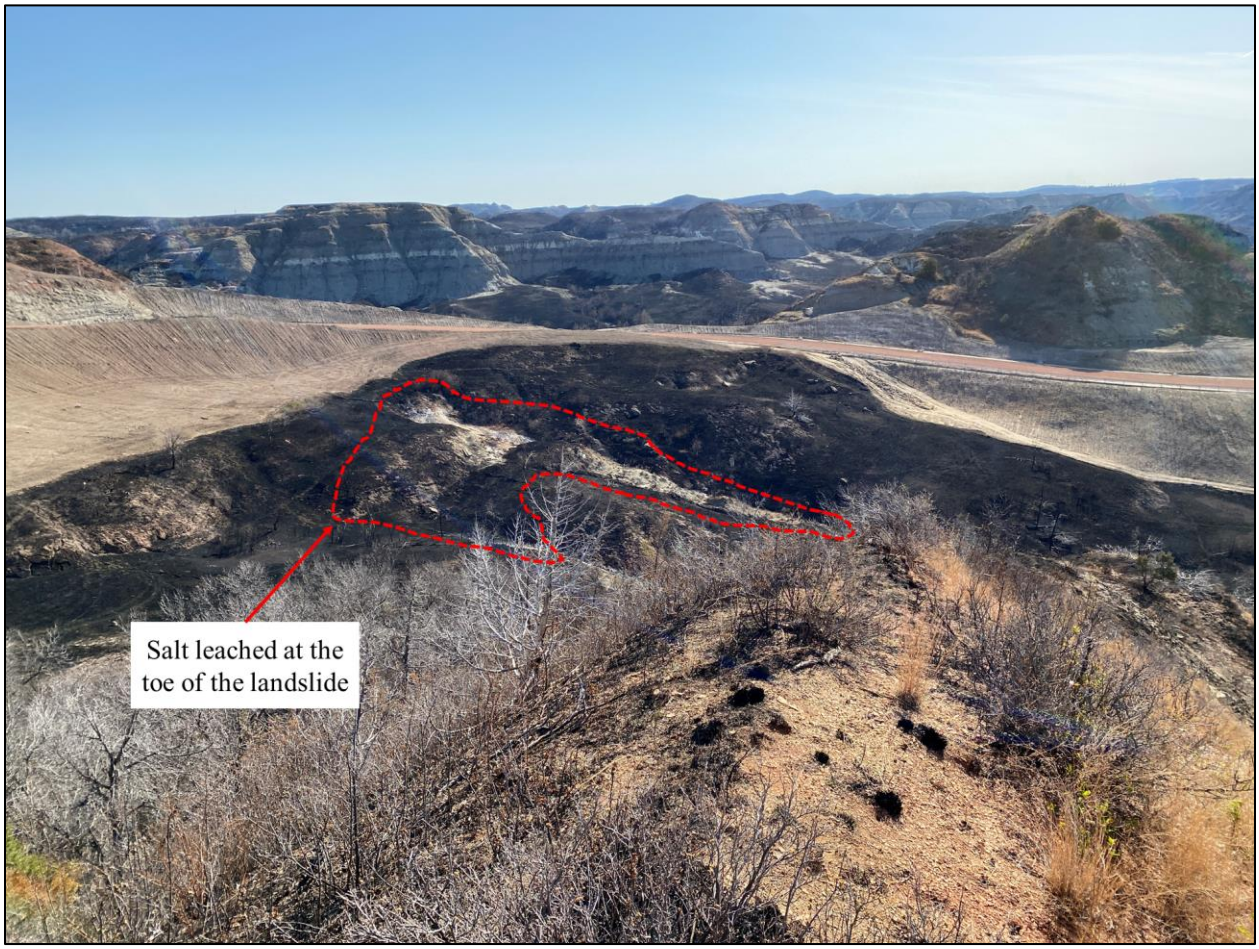

Figure 5.14. Another Example of Leached Salt at Landslide Toe.

The geological map presented in Figure 5.2 shows that the Pierre Formation is primarily found in the eastern part of the state. From the correlation matrix, it can be seen that there was a moderate negative correlation between Pierre Formation and SAR. This correlation indicates that majority of the landslide areas in Pierre Formation also lack dissolved salt concentrations. Similarly, Pierre Formation has a strong positive correlation with rainfall, indicating the majority of landslides in Pierre Formation occur in areas with rainfall. Finally, a moderate positive correlation of Pierre Formation with emergent herbaceous wetlands indicates that area where landslides are encountered in this formation also have saturated soil because this was a common feature of herbaceous vegetation (NLCD 2016). Rainfall with saturated soil deposits makes the slope heavy with a potential loss of cohesion and an increase in the pore water pressure in the soil, which decreases the factor of safety (Kawagoe et al. 2009; Matsuura et al. 2017; Tiwari and Upadhyaya 2014). With a decrease in the salt concentration, the thickness of diffused double layer increases resulting in weak intermolecular bonding between clay particles and a decrease the factor of safety of soil (Mitchell 1993; Tiwari and Ajmera 2015; Tiwari et al. 2005; Yong et al. 1992). These three indicate that the eastern part of the state receives rainfall and has saturated soil with an absence of dissolved salt concentrations in the majority of the landslide areas. Thus, these three factors are responsible for large-scale landslides in this formation.

Two counties, namely Dunn and McKenzie Counties, were found to have the highest and second highest number of large-scale landslides, respectively. These two counties lie in the western part of the state in the Sentinel Butte Formation. Hence, the reason for encountering higher landslides as compared to other counties was expected, with reasons being similar to that of landslides occurrence in the Sentinel Butte Formation.

Large-scale landslides were predominant in three of the land covers, namely, herbaceous vegetation, shrub, and emergent herbaceous wetland. The reason for most of large-scale landslides in herbaceous vegetation and shrub (which include small trees in their early growth period) might be due to their root structures and life spans, as explained above. Emergent herbaceous wetlands include lands that are partially covered with water so, the reason for failure is similar to the one for Pierre Formation. Finally, it appears that most of these large-scale landslides, about 75%, seem to occur with low dissolved salt concentrations and reason might be due to the increase in the diffused double layer that decreases the intermolecular bonding among clay particles with low salt concentrations (Tiwari and Ajmera 2015).

A low dissolved salt concentration, the presence of abundant herbaceous vegetation, the presence of wetlands, and the presence of rainfall at the large-scale landslide areas were causative factors for large-scale landslides, but the common landslides between each of those causative factors were lacking. For instance, about 80% of the landslide locations had a dissolved salt concentration within 600 mg/L, more than half of the large-scale landslide areas had a slope inclination between 6° and 14°, about 57% had rainfall and snowfall ranging from 38 to 43 cm, and from 125 to 145 cm, respectively. Determining the common landslides that had causative factors within those ranges would give a conclusion stating that landslides in North Dakota can occur when factors, such as the one considered in this study, are within a particular range. Thus, this conclusion can be achieved when analyzing the causative factors with machine learning algorithms, which will be the future work for this study.

Comparison of All Landslides with Large-Scale Landslides

After analyzing all the landslides and only the large-scale landslides within the state, a comparison based upon different components and causative factors was made, as presented in

Table 5.4. The highest, second highest, and third highest landslides were observed in Sentinel Butte, Bullion Creek, and Pierre Formations, respectively, for all the landslides. For large-scale landslides, the highest was observed in Sentinel Butte Formation. Presence of steep slope inclination and absence of dissolved salt concentration for majority of the landslides was the potential cause. The positions of geological formations were interchanged for the second and the third highest large-scale landslides.

For all landslides, the top three counties, namely McKenzie, Billings, and Morton had highest, second highest, and third highest number of landslides, respectively, with the first two being located in Sentinel Butte Formation. For large-scale landslides, the top two counties with the most number of landslides, Dunn and McKenzie Counties were both located in the Sentinel Butte Formation. Barnes County had the third highest number of large-scale landslides because it lies primarily in Pierre Formation. Landslides in this formation were due to the presence of rainfall, wetlands, and low dissolved salt concentrations, as explained above. As all of the correlation coefficients between counties and any of the other causative factors were smaller than moderate positive as well negative correlations, the reason why McKenzie County had the highest number of all landslides and the second highest number of large-scale landslides was hard to determine.

Table 5.4. Comparison Based Upon Different Factors Associated with Landslides

Causative Factor	Descriptor	All Landslides	Only Large-Scale Landslides
Geological Formation	Highest Number of Failures	Sentinel Butte Formation	Sentinel Butte Formation
	Second Highest Number of Failures	Bullion Creek Formation	Pierre Formation
	Third Highest Number of Failures	Pierre Formation	Bullion Creek Formation
County	Highest Number of Failures	McKenzie County	Dunn County
	Second Highest Number of Failures	Billings County	McKenzie County
	Third Highest Number of Failures	Morton County	Barnes County
Land Cover	Highest Number of Failures	Herbaceous Vegetation	Herbaceous Vegetation
	Second Highest Number of Failures	Shrubs and Scrub	Shrubs
	Third Highest Number of Failures	Deciduous Forest	Emergent Herbaceous Wetlands
Slope Inclination	6º to 14º	51%	52%
Rainfall	37 to 42 cm	51%	57%
Snowfall	125 to 145 cm	36%	51%
SAR	0 to 1	48%	42%
EC	1 to 2 dS/m	52%	55%
Na_2SO_4	0 to 400 mg/L	80%	81%
$CaSO_4$	200 to 500 mg/L	68%	75%
$MgSO_4$	200 to 500 mg/L	73%	75%

Note: Percentages in the represents the percentage of the landslides considered in the column.

Herbaceous vegetation and shrubs had highest and second highest number of landslides, respectively. Similarly, in both sets of landslides almost half had slope inclinations between 6º and 14º. Finally, low dissolved salt concentrations within similar ranges (Table 5.4) had similar percentage of the landslides observed for both datasets.

Conclusions

A total of 1,497 large-scale landslides were observed in North Dakota. A detailed analysis of the large-scale landslides and their causative factors yielded the following conclusions:

- The Sentinel Butte Formation with 844 landslides had the highest number of large-scale landslides. With 197 landslides, the Pierre Formation had the second highest number of large-scale landslides. These two formations accounted for about 70% of the total large-scale landslides in the state. Steep slope inclination, presence of herbaceous vegetation with root structures only present for part of the year or the absence of tap roots, presence of rainfall with wetlands, and absence of dissolved salt concentrations in a pore fluid for majority of large-scale landslides were some of the causative factors of the large-scale landslides observed within these formations. Dunn and McKenzie Counties had 376 and 369 large-scale landslides, respectively. These two counties accounted for 49.7% of the total large-scale landslides. As both counties are in the Sentinel Butte Formation, the reasons for the failures were the same as the landslides in those geological formations.
- More than half of the large-scale landslide areas in the state had slope inclinations between 6º and 14º.
- More than 80% of the total large-scale landslide locations had sodium sulfate concentrations between 0 and 400 mg/L. Approximately 75% of the total large-scale landslide sites had calcium sulfate and magnesium sulfate concentrations between 200 and 500 mg/L. These low concentrations might be due to leaching of the dissolved salt concentrations.

References

ACS (2006). "Reagent Chemicals: Specifications and Procedures." *American Chemical Society*.

AGI (2021). "How Much do Landslides Cost the US in Terms of Monetary Losses?" *American Geosciences Institute*, <https://www.americangeosciences.org/critical-issues/faq/how-much-do-landslides-cost-terms-monetary-losses#:~:text=Losses%20from%20landslides%20in%20the,and%20%244%20billion%20per%20year>.

AgriMetSoft (2019). "Gamma Distribution Fitting." *Agricultural and Meteorological Software*, <https://agrimetsoft.com/distributions-calculator/Gamma-Distribution-Fitting#toolSection>.

Anderson, F. J., and Maike, C. A. (2017). "Drones Rising from the Prairie: Geological Applications of Unmanned Aerial Systems." *GeoNews*, 44(2), 8-14.

Bluemle, J., and Biek, B. (2007). "No Ordinary Plain-North Dakota's Physiography and Landforms." *North Dakota Geological Survey*.

Collins, T. (2020). "Landslides: Experts Seek Ways to Mitigate Losses, Danger Said Growing Due to Climate Change." *EurekAlert!*, <https://www.eurekalert.org/pub_releases/2006-01/unu-les011106.php>.

Corwin, D. L., and Yemoto, K. (2017). "Salinity: Electrical Conductivity and Total Dissolved Solids." *Soil Science Society of America*, 84(5), 1442-1461.

Day, R. W. (1993). "Surficial Slope Failure: A Case Study." *Journal of Performance of Constructed Facilities*, 7(4), 264-269.

EMDAT (2020). "The International Disaster Database." *Centre for Research on the Epidemiology of Disasters*, <https://www.emdat.be>.

Ghestem, M., Veylon, G., Bernard, A., Vanel, Q., and Stokes, A. (2014). "Influence of Plant Root System Morphology and Architectural Traits on Soil Shear Resistance." *Plant and Soil*, 377(1), 43-61.

Kawagoe, S., Kazama, S., and Sarukkalige, P. R. (2009). "Assessment of Snowmelt Triggered Landslide Hazard and Risk in Japan." *Cold Regions Science and Technology*, 58(3), 120-129.

Matsuura, S., Okamoto, T., Asano, S., Osawa, H., and Shibasaki, T. (2017). "Influences of the Snow Cover on Landslide Displacement in Winter Period: A Case Study in a Heavy Snowfall Area of Japan." *Environmental Earth Sciences*, 76(10), p10.

Mitchell, J. K. (1993). *Fundamentals of Soil Behavior., 2nd Edn.*, John Wiley & Sons, Inc., Wiley, New York.

Moxness, A. D. (2019). "Twenty Thousand Slides and Counting: Recent Advances in Digital Imagery Expedite Landslides Mapping in North Dakota." *GeoNews*, 17-19.

ND (2020). "Climate." *Game and Fish*, <https://gf.nd.gov/wildlife/habitats/climate#:~:text=Annual%20precipitation%20ranges%20from%2013,to%204%20inches%20of%20rain.>.

ND (2021). "North Dakota Plants and Habitats Overview." *North Dakota Game and Fish Department*, <https://gf.nd.gov/wildlife/habitats/vegetation>.

NDGS (2020). "North Dakota Geological Survey: 1:24,000 & 1:100,000 Scale Maps and Data." *North Dakota Geological Survey*, <https://www.dmr.nd.gov/ndgs/SurfaceMap/SurfaceMap.asp?source=landslide24k>.

NLCD (2016). "National Land Cover Database 2016." *Multi-Resolution Land Characteristics Consortium*, <https://www.mrlc.gov/data/legends/national-land-cover-database-2016-

nlcd2016-legend#:~:text=Grassland%2FHerbaceous%2D%20areas%20dominated%20by,can%20be%20utilized%20for%20grazing.>.

NOAA (2017). "Climate of North Dakota." *National Oceanic and Atmospheric Administration*, <https://web.archive.org/web/20070926010149/http://www5.ncdc.noaa.gov/climatenormals/clim60/states/Clim_ND_01.pdf>.

NOAA (2020). "National Weather Service: National Snowfall Analysis." *National Oceanic and Atmospheric Administration*, <https://www.nohrsc.noaa.gov/snowfall_v2/index.html?season=2009-2010&date=2011060912&version=3&format=.tif>.

Ratner, B. (2009). "The Correlation Coefficient: Its Values Range Between+ 1/− 1, or Do They?" *Journal of Targeting, Measurement and Analysis for Marketing*, 17(2), 139-142.

Tiwari, B., and Ajmera, B. (2015). "Reduction in Fully Softened Shear Strength of Natural Clays with NaCl Leaching and its Effect on Slope Stability." *Journal of Geotechnical and Geoenvironmental Engineering*, 141(1), 04014086.

Tiwari, B., Tuladhar, G. R., and Marui, H. (2005). "Variation in Residual Shear Strength of the Soil with the Salinity of Pore Fluid." *Journal of Geotechnical and Geoenvironmental Engineering*, 131(12), 1445-1456.

Tiwari, B., and Upadhyaya, S. (2014). "Influence of Antecedent Rainfall on Stability of Slopes." *Geo-Congress 2014: Geo-Characterization and Modeling for Sustainability*, 3243-3251.

USDA (2013). "National Soil Survey Handbook." *Title 430-VI*.

USDA (2020). "Web Soil Survey." *Natural Resources Conservation Service*, <https://websoilsurvey.nrcs.usda.gov/>.

USGS (2016). "NLCD Land Cover (CONUS)." *MRLC*, <https://www.mrlc.gov/data?f%5B0%5D=category%3ALand%20Cover>.

USGS (2019). "USGS National Elevation Dataset (NED)." *ND State Water Commission*, <https://catalog.data.gov/dataset/usgs-national-elevation-dataset-ned>.

USGS (2020). "North Dakota Geologic Map Data." *United States Geological Survey*, <https://mrdata.usgs.gov/geology/state/state.php?state=ND>.

Xiaoming, Z., Yujie, W., Yiping, X., Yun, W., and Lin, C. (2006). "Shear Strengths of Undisturbed and Remolded Soils of Typical Vegetations in Jinyun Mountain of Chongqing City." *Transactions of the Chinese Society of Agricultural Engineering*, 22(11), 6-9.

Yong, R. N., Mohamed, A.-M. O., and Warkentin, B. P. (1992). *Principles of Contaminant Transport in Soils*, Elsevier Science Publishers, Amsterdam, Netherlands.

Zhang, C.-B., Chen, L.-H., Liu, Y.-P., Ji, X.-D., and Liu, X.-P. (2010). "Triaxial Compression Test of Soil–Root Composites to Evaluate Influence of Roots on Soil Shear Strength." *Ecological Engineering*, 36(1), 19-26.

CHAPTER 6: RESULTS FROM LABORATORY TESTING AND FIELDWORK

Results from the Laboratory Testing

The results for the LL and PL tests for montmorillonite and kaolinite mixed with quartz are shown in Table 6.1. The plasticity chart for montmorillonite and kaolinite, when mixed with quartz, is shown in Figures 6.1 and 6.2, respectively. Figures for LL and PL for each of those clay mixtures are presented in Appendix H. Calculation tables for PL are also presented in that appendix. For mixtures containing montmorillonite, LL and PI was always greater when the sodium sulfate solution was the pore fluid than when distilled water was the pore fluid, as shown in Table 6.1 and Figure 6.1.

When the percentage of kaolinite was greater than quartz in the mixture, the LL and PI was greater when distilled water was a pore fluid than when the sodium sulfate solution was the pore fluid. With an increase in the percentage of quartz in the mixture until the percentage of quartz was equal to or greater than the percentage of kaolinite, the LL and PI of the mixture when sodium sulfate solution was the pore fluid was greater than when distilled water was the pore fluid (Table 6.1 and Figure 6.2). The possible potential reasons for this behavior of both kaolinite and montmorillonite are explained in subsequent paragraphs.

Table 6.1. LL and PI of Mixtures of Different Proportions of Clay Minerals with Sodium Sulfate Solution and Distilled Water as the Pore Fluids

SN	M	K	Q	LL with distilled water	LL with sodium sulfate solution	PI with distilled water	PI with sodium sulfate solution
1	100	0	0	463	659	409	602
2	70	0	30	324	423	259	389
3	50	0	50	232	288	172	261
4	30	0	70	139	177	95	153
5	10	0	90	46	61	29	37
6	0	100	0	69	48	24	18
7	0	70	30	49	45	17	16
8	0	50	50	35	40	12	15
9	0	30	70	21	37	7	13
10	0	10	90	7	27	2	4

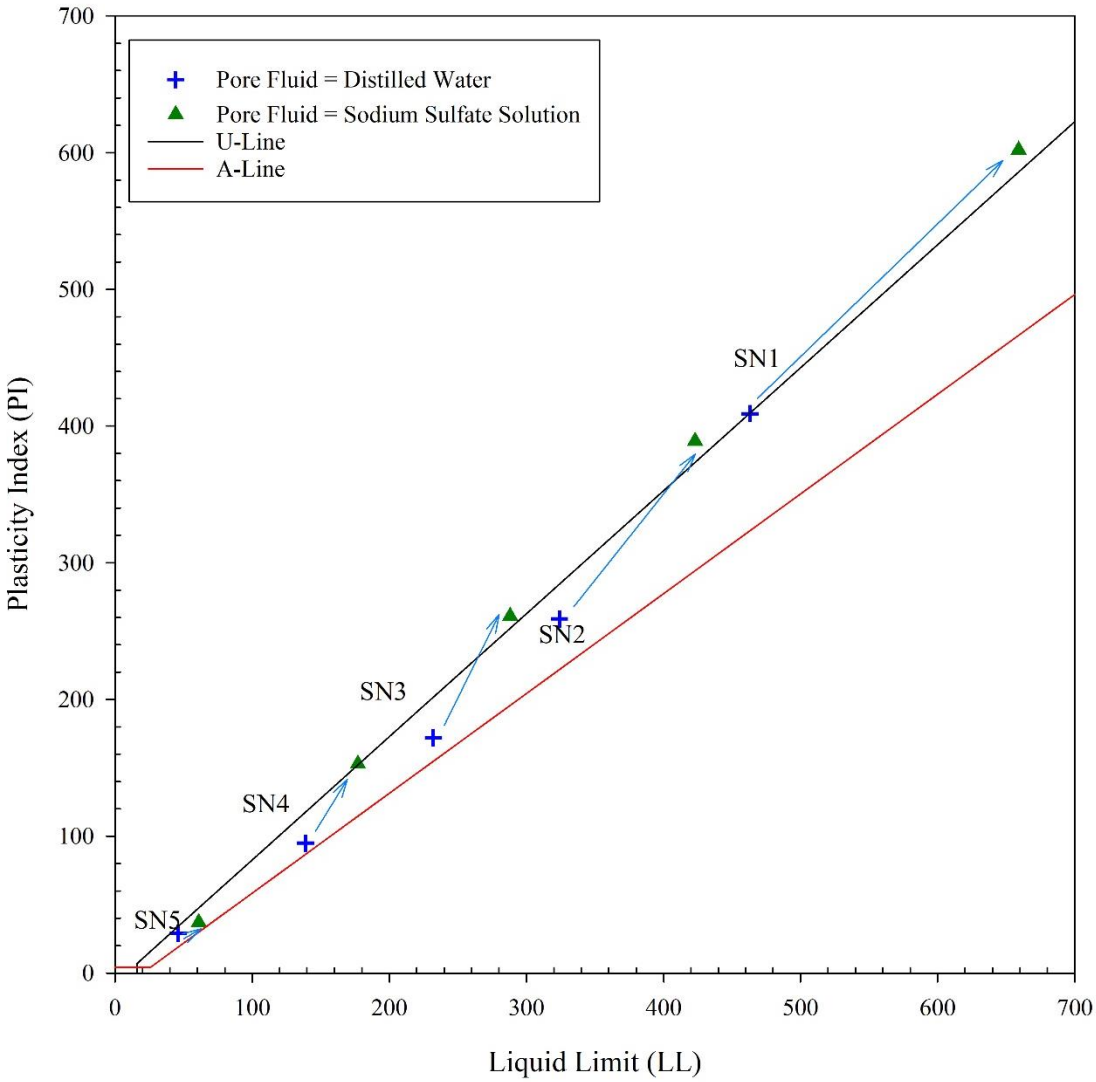

Figure 6.1. Plasticity Chart for the Montmorillonite-Quartz Mixtures Tested in this Study.

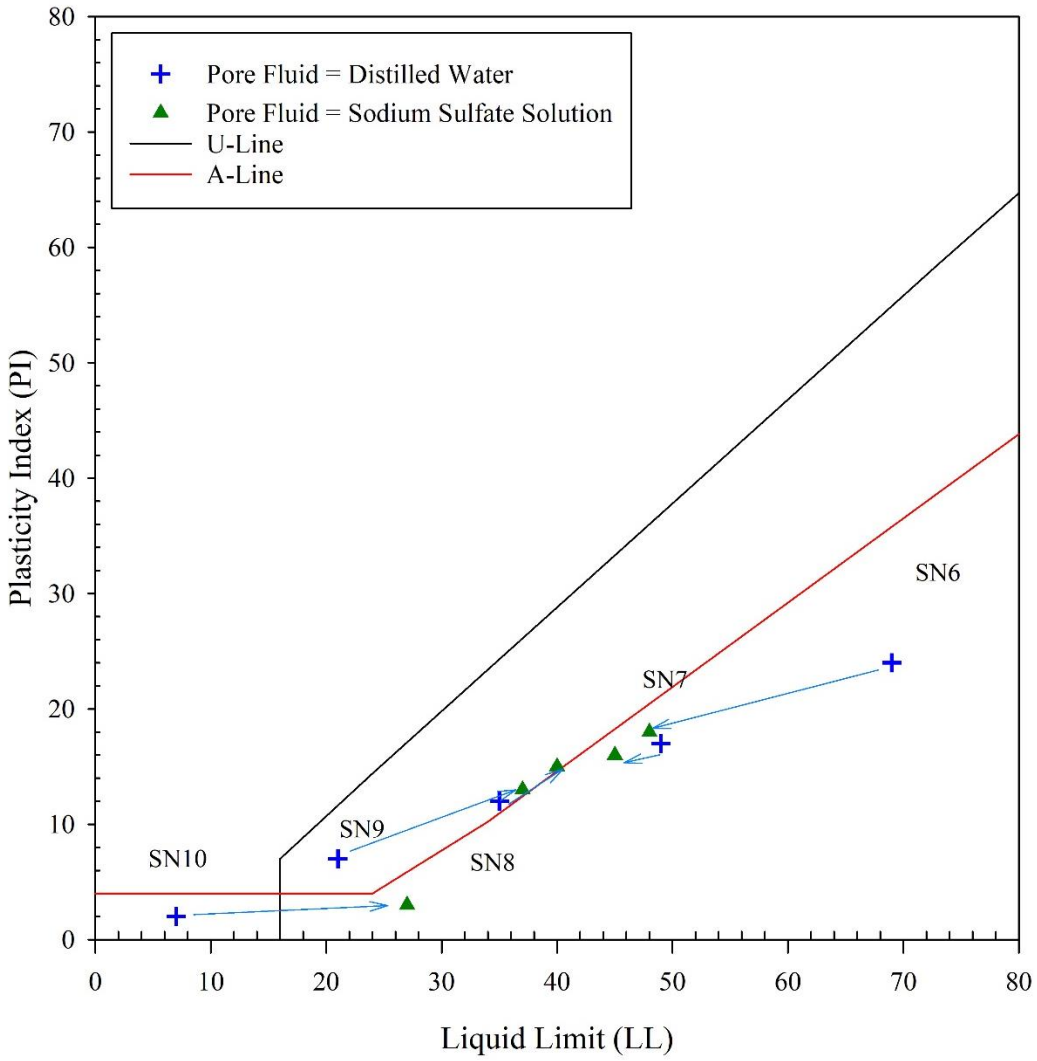

Figure 6.2. Plasticity Chart for the Kaolinite-Quartz Mixtures Tested in this Study.

The variation in the LL and PI with the percentage of kaolinite in the mixtures, as indicated in Table 6.1, is shown in Figures 6.3 and 6.4, respectively. The red squares and green triangles represent the LL with distilled water and sodium sulfate solution as a pore fluid, respectively. Figures 6.5 and 6.6 depicts the variation of the LL and PI with the percentage of montmorillonite for the mixtures of montmorillonite with quartz.

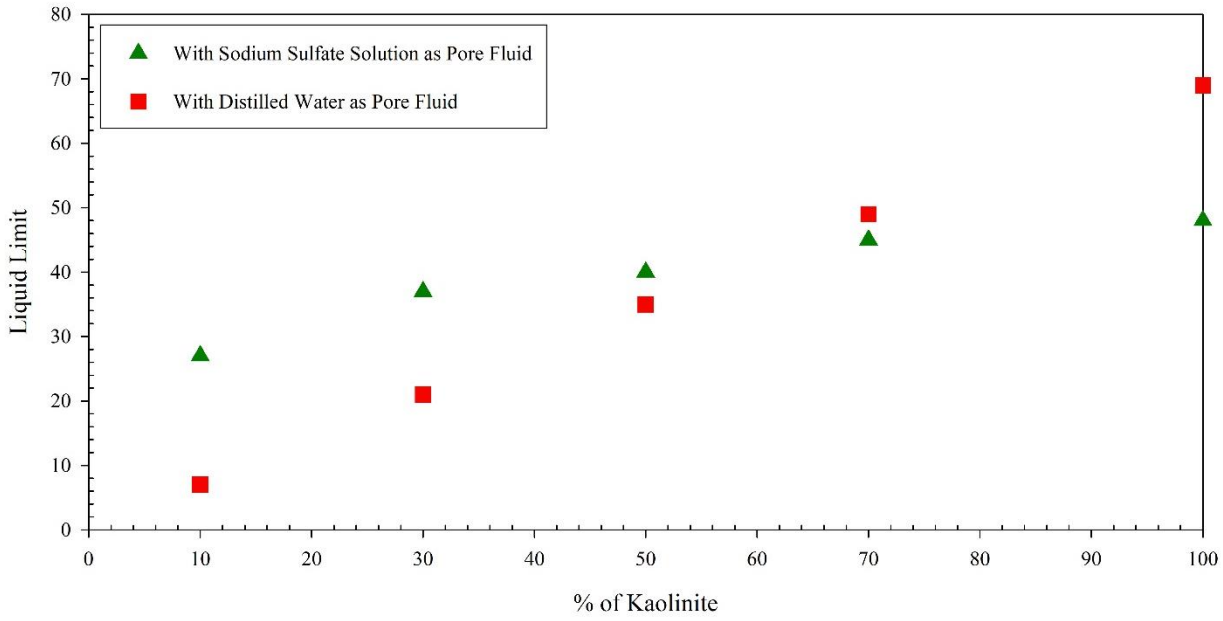

Figure 6.3. Liquid Limit of Kaolinite Mixed with Quartz in Different Ratios with Sodium Sulfate Solution and Distilled Water as the Pore Fluids.

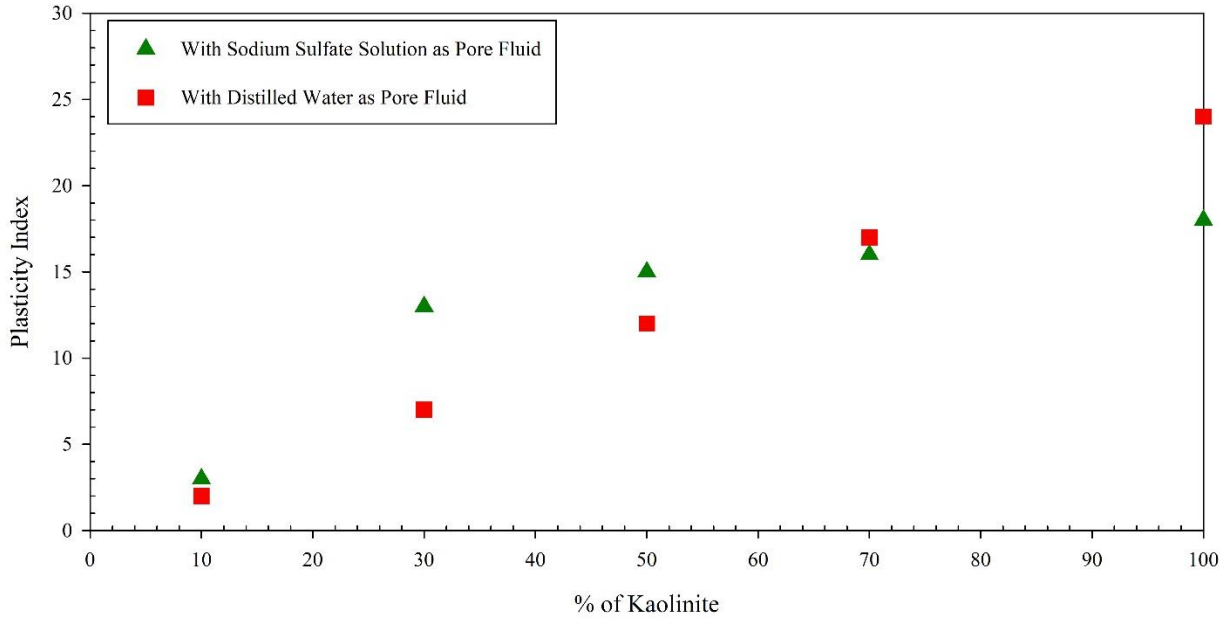

Figure 6.4. Plasticity Index of Kaolinite Mixed with Quartz in Different Ratios with Sodium Sulfate Solution and Distilled Water as the Pore Fluids.

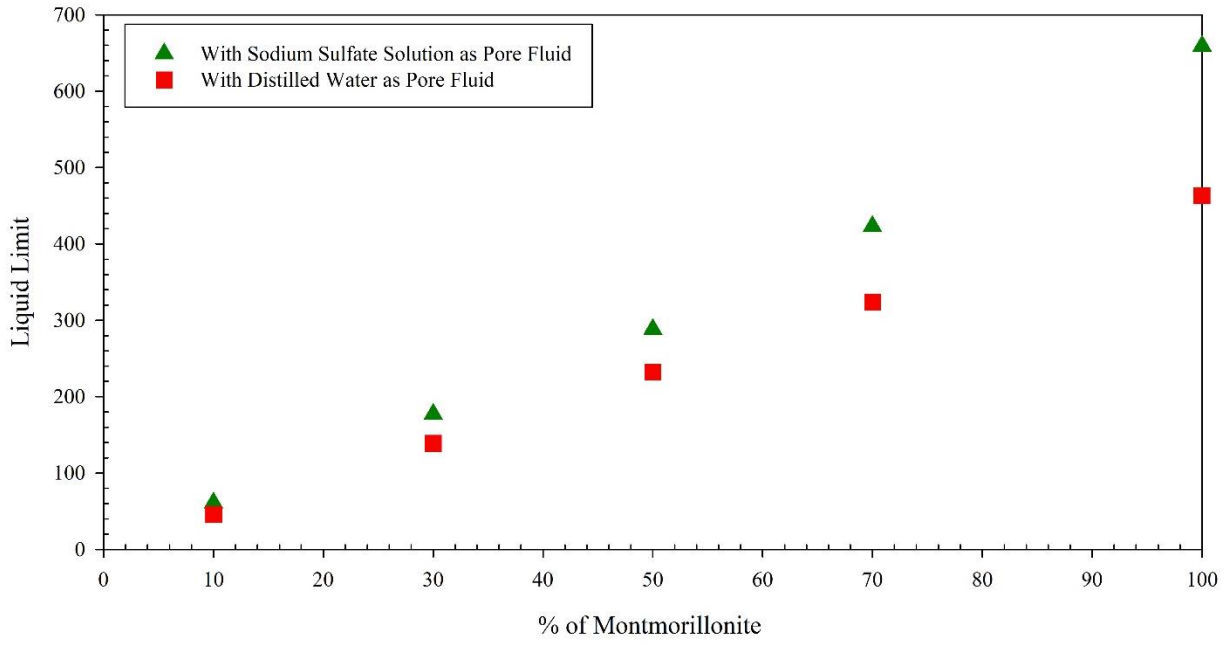

Figure 6.5. Liquid Limit of Montmorillonite Mixed with Quartz in Different Ratios with Sodium Sulfate Solution and Distilled Water as the Pore Fluids.

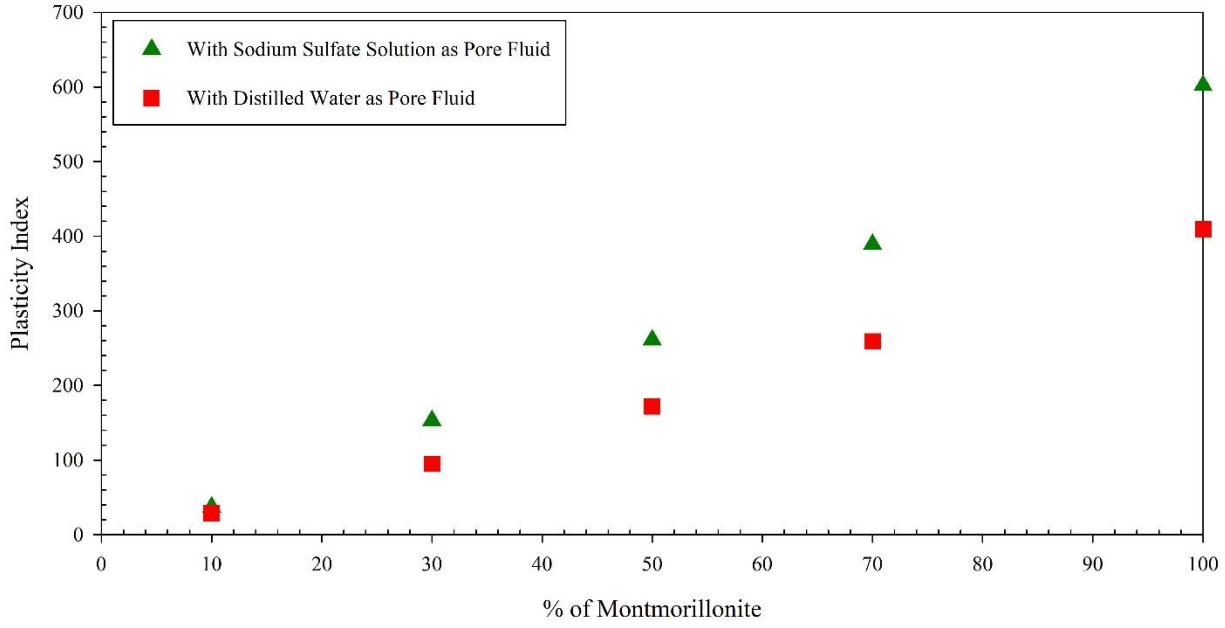

Figure 6.6. Plasticity Index of Montmorillonite Mixed with Quartz in Different Ratios with Sodium Sulfate Solution and Distilled Water as the Pore Fluids.

In the mixtures of kaolinite with quartz, until the percentages of kaolinite and quartz were equal, the LL of the mixture when sodium sulfate solution was the pore fluid was greater than

when distilled water was the pore fluid. After the percentage of kaolinite in the mixture was greater than the percentage of quartz, the LL with distilled water as the pore fluid was greater than when sodium sulfate solution was the pore fluid. Similarly, as shown in Figure 6.4, PI shows the same behavior. This increase in LL and PI for the mixtures of kaolinite and quartz until the ratio was equal was similar to Ajmera et al. (2018) when the pore fluid was saline water of 0.5 M sodium chloride concentration. They found that when the plasticity index of the clay mixtures were less than 100, the LL was lower when sodium sulfate was the pore fluid than when distilled water was the pore fluid.

Similarly, for the mixtures of montmorillonite and quartz, the LL and PI of the mixture when sodium sulfate solution was a pore fluid was higher than when distilled water was the pore fluid (Figures 6.5 and 6.6). These results were opposite as those presented by Tiwari and Ajmera (2015) for samples whose pore fluid was saline water prepared as a 0.5 M sodium chloride solution. In this study, LL and PL were higher for the mixtures of montmorillonite and kaolinite when sodium sulfate solution was the pore fluid than when distilled water was the pore fluid. These results might be due to the presence of sodium sulfate in the pore fluid rather than sodium chloride.

Results from Fieldwork

The results for inclinometers ST-06 and ST-07 from the fieldwork, are presented in Figures 6.7 and 6.8, respectively. The horizontal axis in the figures represents the cumulative displacements, in mm, over a period of seven months. Similarly, the vertical axis represents the depth, in m, below the ground level. During the instrumentation setup, an inclinometer should be assigned a direction to record the movement of slope failure. The first reading is also known as baseline reading. The direction to which the probe of the inclinometer faces is known as A-A

direction and is generally faced in the direction of the primary slope movement. Similarly, B-B is the direction perpendicular to A-A. The results from the inclinometers indicated that slope movement was observed in both directions, A-A and B-B. During the period of observation, ST-06 had movement of 7 mm, which is very small, while ST-07 had movement of 70 mm at a depth of about 5 m below the ground surface.

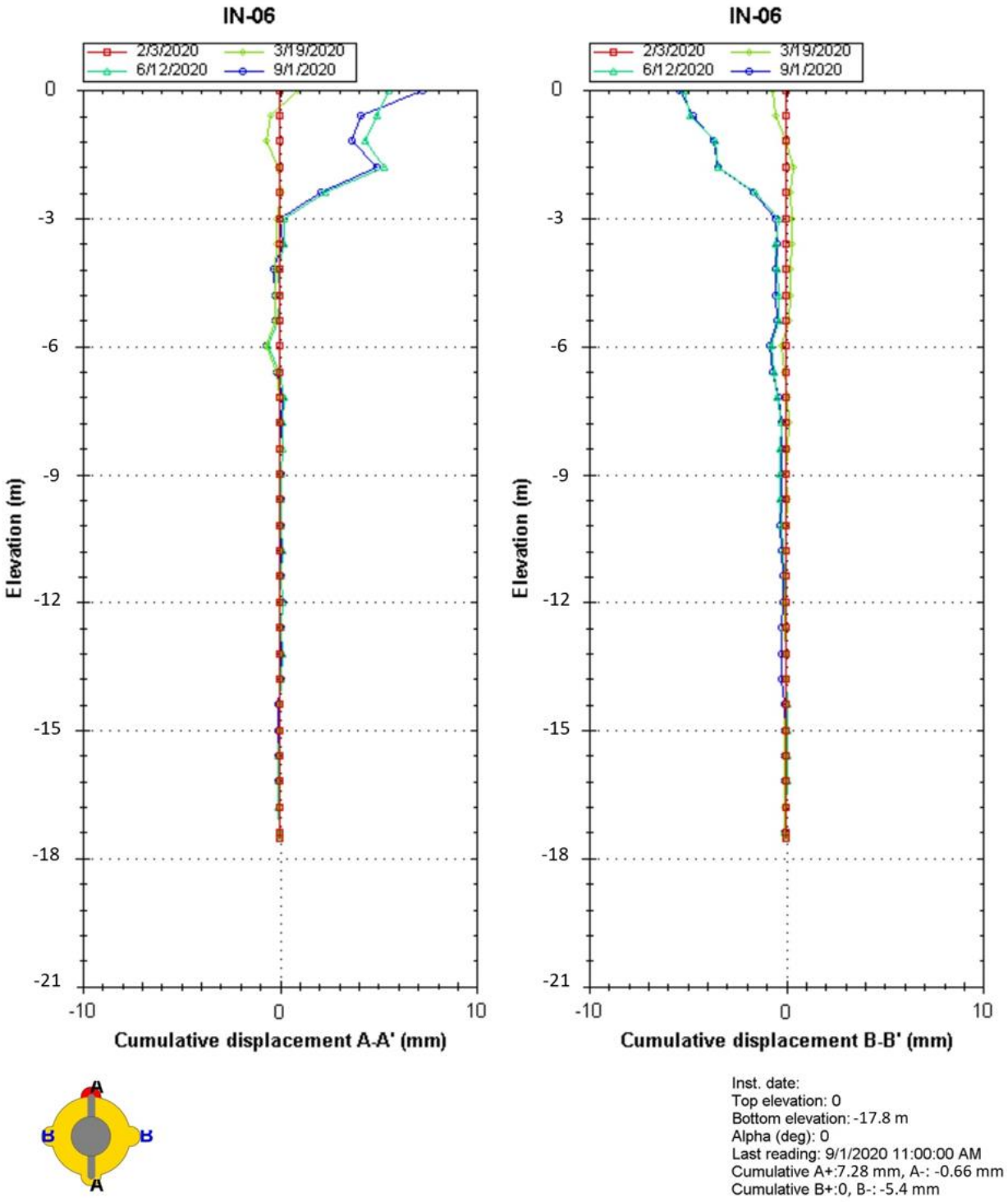

Figure 6.7. Cumulative Displacement Observed for Inclinometer 6.

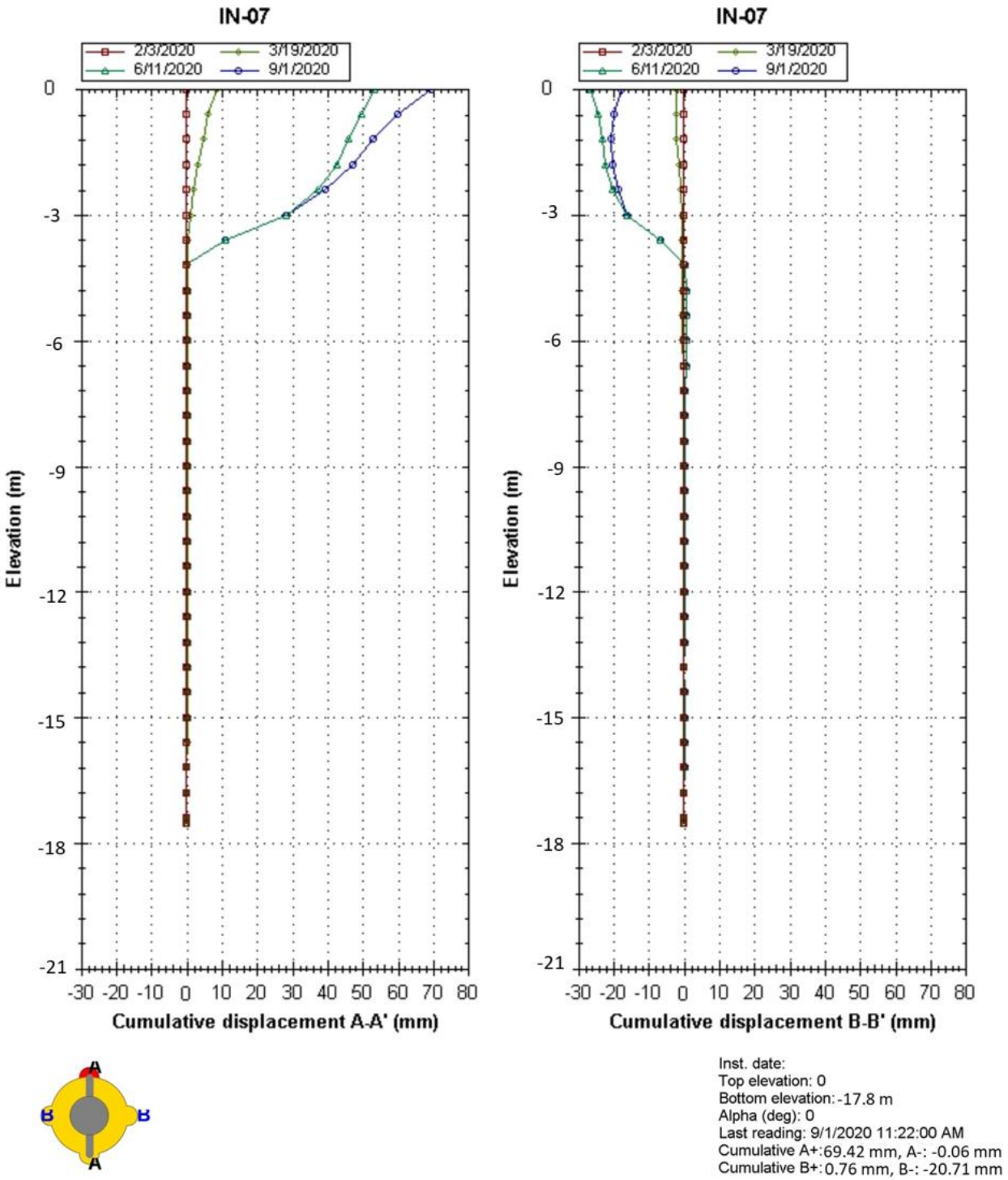

Figure 6.8. Cumulative Displacement Observed for Inclinometer 7.

CHAPTER 7: CONCLUSIONS

North Dakota had 24,098 landslides with areas greater than 100 m^2. Among these landslides, 1,497 had areas greater than 100,000 m^2 and were termed large-scale landslides. Separate analyses for all the landslides and the large-scale landslides, along with the causative factors, yielded the following results:

- The Sentinel Butte and Bullion Creek Formations, with 12,252 and 5,829 landslides, accounted for 50.8% and 24.2% of the total landslides, respectively. These formations had the highest and second highest number of landslides. Landslides in Sentinel Butte Formation were due to steep slope inclinations and the absence of dissolved salt concentrations for the majority of landslides. Landslides in Bullion Creek Formation were due to presence of rainfall which might fluctuate the groundwater table resulting in a decrease in the cohesion and an increase in the pore water pressure.
- The Sentinel Butte and Pierre Formations, with 844 and 197 large-scale landslides, respectively, accounted for 69.6% of the large-scale landslides. Steep slope inclination with the presence of herbaceous vegetation and leaching of dissolved salt concentrations were some of the main potential reasons for the large-scale landslides within Sentinel Butte Formations. Presence of rainfall and wetlands with saturated soils were the potential reason for landslides in the Pierre Formation.
- With 5,139 landslides, McKenzie County had the highest number of landslides. Among these landslides, 369 were large-scale landslides. Billings County, with 3,402 landslides, had the second highest number of landslides. These two counties, accounted for 21.3% and 7.7%, respectively, of the total landslides throughout the

state. As these two counties are underlain by the Sentinel Butte and Bullion Creek Formations, these slope failures were expected.

- More than half of the landslides occurred in topographies with slope inclinations between 6º and 14º.
- About 80% of the total landslide areas had sodium sulfate concentrations between 0 and 400 mg/L. Approximately 67% and 72% of the total landslides had calcium sulfate and magnesium sulfate concentrations between 200 and 500 mg/L. The low dissolved salt concentrations were due to the leaching of salts from the exposed surface.
- For montmorillonite-quartz mixtures, LL and PI were greater when sodium sulfate solution was the pore fluid than when distilled water was the pore fluid.
- When the percentage of quartz was equal or greater than the percentage of montmorillonite in the mixture, the LL and PI was greater when sodium sulfate was the pore fluid. When the percentage of kaolinite was greater than the percentage of quartz in the mixture, the LL and PI were higher when distilled water was the pore fluid than when sodium sulfate solution was the pore fluid.
- Results from fieldwork showed that about 70 mm of movement was observed at a depth of about 5 m from the ground surface at the slope failure monitored.

REFERENCES

Abrol, I. P., Yadav, J. S. P., and Massoud, F. I. (1988). *Salt-Affected Soils and Their Management*, Food & Agriculture Org.

ACIS (2020). "NOAA: Regional Climate Centers." *Applied Climate Information System*, <http://scacis.rcc-acis.org/>.

ACS (2006). "Reagent Chemicals: Specifications and Procedures." *American Chemical Society*.

AGI (2021). "How Much do Landslides Cost the US in Terms of Monetary Losses?" *American Geosciences Institute*, <https://www.americangeosciences.org/critical-issues/faq/how-much-do-landslides-cost-terms-monetary-losses#:~:text=Losses%20from%20landslides%20in%20the,and%20%244%20billion%20per%20year>.

AgriMetSoft (2019). "Gamma Distribution Fitting." *Agricultural and Meteorological Software*, <https://agrimetsoft.com/distributions-calculator/Gamma-Distribution-Fitting#toolSection>.

Ajmera, B., Tiwari, B., and Ostrova, F. (2018). "Influence of Salinity of Pore Fluid on the Undrained Shear Strength of Clays." *IFCEE 2018*, 94-102.

Anderson, F. J., and Maike, C. A. (2017). "Drones Rising from the Prairie: Geological Applications of Unmanned Aerial Systems." *GeoNews*, 44(2), 8-14.

Andrews, D. A. (1939). "Geology and Coal Resources of the Minot Region North Dakota." *United States Government Printing Office*, <https://pubs.usgs.gov/bul/0906b/report.pdf>.

ASTM D4318 (2010). "Standard Test Methods for Liquid Limit, Plastic Limit, and Plasticity Index of Soils." *ASTM International*.

Bluemle, J., and Biek, B. (2007). "No Ordinary Plain-North Dakota's Physiography and Landforms." *North Dakota Geological Survey*.

Booth, A. M., Roering, J. J., and Perron, J. T. (2009). "Automated Landslide Mapping Using Spectral Analysis and High-Resolution Topographic Data: Puget Sound Lowlands, Washington, and Portland Hills, Oregon." *Geomorphology*, 109(3-4), 132-147.

Brouwer, C., Goffeau, A., and Heibloem, M. (1985). "Irrigation Water Management: Training Manual No. 1-Introduction to Irrigation." *Food and Agriculture Organization of the United Nations, Rome, Italy*, 102-103.

Burette, S. (2012). "Mapping of Landslides and Correlations With Morphological Factors Based on Remote Sensing, Field Observations and Measurements in the Central Tien Shan (Kyrgyzstan)." *Master's Thesis in Geological Sciences), University of Liege, Belgium (112pp.)*.

City-Data (2020). "North Dakota Location, Size and Extent." *North Dakota*, <http://www.city-data.com/states/North-Dakota-Location-size-and-extent.html>.

Clayton, L. (1980a). *Geologic Map of North Dakota*, US Geological Survey.

Clayton, L. (1980b). *Explanatory Text to Accompany the Geologic Map of North Dakota*, North Dakota Geological Survey, Grand Forks.

Collins, T. (2020). "Landslides: Experts Seek Ways to Mitigate Losses, Danger Said Growing Due to Climate Change." *EurekAlert!*, <https://www.eurekalert.org/pub_releases/2006-01/unu-les011106.php>.

Corwin, D. L., and Yemoto, K. (2017). "Salinity: Electrical Conductivity and Total Dissolved Solids." *Soil Science Society of America*, 84(5), 1442-1461.

Cvancara, A. M. (1976). *Geology of the Cannonball Formation (Paleocene) in the Williston Basin, with Reference to Uranium Potential. Report of Investigation No. 57*, North Dakota University, Grand Forks.

Damm, B., and Klose, M. (2015). "The Landslide Database for Germany: Closing the Gap at National Level." *Geomorphology*, 249, 82-93.

Day, R. W. (1993). "Surficial Slope Failure: A Case Study." *Journal of Performance of Constructed Facilities*, 7(4), 264-269.

Dhakal, A. S., and Sidle, R. C. (2004). "Distributed Simulations of Landslides for Different Rainfall Conditions." *Hydrological Processes*, 18(4), 757-776.

EMDAT (2020). "The International Disaster Database." *Centre for Research on the Epidemiology of Disasters*, <https://www.emdat.be>.

Fleming, R. W., and Taylor, F. A. (1980). *Estimating the Costs of Landslide Damage in the United States*, US Department of the Interior, Geological Survey.

Foster, C., Pennington, C. V. L., Culshaw, M. G., and Lawrie, K. (2012). "The National Landslide Database of Great Britain: Development, Evolution and Applications." *Environmental Earth Sciences*, 66(3), 941-953.

Gangwar, P., Singh, R., Trivedi, M., and Tiwari, R. K. (2020). "Sodic Soil: Management and Reclamation Strategies." *Environmental Concerns and Sustainable Development*, Springer, 175-190.

Ghestem, M., Veylon, G., Bernard, A., Vanel, Q., and Stokes, A. (2014). "Influence of Plant Root System Morphology and Architectural Traits on Soil Shear Resistance." *Plant and Soil*, 377(1), 43-61.

Gill, J. R., and Cobban, W. A. (1965). *Stratigraphy of the Pierre Shale, Valley City and Pembina Mountain Areas, North Dakota*, US Government Printing Office, Washington.

Guzzetti, F., Mondini, A. C., Cardinali, M., Fiorucci, F., Santangelo, M., and Chang, K.-T. (2012). "Landslide inventory maps: New tools for an old problem." *Earth-Science Reviews*, 112(1-2), 42-66.

Guzzetti, F., Peruccacci, S., Rossi, M., and Stark, C. P. (2008). "The Rainfall Intensity–Duration Control of Shallow Landslides and Debris Flows: An Update." *Landslides*, 5(1), 3-17.

Harp, E. L., and Crone, A. J. (2006). *Landslides Triggered by the October 8, 2005, Pakistan Earthquake and Associated Landslide-Dammed Reservoirs*, US Geological Survey, Reston, Virginia.

Havenith, H.-B., Strom, A., Torgoev, I., Torgoev, A., Lamair, L., Ischuk, A., and Abdrakhmatov, K. (2015a). "Tien Shan Geohazards Database: Earthquakes and Landslides." *Geomorphology*, 249, 16-31.

Havenith, H.-B., Torgoev, A., Schlögel, R., Braun, A., Torgoev, I., and Ischuk, A. (2015b). "Tien Shan Geohazards Database: Landslide Susceptibility Analysis." *Geomorphology*, 249, 32-43.

Highland, L., and Bobrowsky, P. T. (2008). *The Landslide Handbook: A Guide to Understanding Landslides*, US Geological Survey, Reston, Virginia.

Jacob, A. F. (1976). *Geology of the Upper Part of the Fort Union Group (Paleocene), Williston Basin, with Reference to Uranium*, North Dakota Geological Survey, Grand Forks.

Jiang, Q., Gao, G.-H., Yu, Y.-X., and Qin, Y. (2000). "Solubility of Sodium Dimethyl Isophthalate-5-Sulfonate in Water and in Water+ Methanol Containing Sodium Sulfate." *Journal of Chemical & Engineering Data*, 45(2), 292-294.

Kawagoe, S., Kazama, S., and Sarukkalige, P. R. (2009). "Assessment of Snowmelt Triggered Landslide Hazard and Risk in Japan." *Cold Regions Science and Technology*, 58(3), 120-129.

Keefer, D. K. (1984). "Landslides Caused by Earthquakes." *Geological Society of America Bulletin*, 95(4), 406-421.

Khazai, B., and Sitar, N. (2004). "Evaluation of Factors Controlling Earthquake-Induced Landslides Caused by Chi-Chi Earthquake and Comparison with the Northridge and Loma Prieta Events." *Engineering Geology*, 71(1-2), 79-95.

Kirschbaum, D., Stanley, T., and Zhou, Y. (2015). "Spatial and Temporal Analysis of a Global Landslide Catalog." *Geomorphology*, 249, 4-15.

Klose, M., Damm, B., and Highland, L. M. (2015). "Databases in Geohazard Science: An Introduction." *Geomorphology*, 249, 1-3.

Lee, C.-T. (2014). "Statistical Seismic Landslide Hazard Analysis: An Example from Taiwan." *Engineering Geology*, 182, 201-212.

Lee, C. T., Huang, C. C., Lee, J. F., Pan, K. L., Lin, M. L., and Dong, J. J. (2008). "Statistical Approach to Earthquake-Induced Landslide Susceptibility." *Engineering Geology*, 100(1-2), 43-58.

Lei, X., Chen, W., and Pham, B. T. (2020). "Performance Evaluation of GIS-Based Artificial Intelligence Approaches for Landslide Susceptibility Modeling and Spatial Patterns Analysis." *ISPRS International Journal of Geo-Information*, 9(7), 443.

Li, W., Liu, C., Hong, Y., Zhang, X., Wan, Z., Saharia, M., Sun, W., Yao, D., Chen, W., and Chen, S. (2016). "A Public Cloud-Based China's Landslide Inventory Database (CsLID):

Development, Zone, and Spatiotemporal Analysis for Significant Historical Events, 1949-2011." *Journal of Mountain Science*, 13(7), 1275-1285.

Lin, Q., and Wang, Y. (2018). "Spatial and Temporal Analysis of a Fatal Landslide Inventory in China from 1950 to 2016." *Landslides*, 15(12), 2357-2372.

Mahdavifar, M. R., Solaymani, S., and Jafari, M. K. (2006). "Landslides Triggered by the Avaj, Iran Earthquake of June 22, 2002." *Engineering Geology*, 86(2-3), 166-182.

Maike, C. (2018b). "Mapping in the 21st Century." *GeoNews*, 45(2), 14-15.

Maike, C. A. (2018a). "Drone Applications at the NDGS." *GeoNews*, 45(1), 16-17.

Marjanović, M., Krautblatter, M., Abolmasov, B., Đurić, U., Sandić, C., and Nikolić, V. (2018). "The Rainfall-Induced Landsliding in Western Serbia: A Temporal Prediction Approach using Decision Tree Technique." *Engineering Geology*, 232, 147-159.

Matsuura, S., Okamoto, T., Asano, S., Osawa, H., and Shibasaki, T. (2017). "Influences of the Snow Cover on Landslide Displacement in Winter Period: A Case Study in a Heavy Snowfall Area of Japan." *Environmental Earth Sciences*, 76(10), p10.

Meunier, P., Hovius, N., and Haines, A. J. (2007). "Regional Patterns of Earthquake-Triggered Landslides and their Relation to Ground Motion." *Geophysical Research Letters*, 34(20).

Mitchell, J. K. (1993). *Fundamentals of Soil Behavior., 2nd Edn.*, John Wiley & Sons, Inc., Wiley, New York.

Moxness, A. D. (2019). "Twenty Thousand Slides and Counting: Recent Advances in Digital Imagery Expedite Landslides Mapping in North Dakota." *GeoNews*, 17-19.

Mukhlisin, M., and Taha, M. R. (2012). "Numerical Model of Antecedent Rainfall Effect on Slope Stability at a Hillslope of Weathered Granitic Soil Formation." *Journal of the Geological Society of India*, 79(5), 525-531.

Murphy, E. C. (2017). "Landslides in North Dakota." *GeoNews*, 44(1), 1-5.

Murphy, E. C., Nordeng, S. H., Juenker, B. J., and Hoganson, J. W. (2009). "North Dakota Stratigraphic Column: North Dakota Geological Survey Miscellaneous Series 91." *North Dakota Geological Survey*.

ND (2020). "Climate." *Game and Fish*, <https://gf.nd.gov/wildlife/habitats/climate#:~:text=Annual%20precipitation%20ranges%20from%2013,to%204%20inches%20of%20rain.>.

ND (2021). "North Dakota Plants and Habitats Overview." *North Dakota Game and Fish Department*, <https://gf.nd.gov/wildlife/habitats/vegetation>.

NDGS (2020). "North Dakota Geological Survey: 1:24,000 & 1:100,000 Scale Maps and Data." *North Dakota Geological Survey*, <https://www.dmr.nd.gov/ndgs/SurfaceMap/SurfaceMap.asp?source=landslide24k>.

NDSU (2019). "Sodicity and Remediation of Sodic Soils in North Dakota." *North Dakota State University*, <https://www.ag.ndsu.edu/publications/crops/sodicity-and-remediation-of-sodic-soils-in-north-dakota#section-6>.

Ng, C. W. W., and Shi, Q. (1998). "Influence of Rainfall Intensity and Duration on Slope Stability in Unsaturated Soils." *Quarterly Journal of Engineering Geology and Hydrogeology*, 31(2), 105-113.

NLCD (2016). "National Land Cover Database 2016." *Multi-Resolution Land Characteristics Consortium*, <https://www.mrlc.gov/data/legends/national-land-cover-database-2016-nlcd2016-legend#:~:text=Grassland%2FHerbaceous%2D%20areas%20dominated%20by,can%20be%20utilized%20for%20grazing.>.

NOAA (2017). "Climate of North Dakota." *National Oceanic and Atmospheric Administration*, <https://web.archive.org/web/20070926010149/http://www5.ncdc.noaa.gov/climatenormals/clim60/states/Clim_ND_01.pdf>.

NOAA (2020). "National Weather Service: National Snowfall Analysis." *National Oceanic and Atmospheric Administration*, <https://www.nohrsc.noaa.gov/snowfall_v2/index.html?season=2009-2010&date=2011060912&version=3&format=.tif>.

Owen, L. A., Kamp, U., Khattak, G. A., Harp, E. L., Keefer, D. K., and Bauer, M. A. (2008). "Landslides Triggered by the 8 October 2005 Kashmir Earthquake." *Geomorphology*, 94(1-2), 1-9.

Pearson, K. E. (2020). "Basics of Salinity and Sodicity Effects on Soil Physical Properties." *Montana State University*, <https://waterquality.montana.edu/energy/cbm/background/soil-prop.html>.

Pennington, C., Dijkstra, T., Lark, M., Dashwood, C., Harrison, A., and Freeborough, K. (2014). "Antecedent Precipitation as a Potential Proxy for Landslide Incidence in South West United Kingdom." *Landslide Science for a Safer Geoenvironment*, 253-259.

Rahardjo, H., Leong, E. C., and Rezaur, R. B. (2008). "Effect of Antecedent Rainfall on Pore-Water Pressure Distribution Characteristics in Residual Soil Slopes under Tropical Rainfall." *Hydrological Processes: An International Journal*, 22(4), 506-523.

Rahardjo, H., Li, X. W., Toll, D. G., and Leong, E. C. (2001). "The Effect of Antecedent Rainfall on Slope Stability." *Unsaturated Soil Concepts and Their Application in Geotechnical Practice*, 19, 371-399.

Ratner, B. (2009). "The Correlation Coefficient: Its Values Range Between+ 1/− 1, or Do They?" *Journal of Targeting, Measurement and Analysis for Marketing*, 17(2), 139-142.

Ritchie, H., and Roser, M. (2014). "Natural Disasters." *Our World in Data*, <https://ourworldindata.org/natural-disasters>.

Rodrıguez, C. E., Bommer, J. J., and Chandler, R. J. (1999). "Earthquake-Induced Landslides: 1980–1997." *Soil Dynamics and Earthquake Engineering*, 18(5), 325-346.

Schlögel, R. (2009). "Detection of Recent Landslides in Maily-Say Valley, Kyrgyz Tien Shan, Based on Field Observations and Remote Sensing Data." *Master's Thesis, Geological Sciences. University of Liege, Belgium (133 pp.)*.

Statistics, S. (2020). "Correlation (Pearson, Kendall, Spearman)." *Complete Dissertation*, <https://www.statisticssolutions.com/free-resources/directory-of-statistical-analyses/correlation-pearson-kendall-spearman/#:~:text=Usually%2C%20in%20statistics%2C%20we%20measure,and%20the%20Point%2DBiserial%20correlation>.

Strom, A. L., and Korup, O. (2006). "Extremely Large Rockslides and Rock Avalanches in the Tien Shan Mountains, Kyrgyzstan." *Landslides*, 3(2), 125-136.

Timpson, M. E., and Richardson, J. L. (1986). "Ionic Composition and Distribution in Saline Seeps of Southwestern North Dakota, USA." *Geoderma*, 37(4), 295-305.

Tiwari, B., and Ajmera, B. (2011). "A New Correlation Relating the Shear Strength of Reconstituted Soil to the Proportions of Clay Minerals and Plasticity Characteristics." *Applied Clay Science*, 53(1), 48-57.

Tiwari, B., and Ajmera, B. (2015). "Reduction in Fully Softened Shear Strength of Natural Clays with NaCl Leaching and its Effect on Slope Stability." *Journal of Geotechnical and Geoenvironmental Engineering*, 141(1), 04014086.

Tiwari, B., Ajmera, B., and Dhital, S. (2017). "Characteristics of Moderate-to Large-Scale Landslides Triggered by the MW 7.8 2015 Gorkha Earthquake and its Aftershocks." *Landslides*, 14(4), 1297-1318.

Tiwari, B., Tuladhar, G. R., and Marui, H. (2005). "Variation in Residual Shear Strength of the Soil with the Salinity of Pore Fluid." *Journal of Geotechnical and Geoenvironmental Engineering*, 131(12), 1445-1456.

Tiwari, B., and Upadhyaya, S. (2014). "Influence of Antecedent Rainfall on Stability of Slopes." *Geo-Congress 2014: Geo-Characterization and Modeling for Sustainability*, 3243-3251.

Trigila, A., Iadanza, C., Esposito, C., and Scarascia-Mugnozza, G. (2015). "Comparison of Logistic Regression and Random Forests Techniques for Shallow Landslide Susceptibility Assessment in Giampilieri (NE Sicily, Italy)." *Geomorphology*, 249, 119-136.

Trimble, D. E. (1979). *Unstable Ground in Eestern North Dakota*, Branch of Distribution, US Geological Survey, Arlington, VA.

USDA (2013). "National Soil Survey Handbook." *Title 430-VI*.

USDA (2020). "Web Soil Survey." *Natural Resources Conservation Service*, <https://websoilsurvey.nrcs.usda.gov/>.

USGS (1980). "Estimating the costs of Landslide Damage in the United States." *United States Geological Survey*, <https://pubs.er.usgs.gov/publication/cir832>.

USGS (2003). "National Landslide Hazards Mitigation Strategy - A Framework for Loss Reduction." *United States Geological Survey*, <https://pubs.usgs.gov/circ/c1244/c1244.pdf>.

USGS (2016a). "NLCD Land Cover Change Index." *Multi-Resolution Land Characteristics Consortium*, <https://www.mrlc.gov/data/nlcd-land-cover-change-index-conus>.

USGS (2016b). "NLCD Land Cover (CONUS)." *MRLC*, <https://www.mrlc.gov/data?f%5B0%5D=category%3ALand%20Cover>.

USGS (2019). "USGS National Elevation Dataset (NED)." *ND State Water Commission*, <https://catalog.data.gov/dataset/usgs-national-elevation-dataset-ned>.

USGS (2020a). "What is a Landslide and What Causes One?" *United States Geological Survey*, <https://www.usgs.gov/faqs/what-a-landslide-and-what-causes-one?qt-news_science_products=0#qt-news_science_products>.

USGS (2020b). "North Dakota Geologic Map Data." *United States Geological Survey*, <https://mrdata.usgs.gov/geology/state/state.php?state=ND>.

Wang, L.-J., Guo, M., Sawada, K., Lin, J., and Zhang, J. (2016). "A Comparative Study of Landslide Susceptibility Maps Using Logistic Regression, Frequency Ratio, Decision Tree, Weights of Evidence and Artificial Neural Network." *Geosciences Journal*, 20(1), 117-136.

Wieczorek, G. F. (1996). "Landslides: Investigation and Mitigation. Chapter 4-Landslide Triggering Mechanisms." *Transportation Research Board Special Report*(247), 76-90.

Wood, J. L., Harrison, S., and Reinhardt, L. (2015). "Landslide Inventories for Climate Impacts Research in the European Alps." *Geomorphology*, 228, 398-408.

Xiaoming, Z., Yujie, W., Yiping, X., Yun, W., and Lin, C. (2006). "Shear Strengths of Undisturbed and Remolded Soils of Typical Vegetations in Jinyun Mountain of Chongqing City." *Transactions of the Chinese Society of Agricultural Engineering*, 22(11), 6-9.

Xu, C., Shyu, J. B. H., and Xu, X. (2014). "Landslides Triggered by the 12 January 2010 Port-au-Prince, Haiti, M w= 7.0 Earthquake: Visual Interpretation, Inventory Compiling, and Spatial Distribution Statistical Analysis." *Natural Hazards and Earth System Sciences*, 14(7), 1789-1818.

Xu, C., Xu, X., Dai, F., Wu, Z., He, H., Shi, F., Wu, X., and Xu, S. (2013). "Application of an Incomplete Landslide Inventory, Logistic Regression Model and its Validation for Landslide Susceptibility Mapping Related to the May 12, 2008 Wenchuan Earthquake of China." *Natural Hazards*, 68(2), 883-900.

Xue, K., Ajmera, B., Tiwari, B., and Hu, Y. (2016). "Effect of Long Duration Rainstorm on Stability of Red-clay Slopes." *Geoenvironmental Disasters*, 3(1), 12.

Yagi, H., Sato, G., Higaki, D., Yamamoto, M., and Yamasaki, T. (2009). "Distribution and Characteristics of Landslides Induced by the Iwate–Miyagi Nairiku Earthquake in 2008 in Tohoku District, Northeast Japan." *Landslides*, 6(4), 335.

Yong, R. N., Mohamed, A.-M. O., and Warkentin, B. P. (1992). *Principles of Contaminant Transport in Soils*, Elsevier Science Publishers, Amsterdam, Netherlands.

Zhang, C.-B., Chen, L.-H., Liu, Y.-P., Ji, X.-D., and Liu, X.-P. (2010). "Triaxial Compression Test of Soil–Root Composites to Evaluate Influence of Roots on Soil Shear Strength." *Ecological Engineering*, 36(1), 19-26.

APPENDIX A: GEOLOGICAL COMPOSITIONS WITH THEIR LITHOLOGY AND DEPOSITIONAL ENVIRONMENT IN NORTH DAKOTA ADAPTED FROM MURPHY ET AL. (2009)

Geological Formation	Lithology, description copied from Murphy et al. (2009).	Depositional Environments
Belle Fourche	"Shale; medium to dark gray; micaceous; soft; lumpy to massive; includes beds of bluish gray bentonitic clay; sandstone and siltstone near the base in eastern North Dakota"	Offshore marine deposits
Bullion Creek	"Sandstone, siltstone, claystone, mudstone, clinker, and lignite; generally brightly colored, yellow, brown, gray; poorly-cemented to well-cemented sandstones; swelling and non-swelling clay stones; limestone and iron oxide nodules and concretions" "Contains the Harmon Bed, 16 m thick, the thickest lignite in North Dakota"	River, lake, and swamp deposits
Cannonball	"Mudstones and sandstones; dark gray to black mudstones, greenish gray to yellow sandstone; glauconitic; mudstone contains lenses of siltstone and sandstones; sandstone is poorly-cemented to well-cemented; contains at least three well-cemented, lenticular, ledge forming sandstones in south-central North Dakota; abundant marine fossils"	Marine and brackish deposits
Carlile	"Shale; medium gray to black; non-calcareous; soft; a zone of selenite and large ellipsoidal concretions and septarian nodules near the top; marine fossils; forms rounded slopes"	Offshore marine deposits
Fox Hills	"Mudstone, siltstone, sandstone; yellowish brown to gray; poorly-cemented to well-cemented sandstone; organic laminae; tuffaceous bed(s); mollusk-rich beds; abundant marine and brackish-water fossils. Generally forms gentle, rounded slopes, but can form flat-topped hills and buttes"	Offshore marine and nearshore deposits
Golden Valley	"Camels Butte Member: 350 feet (107 m) thick, sandstone, siltstone, mudstone, claystone, and thin lignite; shades of yellow and brown; sandstone is poorly-cemented to well-cemented; the lower part is very similar lithologically to the Sentinel Butte Formation except that it is generally micaceous; the upper part contains a massive fluvial sandstone that caps many of the major buttes in southwestern North Dakota"	River, lake, and swamp deposits
Greenhorn	"Shale; dark gray; micaceous; soft; thin-bedded shaly limestone; referred to as the Second White Speaks by drillers; the top is a good marker on a gamma-ray and resistivity logs"	Offshore marine deposits
Hell Creek	"Sandstone, siltstone, claystone, mudstone, and thin, discontinuous lignite; somber tones of gray, brown, and purple; moderately-cemented to poorly-cemented, organic-rich, cross-bedded sandstone; bentonitic claystone; tuffaceous beds; limestone, manganese-oxide, and iron-oxide nodules and concretions; dinosaur fossils"	River, lake, and swamp deposits

Geological Formation	Lithology, description copied from Murphy et al. (2009).	Depositional Environments
Inyan Kara	"Upper part: Sandstone; light gray; quartzose; fine-grained to coarse-grained. Shale: gray; silty; lumpy" "Lower part: Sandstone; gray; quartzose; medium-grained to coarse-grained; angular to subrounded; occasional lenses of shale; gray; bentonitic; contains manganese and siderite spheres"	Primarily nonmarine
Ludlow	"Sandstone, siltstone, claystone, clinker, and lignite; brown and gray; poorly-cemented to well-cemented sandstones; swelling and non-swelling claystone, limestone and iron oxide nodules and concretions. Forms steep, rilled slopes and badlands topography in southwestern North Dakota"	River Lakes and swamp deposits
Mowry-Skull Creek	"Shale; medium to dark gray; soft; flaky; traces of bluish gray bentonitic claystone; top is marked by a persistent bentonitic that has a strong response on a gamma ray log"	Offshore marine deposits
Niobrara	"Shale, chalk; light to medium gray, upper exposures weather to yellow; calcareous; zones contain limy inclusions or specks that are referred to as the First White Specks by drillers an are used to differentiate it from the overlying Pierre Formation"	Offshore Marine deposits
Pierre	"Shale; light to dark gray; generally non-calcareous; fissile to blocky"	Offshore marine deposits
Piper	"Shale; red, purple, and greenish gray; silty; gypsum and anhydrite layers. Limestone; white, brown, or gray; dolomitic; finely crystalline, dense; fossiliferous"	Offshore marine deposits
Precambrian Rocks	"These rocks include granite, granodiorites, biotite-garnet gneiss, charnockite, hornblende schist, monzonite, and diabase" "Granites, granodiorites, diorites, chlorite schists (greenstone), granitic metamorphic rocks, stretched pebble conglomerates, porphyritic granodiorite-gneiss, banded gneiss, phyllites, metasedimentary and metavolcanics rocks, adamellites, syenites, banded iron formations, and tuffs"	Offshore marine deposits
Red River	"Upper one-third: limestone; gray to brown, mottled; dolomitic in part; medium-grained to fine-grained; zones of brown to black organic detritus; bioturbated zones; some vugs; nodular anhydrite; fossiliferous" "Lower two thirds: limestone; yellowish gray to brown; mottled; occasional vugs; fossiliferous, bioturbated"	Shallow marine to restricted marine deposits
Sentinel Butte	"Sandstone, siltstone, clay stone, mudstone, clinker and lignite; generally somber colored gray, blue, and brown; poorly-cemented to well-cemented sandstones; swelling bentonitic and non-swelling clay stones; limestone and iron oxide nodules and concretions; abundant petrified wood, tuffaceous bed(s); forms steep, rilled slopes and badlands topography throughout much of southwestern North Dakota"	River, lake, and swamp deposits
Slope	"Sandstone, siltstone, clay stone, mudstone, clinker and lignite; generally dark colored, brown and gray; poorly-cemented to well-cemented sandstones; swelling and non-swelling clay stones; limestone and iron oxide nodules and concretions; forms steep, rilled slopes and badlands topography in southwestern North Dakota"	River, lake, and swamp deposits

Geological Formation	Lithology, description copied from Murphy et al. (2009).	Depositional Environments
Jurassic Sediments	Dark-gray, greenish, and varicolored shale with local limestone.	Marine deposits
Upper and Middle Tertiary Rock	"Butte caprock consisting of fluvial or lacustrine sandstone or limestone of Oligocene, Miocene, or Pliocene age"	Offshore marine deposits
White River Group	"Brule Formation: siltstone, sandstone, and claystone; brown to pink; nodular, siltstones may contain claystone inclusions; weathers to steep slopes with rounded pitted surfaces" "South Heart Member; claystone; brown, pink, and green; contains silicified zones; bentonitic; popcorn weathering surfaces" "Chalky Buttes Member; sandstone and conglomerate; grayish green to white; cross-bedded, poorly-cemented sandstone"	River and lake deposits
Winnipeg Group	"Shale; medium to dark gray; silty; calcareous; fossiliferous; contains nodules of light gray limestone' "shale; greenish gray to black; carbonaceous; bioturbated; locally fossiliferous; black phosphate nodules"	Offshore marine deposits

APPENDIX B: ARCGIS PROCEDURES

This section provides detailed information about the steps followed in ArcGIS. The centroid of the polygons was calculated using the following steps:

1. In the Geoprocessing Toolbar, search for the Feature to Point (Figure B.1).
2. Under Input Features, select the landslide polygons for which the centroid needs to be determined (Figure B.2).
3. For the Output Feature Class, select the desired output location (Figure B.2).
4. Click Run.

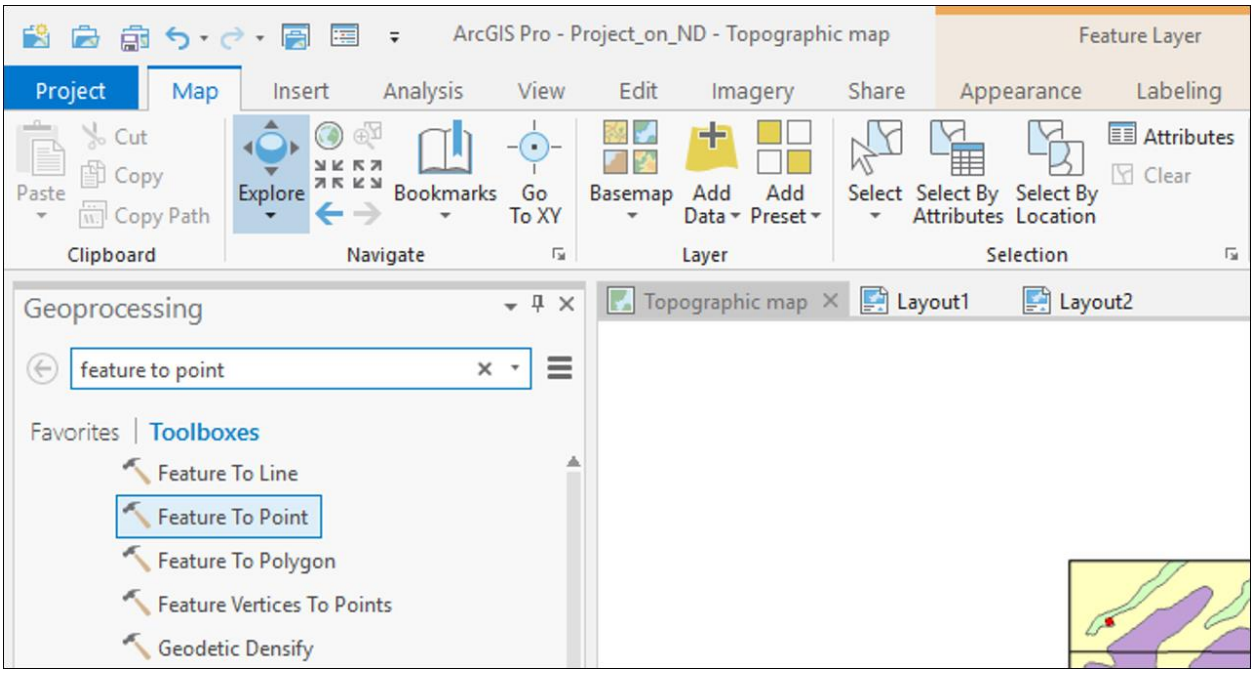

Figure B.1. Searching for Feature to Point in the Geoprocessing Toolbar.

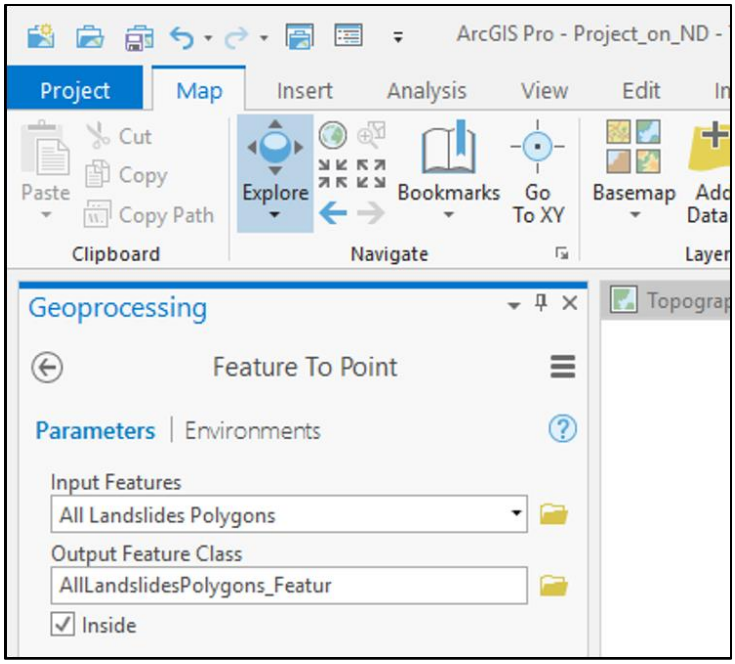

Figure B.2. Input and Output Feature Selection to Calculate the Centroid of Each Landslide.

The steps to calculate the number of slope failures within each geological composition are as follows:

1. In the Geoprocessing Toolbar, search for and select the Spatial Join option under Analysis Tools (Figure B.3).
2. Under Target Features, select Geology (Figure B.4). Geology was selected because the number of slope failures needs to be calculated for each geological composition which acts as a boundary.
3. Under Join Features, select Centroid of Landslide because the number of centroids/landslides with each boundary should be counted.
4. In the Output Feature Class, give the desired location to save the output file. All the other operations were set as the default values.
5. For the Match Option, select Completely Contains as the number of centroids within each boundary that need to be calculated (Figure B.4).

6. Click Run.

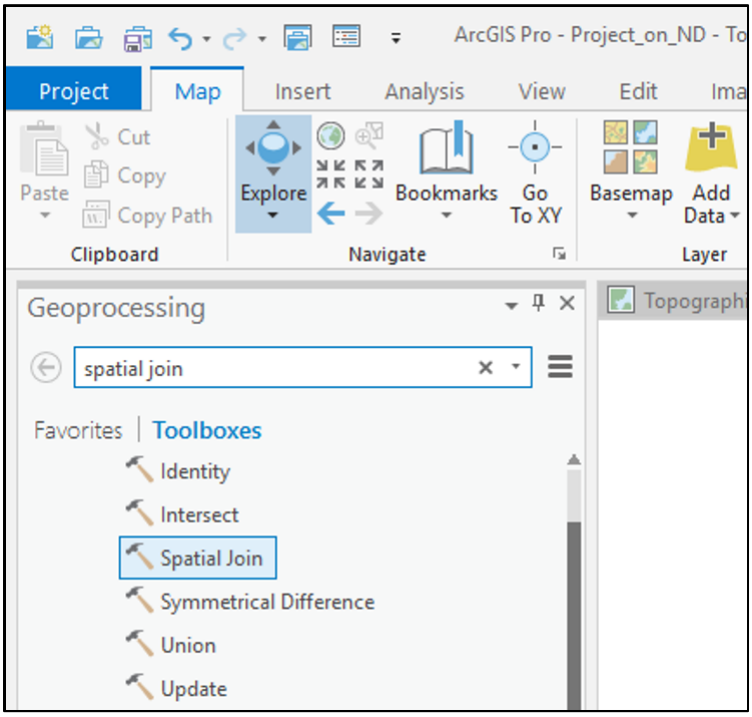

Figure B.3. Searching for Spatial Join in the Geoprocessing Toolbar.

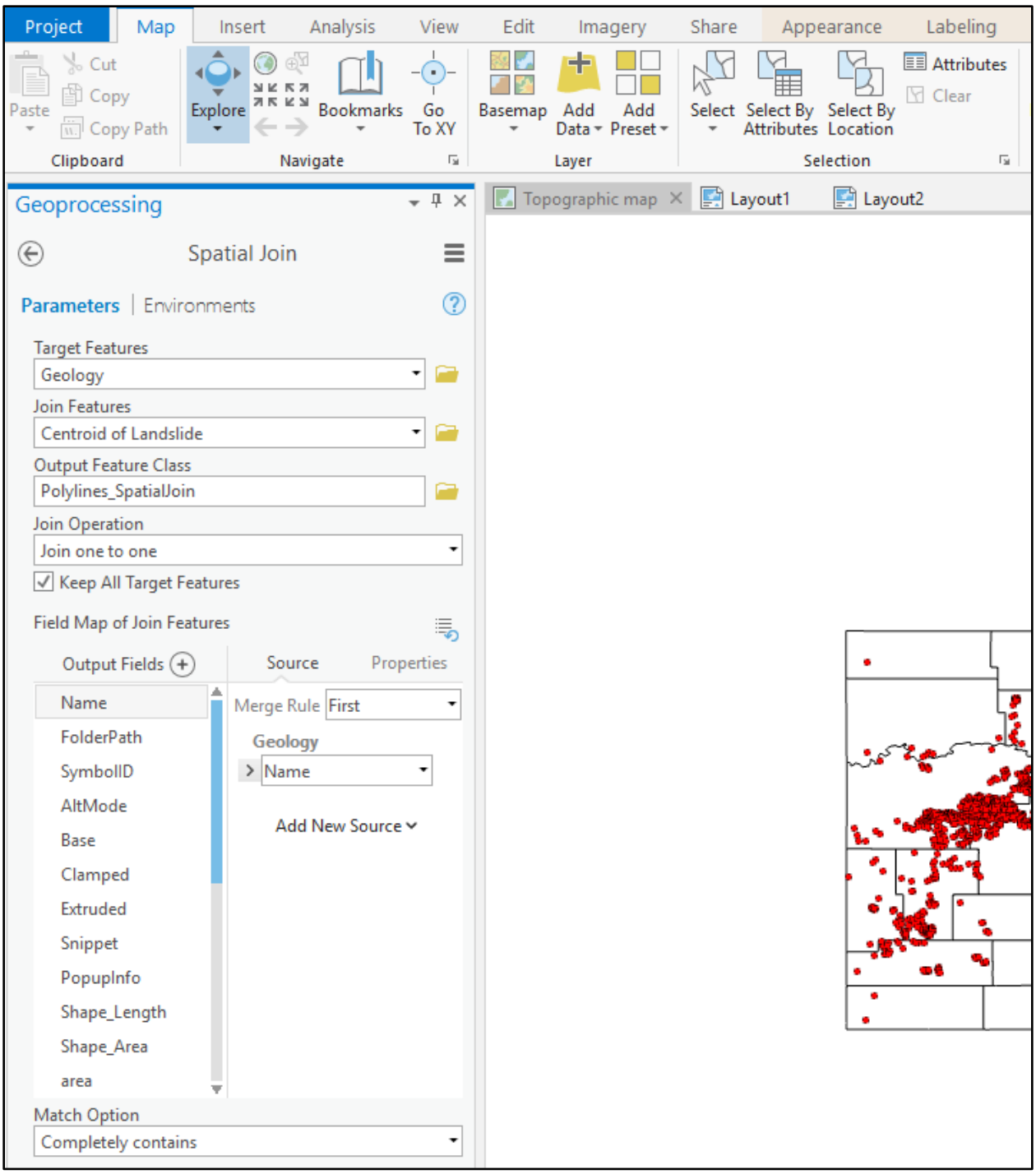

Figure B.4. Target and Join Features to Calculate the Number of Slope Failures within Each Geological Composition.

The steps to calculate the slope map are as follows:

1. Select the Slope option from the Geoprocessing Toolbar (Figure B.5).
2. Select the NED Elevation Map as the Input Raster (Figure B.6).
3. For the Output Raster, an automatic name will be given for the raster data (Figure B.6). This name can be changed, if required. In this study, Slope NED was used.
4. For the Output Measurement, select Degrees (Figure B.6).
5. In Method, select Planer. Calculations will be done considering a flat earth surface.
6. Click Run.

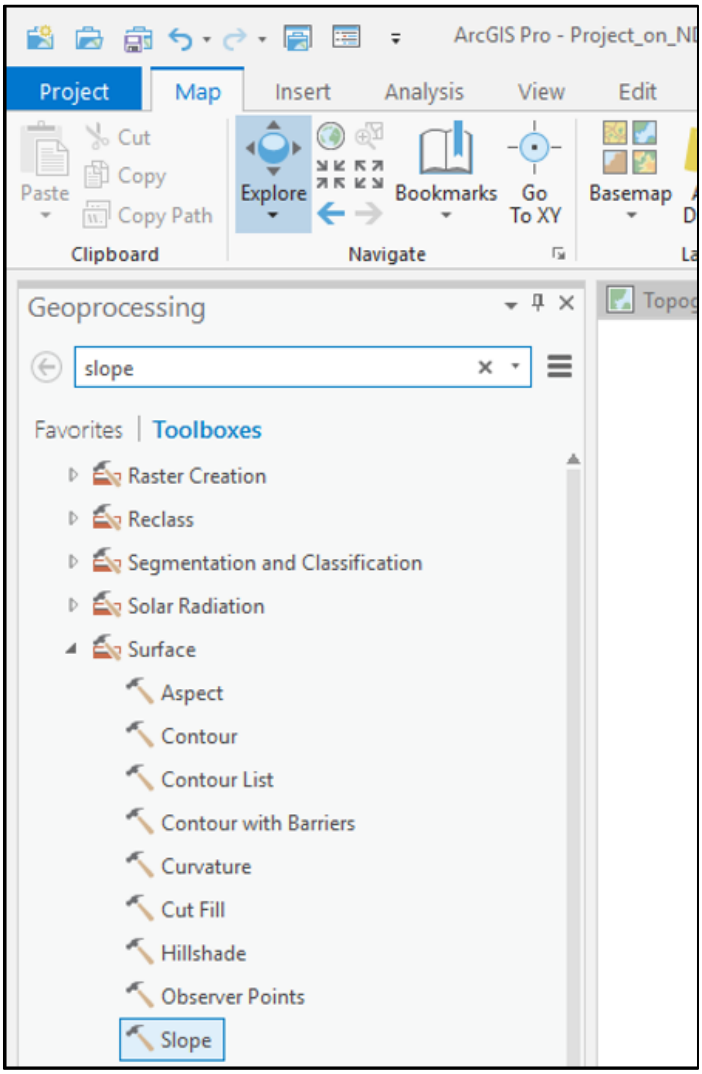

Figure B.5. Searching for Slope in the Geoprocessing Toolbar.

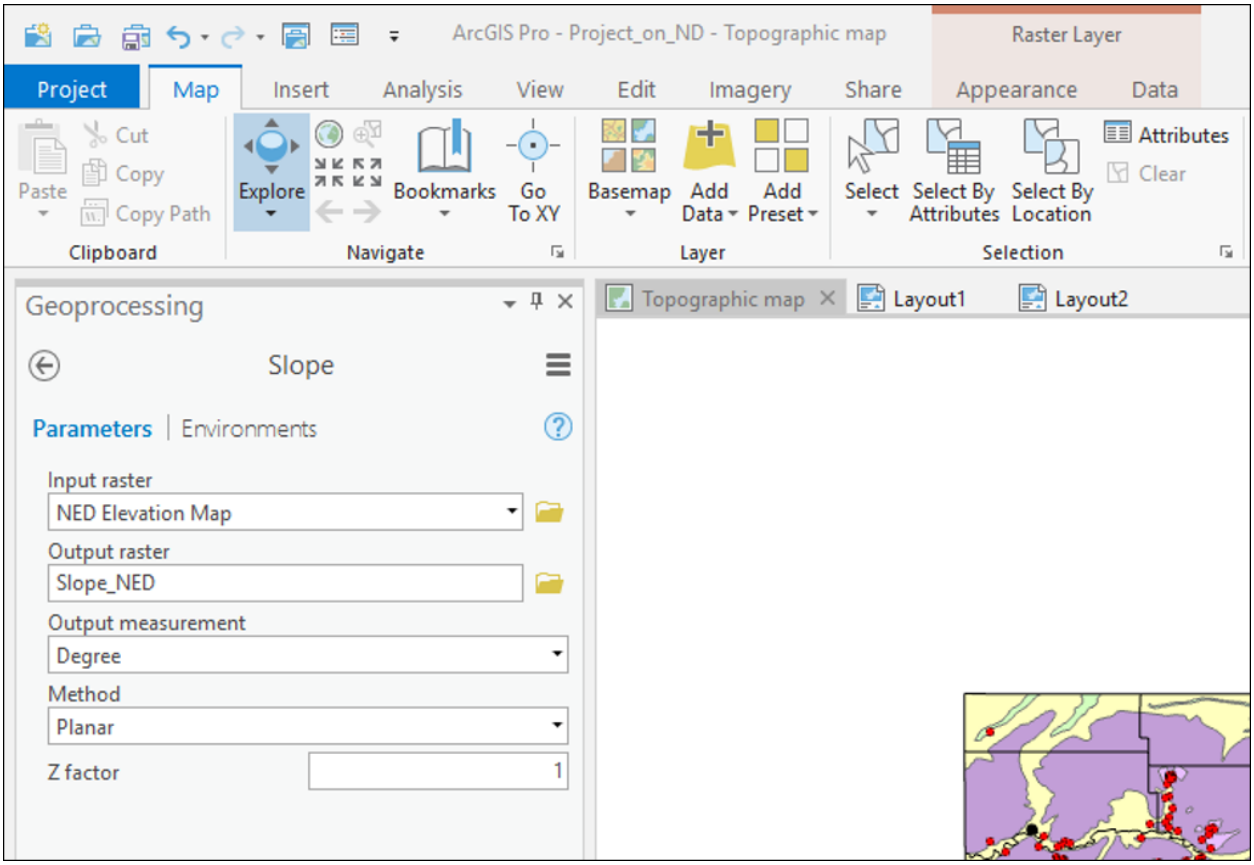

Figure B.6. Input and Output Feature Selection to Calculate the Slope Map.

The steps for calculating the slope inclinations at the centroid of landslides are as follows:

1. Select Extract Multi Values to Points from Geoprocessing Toolbar (Figure B.7).
2. The Centroid of Landslide was selected for the Input Point Features (Figure B.8).
3. Select Slope NED for the Input Rasters (Figure B.8).
4. The Bilinear Interpolation of Values at Point Locations was checked. Checking this option calculates the value of the cell using bilinear interpolation from the adjacent cell values.
5. Click Run.

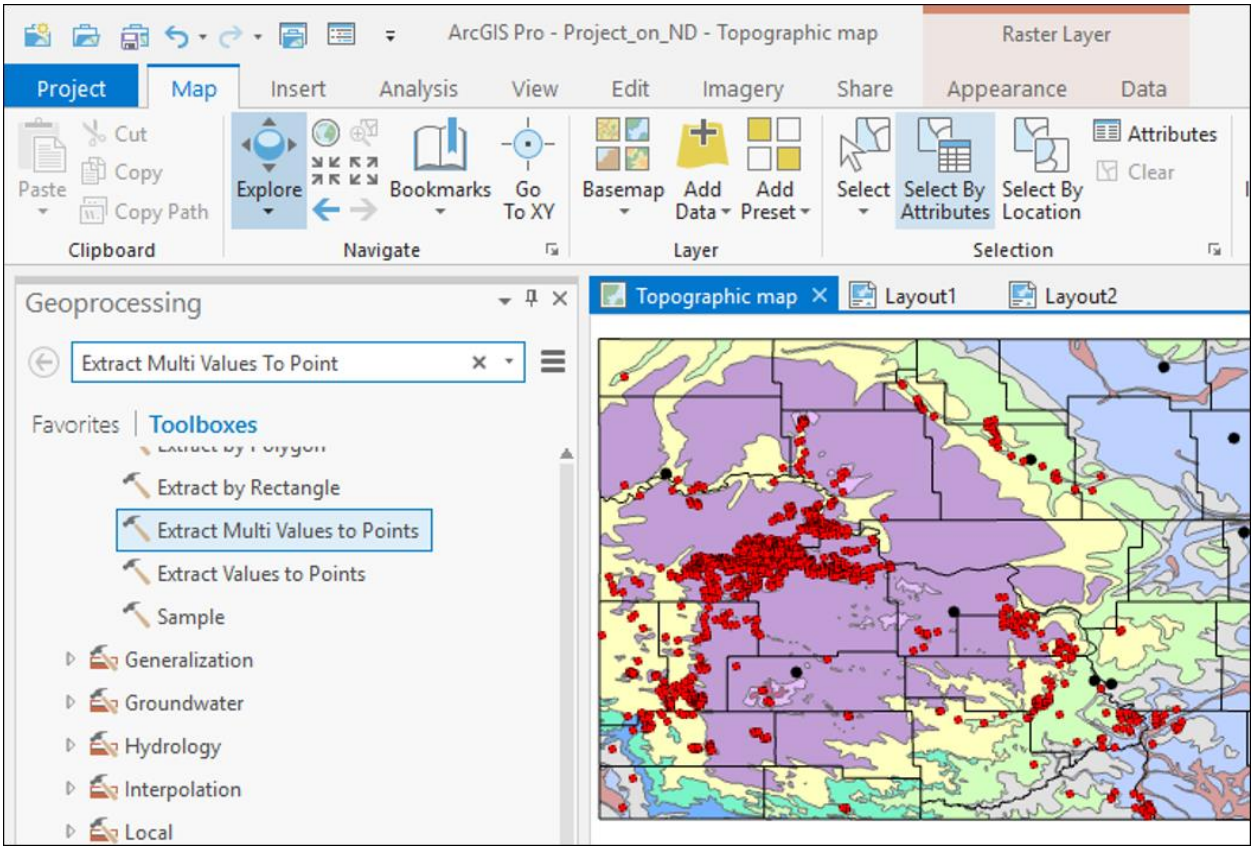

Figure B.7. Searching for Extract Multi Value to Point in the Geoprocessing Toolbar.

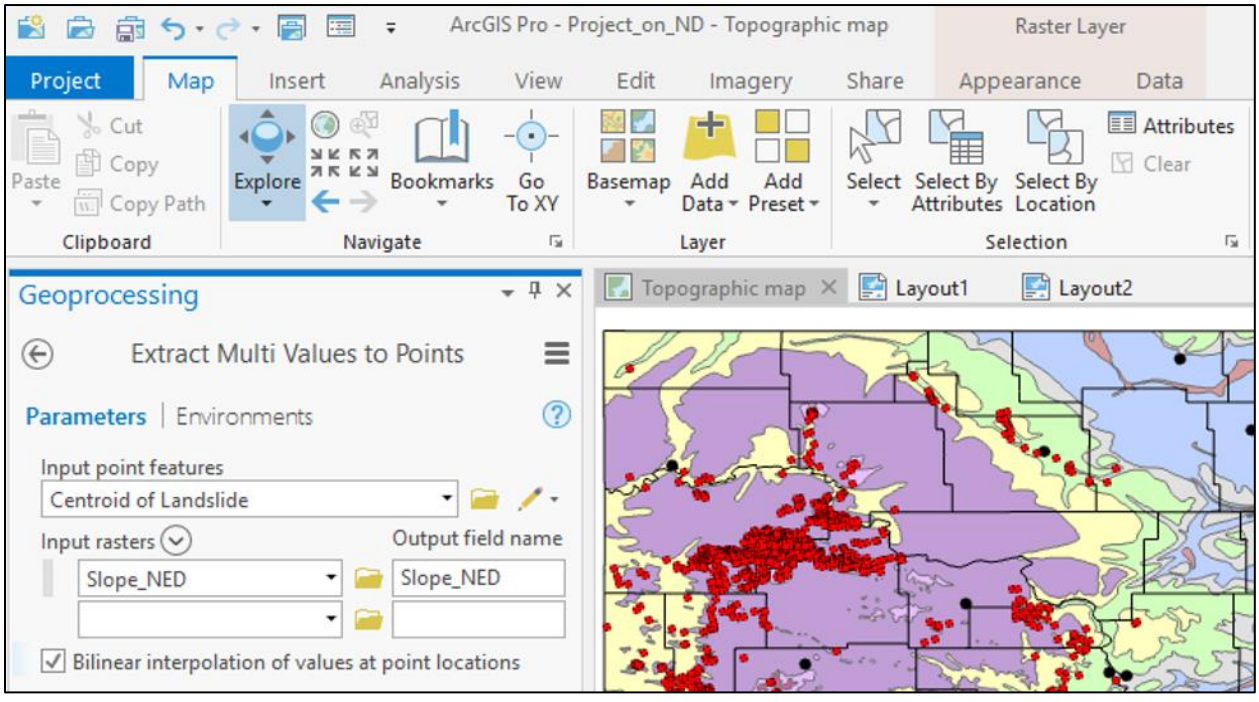

Figure B.8. Input and Output Feature Selection to Calculate the Slope Inclination.

The steps for calculating the land cover at the landslides are as follows:

1. In the Geoprocessing Toolbar, search for and select Zonal Statistics (Figure B.9).
2. For the Input Raster or Feature Zone Data, select the dataset that defines the zone for which the land cover needs to be calculated (Figure B.10). As the land cover within each slope failure area was required, All Landslide Polygons was selected as the Input Raster in the study (Figure B.10).
3. In the Zone Field, different attributes of the previously selected feature class are shown with the dropdown menu, and the one that defines the zone needs to be selected. In the study, Object ID (OID) was selected because OID was unique for each slope failure (Figure B.10).
4. Under Input Value Raster, select the raster that contains the values, which will be utilized to calculate the statistics. For these steps, the raster with the land cover data obtained from the NLCD was selected (Figure B.10).
5. For the Output Raster, the name of the output raster file is generated (Figure B.10).
6. Under Statistics Type, different statistical tools are available. For this study, Maximum was selected (Figure B.10) because the desired calculation was the land cover with the greatest area within each landslide boundary.
7. Click Run.

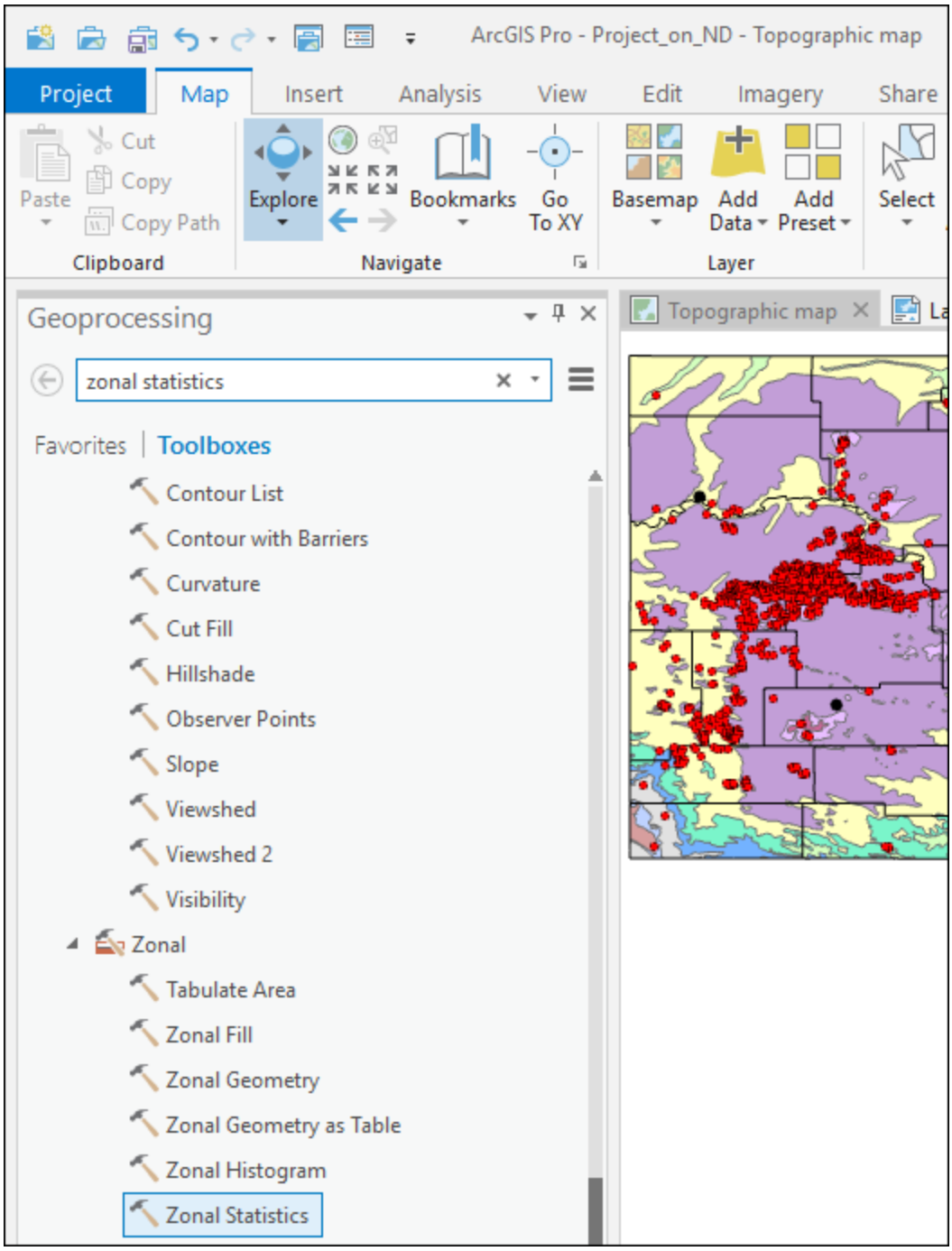

Figure B.9. Searching for Zonal Statistics in the Geoprocessing Toolbar.

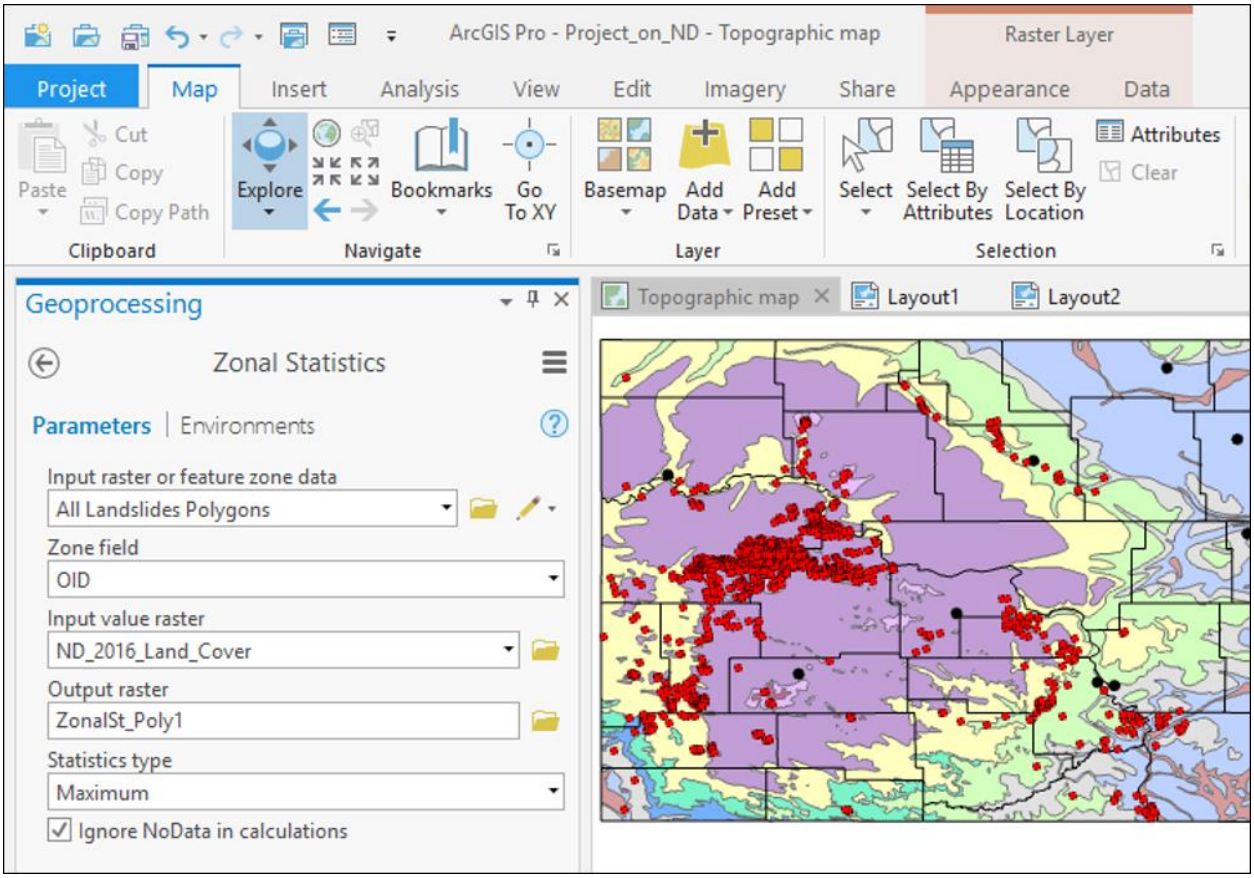

Figure B.10. Input and Output Feature Calculation for the Land Cover.

APPENDIX C: CALCULATIONS IN EXCEL

The following steps were taken in Excel to calculate the concentration of dissolved salts using the Solver function:

1. Columns for each heading shown in Figure C.1 are set.
2. Click on Data and then select Solver from the Ribbon.
3. In the Solver Parameters Dialogue Box, the Set Objective will appear (Figure C.2). In this box, select the column for which the sum of squared error needs to be minimized. In the study, sum of squared error, Column Q of Row 28 as shown in Figure B.1, was selected as the objective because this cell needs to be kept as small as possible.
4. Select the Min check box (Figure C.2).
5. Under By Changing Variable Cells, select the cells for which the calculation is required with the Solver function (Figure C.2). In this study, Columns L, M, and N were selected because the dissolved salt concentration was needed to be calculated.

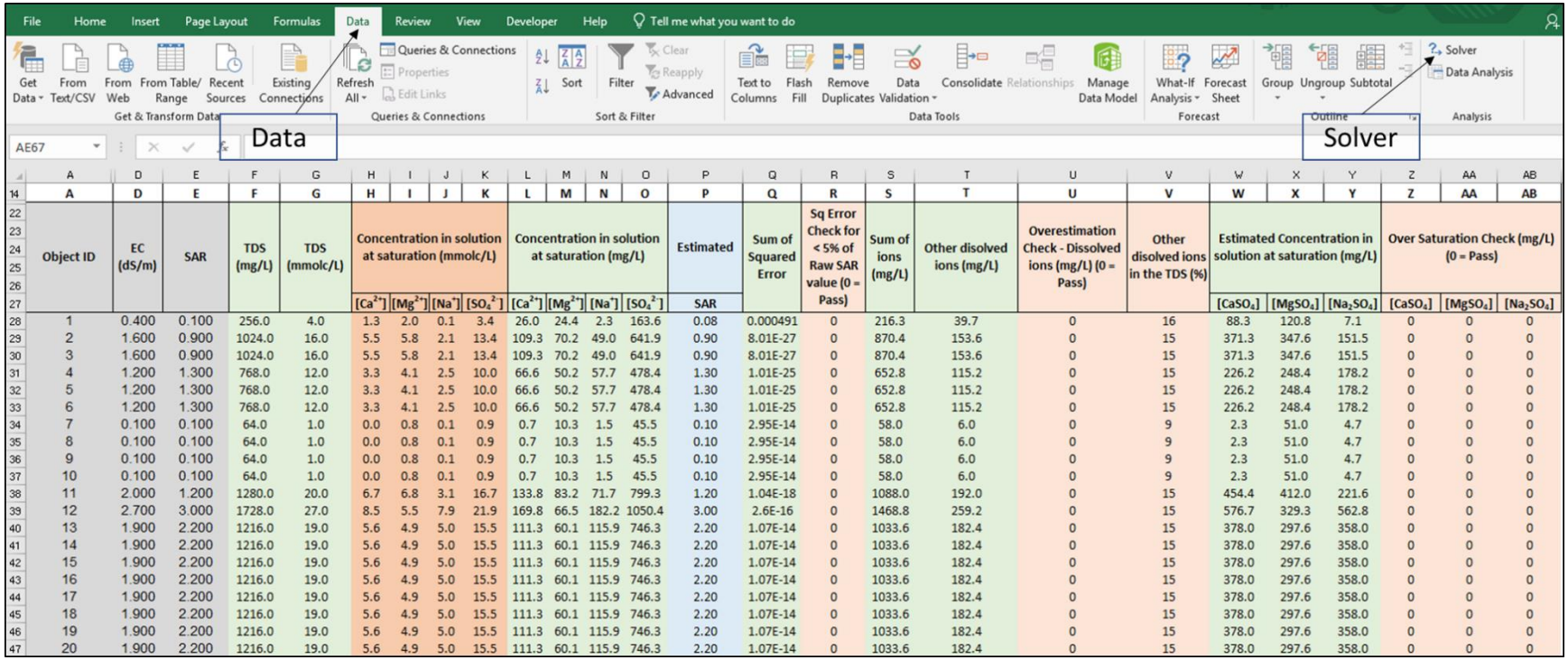

Object ID	EC (dS/m)	SAR	TDS (mg/L)	TDS (mmolc/L)	Concentration in solution at saturation (mmolc/L)				Concentration in solution at saturation (mg/L)				Estimated	Sum of Squared Error	Sq Error Check for < 5% of Raw SAR value (0 = Pass)	Sum of ions (mg/L)	Other disolved ions (mg/L)	Overestimation Check - Dissolved ions (mg/L) (0 = Pass)	Other disolved ions in the TDS (%)	Estimated Concentration in solution at saturation (mg/L)			Over Saturation Check (mg/L) (0 = Pass)		
					$[Ca^{2+}]$	$[Mg^{2+}]$	$[Na^{+}]$	$[SO_4^{2-}]$	$[Ca^{2+}]$	$[Mg^{2+}]$	$[Na^{+}]$	$[SO_4^{2-}]$	SAR							$[CaSO_4]$	$[MgSO_4]$	$[Na_2SO_4]$	$[CaSO_4]$	$[MgSO_4]$	$[Na_2SO_4]$
1	0.400	0.100	256.0	4.0	1.3	2.0	0.1	3.4	26.0	24.4	2.3	163.6	0.08	0.000491	0	216.3	39.7	0	16	88.3	120.8	7.1	0	0	0
2	1.600	0.900	1024.0	16.0	5.5	5.8	2.1	13.4	109.3	70.2	49.0	641.9	0.90	8.01E-27	0	870.4	153.6	0	15	371.3	347.6	151.5	0	0	0
3	1.600	0.900	1024.0	16.0	5.5	5.8	2.1	13.4	109.3	70.2	49.0	641.9	0.90	8.01E-27	0	870.4	153.6	0	15	371.3	347.6	151.5	0	0	0
4	1.200	1.300	768.0	12.0	3.3	4.1	2.5	10.0	66.6	50.2	57.7	478.4	1.30	1.01E-25	0	652.8	115.2	0	15	226.2	248.4	178.2	0	0	0
5	1.200	1.300	768.0	12.0	3.3	4.1	2.5	10.0	66.6	50.2	57.7	478.4	1.30	1.01E-25	0	652.8	115.2	0	15	226.2	248.4	178.2	0	0	0
6	1.200	1.300	768.0	12.0	3.3	4.1	2.5	10.0	66.6	50.2	57.7	478.4	1.30	1.01E-25	0	652.8	115.2	0	15	226.2	248.4	178.2	0	0	0
7	0.100	0.100	64.0	1.0	0.0	0.8	0.1	0.9	0.7	10.3	1.5	45.5	0.10	2.95E-14	0	58.0	6.0	0	9	2.3	51.0	4.7	0	0	0
8	0.100	0.100	64.0	1.0	0.0	0.8	0.1	0.9	0.7	10.3	1.5	45.5	0.10	2.95E-14	0	58.0	6.0	0	9	2.3	51.0	4.7	0	0	0
9	0.100	0.100	64.0	1.0	0.0	0.8	0.1	0.9	0.7	10.3	1.5	45.5	0.10	2.95E-14	0	58.0	6.0	0	9	2.3	51.0	4.7	0	0	0
10	0.100	0.100	64.0	1.0	0.0	0.8	0.1	0.9	0.7	10.3	1.5	45.5	0.10	2.95E-14	0	58.0	6.0	0	9	2.3	51.0	4.7	0	0	0
11	2.000	1.200	1280.0	20.0	6.7	6.8	3.1	16.7	133.8	83.2	71.7	799.3	1.20	1.04E-18	0	1088.0	192.0	0	15	454.4	412.0	221.6	0	0	0
12	2.700	3.000	1728.0	27.0	8.5	5.5	7.9	21.9	169.8	66.5	182.2	1050.4	3.00	2.6E-16	0	1468.8	259.2	0	15	576.7	329.3	562.8	0	0	0
13	1.900	2.200	1216.0	19.0	5.6	4.9	5.0	15.5	111.3	60.1	115.9	746.3	2.20	1.07E-14	0	1033.6	182.4	0	15	378.0	297.6	358.0	0	0	0
14	1.900	2.200	1216.0	19.0	5.6	4.9	5.0	15.5	111.3	60.1	115.9	746.3	2.20	1.07E-14	0	1033.6	182.4	0	15	378.0	297.6	358.0	0	0	0
15	1.900	2.200	1216.0	19.0	5.6	4.9	5.0	15.5	111.3	60.1	115.9	746.3	2.20	1.07E-14	0	1033.6	182.4	0	15	378.0	297.6	358.0	0	0	0
16	1.900	2.200	1216.0	19.0	5.6	4.9	5.0	15.5	111.3	60.1	115.9	746.3	2.20	1.07E-14	0	1033.6	182.4	0	15	378.0	297.6	358.0	0	0	0
17	1.900	2.200	1216.0	19.0	5.6	4.9	5.0	15.5	111.3	60.1	115.9	746.3	2.20	1.07E-14	0	1033.6	182.4	0	15	378.0	297.6	358.0	0	0	0
18	1.900	2.200	1216.0	19.0	5.6	4.9	5.0	15.5	111.3	60.1	115.9	746.3	2.20	1.07E-14	0	1033.6	182.4	0	15	378.0	297.6	358.0	0	0	0
19	1.900	2.200	1216.0	19.0	5.6	4.9	5.0	15.5	111.3	60.1	115.9	746.3	2.20	1.07E-14	0	1033.6	182.4	0	15	378.0	297.6	358.0	0	0	0
20	1.900	2.200	1216.0	19.0	5.6	4.9	5.0	15.5	111.3	60.1	115.9	746.3	2.20	1.07E-14	0	1033.6	182.4	0	15	378.0	297.6	358.0	0	0	0

Figure C.1. Selecting Data and Solver Function in Excel Spreadsheet.

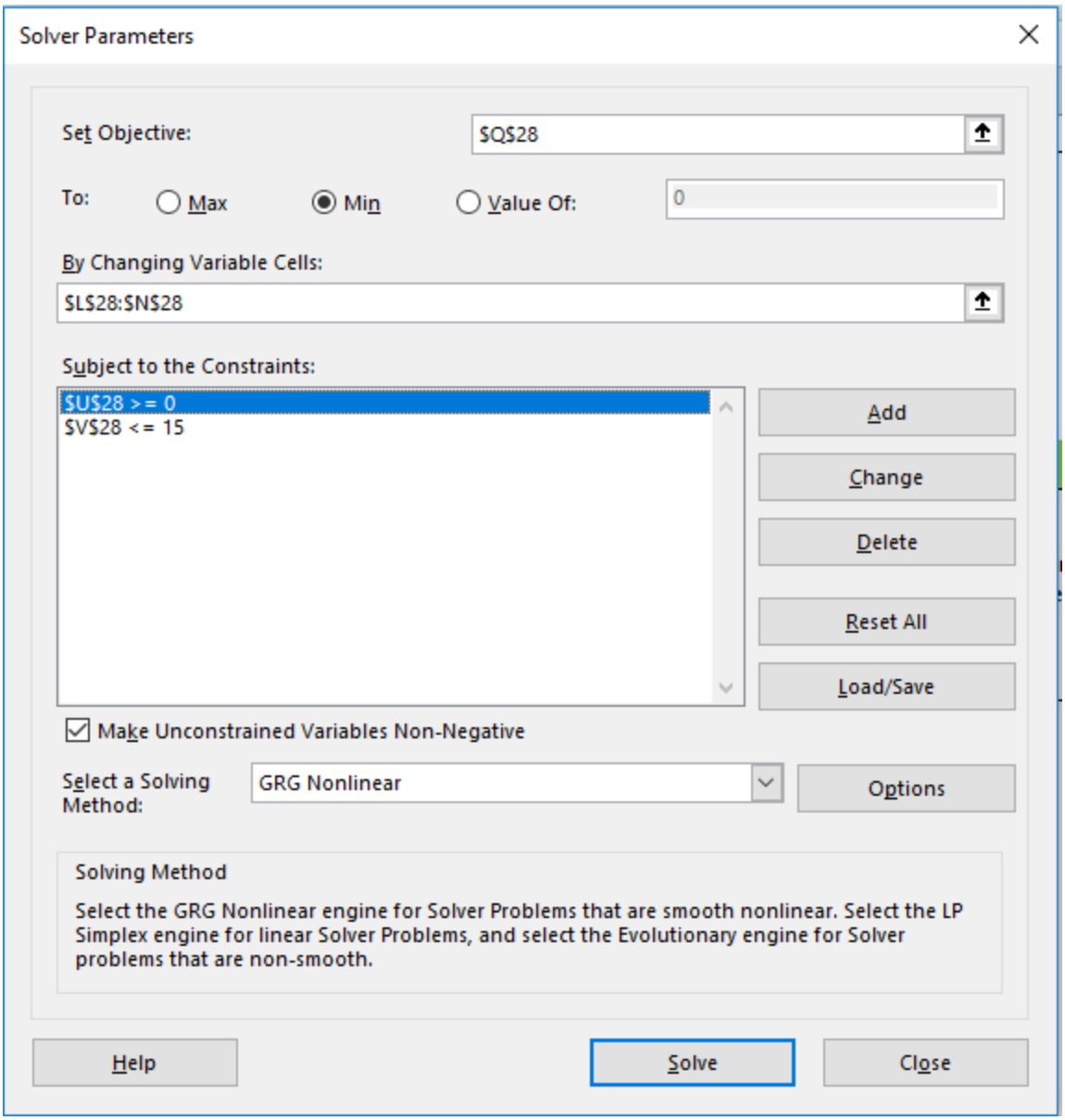

Figure C.2. Solver Parameter Dialogue Box.

6. Click on the Add button to add constraints.
7. A Change Constraint Dialogue Box will appear (Figure C.3). In that box, set the constraints as per the requirements. In the study, Column U of Row 28 (Figure C.1) was selected because the constraint was set for overestimation. As Column U of Row 28 should be at least zero, the ">=" symbol and zero was entered in the Constraint.

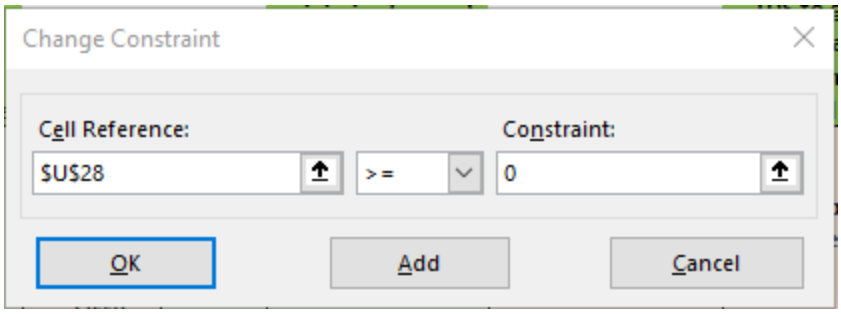

Figure C.3. Constraint Dialogue Box.

8. Click the Add button to add more constraints (Figure C.3). As two constraints were set in the study, this option was selected.
9. Similarly, another constraint was added so that Column V was less than 15%.
10. Click Solve (Figure C.2).
11. Due to the number of slope failures in this study, a VBA code was used to repeat this process for each landslide. This code is provided in Appendix D.

The steps to calculate the correlation matrix are as follows:

1. Object IDs of landslides were exported to the first column in the spreadsheet.
2. Different parameters, such as area, EC, SAR, TDS, slope, latitude, longitude, land cover, geological composition, counties, and calcium sulfate, magnesium sulfate, and sodium sulfate concentrations, were exported to different columns in the spreadsheet.
3. For any factor that did not contain an associated numerical value, a true (1) or false (0) value was assigned. A value of 1 was assigned if the landslide satisfied that non-numerical quantity. Otherwise, a value of 0 was assigned.
4. Click on Data and select Data Analysis from the Ribbon (Figures C.4 and C.5)
5. Click on Correlation and click OK (Figure C.6).

6. In the Input Range of Correlation Dialogue Box (Figure C.7), select the data the correlation matrix should use for the calculation.
7. Click OK.

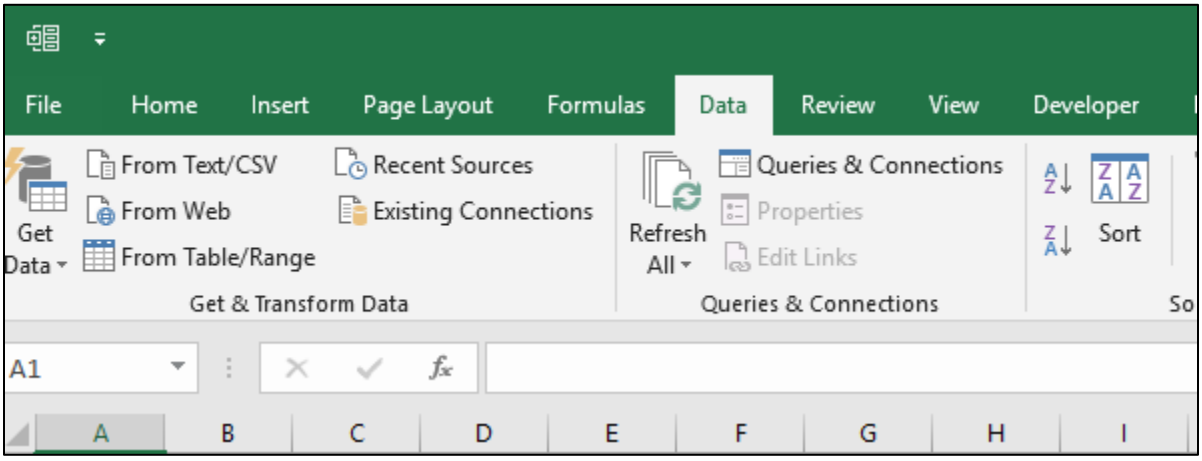

Figure C.4. Data Tab for Correlation Calculation.

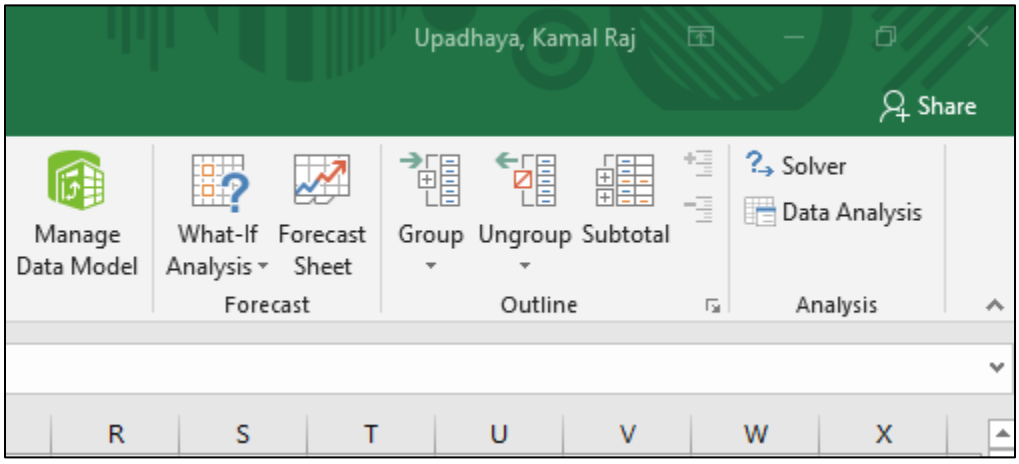

Figure C.5. Data Analysis Ribbon for Correlation Calculation.

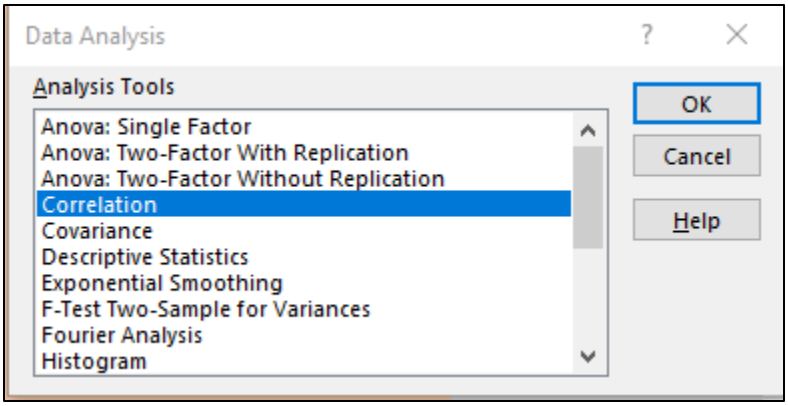

Figure C.6. Data Analysis Dialogue Box with Correlation Option.

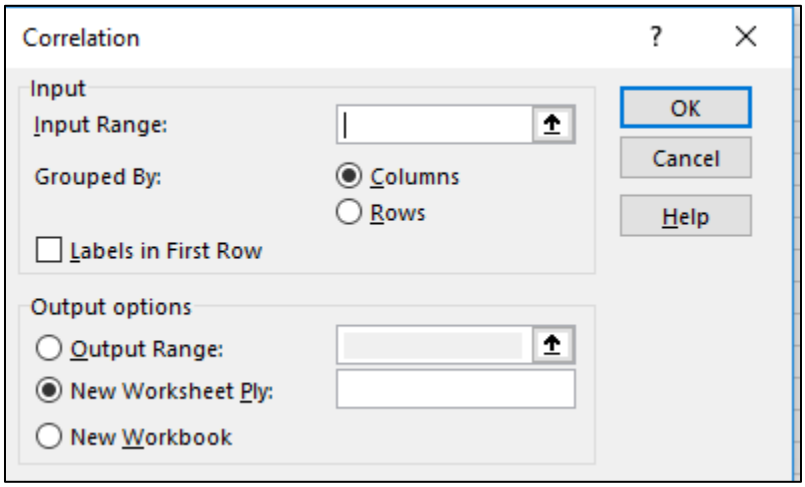

Figure C.7. Correlation Dialogue Box.

APPENDIX D: VBA CODE

This section describes the VBA code used for the dissolved salt concentration calculations. Any of the figures depicted in this section represent Figure C.1.

Sub SolverAutomatev3() #piece of code that is used to perform a specific task: when writing the Sub, it should start with a “Sub” keyword and a name as the procedure name to declare the sub#

' SolverAutomatev3 Macro #syntax, procedure name#

Dim i As Integer #declaring a variable to hold an integer#

For i = 19 To 24057 #starts the loop at cell 19 because the calculation process is for cells 19 to 24,057 in the study#

SolverReset #resets all cell selections and constraints in the Solver parameters after the calculation for previous cell was done to prevent interference from different Solver optimizations#

SolverOk SetCell:="S" & i, MaxMinVal:=2, ValueOf:=0, ByChange:=Range("I" & i, "K" & i), _

Engine:=1, EngineDesc:="GRG Nonlinear" #solverOk defines the cell to optimize, how to optimize it, and what cells to change during the solver optimization#

SolverAdd CellRef:="V" & i, Relation:=3, FormulaText:="0" #adds constraints to the Solver model, in the study, Column V was set to be greater than zero#

SolverAdd CellRef:="X" & i, Relation:=1, FormulaText:="15" #adds constraints to the Solver model, in the study, Column X was set to be less than 15#

SolverSolve (True) #an optional userFinish argument: if userFinish is false or omitted, the dialogue box will appear, asking the user whether to save the optimization. If userFinish is true, the Solver function will end without the dialogue box#

' Approve the solution and avoid the popups

SolverSolve userFinish:=True #stops the Solver function without the dialogue box #

SolverFinish KeepFinal:=1 #keeps the final solution values in the changing cells, replacing any former values#

ActiveWorkbook.Save #saves the calculations for each loop when they are done#

Next i #leads the Solver function to the next cell, until it reaches the final cell for calculations#

End Sub #end of the sub statement#

APPENDIX E: GRAPHS FROM STATISTICAL CALCULATIONS

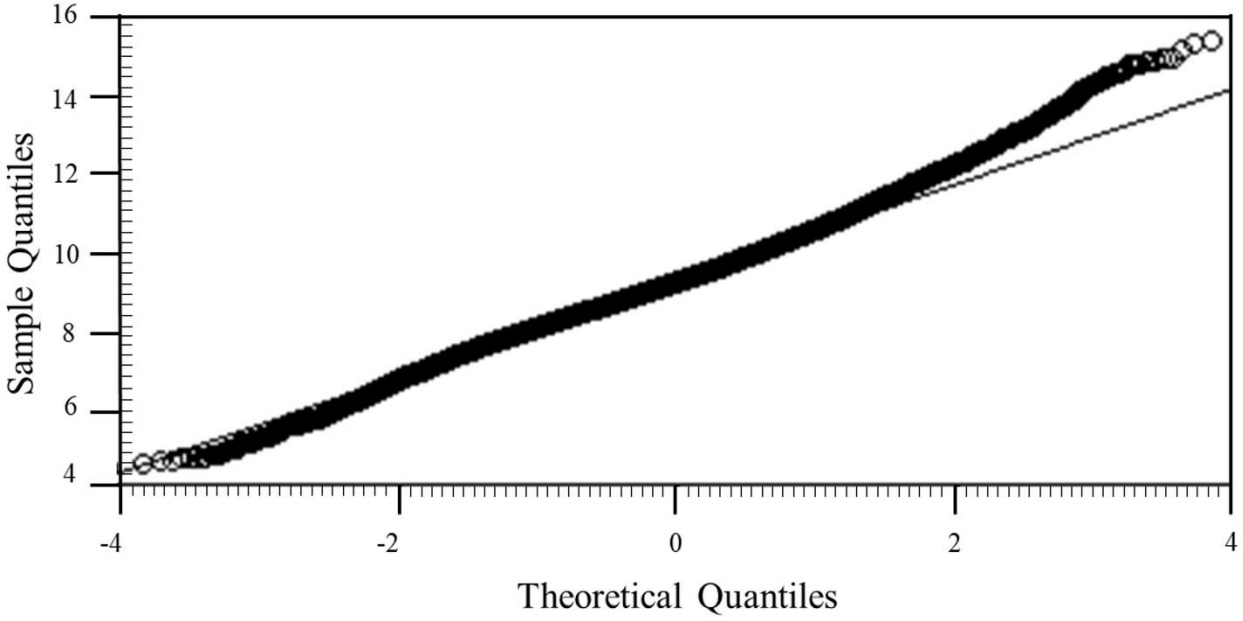

Figure E.1. Q-Q Plot for Logarithm of Area of all Landslides.

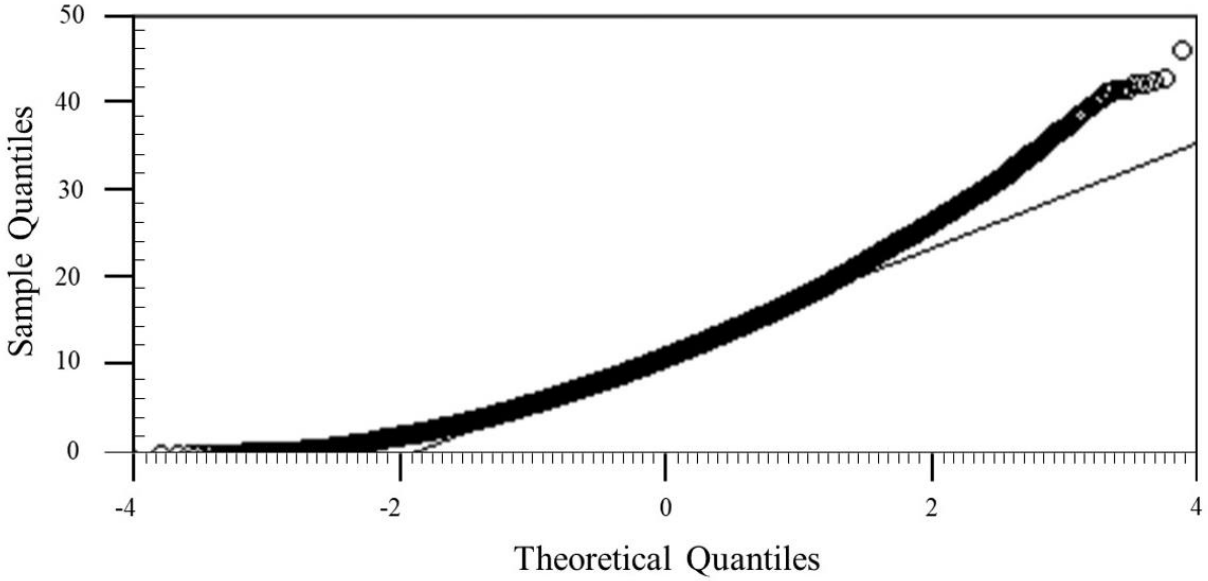

Figure E.2. Q-Q Plot for Slope Inclination of all Landslides.

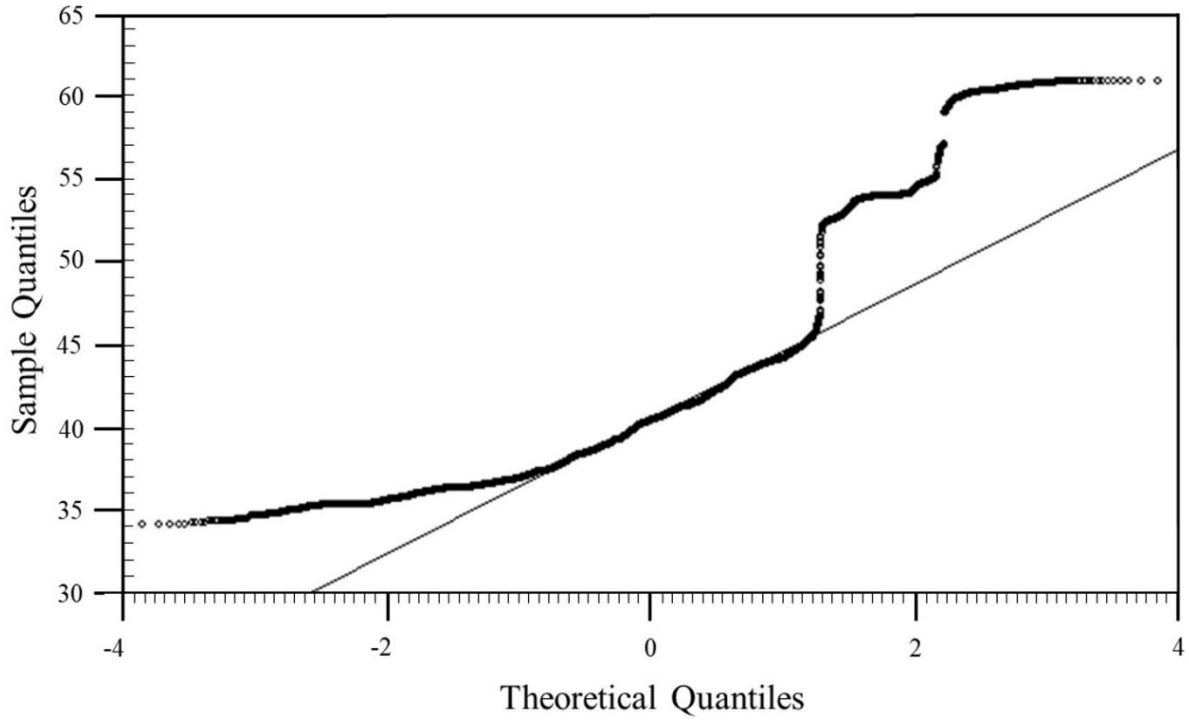

Figure E.3. Q-Q Plot for Distribution of Rainfall at all Landslides.

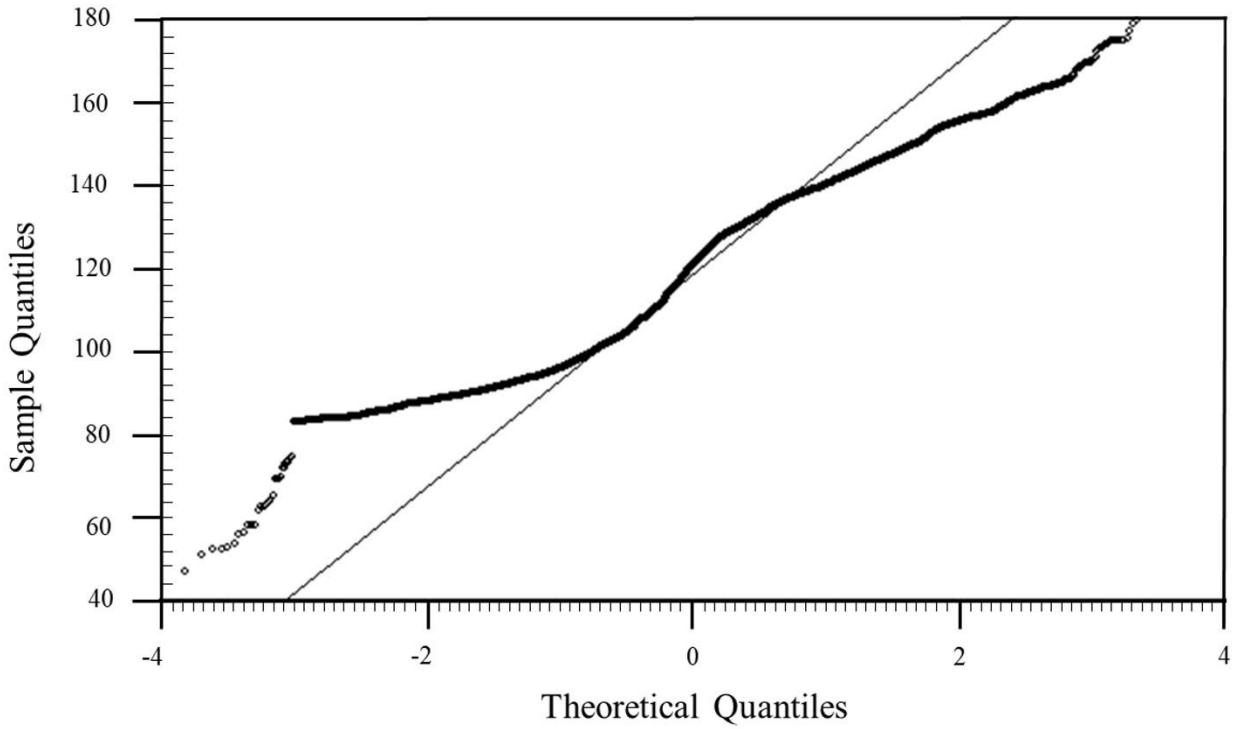

Figure E.4. Q-Q Plot for Distribution of Snowfall at all Landslides.

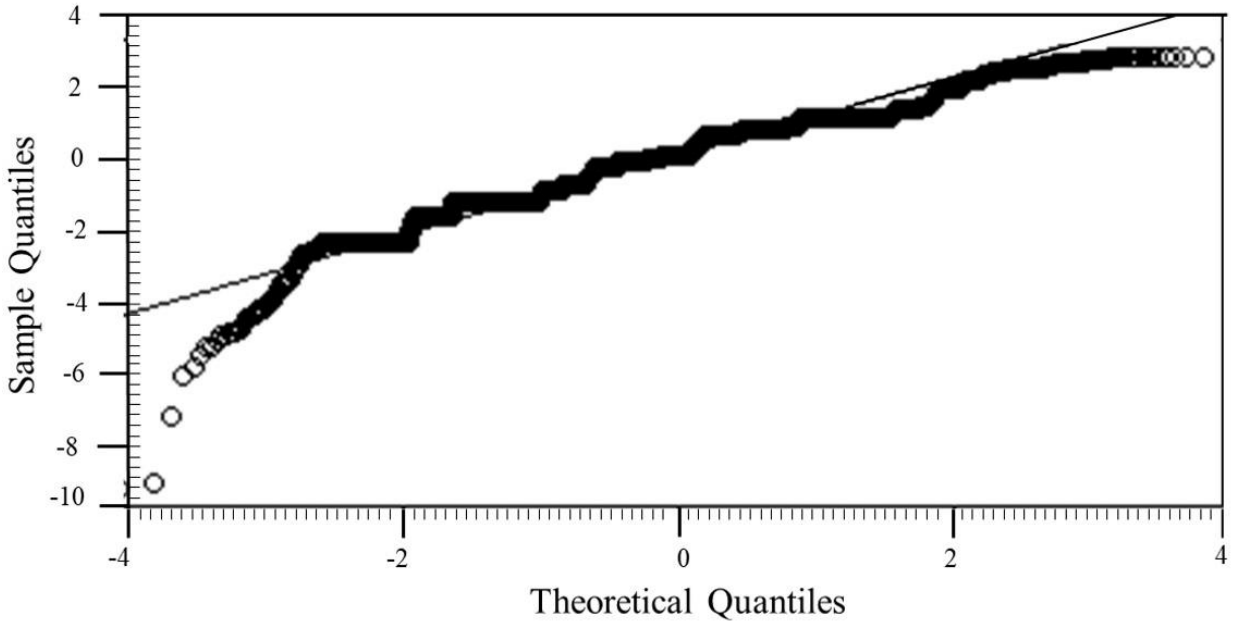

Figure E.5. Q-Q Plot for SAR at all Landslides.

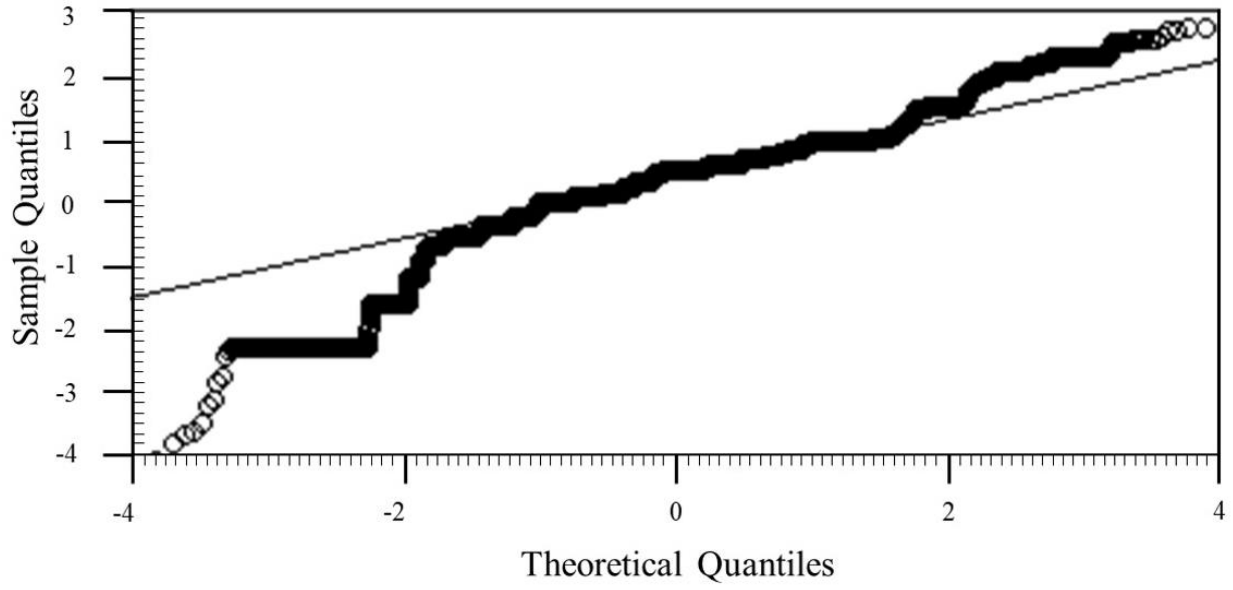

Figure E.6. Q-Q Plot for EC at all Landslides.

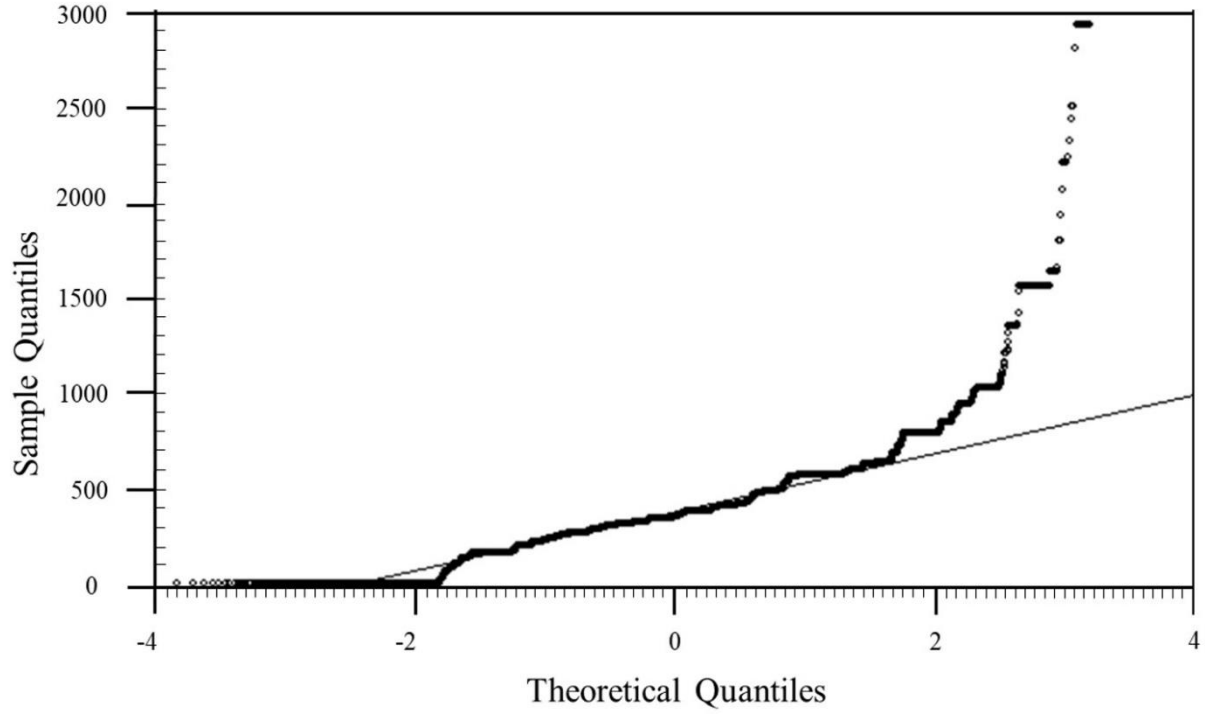

Figure E.7. Q-Q Plot for Calcium Sulfate Concentration at all Landslides.

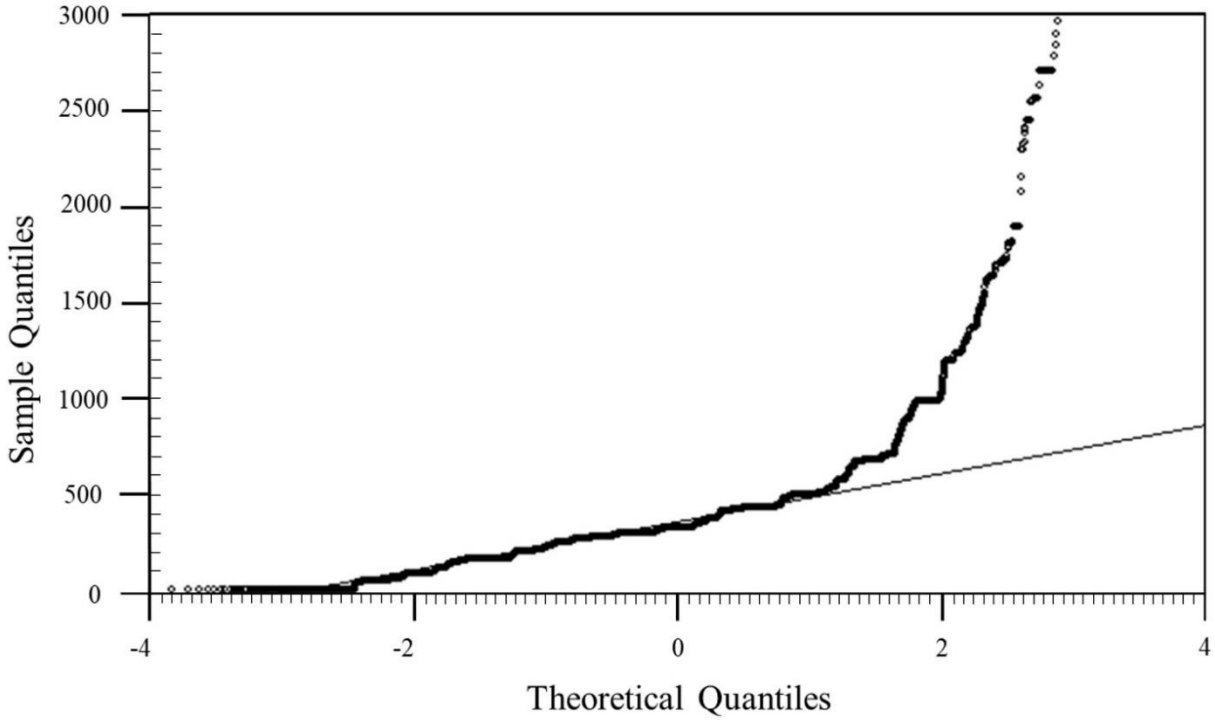

Figure E.8. Q-Q Plot for Magnesium Sulfate Concentration at all Landslides.

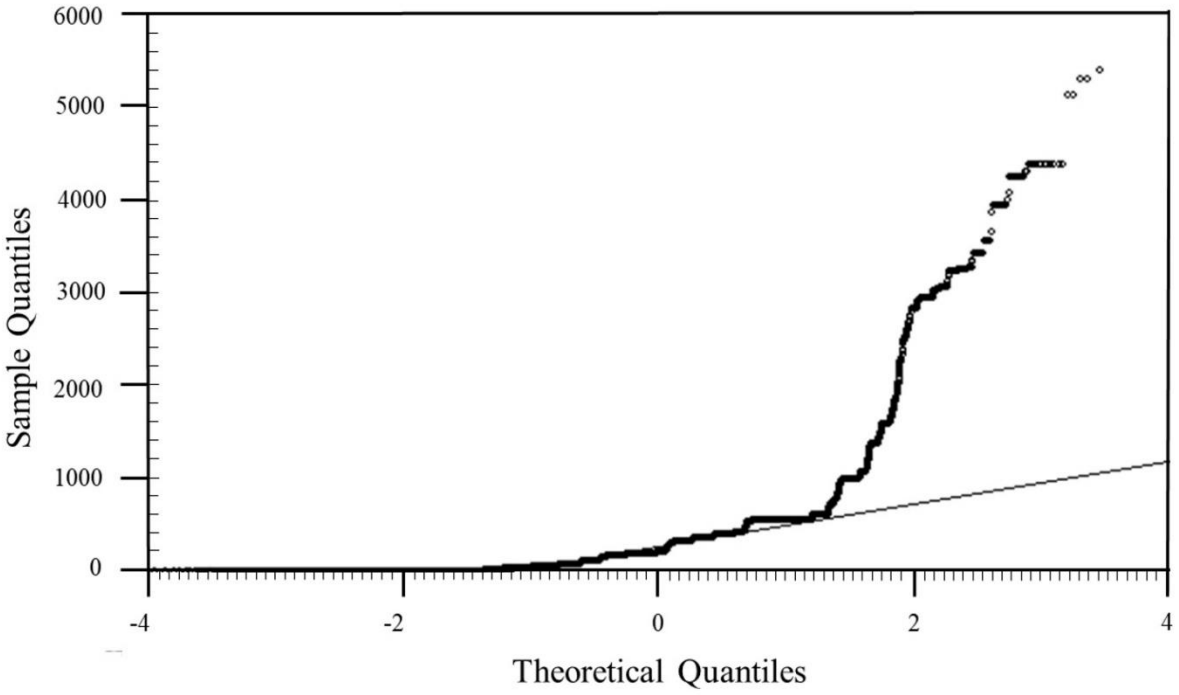

Figure E.9. Q-Q Plot for Sodium Sulfate Concentration at all Landslides.

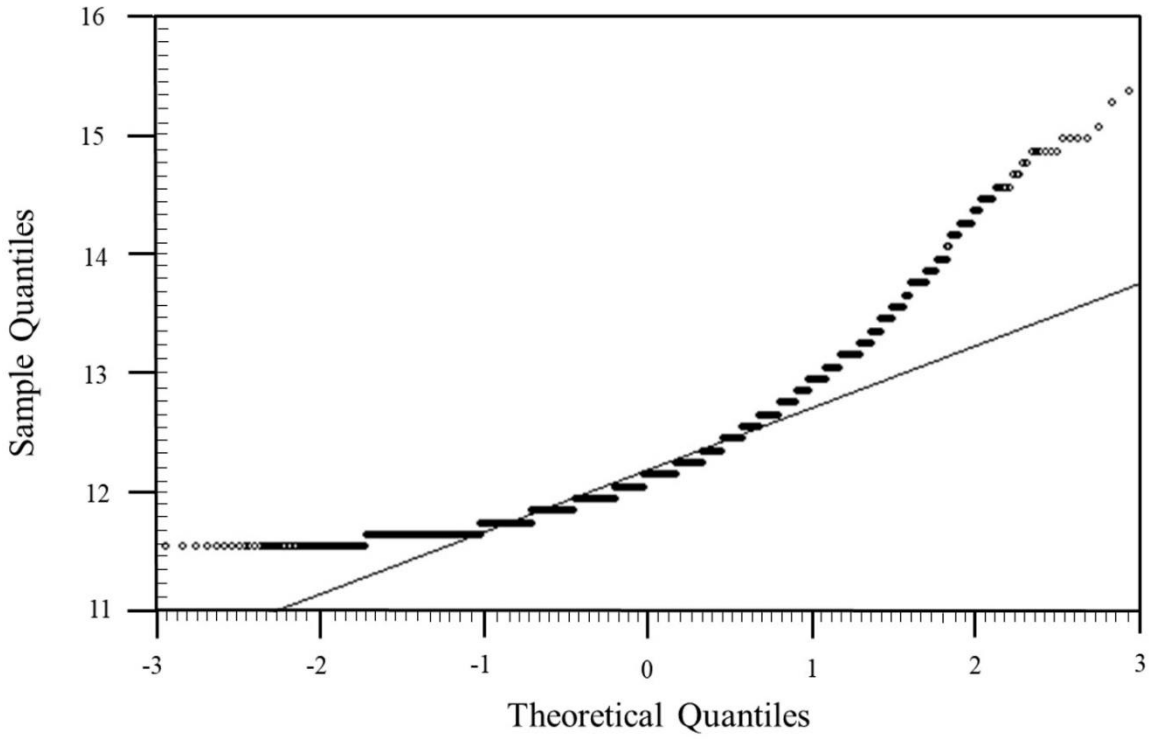

Figure E.10. Q-Q Plot for Logarithm of Area of Large-Scale Landslides.

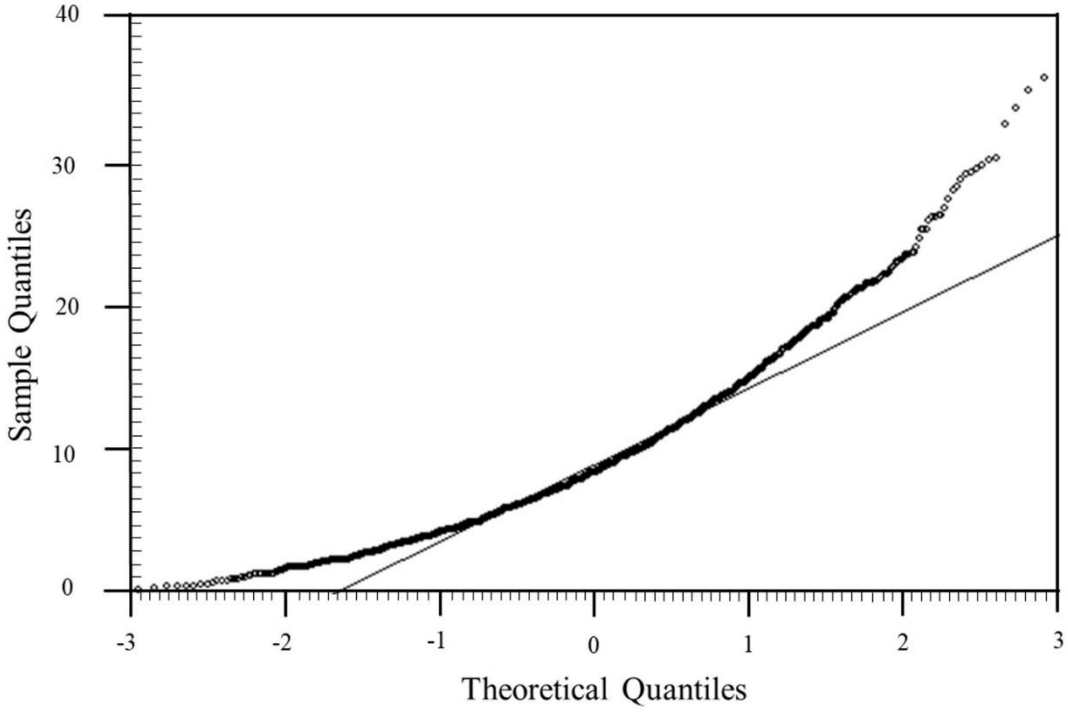

Figure E.11. Q-Q Plot for Slope Inclination of Large-Scale Landslides.

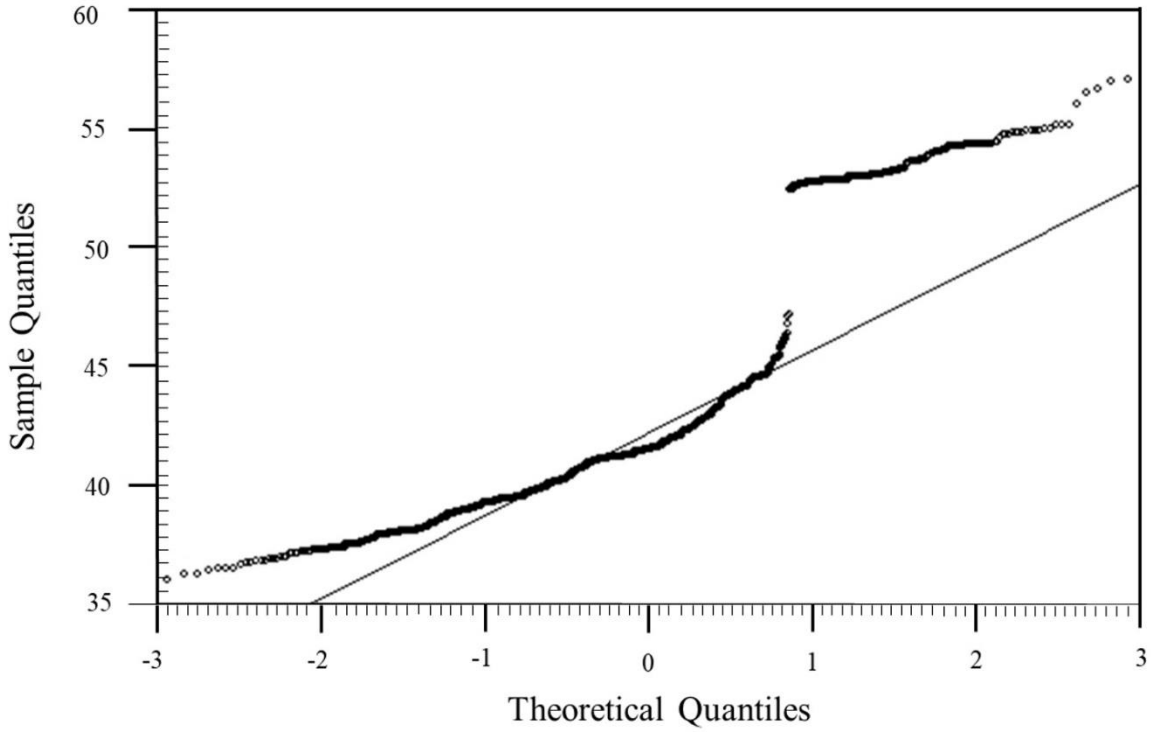

Figure E.12. Q-Q Plot for Distribution of Rainfall at Large-Scale Landslides.

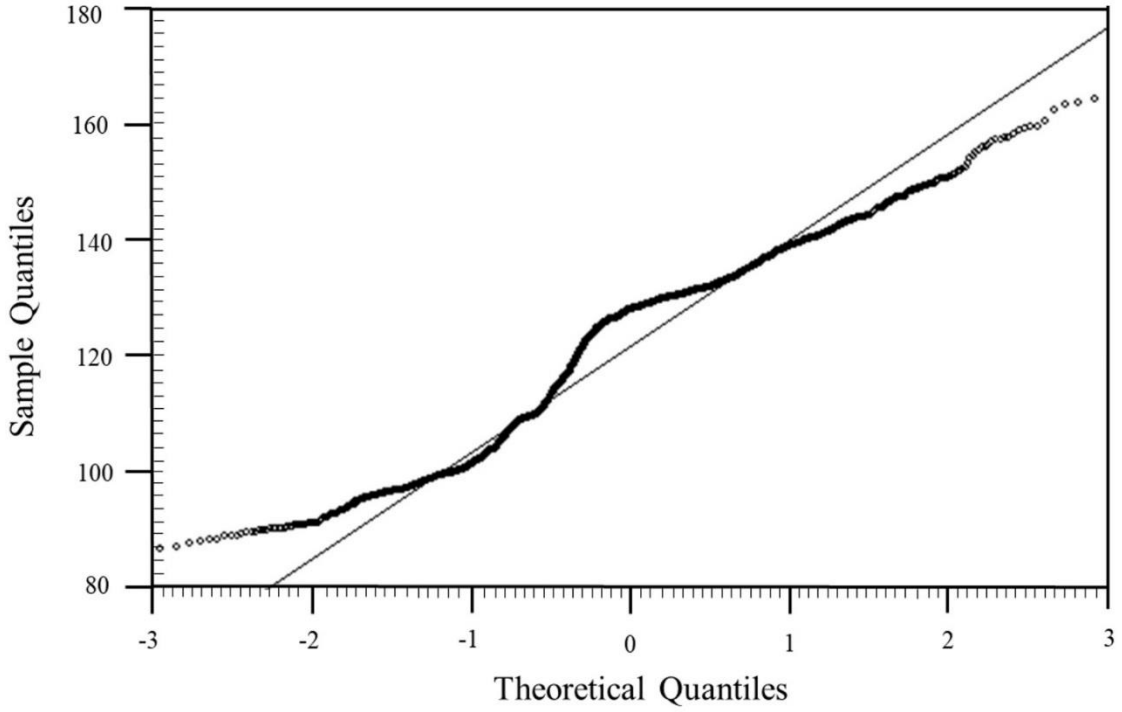

Figure E.13. Q-Q Plot for Distribution of Snowfall at Large-Scale Landslides.

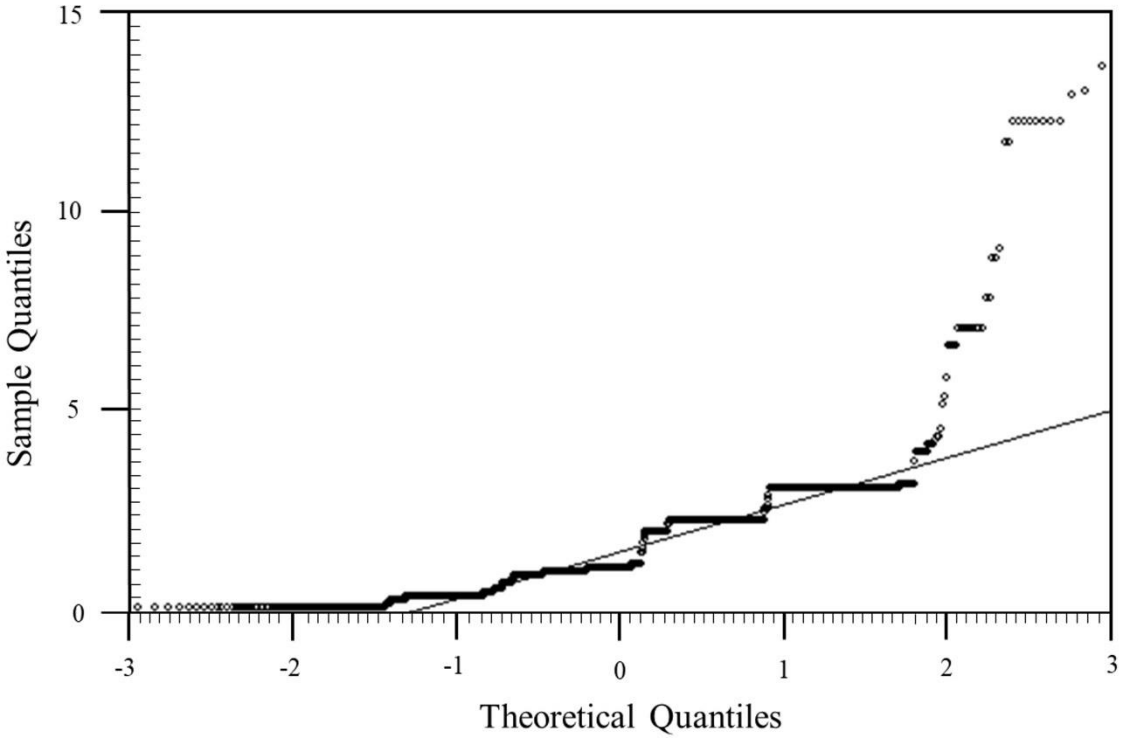

Figure E.14. Q-Q Plot for Distribution of SAR at Large-Scale Landslides.

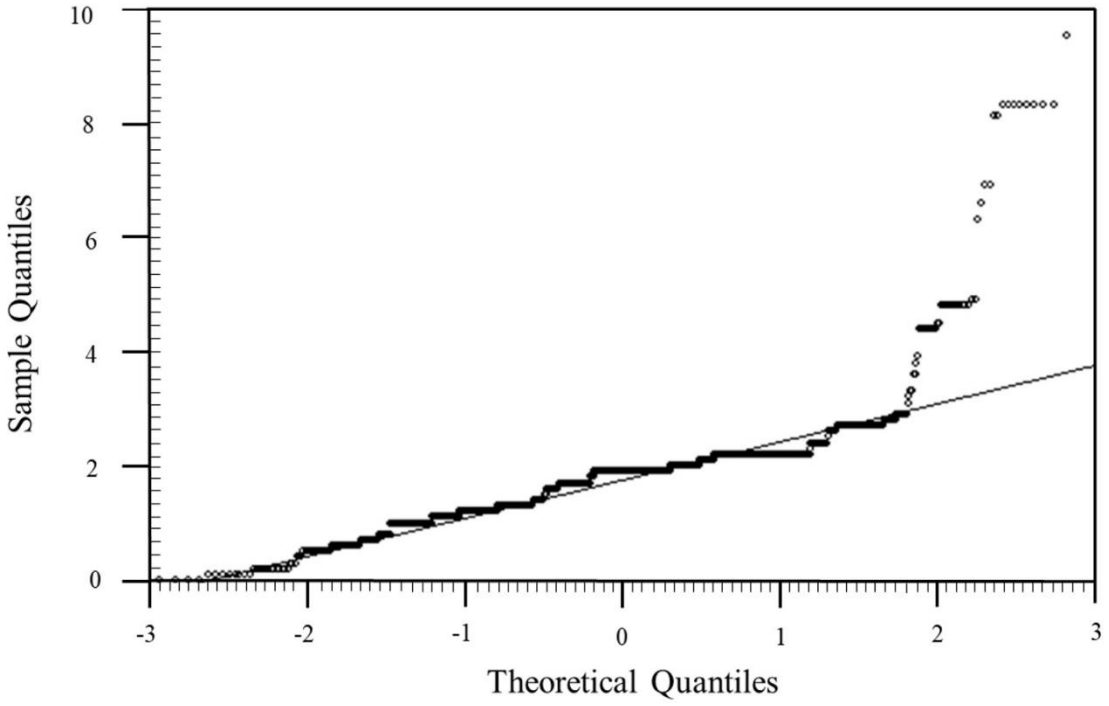

Figure E.15. Q-Q Plot for Distribution of EC at Large-Scale Landslides.

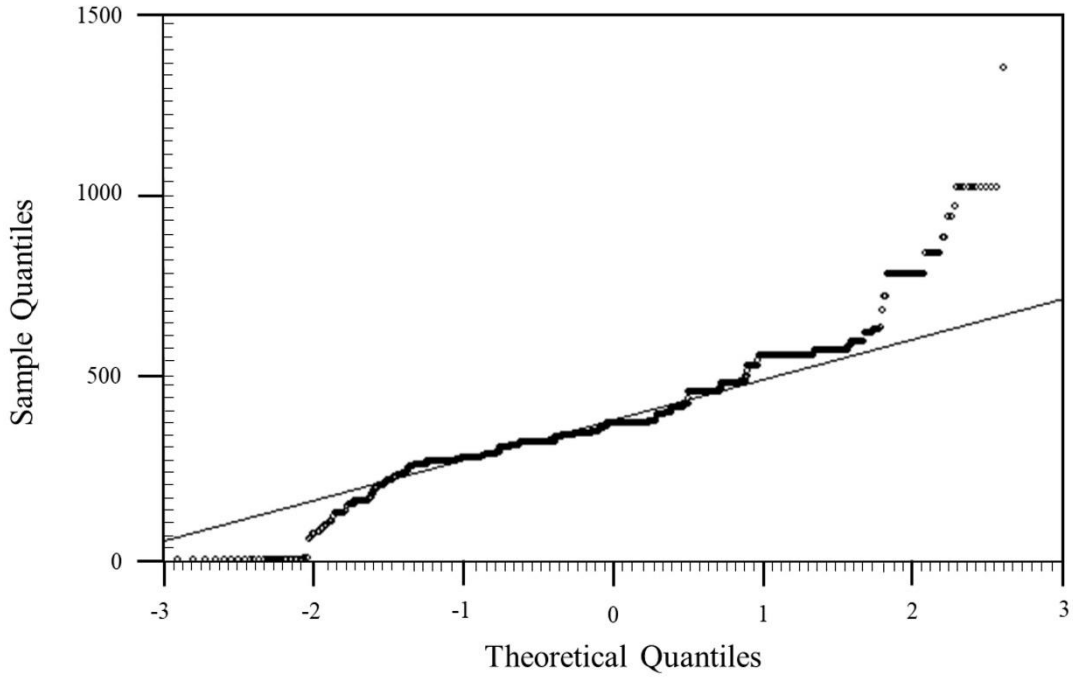

Figure E.16. Q-Q Plot for Distribution of Calcium Sulfate Concentration at Large-Scale Landslides.

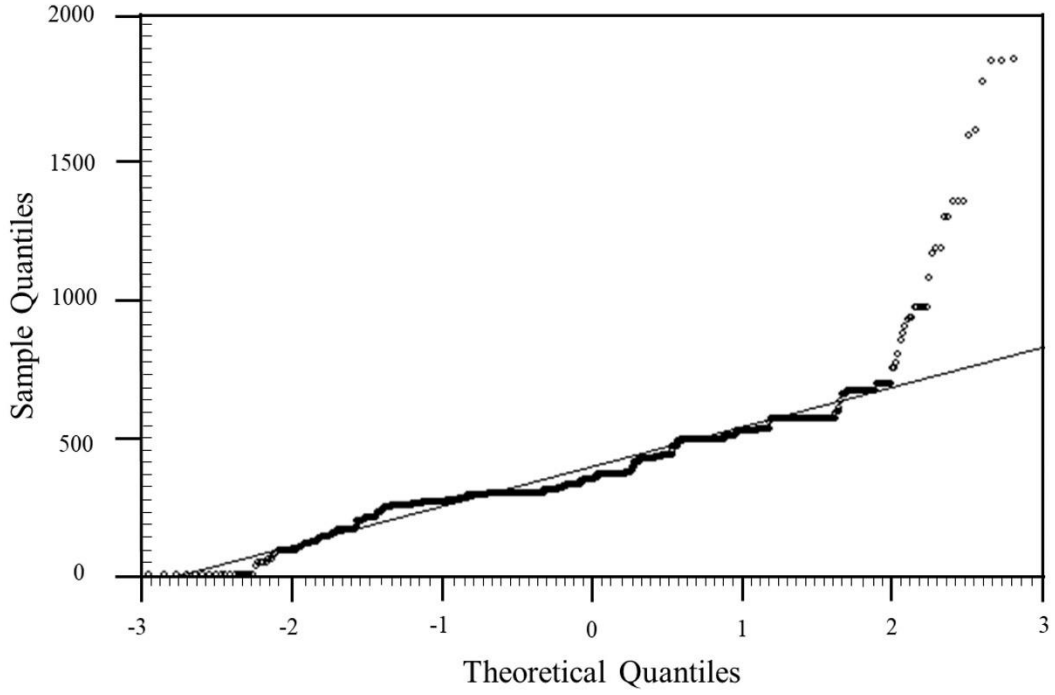

Figure E.17. Q-Q Plot for Distribution of Magnesium Sulfate Concentration at Large-Scale Landslides.

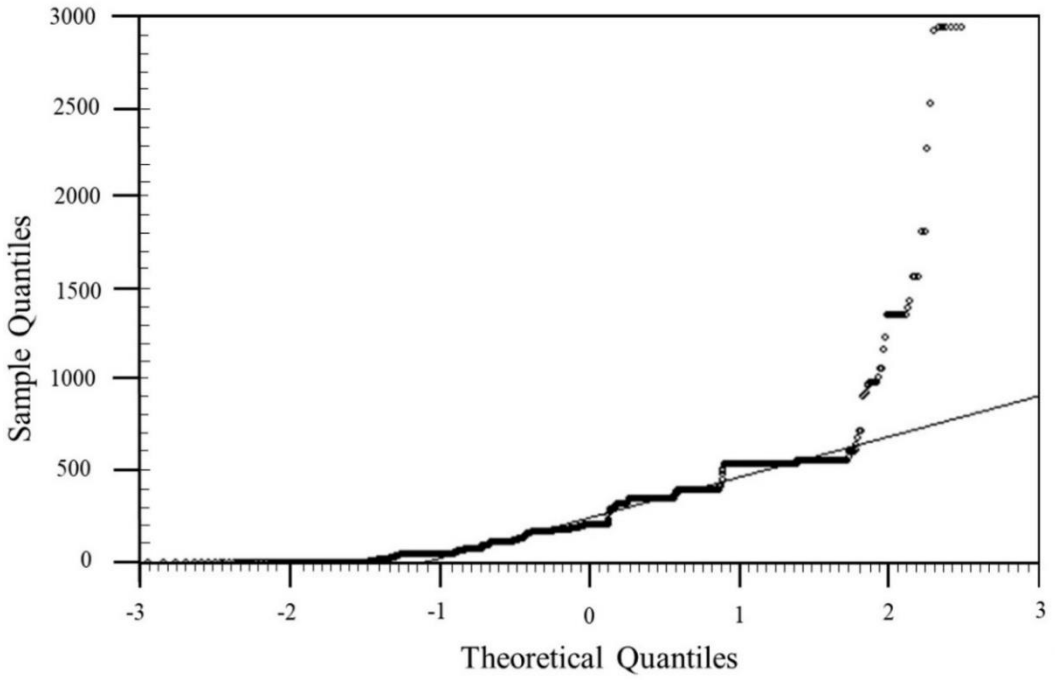

Figure E.18. Q-Q Plot for Distribution of Sodium Sulfate Concentration at Large-Scale Landslides.

APPENDIX F: COMPLETE CORRELATION MATRIX FROM DRAFT PAPER IN CHAPTER 4

Factors	Area	TDS	SAR	Ca^{2+}	Mg^{2+}	Na^{+}	SO^{2-}_4	Slope Inclination	Latitude	Longitude	Belle Fourche-Skull Creek	Bullion Creek Formation	Cannonball Formation	Carlile Formation	Fox Hills Formation	Golden Valley Formation	Greenhorn Formation	Hell Creek Formation	Inyan Kara	Ludlow Formation	Mowry-Skull Creek	Niobrara Formation	Pierre Formation	Piper Formation	Precambrian Rocks	Red River Formation	Sentinel Butte Formation	Slope Formation	Jurassic Sediments	Upper and Middle Tertiary Rock	White River Group	Winnipeg Group	Average Rainfall	Average Snowfall	Adams County	Barnes County	Benson County	Billings County	Bottineau County	Bowman County	Burke County	Burleigh County	Cass County	Cavalier County	Dickey County	Divide County
Area	1.00																																												
TDS	<0.01	1.00																																												
SAR	0.01	0.86	1.00																																											
Ca^{2+}	0.01	0.60	0.29	1.00																																										
Mg^{2+}	<0.01	0.79	0.53	0.36	1.00																																										
Na^{+}	<0.01	0.91	0.97	0.33	0.66	1.00																																									
SO^{2-}_4	<0.01	0.98	0.82	0.59	0.86	0.90	1.00																																								
Slope Inclination	-0.08	-0.04	-0.04	0.03	-0.04	-0.07	-0.05	1.00																																							
Latitude	0.08	-0.12	-0.08	-0.12	-0.07	-0.09	-0.11	0.01	1.00																																						
Longitude	0.05	-0.15	-0.20	-0.13	-0.06	-0.13	-0.13	-0.21	-0.13	1.00																																					
Belle Fourche-Skull Creek	-0.01	-0.09	-0.05	-0.11	-0.08	-0.04	-0.08	-0.09	-0.07	0.27	1.00																																				
Bullion Creek Formation	-0.06	0.06	0.04	0.08	0.04	0.03	0.05	0.06	-0.06	-0.25	-0.05	1.00																																			
Cannonball Formation	<-0.01	-0.11	-0.12	-0.10	-0.07	-0.08	-0.10	<-0.01	-0.18	0.13	-0.02	-0.13	1.00																																		
Carlile Formation	0.07	0.02	-0.02	0.05	0.04	-0.01	0.02	-0.02	0.14	0.18	<-0.01	-0.04	-0.02	1.00																																	
Fox Hills Formation	<-0.01	-0.03	-0.01	-0.07	-0.02	<0.01	-0.03	-0.04	-0.24	0.18	-0.02	-0.10	-0.04	-0.01	1.00																																
Golden Valley Formation	<0.01	-0.02	-0.01	-0.02	<-0.01	-0.01	-0.02	<-0.01	0.03	-0.03	-0.01	-0.07	-0.03	<-0.01	-0.02	1.00																															
Greenhorn Formation	<-0.01	<0.01	<-0.01	0.01	0.01	<-0.01	<0.01	<-0.01	-0.03	0.07	<-0.01	-0.02	<-0.01	<-0.01	<-0.01	<-0.01	1.00																															
Hell Creek Formation	<-0.01	0.07	0.06	<0.01	0.06	0.08	0.07	-0.02	-0.22	0.09	-0.01	-0.09	-0.04	-0.01	-0.03	-0.02	<-0.01	1.00																													
Inyan Kara	<-0.01	-0.06	-0.03	-0.05	-0.04	-0.03	-0.04	-0.05	0.08	0.15	<-0.01	-0.03	-0.01	<-0.01	<-0.01	<-0.01	<-0.01	<-0.01	1.00																													
Ludlow Formation	<-0.01	0.07	0.04	0.11	0.04	0.03	0.06	0.02	-0.12	-0.09	<-0.01	-0.06	-0.02	<-0.01	-0.02	-0.01	<-0.01	-0.02	<-0.01	1.00																												
Mowry-Skull Creek	<-0.01	<0.01	<0.01	<0.01	<-0.01	<0.01	<0.01	<-0.01	<0.01	<-0.01	<-0.01	<-0.01	<-0.01	<-0.01	<-0.01	<-0.01	<-0.01	<-0.01	<-0.01	<-0.01	1.00																											
Niobrara Formation	0.08	0.02	-0.02	0.03	0.04	-0.01	0.02	-0.05	0.08	0.23	<-0.01	-0.05	-0.02	<-0.01	-0.02	-0.01	<-0.01	-0.02	<-0.01	<-0.01	<-0.01	1.00																											
Pierre Formation	0.03	-0.02	-0.10	0.06	0.02	-0.08	-0.02	-0.08	-0.11	0.61	-0.02	-0.15	-0.06	-0.02	-0.05	-0.03	<-0.01	-0.05	-0.01	-0.03	<-0.01	-0.03	1.00																										
Piper Formation	0.00	-0.01	<-0.01	-0.01	<-0.01	<-0.01	-0.01	<-0.01	0.02	0.02	<-0.01	<-0.01	<-0.01	<-0.01	<-0.01	<-0.01	<-0.01	<-0.01	<-0.01	<-0.01	<-0.01	<-0.01	<-0.01	1.00																									
Precambrian Rocks	<-0.01	-0.08	-0.04	-0.10	-0.06	-0.04	-0.07	-0.08	-0.04	0.24	<-0.01	-0.04	-0.02	<-0.01	-0.01	<-0.01	<-0.01	-0.01	<-0.01	<-0.01	<-0.01	<-0.01	-0.02	<-0.01	1.00																								
Red River Formation	<-0.01	-0.07	-0.04	-0.10	-0.06	-0.03	-0.07	-0.07	0.12	0.16	<-0.01	-0.03	-0.01	<-0.01	<-0.01	<-0.01	<-0.01	<-0.01	<-0.01	<-0.01	<-0.01	<-0.01	-0.02	<-0.01	<-0.01	1.00																							
Sentinel Butte Formation	0.02	0.03	0.08	<0.01	<-0.01	0.04	0.02	0.07	0.34	-0.41	-0.09	-0.57	-0.23	-0.07	-0.18	-0.13	-0.03	-0.17	-0.06	-0.11	-0.01	-0.09	-0.28	-0.01	-0.08	-0.06	1.00																					
Slope Formation	-0.02	<-0.01	<-0.01	<0.01	<-0.01	<-0.01	<-0.01	-0.02	-0.12	-0.04	<-0.01	-0.05	-0.02	<-0.01	-0.02	-0.01	<-0.01	-0.01	<-0.01	<-0.01	<-0.01	<-0.01	-0.02	<-0.01	<-0.01	<-0.01	-0.09	1.00																			
Jurassic Sediments	0.00	-0.03	-0.02	-0.04	-0.03	-0.01	-0.03	-0.03	0.04	0.07	<-0.01	-0.01	<-0.01	<-0.01	<-0.01	<-0.01	<-0.01	<-0.01	<-0.01	<-0.01	<-0.01	<-0.01	<-0.01	<-0.01	<-0.01	<-0.01	-0.02	<-0.01	1.00																		
Upper and Middle Tertiary Rock	<0.01	<-0.01	<-0.01	<0.01	<-0.01	<-0.01	<-0.01	<-0.01	-0.03	-0.01	<-0.01	-0.01	<-0.01	<-0.01	<-0.01	<-0.01	<-0.01	<-0.01	<-0.01	<-0.01	<-0.01	<-0.01	<-0.01	<-0.01	<-0.01	<-0.01	-0.02	<-0.01	<-0.01	1.00																	
White River Group	0.05	<-0.01	<0.01	<-0.01	<-0.01	<-0.01	<-0.01	-0.01	-0.07	-0.04	<-0.01	-0.04	-0.02	<-0.01	-0.01	<-0.01	<-0.01	-0.01	<-0.01	<-0.01	<-0.01	<-0.01	-0.02	<-0.01	<-0.01	<-0.01	-0.07	<-0.01	<-0.01	<-0.01	1.00															
Winnipeg Group	<0.01	-0.05	-0.03	-0.06	-0.04	-0.03	-0.05	-0.06	0.05	0.16	<-0.01	-0.03	-0.01	<-0.01	<-0.01	<-0.01	<-0.01	<-0.01	<-0.01	<-0.01	<-0.01	<-0.01	-0.01	<-0.01	<-0.01	<-0.01	-0.05	<-0.01	<-0.01	<-0.01	<-0.01	1.00													
Average Rainfall	0.06	-0.16	-0.19	-0.14	-0.06	-0.13	-0.14	-0.22	-0.09	0.97	0.32	-0.28	0.11	0.17	0.10	-0.01	0.07	0.06	0.12	-0.11	<-0.01	0.22	0.59	0.02	0.28	0.14	-0.33	-0.05	0.05	-0.01	-0.04	0.15	1.00												
Aerage Snowfall	<0.01	-0.21	-0.21	-0.24	-0.10	-0.14	-0.18	-0.09	<-0.01	0.36	-0.06	-0.23	0.24	-0.06	0.21	0.05	-0.01	0.12	-0.01	-0.14	-0.01	-0.05	0.07	<0.01	-0.03	-0.04	0.02	<-0.01	<-0.01	-0.01	-0.04	0.02	0.37	1.00											
Adams County	<0.01	<-0.01	<-0.01	<-0.01	<-0.01	<-0.01	<-0.01	<0.01	0.02	-0.02	<-0.01	<0.01	-0.01	<0.01	<-0.01	<-0.01	<-0.01	<-0.01	<-0.01	0.02	<-0.01	<-0.01	<-0.01	<-0.01	<-0.01	<-0.01	<0.01	<0.01	<-0.01	<-0.01	<0.01	0.02	-0.02	-0.02	1.00										
Barnes County	0.01	<-0.01	-0.01	<-0.01	<-0.01	<-0.01	<-0.01	-0.01	0.00	<-0.01	<0.01	-0.01	<-0.01	<-0.01	<-0.01	0.02	<-0.01	<0.01	0.02	0.02	<-0.01	<-0.01	<-0.01	<-0.01	<-0.01	<-0.01	<0.01	<0.01	0.01	<0.01	0.02	<0.01	<-0.01	<-0.01	<-0.01	-0.02	1.00							
Benson County	<-0.01	<0.01	<0.01	<0.01	<-0.01	<0.01	<-0.01	<-0.01	<0.01	<-0.01	<-0.01	0.01	<-0.01	<-0.01	<-0.01	<-0.01	<-0.01	<-0.01	<-0.01	<-0.01	<-0.01	<-0.01	<-0.01	<-0.01	<-0.01	<-0.01	<-0.01	<-0.01	<-0.01	<-0.01	<-0.01	<-0.01	<-0.01	<-0.01	<-0.01	<-0.01	<-0.01	1.00						
Billings County	<-0.01	<0.01	<0.01	<0.01	<0.01	<0.01	<0.01	<0.01	-0.02	0.01	<0.01	<-0.01	0.01	<-0.01	<0.01	<-0.01	<-0.01	<-0.01	<-0.01	<-0.01	<-0.01	-0.01	<0.01	<-0.01	<-0.01	<-0.01	<-0.01	0.01	<-0.01	<-0.01	-0.01	-0.03	-0.09	<-0.01	1.00									
BottineauCounty	<-0.01	<-0.01	<-0.01	<0.01	<0.01	<-0.01	<-0.01	<0.01	<0.01	<-0.01	<-0.01	<-0.01	<-0.01	<-0.01	<-0.01	<-0.01	<-0.01	<-0.01	<-0.01	<-0.01	<-0.01	<-0.01	<-0.01	<-0.01	<-0.01	<-0.01	<-0.01	<0.01	<-0.01	<-0.01	<-0.01	<-0.01	<-0.01	<-0.01	<-0.01	<-0.01	<-0.01	1.00						
Bowman County	<-0.01	<-0.01	<0.01	<-0.01	<-0.01	<0.01	<-0.01	<-0.01	<0.01	-0.01	<-0.01	<0.01	<-0.01	0.02	<0.01	<-0.01	<-0.01	<-0.01	<-0.01	<-0.01	0.00	<-0.01	<-0.01	0.00	<-0.01	<-0.01	<0.01	<0.01	<-0.01	<-0.01	<-0.01	<-0.01	-0.01	<-0.01	<-0.01	-0.02	<-0.01	-0.03	<-0.01	1.00				
Burke County	<0.01	0.01	<0.01	0.03	<0.01	<0.01	<0.01	<-0.01	<0.01	-0.01	<-0.01	<-0.01	<0.01	<-0.01	<0.01	<-0.01	<-0.01	<-0.01	<-0.01	<-0.01	<-0.01	<-0.01	<-0.01	<-0.01	<-0.01	<0.01	<0.01	<-0.01	<-0.01	<-0.01	<-0.01	0.01	<-0.01	-0.02	-0.01	<-0.01	-0.01	<-0.01	-0.02	<-0.01	<-0.01	1.00		
Burleigh County	0.00	<-0.01	<-0.01	<0.01	<-0.01	<-0.01	<-0.01	<-0.01	-0.01	<0.01	<0.01	<0.01	<0.01	<0.01	<0.01	<0.01	<-0.01	<-0.01	<-0.01	<-0.01	<-0.01	<-0.01	<-0.01	<-0.01	<-0.01	<-0.01	-0.01	<-0.01	<-0.01	<-0.01	<-0.01	<-0.01	0.01	<0.01	<-0.01	<-0.01	<-0.01	-0.01	<-0.01	-0.02	<-0.01	<-0.01	<-0.01	1.00	
Cass County	0.01	<-0.01	<0.01	<-0.01	<-0.01	<-0.01	<-0.01	<0.01	<0.01	<0.01	<0.01	<-0.01	<-0.01	<-0.01	<0.01	<-0.01	<0.01	<-0.01	<0.01	<0.01	<-0.01	<-0.01	<-0.01	<-0.01	<0.01	<-0.01	<-0.01	<-0.01	<-0.01	<-0.01	<-0.01	<0.01	<0.01	<0.01	<-0.01	<-0.01	<-0.01	<-0.01	-0.03	0.00	-0.05	0.00	<-0.01	<-0.01	<-0.01	1.00
Cavalier County	<-0.01	-0.02	-0.02	<-0.01	<-0.01	-0.02	-0.01	-0.01	<-0.01	<0.01	<0.01	0.01	<0.01	<-0.01	-0.01	<0.01	<-0.01	-0.01	0.02	<-0.01	<-0.01	<0.01	<0.01	<-0.01	<-0.01	<-0.01	-0.01	<0.01	<-0.01	<-0.01	0.01	<0.01	<-0.01	<0.01	<0.01	<-0.01	<-0.01	<-0.01	-0.03	0.00	-0.05	0.00	<-0.01	<-0.01	<-0.01	-0.01	1.00	
Dickey County	<0.01	<-0.01	<0.01	<-0.01	<-0.01	<-0.01	<-0.01	<-0.01	<-0.01	0.01	<0.01	<-0.01	<-0.01	<-0.01	<-0.01	<-0.01	<-0.01	<-0.01	0.01	<0.01	<-0.01	<-0.01	0.01	<-0.01	<0.01	<-0.01	<-0.01	<-0.01	<-0.01	<-0.01	<-0.01	0.01	0.01	<0.01	<-0.01	<-0.01	<-0.01	<-0.01	<-0.01	<-0.01	-0.02	<-0.01	<-0.01	<-0.01	<-0.01	<-0.01	<-0.01	1.00	
Divide County	<-0.01	<-0.01	<-0.01	<-0.01	-0.01	<-0.01	<-0.01	<-0.01	0.03	-0.01	<0.01	<0.01	<-0.01	0.02	<-0.01	<-0.01	<-0.01	<-0.01	<-0.01	<-0.01	<-0.01	<-0.01	<0.01	<-0.01	<-0.01	<-0.01	<0.01	<0.01	<-0.01	<-0.01	<-0.01	<-0.01	<-0.01	-0.02	-0.02	<-0.01	-0.01	<-0.01	-0.02	<-0.01	<-0.01	<-0.01	<-0.01	<-0.01	<-0.01	<-0.01	<-0.01	1.00
Dunn County	<-0.01	-0.01	-0.02	<-0.01	<-0.01	<-0.01	<-0.01	-0.01	-0.01	0.01	<-0.01	<0.01	<-0.01	-0.02	<0.01	0.01	<-0.01	<0.01	0.02	-0.01	0.01	-0.02	<0.01	0.01	<0.01	<-0.01	<-0.01	<0.01	<-0.01	<-0.01	0.01	<0.01	0.01	0.02	-0.02	-0.06	<-0.01	-0.11	<-0.01	-0.02	-0.02	-0.01	-0.03	-0.03	-0.01	-0.02
Emmons County	<-0.01	<-0.01	<-0.01	0.00	<-0.01	<-0.01	<-0.01	<0.01	-0.01	<0.01	<-0.01	<0.01	<-0.01	<-0.01	<-0.01	<-0.01	<0.01	<0.01	<-0.01	<0.01	<-0.01	<-0.01	0.01	<-0.01	<0.01	<-0.01	<-0.01	<-0.01	<0.01	<-0.01	<-0.01	<-0.01	-0.01	<0.01	<0.01	<-0.01	<-0.01	-0.04	<-0.01	-0.08	<-0.01	-0.01	-0.01	<-0.01	-0.02	-0.02	-0.01	-0.01
Golden Valley County	<0.01	<0.01	<0.01	<0.01	<0.01	<0.01	<0.01	<-0.01	<-0.01	<0.01	<-0.01	<-0.01	<0.01	<-0.01	<-0.01	<-0.01	<-0.01	<-0.01	<-0.01	<-0.01	<-0.01	0.02	<-0.01	<-0.01	<0.01	<0.01	<0.01	<-0.01	<-0.01	<-0.01	<-0.01	<0.01	-0.01	<0.01	<0.01	-0.02	-0.06	<-0.01	-0.10	<-0.01	-0.02	-0.02	-0.01	-0.03	-0.03	-0.01	-0.01
Grand Forks County	<0.01	<0.01	<-0.01	<-0.01	<0.01	<0.01	<0.01	<0.01	0.01	<-0.01	<-0.01	<0.01	<-0.01	<0.01	-0.01	<-0.01	<-0.01	<0.01	<-0.01	<-0.01	<-0.01	<-0.01	<-0.01	<-0.01	<-0.01	<-0.01	<0.01	<0.01	<-0.01	<-0.01	<-0.01	<-0.01	0.01	<-0.01	-0.01	<-0.01	-0.03	<-0.01	<-0.01	<-0.01	<-0.01	<-0.01	<-0.01	<-0.01	<-0.01	<-0.01	<-0.01
Grant County	<-0.01	<0.01	<0.01	<0.01	<0.01	<0.01	<0.01	<-0.01	<0.01	<0.01	<0.01	<-0.01	0.01	<0.01	<-0.01	<-0.01	<0.01	<-0.01	0.01	<-0.01	<-0.01	0.01	<-0.01	<-0.01	<0.01	<-0.01	<-0.01	<0.01	<-0.01	<-0.01	<-0.01	<0.01	<-0.01	-0.01	<-0.01	-0.01	-0.04	<-0.01	-0.07	<-0.01	-0.01	-0.01	<-0.01	-0.02	-0.02	<-0.01	-0.01
Griggs County	<-0.01	<0.01	<0.01	<-0.01	<-0.01	<0.01	<0.01	<0.01	<-0.01	<-0.01	<-0.01	<0.01	-0.01	<-0.01	<-0.01	<0.01	<-0.01	<0.01	<-0.01	0.02	<-0.01	<-0.01	<0.01	<-0.01	<-0.01	<-0.01	<-0.01	<0.01	0.05	<-0.01	0.01	<-0.01	<-0.01	<-0.01	<-0.01	-0.02	<-0.01	-0.03	<-0.01	<-0.01	<-0.01	<-0.01	<-0.01	<-0.01	<-0.01	<-0.01	<-0.01	<-0.01
Hettinger County	<-0.01	<-0.01	<-0.01	0.00	<-0.01	<-0.01	<-0.01	<0.01	0.05	-0.04	<-0.01	<0.01	<-0.01	<-0.01	0.01	<-0.01	<-0.01	-0.02	<-0.01	0.02	<-0.01	<-0.01	<-0.01	<-0.01	<-0.01	<-0.01	<-0.01	0.01	<0.01	<-0.01	<-0.01	0.01	<0.01	-0.04	-0.04	<-0.01	-0.02	<-0.01	-0.04	<-0.01	<-0.01	<-0.01	-0.01	-0.01	<-0.01	<-0.01	<-0.01	<-0.01
LaMoure County	<-0.01	<-0.01	<-0.01	<-0.01	<-0.01	<-0.01	<-0.01	<-0.01	<0.01	<-0.01	0.00	<-0.01	<-0.01	<-0.01	<-0.01	<-0.01	<-0.01	<-0.01	<-0.01	<-0.01	<-0.01	<-0.01	<-0.01	<-0.01	<-0.01	<-0.01	<0.01	0.00	<-0.01	<-0.01	<-0.01	<-0.01	<-0.01	<0.01	0.00	<-0.01	<-0.01	<-0.01	<-0.01	<-0.01	<-0.01	<-0.01	<-0.01	<-0.01	<-0.01	<-0.01	<-0.01	<-0.01
Logan County	<0.01	<0.01	<0.01	<-0.01	0.01	<0.01	<0.01	<-0.01	<0.01	<-0.01	<-0.01	-0.01	<-0.01	<-0.01	<-0.01	0.02	<-0.01	<-0.01	<-0.01	<-0.01	<-0.01	<-0.01	<-0.01	<-0.01	<-0.01	<-0.01	0.01	<-0.01	<-0.01	<-0.01	<-0.01	<-0.01	<-0.01	<-0.01	<-0.01	<-0.01	<-0.01	<-0.01	<-0.01	<-0.01	<-0.01	<-0.01	<-0.01	<-0.01	<-0.01	<-0.01	<-0.01	<-0.01

Legend

- Strong Positive Correlation
- Moderate Positive Correlation
- Strong Negative Correlation
- Moderate Negative Correlation

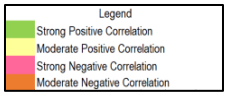

Factors	Area	TDS	SAR	Ca^{2+}	Mg^{2-}	Na^{-}	SO^{2-}_4	Slope Inclination	Latitude	Longitude	Belle Fourche-Skull Creek	Bullion Creek Formation	Cannonball Formation	Carlile Formation	Fox Hills Formation	Golden Valley Formation	Greenhorn Formation	Hell Creek Formation	Inyan Kara	Ludlow Formation	Mowry-Skull Creek	Niobrara Formation	Pierre Formation	Piper Formation	Precambrian Rocks	Red River Formation	Sentinel Butte Formation	Slope Formation	Jurassic Sediments	Upper and Middle Tertiary Rock	White River Group	Winnipeg Group	Average Rainfall	Average Snowfall	Adams County	Barnes County	Benson County	Billings County	Bottineau County	Bowman County	Burke County	Burleigh County	Cass County	Cavalier County	Dickey County	Divide County
McHenry County	<0.01	<-0.01	<-0.01	<0.01	<0.01	<-0.01	<0.01	<-0.01	<0.01	<-0.01	<0.01	<0.01	<-0.01	0.01	<0.01	0.01	<-0.01	<-0.01	<-0.01	<0.01	<-0.01	<-0.01	<-0.01	<-0.01	<-0.01	<-0.01	0.00	<-0.01	<-0.01	<-0.01	<-0.01	<-0.01	<-0.01	<0.01	<-0.01	<-0.01	<-0.01	-0.02	<-0.01	<-0.01	<-0.01	<-0.01	<-0.01	<-0.01	<-0.01	<-0.01
McIntosh County	0.00	<-0.01	<0.01	<-0.01	<-0.01	<0.01	<-0.01	<-0.01	-0.01	<0.01	<-0.01	<0.01	0.01	<-0.01	0.01	<-0.01	<-0.01	<-0.01	0.00	<-0.01	<-0.01	<-0.01	<-0.01	<-0.01	<-0.01	<-0.01	<-0.01	<-0.01	<-0.01	<-0.01	<-0.01	<-0.01	0.00	<0.01	<0.01	<-0.01	<-0.01	<-0.01	<-0.01	<-0.01	0.00	<-0.01	<-0.01	0.00	<-0.01	<-0.01
McKenzie County	<-0.01	<-0.01	<0.01	-0.01	<-0.01	<0.01	<-0.01	<0.01	<-0.01	<0.01	<0.01	-0.02	<-0.01	-0.02	<0.01	<-0.01	<0.01	<0.01	<-0.01	-0.01	<0.01	<0.01	<0.01	<-0.01	0.00	<0.01	0.02	<-0.01	≤0.01	<0.01	<-0.01	<-0.01	0.01	0.02	-0.04	-0.12	<-0.01	-0.21	<-0.01	-0.04	-0.03	-0.03	-0.06	-0.06	-0.03	-0.03
McLean County	<0.01	<0.01	<-0.01	0.01	<0.01	<0.01	≤0.01	0.00	0.01	-0.02	<-0.01	0.02	<0.01	0.02	<-0.01	-0.01	0.01	-0.01	<-0.01	0.01	<-0.01	0.02	-0.01	<-0.01	<-0.01	<-0.01	<-0.01	<-0.01	<-0.01	<-0.01	<-0.01	<0.01	<-0.01	-0.02	-0.02	<-0.01	-0.02	0.00	-0.04	0.00	<-0.01	<-0.01	<-0.01	-0.01	-0.01	<-0.01	<-0.01
Mercer County	<0.01	<0.01	0.01	<-0.01	<0.01	<0.01	<0.01	<-0.01	<-0.01	<-0.01	<-0.01	<0.01	<-0.01	<-0.01	<-0.01	<-0.01	<0.01	<-0.01	<-0.01	<0.01	<-0.01	<-0.01	<0.01	<-0.01	<-0.01	<-0.01	<0.01	<-0.01	<0.01	0.02	<-0.01	<-0.01	<-0.01	<-0.01	-0.02	-0.04	<-0.01	-0.08	<-0.01	-0.01	-0.01	<-0.01	-0.02	-0.02	-0.01	-0.01
Morton County	<-0.01	<0.01	<0.01	<-0.01	<0.01	<0.01	<0.01	<0.01	<-0.01	<0.01	<0.01	-0.01	<0.01	<0.01	0.01	<0.01	<-0.01	<-0.01	<-0.01	<-0.01	<-0.01	<0.01	<0.01	0.01	<0.01	<0.01	<0.01	<-0.01	<-0.01	<0.01	-0.01	<-0.01	0.01	<0.01	-0.02	-0.06	<-0.01	-0.12	<-0.01	-0.02	-0.02	-0.01	-0.03	-0.04	-0.02	-0.02
Mountrail County	<0.01	<-0.01	<0.01	<-0.01	<0.01	0.00	<0.01	<0.01	<-0.01	<0.01	<-0.01	<-0.01	0.01	<-0.01	<0.01	<-0.01	<-0.01	<0.01	<-0.01	<-0.01	<-0.01	<-0.01	<0.01	<-0.01	<-0.01	<0.01	<0.01	<-0.01	<-0.01	<-0.01	<-0.01	<0.01	<0.01	<0.01	-0.02	-0.05	<-0.01	-0.08	<-0.01	-0.01	-0.01	-0.01	-0.02	-0.03	-0.01	-0.01
Oliver County	<-0.01	<-0.01	<-0.01	0.00	<-0.01	<-0.01	<-0.01	<-0.01	<0.01	<0.01	<0.01	<-0.01	0.01	0.02	-0.01	<-0.01	<-0.01	<0.01	<0.01	<-0.01	<-0.01	<-0.01	<-0.01	<-0.01	<-0.01	<0.01	<-0.01	<-0.01	<-0.01	<-0.01	0.01	<0.01	<-0.01	<0.01	<0.01	-0.01	-0.03	<-0.01	-0.05	<-0.01	<-0.01	<-0.01	-0.01	-0.02	<-0.01	<-0.01
Pembina County	0.00	<-0.01	<-0.01	-0.02	<-0.01	<-0.01	<-0.01	-0.03	<-0.01	0.02	0.04	<0.01	<-0.01	<-0.01	<-0.01	<-0.01	<-0.01	<0.01	<-0.01	<-0.01	<-0.01	<-0.01	<-0.01	0.00	<-0.01	0.02	<-0.01	<-0.01	<-0.01	<-0.01	<-0.01	<0.01	<-0.01	<0.01	<0.01	<-0.01	-0.01	<-0.01	-0.02	<-0.01	<-0.01	<-0.01	<-0.01	<-0.01	<-0.01	<-0.01	<-0.01
Ransom County	<-0.01	<-0.01	<-0.01	<0.01	<-0.01	<-0.01	<-0.01	-0.01	<0.01	<0.01	<-0.01	<0.01	<-0.01	<-0.01	<-0.01	<-0.01	<-0.01	<-0.01	0.03	<-0.01	<-0.01	0.01	<0.01	<-0.01	<-0.01	<-0.01	<-0.01	<-0.01	<-0.01	<-0.01	<-0.01	<0.01	<-0.01	<0.01	<0.01	<-0.01	<-0.01	<-0.01	-0.01	<-0.01	<-0.01	<-0.01	<-0.01	<-0.01	<-0.01	<-0.01	<-0.01
Renville County	<0.01	<0.01	<-0.01	<0.01	<0.01	<-0.01	<0.01	<-0.01	<-0.01	0.01	<-0.01	<-0.01	<-0.01	<-0.01	<-0.01	<-0.01	<-0.01	0.02	0.00	<-0.01	<-0.01	<-0.01	0.02	<-0.01	<-0.01	<-0.01	<-0.01	<-0.01	<-0.01	<-0.01	<-0.01	<-0.01	0.00	<0.01	<0.01	<-0.01	<-0.01	<-0.01	<-0.01	<-0.01	<-0.01	<-0.01	<-0.01	0.00	<-0.01	<-0.01
Richland County	<-0.01	<-0.01	<-0.01	<-0.01	<-0.01	<-0.01	<-0.01	<0.01	0.01	-0.01	<-0.01	<0.01	<-0.01	<-0.01	<-0.01	<-0.01	<-0.01	<-0.01	<-0.01	0.02	<-0.01	<-0.01	<-0.01	<-0.01	<-0.01	<-0.01	<-0.01	<-0.01	<-0.01	<-0.01	<-0.01	<-0.01	<-0.01	<-0.01	-0.02	<-0.01	<-0.01	<-0.01	-0.01	<-0.01	<-0.01	<-0.01	<-0.01	<-0.01	<-0.01	<-0.01	<-0.01
Rolette County	<0.01	0.02	<0.01	0.02	0.02	<0.01	0.02	-0.01	<0.01	<-0.01	<-0.01	0.02	<-0.01	<-0.01	<0.01	0.01	0.00	<-0.01	<-0.01	<-0.01	<-0.01	0.02	<-0.01	<-0.01	<-0.01	<-0.01	-0.01	<-0.01	<-0.01	<-0.01	<-0.01	<-0.01	<-0.01	<-0.01	-0.01	-0.02	<-0.01	<-0.01	<-0.01	<-0.01	<-0.01	<-0.01	<-0.01	<-0.01	<-0.01	<-0.01	<-0.01
Sioux County	<-0.01	<0.01	<-0.01	<0.01	<0.01	<0.01	<0.01	0.01	<0.01	<-0.01	<-0.01	<0.01	<-0.01	<0.01	<-0.01	<-0.01	<-0.01	-0.01	<-0.01	<-0.01	<-0.01	<0.01	<0.01	<-0.01	<-0.01	<0.01	<-0.01	<-0.01	<-0.01	<-0.01	<-0.01	<0.01	<0.01	<-0.01	<0.01	<-0.01	-0.02	<-0.01	-0.03	<-0.01	<-0.01	<-0.01	<-0.01	<-0.01	<-0.01	<-0.01	<-0.01
Slope County	<-0.01	<0.01	<0.01	<0.01	<0.01	<0.01	<0.01	0.00	<0.01	<-0.01	<-0.01	0.02	<0.01	<0.01	<-0.01	<-0.01	0.00	<0.01	<-0.01	0.00	<-0.01	<-0.01	<-0.01	<-0.01	<-0.01	<0.01	-0.01	<-0.01	<0.01	<0.01	<0.01	<0.01	<0.01	<-0.01	-0.01	-0.02	-0.05	<-0.01	-0.09	<-0.01	-0.01	-0.01	-0.02	-0.03	-0.01	-0.01
Stark County	<0.01	<-0.01	<-0.01	<-0.01	<-0.01	<-0.01	<-0.01	<-0.01	0.01	-0.02	<-0.01	<0.01	-0.01	<0.01	<-0.01	-0.01	<-0.01	<-0.01	<-0.01	0.02	<-0.01	<-0.01	-0.01	0.02	<0.01	<-0.01	0.01	<-0.01	<-0.01	<-0.01	<-0.01	<-0.01	0.01	-0.02	-0.02	-0.01	-0.03	<-0.01	-0.06	<-0.01	-0.01	<-0.01	<-0.01	-0.02	-0.02	<-0.01	<-0.01
Steele County	<-0.01	0.03	0.02	0.03	0.02	0.03	0.03	<-0.01	<0.01	<-0.01	<-0.01	<0.01	<-0.01	<-0.01	<-0.01	<-0.01	<-0.01	<-0.01	<-0.01	0.01	<-0.01	<-0.01	<0.01	<-0.01	<-0.01	<0.01	<-0.01	<-0.01	<-0.01	<-0.01	<-0.01	<-0.01	<-0.01	<-0.01	-0.01	<-0.01	<-0.01	<-0.01	-0.01	<-0.01	<-0.01	<-0.01	<-0.01	<-0.01	<-0.01	<-0.01	<-0.01
Stutsman County	<-0.01	<-0.01	<-0.01	<0.01	<-0.01	<-0.01	<-0.01	<0.01	<-0.01	<-0.01	<-0.01	<0.01	<-0.01	<-0.01	<-0.01	<-0.01	<-0.01	0.01	<-0.01	<-0.01	<-0.01	<-0.01	<-0.01	<-0.01	<-0.01	<-0.01	<0.01	<-0.01	<-0.01	<-0.01	<-0.01	<-0.01	<-0.01	<-0.01	<-0.01	<-0.01	<-0.01	<-0.01	<-0.01	<-0.01	<-0.01	<-0.01	<-0.01	<-0.01	<-0.01	<-0.01	<-0.01
Towner County	<-0.01	<0.01	<0.01	<-0.01	<-0.01	<0.01	<-0.01	0.01	<-0.01	<-0.01	<-0.01	<-0.01	<-0.01	<-0.01	<-0.01	<-0.01	<-0.01	<-0.01	<-0.01	<-0.01	<-0.01	<-0.01	<-0.01	<-0.01	<-0.01	<-0.01	<0.01	<-0.01	<-0.01	<-0.01	<-0.01	<-0.01	<-0.01	<-0.01	<-0.01	<-0.01	<-0.01	<-0.01	<-0.01	<-0.01	<-0.01	<-0.01	<-0.01	<-0.01	<-0.01	<-0.01	<-0.01
Walsh County	<0.01	<0.01	<0.01	<0.01	<0.01	<0.01	<0.01	<-0.01	<0.01	-0.02	<-0.01	0.01	<-0.01	<0.01	<-0.01	<-0.01	<-0.01	<0.01	<-0.01	<0.01	<-0.01	<-0.01	<-0.01	<-0.01	<0.01	<-0.01	<0.01	<-0.01	<-0.01	<-0.01	<-0.01	<0.01	<-0.01	-0.02	-0.02	<-0.01	-0.01	<-0.01	-0.02	<-0.01	<-0.01	<-0.01	<-0.01	<-0.01	<-0.01	<-0.01	<-0.01
Ward County	<0.01	<-0.01	<0.01	<-0.01	<-0.01	<0.01	<-0.01	0.01	0.02	-0.01	<-0.01	<0.01	<-0.01	<-0.01	<0.01	<0.01	<-0.01	<-0.01	<0.01	<-0.01	<-0.01	<-0.01	<-0.01	<-0.01	<0.01	<-0.01	<0.01	<-0.01	<-0.01	<-0.01	<-0.01	<-0.01	<-0.01	<-0.01	-0.01	<0.01	<-0.01	-0.02	<-0.01	-0.03	<-0.01	<-0.01	<-0.01	<-0.01	<-0.01	<-0.01	<-0.01	<-0.01
Williams County	<0.01	<0.01	<0.01	<0.01	<0.01	<-0.01	<0.01	<0.01	<0.01	<0.01	<0.01	<-0.01	<-0.01	0.01	<0.01	-0.01	<-0.01	<-0.01	<-0.01	<0.01	<-0.01	0.02	<0.01	<-0.01	-0.01	0.02	<0.01	<-0.01	<-0.01	<-0.01	<-0.01	<-0.01	<0.01	<0.01	<-0.01	-0.02	-0.05	<-0.01	-0.10	<-0.01	-0.02	-0.01	-0.01	-0.03	-0.03	-0.01	-0.01
Barren Land	<-0.01	<-0.01	<-0.01	<-0.01	<-0.01	<-0.01	<-0.01	0.02	0.01	<0.01	<0.01	<0.01	<-0.01	<-0.01	<-0.01	0.05	<-0.01	<0.01	<-0.01	<-0.01	<-0.01	<-0.01	<-0.01	<-0.01	0.03	0.04	-0.02	<-0.01	<-0.01	0.00	0.04	<-0.01	<0.01	0.01	<-0.01	<0.01	<-0.01	<-0.01	<-0.01	<-0.01	<-0.01	<-0.01	<-0.01	<-0.01	<0.01	<-0.01	<-0.01	<-0.01
Cultivated Crops	0.03	-0.04	-0.06	-0.02	<-0.01	-0.04	-0.03	-0.13	-0.02	0.19	0.05	-0.02	<0.01	0.04	<-0.01	-0.02	0.03	<-0.01	0.12	-0.02	<-0.01	0.12	0.09	<-0.01	0.02	<-0.01	-0.08	<-0.01	0.02	<-0.01	<-0.01	<0.01	0.18	0.06	<-0.01	0.02	<-0.01	<-0.01	<-0.01	<-0.01	-0.01	<0.01	0.01	0.01	<-0.01	<0.01
Deciduous Forest	-0.04	-0.05	-0.04	-0.04	-0.04	-0.04	-0.05	0.08	0.08	0.02	<-0.01	-0.04	0.02	0.04	-0.03	0.04	<-0.01	<-0.01	-0.01	-0.02	<-0.01	0.03	-0.01	<-0.01	-0.01	-0.01	0.03	<-0.01	<-0.01	<-0.01	-0.01	-0.01	0.03	0.05	<-0.01	<0.01	<-0.01	<0.01	<-0.01	0.03	<-0.01	<-0.01	<0.01	<0.01	0.01	<-0.01
High Intensity Development	<-0.01	-0.01	-0.01	<-0.01	<-0.01	-0.01	-0.01	-0.02	-0.01	0.02	0.02	<0.01	<-0.01	<-0.01	<-0.01	<-0.01	<-0.01	<-0.01	<-0.01	<-0.01	<-0.01	<-0.01	<-0.01	<-0.01	0.08	<-0.01	-0.01	0.02	<-0.01	<-0.01	<-0.01	<-0.01	<-0.01	0.03	<-0.01	<-0.01	0.01	<-0.01	<-0.01	<-0.01	<-0.01	<-0.01	0.02	<-0.01	<-0.01	<-0.01	<-0.01
Low Intensity Development	<-0.01	-0.01	<-0.01	-0.02	-0.01	<-0.01	-0.01	-0.03	<0.01	0.03	<-0.01	-0.01	<0.01	<-0.01	<-0.01	<-0.01	<-0.01	<-0.01	<-0.01	<-0.01	<-0.01	<-0.01	<-0.01	<-0.01	0.10	<-0.01	<-0.01	<-0.01	0.08	<-0.01	<-0.01	0.04	0.04	<-0.01	<-0.01	<-0.01	<-0.01	<0.01	<-0.01	<-0.01	<-0.01	<-0.01	<-0.01	<-0.01	<-0.01	<-0.01	<-0.01
Medium Intensity Development	<-0.01	-0.01	<-0.01	-0.01	-0.01	<-0.01	-0.01	-0.02	0.02	0.03	0.07	0.01	<0.01	<-0.01	<-0.01	<-0.01	0.00	<-0.01	<-0.01	<-0.01	<-0.01	<-0.01	<-0.01	<-0.01	0.04	<-0.01	-0.03	<-0.01	<-0.01	<-0.01	<-0.01	<-0.01	0.06	0.03	<-0.01	<-0.01	<-0.01	<-0.01	<0.01	0.02	0.02	<-0.01	<-0.01	<0.01	<-0.01	<-0.01	<-0.01
Open Space	<-0.01	<-0.01	<-0.01	-0.01	<-0.01	<-0.01	<-0.01	-0.03	<0.01	0.05	0.08	<0.01	<-0.01	<-0.01	<-0.01	<-0.01	0.04	<-0.01	0.02	<-0.01	<-0.01	<0.01	<-0.01	<-0.01	0.03	0.02	-0.02	0.01	<-0.01	0.00	<-0.01	0.02	0.06	<-0.01	0.01	<-0.01	<-0.01	<0.01	<-0.01	<-0.01	<-0.01	<-0.01	<0.01	<0.01	<-0.01	<-0.01	<-0.01
Emergent Herbaceuous Wetlands	0.15	0.01	<-0.01	<-0.01	0.04	0.01	0.02	-0.07	0.04	0.14	<-0.01	-0.02	0.02	0.04	0.01	-0.01	0.03	<-0.01	0.04	-0.01	<-0.01	0.04	0.07	<-0.01	<0.01	0.14	-0.06	<-0.01	0.02	<-0.01	<-0.01	<0.01	0.13	0.05	<0.01	<0.01	<-0.01	<-0.01	<-0.01	0.01	0.01	<0.01	<-0.01	0.01	<0.01	<-0.01	<-0.01
Evergreen Forest	-0.01	<0.01	0.02	<-0.01	<-0.01	<0.01	<-0.01	0.07	<0.01	-0.04	<-0.01	0.04	-0.01	0.00	-0.01	-0.01	<-0.01	-0.01	<-0.01	<0.01	<-0.01	<0.01	<-0.01	<-0.01	<-0.01	<-0.01	<-0.01	<-0.01	<0.01	<-0.01	<-0.01	<-0.01	<-0.01	-0.04	-0.08	<-0.01	<-0.01	<-0.01	-0.01	<-0.01	<-0.01	<0.01	<-0.01	<-0.01	-0.01	<0.01	0.01
Hay/Pasture	<0.01	-0.02	-0.03	<-0.01	0.00	-0.02	-0.02	-0.06	-0.02	0.14	<-0.01	-0.01	<0.01	0.02	<0.01	<-0.01	<-0.01	-0.02	<-0.01	-0.01	<-0.01	0.02	0.16	<-0.01	<0.01	<-0.01	-0.07	0.02	<-0.01	<-0.01	<-0.01	<-0.01	<-0.01	0.14	0.06	<-0.01	<-0.01	<-0.01	<0.01	<-0.01	<-0.01	<0.01	<-0.01	<-0.01	0.01	<0.01	<0.01
Herbaceuous	0.02	0.05	0.01	0.06	0.04	0.02	0.05	-0.01	-0.08	<0.01	-0.10	0.08	0.10	-0.07	0.10	-0.04	<-0.01	0.10	-0.06	<0.01	<0.01	-0.04	0.05	<-0.01	-0.08	-0.07	-0.12	-0.02	-0.03	<0.01	<-0.01	-0.06	-0.03	0.11	<-0.01	-0.02	<0.01	0.01	<0.01	<-0.01	<-0.01	<-0.01	<-0.01	<-0.01	<-0.01	<-0.01	<-0.01
Mixed Forest	-0.02	-0.01	<0.01	-0.02	<-0.01	<-0.01	<-0.01	0.08	0.04	-0.05	<0.01	0.02	-0.03	<-0.01	-0.01	<-0.01	<-0.01	-0.02	<-0.01	-0.01	<-0.01	<-0.01	-0.02	0.03	<-0.01	<0.01	0.02	<-0.01	<-0.01	<-0.01	<-0.01	<-0.01	<-0.01	-0.05	-0.05	<0.01	<-0.01	0.00	<-0.01	0.00	<-0.01	<-0.01	<-0.01	<-0.01	<-0.01	<-0.01	<0.01	<-0.01
Open Water	-0.01	-0.04	-0.02	-0.02	<-0.01	-0.02	-0.02	-0.02	0.03	0.06	0.03	0.01	-0.01	<-0.01	<0.01	<-0.01	<-0.01	<-0.01	0.11	<-0.01	<-0.01	<-0.01	0.01	<-0.01	0.04	0.03	-0.04	<-0.01	<-0.01	<-0.01	<-0.01	<-0.01	0.05	0.06	<0.01	<-0.01	<-0.01	<-0.01	-0.02	<-0.01	<-0.01	<-0.01	0.02	0.01	<-0.01	<-0.01	0.01
Shrub/Scrub	-0.07	0.03	0.07	0.02	<-0.01	0.04	0.02	0.07	0.04	-0.29	-0.04	-0.05	-0.12	-0.04	-0.10	0.04	-0.01	-0.09	-0.03	0.03	<0.01	-0.05	-0.15	<-0.01	-0.04	-0.03	0.24	0.02	-0.01	<0.01	0.02	-0.03	-0.25	-0.17	<0.01	0.01	<-0.01	<-0.01	<-0.01	<0.01	<0.01	<-0.01	<-0.01	<-0.01	<-0.01	<-0.01	<-0.01
Woody Wetlands	0.05	-0.11	-0.08	-0.11	-0.07	-0.07	-0.10	-0.08	0.02	0.34	0.32	-0.06	0.01	0.17	-0.02	-0.02	<0.01	-0.02	0.09	-0.02	<-0.01	0.04	0.02	0.02	0.27	0.16	-0.13	<-0.01	0.08	<-0.01	<-0.01	0.24	0.35	<-0.01	0.01	<0.01	<-0.01	<-0.01	<-0.01	<-0.01	<-0.01	<-0.01	<-0.01	<-0.01	<-0.01	0.01	<-0.01

Factors	Dunn County	Emmons County	Golden Valley County	Grand Forks County	Grant County	Griggs County	Hettinger County	LaMoure County	Logan County	McHenry County	McIntosh County	McKenzie County	McLean County	Mercer County	Morton County	Mountrail County	Oliver County	Pembina County	Ransom County	Renville County	Richland County	Rolette County	Sioux County	Slope County	Stark County	Steele County	Stutsman County	Towner County	Walsh County	Ward County	Williams County	Barren Land	Cultivated Crops	Deciduous Forest	High Intensity Development	Low Intensity Development	Medium Intensity Development	Open Space	Emergent Herbaceuous Wetlands	Evergreen Forest	Hay/Pasture	Herbaceuous	Mixed Forest	Open Water	Shrub/Scrub	Woody Wetlands
Area																																														
TDS																																														
SAR																																														
Ca^{2+}																																														
Mg^{2+}																																														
Na^{-}																																														
SO^{2-}_{4}																																														
Slope Inclination																																														
Latitude																																														
Longitude																																														
Belle Fourche-Skull Creek																																														
Bullion Creek Formation																																														
Cannonball Formation																																														
Carlile Formation																																														
Fox Hills Formation																																														
Golden Valley Formation																																														
Greenhorn Formation																																														
Hell Creek Formation																																														
Inyan Kara																																														
Ludlow Formation																																														
Mowry-Skull Creek																																														
Niobrara Formation																																														
Pierre Formation																																														
Piper Formation																																														
Precambrian Rocks																																														
Red River Formation																																														
Sentinel Butte Formation																																														
Slope Formation																																														
Jurassic Sediments																																														
Upper and Middle Tertiary Rock																																														
White River Group																																														
Winnipeg Group																																														
Average Rainfall																																														
Aerage Snowfall																																														
Adams County																																														
Barnes County																																														
Benson County																																														
Billings County																																														
BottineauCounty																																														
Bowman County																																														
Burke County																																														
Burleigh County																																														
Cass County																																														
Cavalier County																																														
Dickey County																																														
Divide County																																														
Dunn County	1.00																																														
Emmons County	-0.05	1.00																																												
Golden Valley County	-0.07	-0.05	1.00																																											
Grand Forks County	-0.02	-0.01	-0.02	1.00																																									
Grant County	-0.05	-0.03	-0.05	-0.01	1.00																																								
Griggs County	-0.02	-0.01	-0.02	<-0.01	-0.01	1.00																																							
Hettinger County	-0.03	-0.02	-0.03	<-0.01	-0.02	<-0.01	1.00																																						
LaMoure County	<-0.01	<-0.01	<-0.01	<-0.01	<-0.01	<-0.01	<-0.01	1.00																																					
Logan County	<-0.01	<-0.01	<-0.01	<-0.01	<-0.01	<-0.01	<-0.01	<-0.01	1.00																																				

Legend

- Strong Positive Correlation
- Moderate Positive Correlation
- Strong Negative Correlation
- Moderate Negative Correlation

Factors	Dunn County	Emmons County	Golden Valley County	Grand Forks County	Grant County	Griggs County	Hettinger County	LaMoure County	Logan County	McHenry County	McIntosh County	McKenzie County	McLean County	Mercer County	Morton County	Mountrail County	Oliver County	Pembina County	Ransom County	Renville County	Richland County	Rolette County	Sioux County	Slope County	Stark County	Steele County	Stutsman County	Towner County	Walsh County	Ward County	Williams County	Barren Land	Cultivated Crops	Deciduous Forest	High Intensity Development	Low Intensity Development	Medium Intensity Development	Open Space	Emergent Herbaceuous Wetlands	Evergreen Forest	Hay/Pasture	Herbaceuous	Mixed Forest	Open Water	Shrub/Scrub	Woody Wetlands
McHenry County	-0.01	<-0.01	-0.01	<-0.01	<-0.01	<-0.01	<-0.01	<-0.01	0.00	1.00																																						
McIntosh County	<-0.01	<-0.01	<-0.01	<-0.01	<-0.01	<-0.01	<-0.01	<-0.01	<-0.01	<-0.01	1.00																																					
McKenzie County	-0.14	-0.10	-0.13	-0.03	-0.09	-0.04	-0.06	<-0.01	<-0.01	-0.02	<-0.01	1.00																																				
McLean County	-0.03	-0.02	-0.03	<-0.01	-0.02	<-0.01	-0.01	<-0.01	<-0.01	<-0.01	<-0.01	-0.06	1.00																																				
Mercer County	-0.05	-0.04	-0.05	-0.01	-0.03	-0.01	-0.02	<-0.01	<-0.01	<-0.01	<-0.01	-0.10	-0.02	1.00																																			
Morton County	-0.08	-0.06	-0.07	-0.02	-0.05	-0.02	-0.03	<-0.01	<-0.01	-0.01	<-0.01	-0.15	-0.03	-0.06	1.00																																		
Mountrail County	-0.06	-0.04	-0.05	-0.01	-0.04	-0.02	-0.02	<-0.01	<-0.01	<-0.01	<-0.01	-0.11	-0.02	-0.04	-0.06	1.00																																	
Oliver County	-0.03	-0.02	-0.03	<-0.01	-0.02	<-0.01	-0.01	<-0.01	<-0.01	<-0.01	<-0.01	-0.06	-0.01	-0.02	-0.04	-0.03	1.00																																	
Pembina County	-0.01	<-0.01	-0.01	<-0.01	<-0.01	<-0.01	<-0.01	<-0.01	<-0.01	<-0.01	0.00	-0.03	<-0.01	-0.01	-0.01	-0.01	<-0.01	1.00																																	
Ransom County	<-0.01	<-0.01	<-0.01	<-0.01	<-0.01	<-0.01	<-0.01	<-0.01	<-0.01	<-0.01	<-0.01	-0.01	<-0.01	<-0.01	<-0.01	<-0.01	<-0.01	<-0.01	1.00																																	
Renville County	<-0.01	<-0.01	<-0.01	<-0.01	<-0.01	<-0.01	<-0.01	<-0.01	<-0.01	<-0.01	<-0.01	<-0.01	<-0.01	<-0.01	<-0.01	<-0.01	<-0.01	0.00	<-0.01	1.00																																	
Richland County	<-0.01	<-0.01	<-0.01	<-0.01	<-0.01	<-0.01	<-0.01	<-0.01	<-0.01	<-0.01	<-0.01	-0.02	<-0.01	<-0.01	<-0.01	<-0.01	<-0.01	<-0.01	<-0.01	<-0.01	1.00																																
Rolette County	<-0.01	<-0.01	<-0.01	<-0.01	<-0.01	<-0.01	<-0.01	<-0.01	<-0.01	<-0.01	<-0.01	-0.01	<-0.01	<-0.01	<-0.01	<-0.01	<-0.01	<-0.01	0.00	<-0.01	<-0.01	1.00																															
Sioux County	-0.02	-0.02	-0.02	<-0.01	-0.01	<-0.01	<-0.01	0.00	<-0.01	<-0.01	<-0.01	-0.04	<-0.01	-0.02	-0.02	-0.02	<-0.01	<-0.01	<-0.01	<-0.01	<-0.01	<-0.01	1.00																														
Slope County	-0.06	-0.04	-0.06	-0.01	-0.04	-0.02	-0.02	<-0.01	<-0.01	<-0.01	<-0.01	-0.11	-0.02	-0.04	-0.06	-0.05	-0.03	-0.01	<-0.01	<-0.01	<-0.01	<-0.01	-0.02	1.00																													
Stark County	-0.04	-0.03	-0.04	<-0.01	-0.03	-0.01	-0.02	<-0.01	<-0.01	<-0.01	<-0.01	-0.08	-0.02	-0.03	-0.04	-0.03	-0.02	<-0.01	<-0.01	<-0.01	<-0.01	<-0.01	-0.01	-0.03	1.00																													
Steele County	<-0.01	<-0.01	<-0.01	<-0.01	<-0.01	<-0.01	<-0.01	<-0.01	<-0.01	<-0.01	<-0.01	-0.02	<-0.01	<-0.01	<-0.01	<-0.01	<-0.01	<-0.01	<-0.01	<-0.01	<-0.01	0.00	<-0.01	<-0.01	<-0.01	1.00																													
Stutsman County	<-0.01	<-0.01	<-0.01	<-0.01	<-0.01	<-0.01	<-0.01	<-0.01	<-0.01	0.00	<-0.01	<-0.01	<-0.01	<-0.01	<-0.01	<-0.01	<-0.01	<-0.01	<-0.01	<-0.01	<-0.01	<-0.01	<-0.01	<-0.01	<-0.01	<-0.01	1.00																													
Towner County	<-0.01	<-0.01	<-0.01	<-0.01	<-0.01	<-0.01	<-0.01	<-0.01	<-0.01	<-0.01	<-0.01	<-0.01	0.00	<-0.01	<-0.01	<-0.01	<-0.01	<-0.01	<-0.01	<-0.01	<-0.01	<-0.01	<-0.01	<-0.01	<-0.01	<-0.01	<-0.01	1.00																													
Walsh County	-0.02	-0.01	-0.01	<-0.01	<-0.01	<-0.01	<-0.01	<-0.01	<-0.01	<-0.01	<-0.01	-0.03	<-0.01	-0.01	-0.02	-0.01	<-0.01	<-0.01	<-0.01	<-0.01	<-0.01	<-0.01	<-0.01	<-0.01	<-0.01	<-0.01	<-0.01	<-0.01	1.00																													
Ward County	-0.02	-0.02	-0.02	<-0.01	-0.01	<-0.01	<-0.01	0.00	<-0.01	<-0.01	<-0.01	-0.04	<-0.01	-0.02	-0.02	-0.02	-0.01	<-0.01	<-0.01	<-0.01	<-0.01	<-0.01	<-0.01	<-0.01	<-0.01	<-0.01	<-0.01	<-0.01	<-0.01	1.00																													
Williams County	-0.06	-0.05	-0.06	-0.01	-0.04	-0.02	-0.03	<-0.01	<-0.01	-0.01	<-0.01	-0.12	-0.03	-0.05	-0.07	-0.05	-0.03	-0.01	<-0.01	<-0.01	<-0.01	<-0.01	-0.02	-0.05	-0.04	<-0.01	<-0.01	<-0.01	-0.01	-0.02	1.00																												
Barren Land	<0.01	0.02	<-0.01	<-0.01	<-0.01	<-0.01	<-0.01	<-0.01	0.00	<-0.01	<-0.01	<0.01	0.03	<-0.01	<-0.01	<-0.01	<-0.01	<-0.01	<-0.01	<-0.01	<-0.01	<-0.01	<-0.01	<0.01	<0.01	<-0.01	<-0.01	<-0.01	<-0.01	<0.01	<-0.01	1.00																												
Cultivated Crops	0.01	<0.01	<0.01	<-0.01	<0.01	<-0.01	<-0.01	<-0.01	<-0.01	<-0.01	<-0.01	<-0.01	<-0.01	<-0.01	<-0.01	<-0.01	0.01	0.01	0.01	<-0.01	<-0.01	<-0.01	<-0.01	-0.01	<-0.01	<-0.01	<-0.01	<-0.01	<0.01	<-0.01	<-0.01	<-0.01	1.00																												
Deciduous Forest	<0.01	<-0.01	<-0.01	<0.01	<-0.01	<-0.01	-0.01	<-0.01	0.03	<-0.01	<-0.01	<-0.01	<-0.01	<-0.01	0.00	<0.01	<0.01	<0.01	<0.01	<-0.01	<-0.01	<-0.01	<-0.01	<-0.01	<-0.01	<-0.01	<-0.01	<0.01	<-0.01	<0.01	<0.01	<-0.01	-0.04	1.00																												
High Intensity Development	<-0.01	<0.01	<-0.01	<-0.01	<-0.01	<-0.01	<-0.01	<-0.01	<-0.01	0.05	<-0.01	<-0.01	<-0.01	<-0.01	<0.01	<-0.01	<-0.01	<-0.01	<-0.01	<-0.01	<-0.01	<-0.01	<-0.01	<-0.01	<-0.01	<-0.01	<-0.01	<-0.01	<-0.01	<-0.01	<-0.01	<-0.01	<-0.01	<-0.01	1.00																												
Low Intensity Development	<-0.01	<0.01	<0.01	<-0.01	<-0.01	<-0.01	<-0.01	<-0.01	<-0.01	<-0.01	<-0.01	0.01	0.02	<-0.01	<-0.01	<-0.01	<-0.01	<-0.01	<-0.01	<-0.01	<-0.01	<-0.01	<-0.01	0.00	<-0.01	<-0.01	<-0.01	<-0.01	<-0.01	<-0.01	<-0.01	<-0.01	<-0.01	<-0.01	<-0.01	1.00																												
Medium Intensity Development	<-0.01	<-0.01	<-0.01	<-0.01	<0.01	<-0.01	0.01	<-0.01	<-0.01	<-0.01	<-0.01	<-0.01	<-0.01	<-0.01	<-0.01	0.01	<0.01	<-0.01	0.00	<-0.01	0.04	<-0.01	<-0.01	<0.01	0.03	0.00	<-0.01	<-0.01	<-0.01	<-0.01	<-0.01	<-0.01	<-0.01	<-0.01	<-0.01	<-0.01	1.00																												
Open Space	<0.01	<-0.01	<0.01	<-0.01	<-0.01	<-0.01	<-0.01	<-0.01	<-0.01	<-0.01	<-0.01	<0.01	<-0.01	<-0.01	<0.01	<0.01	<0.01	<-0.01	<-0.01	<-0.01	<-0.01	<-0.01	<-0.01	<-0.01	<-0.01	<-0.01	<-0.01	<-0.01	<-0.01	<-0.01	<-0.01	<-0.01	<-0.01	<-0.01	<-0.01	<-0.01	<-0.01	1.00																												
Emergent Herbaceuous Wetlands	<0.01	-0.01	<0.01	<0.01	-0.01	<0.01	<-0.01	<-0.01	<-0.01	<-0.01	<-0.01	<0.01	<-0.01	<-0.01	<-0.01	-0.01	<0.01	<-0.01	<-0.01	<-0.01	<0.01	<-0.01	<-0.01	<0.01	<-0.01	<-0.01	<-0.01	<-0.01	<-0.01	<-0.01	<-0.01	<-0.01	<-0.01	<-0.01	<-0.01	<-0.01	<-0.01	<-0.01	1.00																												
Evergreen Forest	<-0.01	<0.01	<-0.01	<0.01	<-0.01	<-0.01	<0.01	0.00	<-0.01	<-0.01	<-0.01	<-0.01	0.02	<-0.01	<0.01	0.01	<-0.01	<-0.01	<-0.01	<-0.01	0.02	<-0.01	<-0.01	<-0.01	<-0.01	0.02	<-0.01	<-0.01	<-0.01	<-0.01	<0.01	0.01	0.03	<-0.01	<-0.01	<-0.01	<-0.01	<-0.01	<-0.01	<-0.01	1.00																												
Hay/Pasture	<-0.01	<0.01	<0.01	<-0.01	<0.01	<0.01	<-0.01	<-0.01	<-0.01	<-0.01	<-0.01	<-0.01	0.00	-0.01	<0.01	<0.01	<0.01	<-0.01	<-0.01	0.03	<-0.01	<-0.01	<0.01	<0.01	<0.01	<-0.01	<-0.01	<-0.01	<-0.01	<-0.01	<-0.01	<-0.01	-0.02	-0.02	<-0.01	<-0.01	<-0.01	<-0.01	<-0.01	<-0.01	-0.01	<-0.01	1.00																												
Herbaceuous	<-0.01	<0.01	<-0.01	<-0.01	<0.01	<-0.01	0.01	<-0.01	<-0.01	<0.01	<-0.01	<-0.01	<0.01	<-0.01	<-0.01	<0.01	<0.01	<-0.01	<-0.01	<-0.01	<0.01	<0.01	<-0.01	0.01	<0.01	0.01	<0.01	<0.01	<0.01	0.01	0.00	-0.05	-0.22	-0.23	-0.02	-0.03	-0.03	-0.04	-0.17	-0.10	-0.12	1.00																												
Mixed Forest	<0.01	<0.01	0.01	0.01	<0.01	<-0.01	<-0.01	<-0.01	<-0.01	<-0.01	<-0.01	<0.01	<0.01	<-0.01	<-0.01	<-0.01	-0.01	<0.01	<-0.01	<-0.01	<-0.01	<0.01	<-0.01	<-0.01	-0.02	<-0.01	<-0.01	<-0.01	0.00	<0.01	<0.01	0.01	<-0.01	-0.02	-0.02	<-0.01	<-0.01	<-0.01	<-0.01	-0.02	<-0.01	-0.01	###	1.00																												
Open Water	<0.01	<-0.01	0.02	<-0.01	<0.01	<0.01	<0.01	<-0.01	<-0.01	<-0.01	0.02	<-0.01	<-0.01	<0.01	<-0.01	<-0.01	<-0.01	0.01	<-0.01	<-0.01	<-0.01	0.01	<-0.01	<-0.01	<-0.01	<-0.01	<-0.01	<-0.01	0.01	<-0.01	<0.01	<-0.01	<-0.01	<-0.01	<-0.01	<-0.01	<-0.01	<-0.01	<-0.01	<-0.01	<-0.01	<-0.01	###	<-0.01	1.00																												
Shrub/Scrub	<0.01	<-0.01	<0.01	<-0.01	<-0.01	0.01	<-0.01	<0.01	<-0.01	<-0.01	<-0.01	<-0.01	<-0.01	0.01	<0.01	<-0.01	<-0.01	<-0.01	<-0.01	<-0.01	<-0.01	<0.01	<-0.01	<-0.01	-0.01	<-0.01	<-0.01	<-0.01	<-0.01	<-0.01	<-0.01	-0.02	-0.11	-0.11	-0.01	-0.01	-0.02	-0.02	-0.08	-0.05	-0.06	###	-0.07	-0.03	1.00																												
Woody Wetlands	<-0.01	-0.01	<-0.01	-0.01	<-0.01	<-0.01	<-0.01	<-0.01	<-0.01	<-0.01	<-0.01	-0.01	0.01	<-0.01	<-0.01	<-0.01	<-0.01	0.02	<-0.01	<-0.01	<-0.01	<-0.01	<-0.01	<-0.01	<-0.01	<-0.01	<-0.01	<-0.01	<-0.01	<-0.01	0.01	<-0.01	-0.03	-0.03	<-0.01	<-0.01	<-0.01	<-0.01	-0.02	-0.01	-0.02	###	-0.02	<-0.01	###	1.00																												

Legend

- Strong Positive Correlation
- Moderate Positive Correlation
- Strong Negative Correlation
- Moderate Negative Correlation

APPENDIX G: COMPLETE CORRELATION MATRIX FROM DRAFT PAPER IN CHAPTER 5

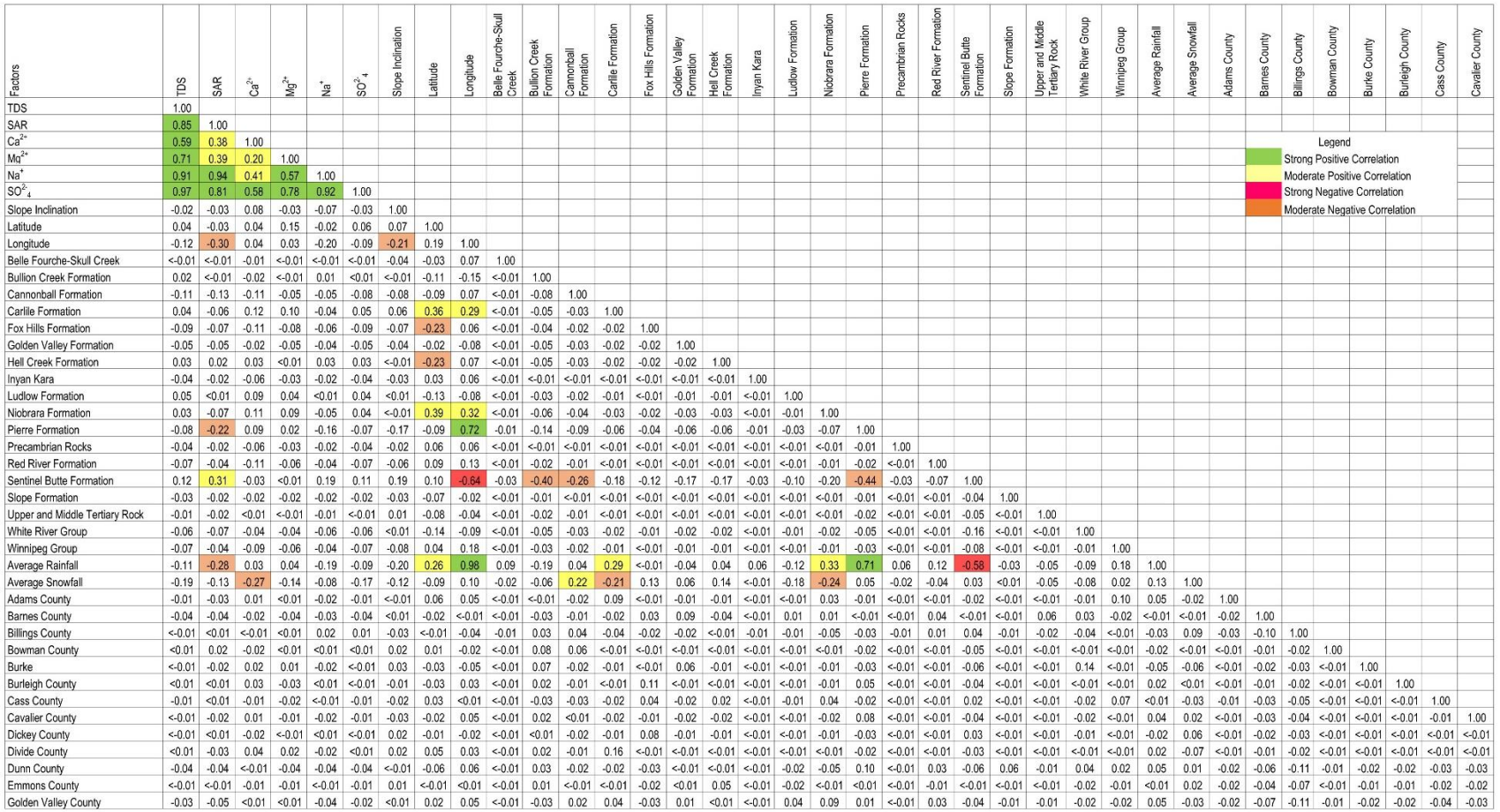

Factors	TDS	SAR	Ca^{2+}	Mg^{2+}	Na^{+}	SO^{2-}_4	Slope Inclination	Latitude	Longitude	Belle Fourche-Skull Creek	Bullion Creek Formation	Cannonball Formation	Carlile Formation	Fox Hills Formation	Golden Valley Formation	Hell Creek Formation	Inyan Kara	Ludlow Formation	Niobrara Formation	Pierre Formation	Precambrian Rocks	Red River Formation	Sentinel Butte Formation	Slope Formation	Upper and Middle Tertiary Rock	White River Group	Winnipeg Group	Average Rainfall	Average Snowfall	Adams County	Barnes County	Billings County	Bowman County	Burke County	Burleigh County	Cass County	Cavalier County
TDS	1.00																																			
SAR	0.85	1.00																																		
Ca^{2+}	0.59	0.38	1.00																																	
Mg^{2+}	0.71	0.39	0.20	1.00																																
Na^{+}	0.91	0.94	0.41	0.57	1.00																															
SO^{2-}_4	0.97	0.81	0.58	0.78	0.92	1.00																														
Slope Inclination	-0.02	-0.03	0.08	-0.03	-0.07	-0.03	1.00																													
Latitude	0.04	-0.03	0.04	0.15	-0.02	0.06	0.07	1.00																												
Longitude	-0.12	-0.30	0.04	0.03	-0.20	-0.09	-0.21	0.19	1.00																											
Belle Fourche-Skull Creek	<-0.01	<-0.01	-0.01	<-0.01	<-0.01	<-0.01	-0.04	-0.03	0.07	1.00																										
Bullion Creek Formation	0.02	<-0.01	-0.02	<-0.01	0.01	<0.01	<-0.01	-0.11	-0.15	<-0.01	1.00																									
Cannonball Formation	-0.11	-0.13	-0.11	-0.05	-0.05	-0.08	-0.08	-0.09	0.07	<-0.01	-0.08	1.00																								
Carlile Formation	0.04	-0.06	0.12	0.10	-0.04	0.05	0.06	0.36	0.29	<-0.01	-0.05	-0.03	1.00																							
Fox Hills Formation	-0.09	-0.07	-0.11	-0.08	-0.06	-0.09	-0.07	-0.23	0.06	<-0.01	-0.04	-0.02	-0.02	1.00																						
Golden Valley Formation	-0.05	-0.05	-0.02	-0.05	-0.04	-0.05	-0.04	-0.02	-0.08	<-0.01	-0.05	-0.03	-0.02	-0.02	1.00																					
Hell Creek Formation	0.03	0.02	0.03	<0.01	0.03	0.03	<-0.01	-0.23	0.07	<-0.01	-0.05	-0.03	-0.02	-0.02	-0.02	1.00																				
Inyan Kara	-0.04	-0.02	-0.06	-0.03	-0.02	-0.04	-0.03	0.03	0.06	<-0.01	<-0.01	<-0.01	<-0.01	<-0.01	<-0.01	<-0.01	1.00																			
Ludlow Formation	0.05	<0.01	0.09	0.04	<0.01	0.04	<0.01	-0.13	-0.08	<-0.01	-0.03	-0.02	-0.01	<-0.01	-0.01	-0.01	<-0.01	1.00																		
Niobrara Formation	0.03	-0.07	0.11	0.09	-0.05	0.04	<-0.01	0.39	0.32	<-0.01	-0.06	-0.04	-0.03	-0.02	-0.03	-0.03	<-0.01	-0.01	1.00																	
Pierre Formation	-0.08	-0.22	0.09	0.02	-0.16	-0.07	-0.17	-0.09	0.72	-0.01	-0.14	-0.09	-0.06	-0.04	-0.06	-0.06	-0.01	-0.03	-0.07	1.00																
Precambrian Rocks	-0.04	-0.02	-0.06	-0.03	-0.02	-0.04	-0.02	0.06	0.06	<-0.01	<-0.01	<-0.01	<-0.01	<-0.01	<-0.01	<-0.01	<-0.01	<-0.01	<-0.01	-0.01	1.00															
Red River Formation	-0.07	-0.04	-0.11	-0.06	-0.04	-0.07	-0.06	0.09	0.13	<-0.01	-0.02	-0.01	<-0.01	<-0.01	<-0.01	<-0.01	<-0.01	<-0.01	-0.01	-0.02	<-0.01	1.00														
Sentinel Butte Formation	0.12	0.31	-0.03	<0.01	0.19	0.11	0.19	0.10	-0.64	-0.03	-0.40	-0.26	-0.18	-0.12	-0.17	-0.17	-0.03	-0.10	-0.20	-0.44	-0.03	-0.07	1.00													
Slope Formation	-0.03	-0.02	-0.02	-0.02	-0.02	-0.02	-0.03	-0.07	-0.02	<-0.01	-0.01	<-0.01	<-0.01	<-0.01	<-0.01	<-0.01	<-0.01	<-0.01	<-0.01	-0.01	<-0.01	<-0.01	-0.04	1.00												
Upper and Middle Tertiary Rock	-0.01	-0.02	<0.01	<-0.01	-0.01	<-0.01	0.01	-0.08	-0.04	<-0.01	-0.02	-0.01	<-0.01	<-0.01	<-0.01	<-0.01	<-0.01	<-0.01	<-0.01	-0.02	<-0.01	<-0.01	-0.05	<-0.01	1.00										
White River Group	-0.06	-0.07	-0.04	-0.04	-0.06	-0.06	<0.01	-0.14	-0.09	<-0.01	-0.05	-0.03	-0.02	-0.01	-0.02	-0.02	<-0.01	-0.01	-0.02	-0.05	<-0.01	<-0.01	-0.16	<-0.01	<-0.01	1.00									
Winnipeg Group	-0.07	-0.04	-0.09	-0.06	-0.04	-0.07	-0.08	0.04	0.18	<-0.01	-0.03	-0.02	-0.01	<-0.01	-0.01	-0.01	<-0.01	<-0.01	-0.01	-0.03	<-0.01	<-0.01	-0.08	<-0.01	<-0.01	-0.01	1.00								
Average Rainfall	-0.11	-0.28	0.03	0.04	-0.19	-0.09	-0.20	0.26	0.98	0.09	-0.19	0.04	0.29	<-0.01	-0.04	0.04	0.06	-0.12	0.33	0.71	0.06	0.12	-0.58	-0.03	-0.05	-0.09	0.18	1.00							
Average Snowfall	-0.19	-0.13	-0.27	-0.14	-0.08	-0.17	-0.12	-0.09	0.10	-0.02	-0.06	0.22	-0.21	0.13	0.06	0.14	<-0.01	-0.18	-0.24	0.05	-0.02	-0.04	0.03	<0.01	-0.05	-0.08	0.02	0.13	1.00						
Adams County	-0.01	-0.03	0.01	<0.01	-0.02	-0.01	<-0.01	0.06	0.05	<-0.01	<-0.01	-0.02	0.09	<-0.01	-0.01	-0.01	<-0.01	<-0.01	0.03	-0.01	<-0.01	<-0.01	-0.02	<-0.01	<-0.01	-0.01	0.10	0.05	-0.02	1.00					
Barnes County	-0.04	-0.04	-0.02	-0.04	-0.03	-0.04	<0.01	-0.02	<-0.01	<-0.01	-0.03	-0.01	-0.02	0.03	0.09	-0.04	<-0.01	0.01	0.01	<-0.01	<-0.01	0.04	<-0.01	<-0.01	0.06	0.03	-0.02	<-0.01	<-0.01	-0.02	1.00				
Billings County	<-0.01	<0.01	<-0.01	<0.01	0.02	0.01	-0.03	<-0.01	-0.04	-0.01	0.03	0.04	-0.04	-0.02	-0.02	<-0.01	-0.01	-0.01	-0.05	-0.03	-0.01	0.01	0.04	-0.01	-0.02	-0.04	<-0.01	-0.03	0.09	-0.03	-0.10	1.00			
Bowman County	<0.01	0.02	-0.02	<0.01	<0.01	<0.01	0.02	0.01	-0.02	<-0.01	0.08	0.06	<-0.01	<-0.01	<-0.01	<-0.01	<-0.01	<-0.01	<-0.01	-0.02	<-0.01	<-0.01	-0.05	<-0.01	<-0.01	<-0.01	<-0.01	-0.02	<-0.01	<-0.01	-0.01	-0.02	1.00		
Burke	<-0.01	-0.02	0.02	0.01	-0.02	<-0.01	0.03	-0.03	-0.05	<-0.01	0.07	-0.02	-0.01	<-0.01	0.06	-0.01	<-0.01	<-0.01	-0.01	-0.03	<-0.01	<-0.01	-0.06	<-0.01	<-0.01	0.14	<-0.01	-0.05	-0.06	<-0.01	-0.02	-0.03	<-0.01	1.00	
Burleigh County	<0.01	<0.01	0.03	-0.03	<0.01	<-0.01	-0.01	-0.03	0.03	<-0.01	0.02	-0.01	<-0.01	0.11	<-0.01	<-0.01	<-0.01	<-0.01	-0.01	0.05	<-0.01	<-0.01	-0.04	<-0.01	<-0.01	<-0.01	<-0.01	0.02	<0.01	<-0.01	-0.01	-0.02	<-0.01	<-0.01	1.00
Cass County	-0.01	<0.01	-0.01	-0.02	<-0.01	-0.01	-0.02	0.03	<0.01	<-0.01	-0.03	-0.03	-0.02	0.04	-0.02	0.02	<-0.01	-0.01	0.04	-0.02	<-0.01	<-0.01	0.02	<-0.01	<-0.01	-0.02	0.07	<0.01	-0.03	-0.01	-0.03	-0.05	<-0.01	<-0.01	<-0.01	1.00
Cavalier County	<-0.01	-0.02	0.01	-0.01	-0.02	-0.01	-0.03	-0.02	0.05	<-0.01	0.02	<0.01	-0.02	-0.01	-0.02	-0.02	<-0.01	<-0.01	-0.02	0.08	<-0.01	<-0.01	-0.04	<-0.01	<-0.01	-0.02	<-0.01	0.04	0.02	<-0.01	-0.03	-0.04	<-0.01	<-0.01	<-0.01	-0.01	1.00
Dickey County	<-0.01	<0.01	-0.02	<-0.01	<0.01	<-0.01	0.02	-0.01	-0.02	<-0.01	<0.01	-0.02	-0.01	0.08	-0.01	-0.01	<-0.01	<-0.01	-0.01	-0.03	<-0.01	<-0.01	0.03	<-0.01	<-0.01	-0.01	<-0.01	-0.02	0.06	<-0.01	-0.02	-0.03	<-0.01	<-0.01	<-0.01	<-0.01	<-0.01
Divide County	<0.01	-0.03	0.04	0.02	-0.02	<0.01	0.02	0.05	0.03	<-0.01	0.02	-0.01	0.16	<-0.01	<-0.01	<-0.01	<-0.01	<-0.01	<-0.01	-0.02	<-0.01	<-0.01	-0.03	<-0.01	<-0.01	<-0.01	<-0.01	0.02	-0.07	<-0.01	-0.01	-0.02	<-0.01	<-0.01	<-0.01	<-0.01	<-0.01
Dunn County	-0.04	-0.04	<-0.01	-0.04	-0.04	-0.04	<-0.01	-0.06	0.06	<-0.01	0.03	-0.02	-0.02	-0.03	<-0.01	<-0.01	<-0.01	-0.02	-0.05	0.10	<-0.01	0.03	-0.06	0.06	-0.01	0.04	0.02	0.05	0.01	-0.02	-0.06	-0.11	-0.01	-0.02	-0.02	-0.03	-0.03
Emmons County	<-0.01	<-0.01	-0.01	-0.01	<-0.01	-0.01	0.01	<-0.01	<0.01	<-0.01	0.01	<-0.01	<-0.01	-0.02	<0.01	0.05	<-0.01	-0.02	<-0.01	<0.01	<-0.01	-0.01	<-0.01	<-0.01	<-0.01	-0.02	-0.01	<0.01	0.02	-0.02	-0.04	-0.07	<-0.01	-0.01	-0.02	-0.01	-0.02
Golden Valley County	-0.03	-0.05	<0.01	<0.01	-0.04	-0.02	<0.01	0.02	0.05	<-0.01	-0.03	0.02	0.04	-0.03	0.01	<0.01	<-0.01	0.04	0.09	0.01	<-0.01	0.03	-0.04	-0.01	-0.01	-0.02	-0.02	0.05	-0.03	-0.02	-0.07	-0.11	-0.01	-0.02	-0.02	-0.04	-0.03

Legend

- Strong Positive Correlation
- Moderate Positive Correlation
- Strong Negative Correlation
- Moderate Negative Correlation

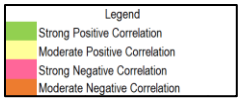

Factors	TDS	SAR	Ca^{2+}	Mg^{2+}	Na^{+}	SO^{2-}_{4}	Slope Inclination	Latitude	Longitude	Belle Fourche-Skull Creek	Bullion Creek Formation	Cannonball Formation	Carlile Formation	Fox Hills Formation	Golden Valley Formation	Hell Creek Formation	Inyan Kara	Ludlow Formation	Niobrara Formation	Pierre Formation	Precambrian Rocks	Red River Formation	Sentinel Butte Formation	Slope Formation	Upper and Middle Tertiary Rock	White River Group	Winnipeg Group	Average Rainfall	Average Snowfall	Adams County	Barnes County	Billings County	Bowman County	Burke County	Burleigh County	Cass County	Cavalier County
Grand Forks County	0.10	0.03	0.01	0.14	0.08	0.11	0.02	0.04	<-0.01	<-0.01	-0.03	0.06	-0.01	<-0.01	-0.01	-0.01	<-0.01	<-0.01	-0.01	<-0.01	<-0.01	<-0.01	0.02	<-0.01	<-0.01	-0.01	<-0.01	<0.01	0.03	<-0.01	-0.02	-0.03	<-0.01	<-0.01	<-0.01	<-0.01	<-0.01
Grant County	0.02	0.03	0.01	-0.03	0.02	<0.01	-0.03	-0.04	-0.03	<-0.01	<-0.01	-0.02	<-0.01	-0.02	<0.01	0.03	<-0.01	0.08	<-0.01	-0.03	<-0.01	-0.01	<0.01	<-0.01	<-0.01	0.06	-0.01	-0.03	<0.01	-0.02	-0.04	-0.07	<-0.01	-0.01	-0.01	-0.02	-0.02
Griggs County	-0.04	-0.04	-0.03	-0.03	-0.03	-0.03	0.04	-0.03	<0.01	<-0.01	0.04	-0.02	-0.01	<-0.01	0.06	0.06	<-0.01	<-0.01	-0.01	<0.01	<-0.01	<-0.01	-0.04	<-0.01	<-0.01	<-0.01	<-0.01	<0.01	0.02	<-0.01	-0.02	-0.03	<-0.01	<-0.01	<-0.01	<-0.01	<-0.01
Hettinger County	0.04	0.02	0.05	<-0.01	0.03	0.02	-0.04	-0.02	0.03	<-0.01	-0.03	0.02	-0.01	<-0.01	-0.01	-0.01	<-0.01	<-0.01	-0.01	0.04	<-0.01	<-0.01	-0.01	<-0.01	<-0.01	0.05	<-0.01	0.03	0.05	<-0.01	-0.02	-0.03	<-0.01	<-0.01	<-0.01	-0.01	<-0.01
Logan County	<-0.01	<-0.01	<0.01	<0.01	<-0.01	<-0.01	<-0.01	0.01	-0.01	<-0.01	<-0.01	<-0.01	<-0.01	<-0.01	<-0.01	<-0.01	<-0.01	<-0.01	<-0.01	-0.01	<-0.01	<-0.01	0.02	<-0.01	<-0.01	<-0.01	<-0.01	-0.01	0.02	<-0.01	<-0.01	-0.01	<-0.01	<-0.01	<-0.01	<-0.01	<-0.01
McHenry County	<-0.01	-0.02	<0.01	<0.01	-0.01	<-0.01	<0.01	0.05	0.04	<-0.01	0.02	-0.01	0.08	<-0.01	<-0.01	<-0.01	<-0.01	<-0.01	<-0.01	0.02	<-0.01	<-0.01	-0.03	<-0.01	<-0.01	<-0.01	<-0.01	0.04	<0.01	<-0.01	-0.01	-0.02	<-0.01	<-0.01	<-0.01	<-0.01	<-0.01
McIntosh County	-0.04	-0.02	-0.04	-0.03	-0.02	-0.03	-0.02	-0.04	0.01	<-0.01	<-0.01	0.12	<-0.01	<-0.01	<-0.01	<-0.01	<-0.01	<-0.01	<-0.01	-0.01	<-0.01	<-0.01	-0.03	<-0.01	<-0.01	<-0.01	<-0.01	<0.01	0.01	<-0.01	<-0.01	-0.01	<-0.01	<-0.01	<-0.01	<-0.01	<-0.01
McKenzie County	0.03	0.02	0.01	0.03	0.02	0.02	0.01	<-0.01	-0.01	-0.01	-0.04	-0.02	<-0.01	0.02	-0.02	0.02	-0.01	<-0.01	0.02	0.01	-0.01	-0.03	0.03	0.02	-0.02	<-0.01	-0.02	-0.01	-0.03	-0.05	-0.13	-0.21	-0.02	-0.04	-0.03	-0.07	-0.06
McLean County	<-0.01	0.01	-0.02	0.02	<0.01	<0.01	0.02	0.05	<-0.01	<-0.01	<-0.01	0.03	0.02	-0.01	-0.02	-0.02	<-0.01	-0.01	0.08	-0.05	<-0.01	<-0.01	<-0.01	<-0.01	<-0.01	0.03	<-0.01	<-0.01	-0.05	-0.01	-0.03	-0.05	<-0.01	<-0.01	<-0.01	-0.01	-0.01
Mercer County	0.03	0.06	<-0.01	<0.01	0.05	0.03	<-0.01	<0.01	-0.04	<-0.01	-0.04	-0.04	-0.03	0.06	<0.01	<-0.01	0.15	-0.02	<-0.01	-0.05	<-0.01	-0.01	0.06	<-0.01	0.08	<0.01	0.04	-0.03	0.02	-0.02	-0.04	-0.07	<-0.01	-0.01	-0.01	-0.02	-0.02
Morton County	-0.01	-0.01	<0.01	<-0.01	-0.01	<-0.01	-0.03	0.02	0.03	<-0.01	<-0.01	<-0.01	0.03	<0.01	0.02	<-0.01	<-0.01	0.01	-0.01	0.03	0.10	-0.01	-0.02	<-0.01	0.05	-0.04	-0.02	0.03	-0.03	-0.02	-0.06	-0.10	-0.01	-0.02	-0.01	-0.03	-0.03
Mountrail County	-0.02	-0.02	<0.01	-0.02	-0.02	-0.02	<0.01	<0.01	-0.02	<-0.01	0.04	0.02	-0.02	0.03	0.03	-0.01	<-0.01	0.02	<-0.01	-0.04	<-0.01	-0.01	-0.01	<-0.01	-0.01	-0.01	0.02	-0.03	0.03	-0.02	-0.06	-0.09	-0.01	-0.02	-0.01	-0.03	-0.03
Oliver County	<0.01	0.01	0.01	<-0.01	<0.01	<0.01	-0.02	<0.01	<0.01	<-0.01	-0.04	0.05	0.02	-0.01	-0.02	-0.02	<-0.01	-0.01	-0.02	<0.01	<-0.01	<-0.01	0.02	<-0.01	<-0.01	-0.02	<-0.01	<0.01	<-0.01	-0.01	-0.03	-0.05	<-0.01	<-0.01	<-0.01	-0.01	-0.01
Pembina County	<-0.01	<0.01	-0.02	<-0.01	<-0.01	<-0.01	0.02	-0.01	-0.01	<-0.01	-0.02	0.06	<-0.01	<-0.01	<-0.01	<-0.01	<-0.01	<-0.01	<-0.01	-0.02	<-0.01	<-0.01	<0.01	<-0.01	<-0.01	<-0.01	<-0.01	-0.01	0.02	<-0.01	-0.01	-0.02	<-0.01	<-0.01	<-0.01	<-0.01	<-0.01
Richland County	<-0.01	-0.02	<-0.01	<-0.01	-0.01	-0.01	0.03	0.01	0.03	<-0.01	-0.01	<-0.01	<-0.01	<-0.01	<-0.01	<-0.01	<-0.01	<-0.01	<-0.01	0.04	<-0.01	<-0.01	<-0.01	<-0.01	<-0.01	<-0.01	<-0.01	0.03	0.03	<-0.01	<-0.01	-0.01	<-0.01	<-0.01	<-0.01	<-0.01	<-0.01
Rolette County	<0.01	<-0.01	<0.01	<0.01	<-0.01	<0.01	-0.02	0.03	0.02	<-0.01	0.05	<-0.01	<-0.01	<-0.01	<-0.01	<-0.01	<-0.01	<-0.01	0.10	-0.01	<-0.01	<-0.01	-0.04	<-0.01	<-0.01	<-0.01	<-0.01	0.01	-0.05	<-0.01	<-0.01	-0.01	<-0.01	<-0.01	<-0.01	<-0.01	<-0.01
Sioux County	-0.01	-0.02	<-0.01	<-0.01	-0.02	-0.01	-0.02	<0.01	0.03	<-0.01	<0.01	-0.02	-0.01	<-0.01	-0.01	-0.01	<-0.01	<-0.01	-0.01	0.02	<-0.01	<-0.01	-0.02	<-0.01	<-0.01	0.05	0.11	0.03	0.03	<-0.01	-0.02	-0.03	<-0.01	<-0.01	<-0.01	<-0.01	<-0.01
Slope County	0.03	0.05	<-0.01	0.02	0.04	0.03	-0.02	<0.01	-0.05	<-0.01	-0.02	<0.01	<-0.01	-0.02	-0.03	0.04	<-0.01	-0.02	-0.04	-0.04	<-0.01	0.05	0.06	<-0.01	<-0.01	<-0.01	-0.01	-0.05	-0.02	-0.02	-0.05	-0.08	<-0.01	-0.01	-0.01	-0.03	-0.02
Stark County	<-0.01	-0.01	0.02	<-0.01	-0.02	<-0.01	0.07	<0.01	-0.04	<-0.01	-0.02	0.02	0.03	-0.02	<0.01	<0.01	<-0.01	0.04	-0.03	-0.05	<-0.01	<-0.01	0.03	<-0.01	<-0.01	<0.01	-0.01	-0.04	<-0.01	-0.01	-0.04	-0.06	<-0.01	-0.01	<-0.01	-0.02	-0.02
Walsh County	0.03	0.02	0.04	<-0.01	<0.01	0.02	-0.01	-0.06	-0.06	<-0.01	0.06	-0.02	-0.01	<-0.01	-0.01	-0.01	<-0.01	<-0.01	-0.01	-0.03	<-0.01	<-0.01	<0.01	<-0.01	<-0.01	-0.01	<-0.01	-0.07	-0.08	<-0.01	-0.02	-0.03	<-0.01	<-0.01	<-0.01	<-0.01	<-0.01
Ward County	-0.02	-0.01	-0.02	<-0.01	-0.01	-0.02	0.03	-0.02	0.02	<-0.01	-0.03	0.02	-0.01	<-0.01	-0.01	-0.01	<-0.01	<-0.01	-0.01	0.04	<-0.01	<-0.01	<0.01	<-0.01	<-0.01	-0.01	<-0.01	0.02	0.02	<-0.01	-0.02	-0.03	<-0.01	<-0.01	<-0.01	-0.01	<-0.01
Williams County	0.02	0.04	-0.04	0.04	0.03	0.02	0.01	0.03	0.02	0.11	0.04	-0.04	<0.01	-0.03	-0.02	-0.04	<-0.01	-0.02	0.03	0.03	<-0.01	-0.01	<-0.01	<-0.01	-0.01	-0.01	-0.02	0.03	-0.03	-0.02	-0.06	-0.10	-0.01	-0.02	-0.01	-0.03	-0.03
Cultivated Crops	-0.02	-0.11	<0.01	0.04	-0.06	-0.02	-0.11	0.05	0.29	<-0.01	0.02	0.04	<-0.01	<-0.01	<-0.01	-0.02	<-0.01	-0.02	0.07	0.28	<-0.01	-0.02	-0.23	<-0.01	-0.01	<0.01	-0.02	0.29	0.07	-0.02	0.06	<0.01	-0.01	-0.02	0.03	-0.01	0.05
Deciduous Forest	0.02	-0.02	0.05	0.05	-0.01	0.02	<0.01	0.13	0.13	<-0.01	<0.01	-0.02	0.10	<-0.01	-0.01	-0.01	<-0.01	<-0.01	0.14	0.05	<-0.01	<-0.01	-0.09	<-0.01	<-0.01	-0.01	<-0.01	0.13	-0.04	<-0.01	-0.02	-0.03	<-0.01	<-0.01	<-0.01	<-0.01	<-0.01
Open Space	-0.04	-0.02	-0.06	-0.04	-0.02	-0.04	-0.03	0.05	0.06	<-0.01	<-0.01	<-0.01	<-0.01	<-0.01	<-0.01	<-0.01	<-0.01	<-0.01	<-0.01	-0.01	<-0.01	0.45	-0.03	<-0.01	<-0.01	<-0.01	<-0.01	0.04	-0.02	<-0.01	<-0.01	0.06	<-0.01	<-0.01	<-0.01	<-0.01	<-0.01
Herbaceuous Wetlands	-0.05	-0.09	<0.01	<0.01	-0.06	-0.03	-0.12	0.08	0.24	<-0.01	<0.01	0.09	0.09	0.02	-0.04	-0.03	<-0.01	<0.01	0.01	0.22	<-0.01	-0.02	-0.20	-0.01	-0.01	-0.04	0.01	0.23	0.09	0.03	<-0.01	<0.01	0.04	-0.02	-0.02	-0.01	0.02
Evergreen Forest	<0.01	-0.01	0.01	<0.01	<-0.01	<-0.01	-0.01	<0.01	0.05	<-0.01	<-0.01	<-0.01	<-0.01	<-0.01	<-0.01	<-0.01	<-0.01	<-0.01	<-0.01	0.07	<-0.01	<-0.01	-0.03	<-0.01	<-0.01	<-0.01	<-0.01	0.06	0.03	<-0.01	<-0.01	-0.01	<-0.01	<-0.01	<-0.01	<-0.01	<-0.01
Hay/Pasture	<0.01	-0.03	<-0.01	<0.01	<0.01	<0.01	-0.09	-0.06	0.14	<-0.01	<-0.01	<-0.01	0.01	0.03	0.01	-0.02	<-0.01	-0.01	-0.02	0.14	<-0.01	<-0.01	-0.09	0.13	<-0.01	-0.02	-0.01	0.13	0.12	-0.01	-0.03	0.02	<-0.01	<-0.01	<-0.01	-0.02	0.03
Herbaceuous	0.09	0.16	0.03	0.02	0.11	0.08	0.17	-0.15	-0.41	-0.04	0.07	-0.03	-0.20	<-0.01	-0.07	0.06	-0.04	0.04	-0.08	-0.28	-0.04	-0.09	0.29	-0.05	<-0.01	-0.04	-0.11	-0.42	-0.07	-0.04	-0.05	0.02	<-0.01	0.02	0.01	0.01	<-0.01
Mixed Forest	<0.01	0.01	-0.01	<0.01	<0.01	<0.01	0.04	<0.01	-0.02	<-0.01	-0.01	<-0.01	<-0.01	<-0.01	<-0.01	<-0.01	<-0.01	<-0.01	<-0.01	-0.01	<-0.01	<-0.01	0.03	<-0.01	<-0.01	<-0.01	<-0.01	-0.02	<0.01	<-0.01	<-0.01	-0.01	<-0.01	<-0.01	<-0.01	<-0.01	<-0.01
Shrub/Scrub	-0.05	<-0.01	-0.06	-0.10	-0.02	-0.06	0.01	-0.02	-0.17	<-0.01	-0.09	-0.07	-0.05	-0.03	0.18	-0.05	<-0.01	-0.03	-0.05	-0.12	<-0.01	0.02	0.14	0.05	0.04	0.11	-0.02	-0.14	<-0.01	-0.03	0.06	-0.02	-0.01	0.01	-0.02	-0.02	-0.03
Woody Wetlands	-0.04	-0.08	<0.01	0.01	-0.06	-0.03	-0.05	0.18	0.33	0.11	-0.06	<0.01	0.34	<0.01	-0.03	<0.01	0.11	-0.02	0.12	0.06	0.11	0.14	-0.20	<-0.01	-0.01	-0.01	0.27	0.33	-0.10	0.12	<-0.01	-0.02	-0.01	-0.02	-0.01	0.04	-0.03

Factors	Dickey County	Divide County	Dunn County	Emmons County	Golden Valley County	Grand Forks County	Grant County	Griggs County	Hettinger County	Logan County	McHenry County	McIntosh County	McKenzie County	McLean County	Mercer County	Morton County	Mountrail County	Oliver County	Pembina County	Richland County	Rolette County	Sioux County	Slope County	Stark County	Walsh County	Ward County	Williams County	Cultivated Crops	Deciduous Forest	Open Space	Emergent Herbaceuous Wetlands	Evergreen Forest	Hay/Pasture	Herbaceuous	Mixed Forest	Shrub/Scrub	Woody Wetlands
TDS																																					
SAR																																					
Ca^{2+}																																					
Mg^{2+}																																					
Na^{+}																																					
SO^{2-}_{4}																																					
Slope Inclination																																					
Latitude																																					
Longitude																																					
Belle Fourche-Skull Creek																																					
Bullion Creek Formation																																					
Cannonball Formation																																					
Carlile Formation																																					
Fox Hills Formation																																					
Golden Valley Formation																																					
Hell Creek Formation																																					
Inyan Kara																																					
Ludlow Formation																																					
Niobrara Formation																																					
Pierre Formation																																					
Precambrian Rocks																																					
Red River Formation																																					
Sentinel Butte Formation																																					
Slope Formation																																					
Upper and Middle Tertiary Rock																																					
White River Group																																					
Winnipeg Group																																					
Average Rainfall																																					
Average Snowfall																																					
Adams County																																					
Barnes County																																					
Billings County																																					
Bowman County																																					
Burke																																					
Burleigh County																																					
Cass County																																					
Cavalier County																																					
Dickey County	1.00																																				
Divide County	<-0.01	1.00																																			
Dunn County	-0.02	-0.01	1.00																																		
Emmons County	-0.01	<-0.01	-0.05	1.00																																	
Golden Valley County	-0.02	-0.01	-0.07	-0.05	1.00																																

Legend

- Strong Positive Correlation
- Moderate Positive Correlation
- Strong Negative Correlation
- Moderate Negative Correlation

Factors	Dickey County	Divide County	Dunn County	Emmons County	Golden Valley County	Grand Forks County	Grant County	Griggs County	Hettinger County	Logan County	McHenry County	McIntosh County	McKenzie County	McLean County	Mercer County	Morton County	Mountrail County	Oliver County	Pembina County	Richland County	Rolette County	Sioux County	Slope County	Stark County	Walsh County	Ward County	Williams County	Cultivated Crops	Deciduous Forest	Open Space	Emergent Herbaceuous Wetlands	Evergreen Forest	Hay/Pasture	Herbaceuous	Mixed Forest	Shrub/Scrub	Woody Wetlands
Grand Forks County	<-0.01	<-0.01	-0.02	-0.01	-0.02	1.00																															
Grant County	-0.01	<-0.01	-0.05	-0.03	-0.05	-0.01	1.00																														
Griggs County	<-0.01	<-0.01	-0.02	-0.01	-0.02	<-0.01	-0.01	1.00																													
Hettinger County	<-0.01	<-0.01	-0.02	-0.01	-0.02	<-0.01	-0.01	<-0.01	1.00																												
Logan County	<-0.01	<-0.01	<-0.01	<-0.01	<-0.01	<-0.01	<-0.01	<-0.01	<-0.01	1.00																											
McHenry County	<-0.01	<-0.01	-0.01	<-0.01	-0.01	<-0.01	<-0.01	<-0.01	<-0.01	<-0.01	1.00																										
McIntosh County	<-0.01	<-0.01	<-0.01	<-0.01	<-0.01	<-0.01	<-0.01	<-0.01	<-0.01	<-0.01	<-0.01	1.00																									
McKenzie County	-0.04	-0.03	-0.14	-0.09	-0.15	-0.04	-0.09	-0.04	-0.04	-0.01	-0.03	-0.01	1.00																								
McLean County	<-0.01	<-0.01	-0.03	-0.02	-0.03	<-0.01	-0.02	<-0.01	<-0.01	<-0.01	<-0.01	<-0.01	-0.06	1.00																							
Mercer County	-0.01	<-0.01	-0.05	-0.03	-0.05	-0.01	-0.03	-0.01	-0.01	<-0.01	<-0.01	<-0.01	-0.09	-0.02	1.00																						
Morton County	-0.02	-0.01	-0.07	-0.04	-0.07	-0.02	-0.05	-0.02	-0.02	<-0.01	-0.01	<-0.01	-0.13	-0.03	-0.05	1.00																					
Mountrail County	-0.02	-0.01	-0.06	-0.04	-0.07	-0.02	-0.04	-0.02	-0.02	<-0.01	-0.01	<-0.01	-0.12	-0.03	-0.04	-0.06	1.00																				
Oliver County	<-0.01	<-0.01	-0.03	-0.02	-0.03	<-0.01	-0.02	<-0.01	<-0.01	<-0.01	<-0.01	<-0.01	-0.06	-0.01	-0.02	-0.03	-0.03	1.00																			
Pembina County	<-0.01	<-0.01	-0.01	<-0.01	-0.01	<-0.01	<-0.01	<-0.01	<-0.01	<-0.01	<-0.01	<-0.01	-0.02	<-0.01	<-0.01	-0.01	-0.01	<-0.01	1.00																		
Richland County	<-0.01	<-0.01	<-0.01	<-0.01	-0.01	<-0.01	<-0.01	<-0.01	<-0.01	<-0.01	<-0.01	<-0.01	-0.02	<-0.01	<-0.01	<-0.01	<-0.01	<-0.01	<-0.01	1.00																	
Rolette County	<-0.01	<-0.01	<-0.01	<-0.01	-0.01	<-0.01	<-0.01	<-0.01	<-0.01	<-0.01	<-0.01	<-0.01	-0.02	<-0.01	<-0.01	<-0.01	<-0.01	<-0.01	<-0.01	<-0.01	1.00																
Sioux County	<-0.01	<-0.01	-0.02	-0.01	-0.02	<-0.01	-0.01	<-0.01	<-0.01	<-0.01	<-0.01	<-0.01	-0.04	<-0.01	-0.01	-0.02	-0.02	<-0.01	<-0.01	<-0.01	<-0.01	1.00															
Slope County	-0.01	-0.01	-0.05	-0.04	-0.06	-0.02	-0.04	-0.01	-0.02	<-0.01	-0.01	<-0.01	-0.11	-0.02	-0.04	-0.05	-0.05	-0.02	<-0.01	<-0.01	<-0.01	-0.02	1.00													
Stark County	-0.01	<-0.01	-0.04	-0.03	-0.05	-0.01	-0.03	-0.01	-0.01	<-0.01	<-0.01	<-0.01	-0.09	-0.02	-0.03	-0.04	-0.04	-0.02	<-0.01	<-0.01	<-0.01	-0.01	-0.03	1.00												
Walsh County	<-0.01	<-0.01	-0.02	-0.01	-0.02	<-0.01	-0.01	<-0.01	<-0.01	<-0.01	<-0.01	<-0.01	-0.04	<-0.01	-0.01	-0.02	-0.02	<-0.01	<-0.01	<-0.01	<-0.01	<-0.01	-0.01	-0.01	1.00											
Ward County	<-0.01	<-0.01	-0.02	-0.01	-0.02	<-0.01	-0.01	<-0.01	<-0.01	<-0.01	<-0.01	<-0.01	-0.04	<-0.01	-0.01	-0.02	-0.02	<-0.01	<-0.01	<-0.01	<-0.01	<-0.01	-0.02	-0.01	<-0.01	1.00										
Williams County	-0.02	-0.01	-0.06	-0.04	-0.07	-0.02	-0.04	-0.02	-0.02	<-0.01	-0.01	<-0.01	-0.13	-0.03	-0.04	-0.06	-0.06	-0.03	-0.01	<-0.01	<-0.01	-0.02	-0.05	-0.04	-0.02	-0.02	1.00									
Cultivated Crops	0.02	-0.01	<0.01	-0.01	0.03	0.01	0.03	-0.02	0.01	<-0.01	0.04	<-0.01	<-0.01	-0.03	-0.02	<0.01	-0.05	0.01	-0.01	<-0.01	<-0.01	-0.02	-0.04	-0.03	0.02	-0.02	<0.01	1.00								
Deciduous Forest	<-0.01	<-0.01	-0.02	-0.01	-0.02	<-0.01	-0.01	<-0.01	<-0.01	<-0.01	<-0.01	<-0.01	0.06	<-0.01	-0.01	-0.02	-0.02	<-0.01	<-0.01	<-0.01	<-0.01	<-0.01	-0.02	0.04	<-0.01	<-0.01	0.09	-0.02	1.00							
Open Space	<-0.01	<-0.01	<-0.01	<-0.01	<-0.01	<-0.01	<-0.01	<-0.01	<-0.01	<-0.01	<-0.01	<-0.01	-0.01	<-0.01	<-0.01	<-0.01	<-0.01	<-0.01	<-0.01	<-0.01	<-0.01	<-0.01	<-0.01	<-0.01	<-0.01	<-0.01	<-0.01	<-0.01	<-0.01	1.00							
Herbaceuous Wetlands	0.01	0.03	0.04	-0.02	0.03	-0.02	-0.05	0.02	-0.02	<-0.01	-0.01	<-0.01	<-0.01	0.01	<-0.01	-0.03	0.02	<0.01	-0.01	-0.01	-0.01	0.01	<0.01	<0.01	-0.02	-0.02	<-0.01	-0.07	-0.02	<-0.01	1.00					
Evergreen Forest	<-0.01	<-0.01	<-0.01	0.15	<-0.01	<-0.01	<-0.01	<-0.01	<-0.01	<-0.01	<-0.01	<-0.01	-0.01	<-0.01	<-0.01	<-0.01	<-0.01	<-0.01	<-0.01	<-0.01	<-0.01	<-0.01	<-0.01	<-0.01	<-0.01	<-0.01	<-0.01	<-0.01	<-0.01	<-0.01	<-0.01	1.00				
Hay/Pasture	-0.01	<-0.01	<0.01	<0.01	0.02	-0.01	-0.02	<-0.01	-0.01	<-0.01	<-0.01	<-0.01	<-0.01	-0.02	-0.02	<0.01	0.06	0.03	<-0.01	<-0.01	<-0.01	0.05	-0.03	-0.02	-0.01	-0.01	<0.01	-0.04	-0.01	<-0.01	-0.04	<-0.01	1.00			
Herbaceuous	<0.01	<0.01	-0.02	0.02	-0.06	0.01	0.01	<0.01	0.02	0.02	-0.02	0.02	0.03	<0.01	0.02	0.04	<0.01	<-0.01	<-0.01	0.02	0.02	-0.02	0.01	0.03	<0.01	0.05	-0.09	-0.39	-0.12	-0.04	-0.42	-0.04	-0.21	1.00		
Mixed Forest	<-0.01	<-0.01	<-0.01	<-0.01	-0.01	<-0.01	<-0.01	<-0.01	<-0.01	<-0.01	<-0.01	<-0.01	-0.02	<-0.01	<-0.01	<-0.01	0.07	<-0.01	0.41	<-0.01	<-0.01	<-0.01	<-0.01	<-0.01	<-0.01	<-0.01	<-0.01	<-0.01	<-0.01	<-0.01	<-0.01	-0.01	<-0.01	<-0.01	-0.05	1.00	
Shrub/Scrub	-0.02	-0.02	<-0.01	-0.01	<0.01	<0.01	<-0.01	0.01	<0.01	<-0.01	-0.02	<-0.01	<0.01	-0.02	<-0.01	-0.03	<0.01	-0.02	-0.01	-0.01	-0.01	<0.01	<-0.01	<0.01	<0.01	-0.03	0.08	-0.08	-0.02	<-0.01	-0.09	<-0.01	-0.04	-0.47	-0.01	1.00
Woody Wetlands	-0.02	-0.01	0.01	<-0.01	0.05	-0.02	0.03	-0.02	-0.02	<-0.01	0.05	<-0.01	-0.07	0.05	<0.01	<0.01	-0.02	<-0.01	-0.01	<-0.01	<-0.01	0.02	0.04	-0.04	-0.02	-0.02	0.05	-0.06	-0.02	<-0.01	-0.07	<-0.01	-0.03	-0.35	<-0.01	-0.07	1.00

Legend

- Strong Positive Correlation
- Moderate Positive Correlation
- Strong Negative Correlation
- Moderate Negative Correlation

APPENDIX H: LIQUID LIMIT AND PLASTIC LIMIT RESULTS

This section presents the tables and figures for the LL and PL tests for the mixtures of kaolinite and montmorillonite with quartz, as described in Chapter 3. K, M, and Q with numbers in front represent percentage of kaolinite, montmorillonite, and quartz, respectively, in the mixtures of these clay minerals. Any data points with an asterisk (*) in this appendix were considered to be outliers and were not considered in the calculation process.

Table H.1. Measurement of LL for K100

Liquid Limit Test						
Test No.		1	2	3	4	5
Mass of Can	W_1 (g)	13.9	11.0	13.9	11.2	21.1
Mass of Can + Moist Soil	W_2 (g)	33.0	32.2	34.7	27.4	40.4
Mass of Can + Dry Soil	W_3(g)	27.0	25.4	27.9	22.1	34.0
Moisture Content	w%	45.8*	47.5	48.8*	48.9	50.3
Number of Blows	N	31	28	26	22	17

Table H.2. Measurement of PL for K100

Plastic Limit Test						
Test No.		1	2	3	4	5
Mass of Can	W_1 (g)	13.7	11.6	11.8	14.5	13.7
Mass of Can + Moist Soil	W_2 (g)	15.0	13.0	12.9	15.9	14.9
Mass of Can + Dry Soil	W_3 (g)	14.7	12.7	12.6	15.6	14.6
Moisture Content	w%	29.8	30.5	12.6*	30.4	29.3
Average Plastic Limit				30		

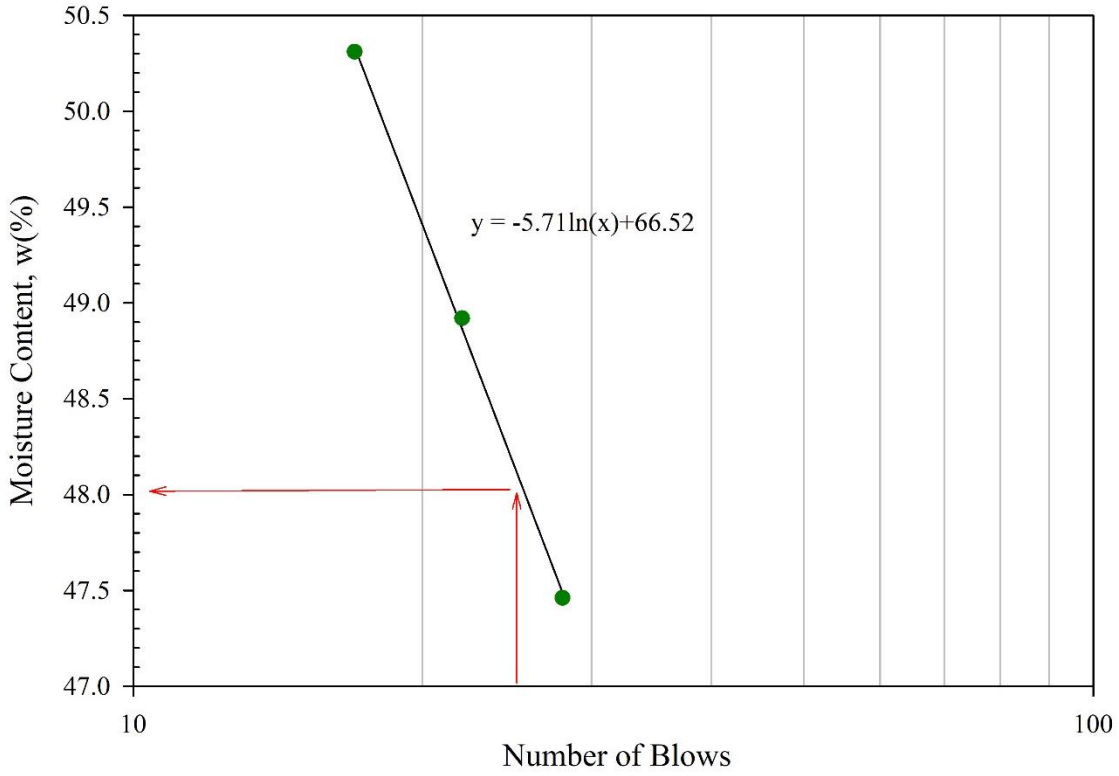

Figure H.1. Moisture Content versus Number of Blows for K100.

Table H.3. Measurement of LL for K70Q30

Liquid Limit Test						
Test No.		1	2	3	4	5
Mass of Can	W_1 (g)	21.5	13.7	14.1	14.4	14.2
Mass of Can + Moist Soil	W_2 (g)	32.2	26.7	26.6	30.7	28.5
Mass of Can + Dry Soil	W_3 (g)	29.0	22.7	22.8	25.6	24.0
Moisture Content	w%	42.5*	43.7	43.9	45.5	45.9
Number of Blows	N	33	30	28	21	19

Table H.4. Measurement of PL for K70Q30

Plastic Limit Test						
Test No.		1	2	3	4	5
Mass of Can	W_1 (g)	14.4	14.1	14.3	14.3	13.8
Mass of Can + Moist Soil	W_2 (g)	15.8	15.9	15.9	16.2	15.2
Mass of Can + Dry Soil	W_3 (g)	15.5	15.5	15.5	15.7	14.9
Moisture Content	w%	27.9	29.1	27.8	30.4	27.3
Average Plastic Limit				28		

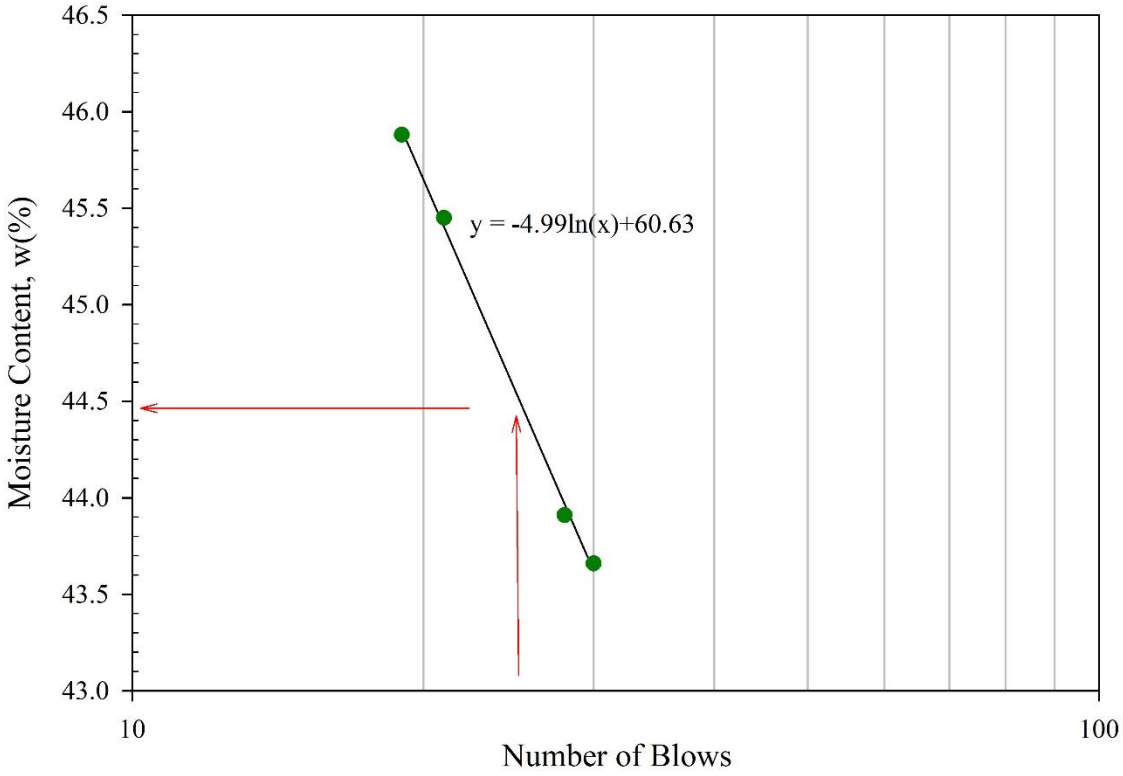

Figure H.2. Moisture Content versus Number of Blows for K70Q30.

Table H.5. Measurement of LL for K50Q50

Liquid Limit Test						
Test No.		1	2	3	4	5
Mass of Can	W_1 (g)	21.5	21.5	14.0	14.3	14.2
Mass of Can + Moist Soil	W_2 (g)	34.0	32.8	23.5	23.6	24.4
Mass of Can + Dry Soil	W_3 (g)	30.4	29.5	20.8	20.9	21.4
Moisture Content	w%	39.6	40.4	40.38*	41.8	42.2
Number of Blows	N	32	26	22	19	15

Table H.6. Measurement of PL for K50Q50

Plastic Limit Test						
Test No.		1	2	3	4	5
Mass of Can	W_1 (g)	21.4	14.1	14.2	14.3	13.8
Mass of Can + Moist Soil	W_2 (g)	22.5	15.3	15.8	15.7	15.3
Mass of Can + Dry Soil	W_3 (g)	22.3	15.0	15.5	15.4	15.1
Moisture Content	w%	28.6	28.6	24.0	27.1	21.1
Average Plastic Limit				25		

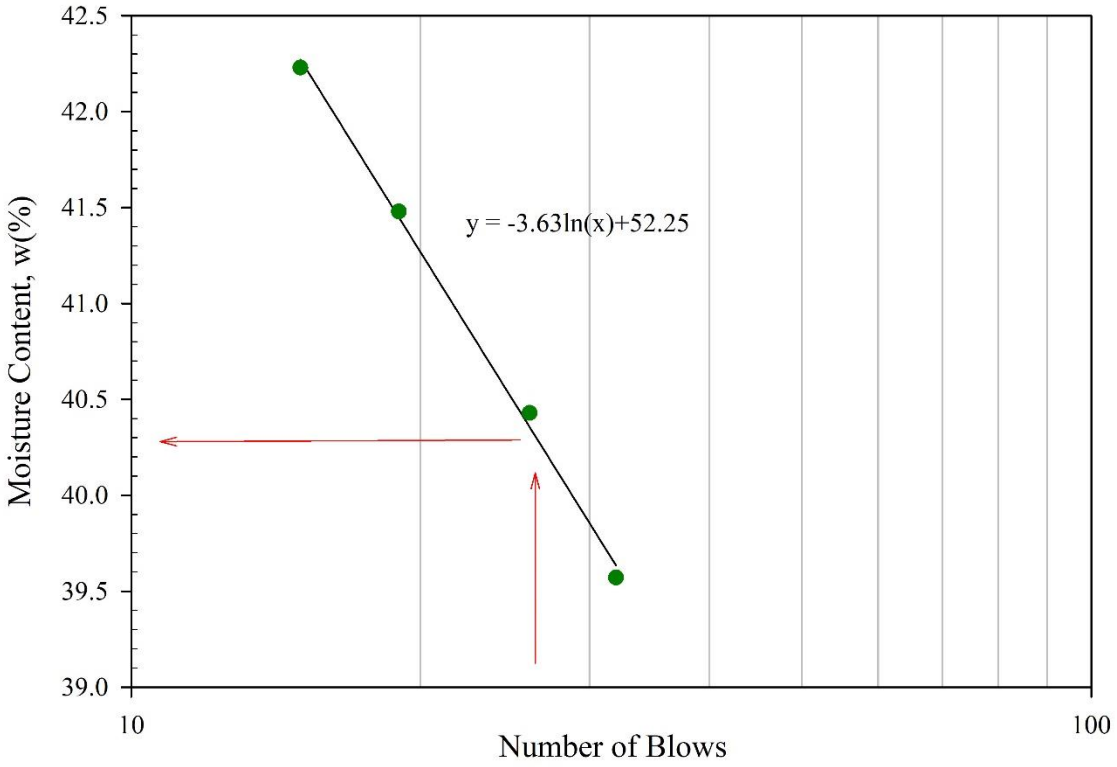

Figure H.3. Moisture Content versus Number of Blows for K50Q50.

Table H.7. Measurement of LL for K30Q70

Liquid Limit Test						
Test No.		1	2	3	4	5
Mass of Can	W_1 (g)	21.5	21.5	14.0	14.4	14.2
Mass of Can + Moist Soil	W_2 (g)	33.2	31.8	24.5	24.8	24.2
Mass of Can + Dry Soil	W_3 (g)	30.0	29.0	21.7	22.0	21.5
Moisture Content	w%	36.6*	37.0	37.1	37.6*	37.5
Number of Blows	N	28	25	20	18	12

Table H.8. Measurement of PL for K30Q70

Plastic Limit Test						
Test No.		1	2	3	4	5
Mass of Can	W_1 (g)	21.4	14.1	14.2	14.3	13.8
Mass of Can + Moist Soil	W_2 (g)	22.7	15.5	15.5	15.5	14.9
Mass of Can + Dry Soil	W_3 (g)	22.4	15.2	15.3	15.3	14.7
Moisture Content	w%	25.2	23.0	26.2	24.0	23.3
Average Plastic Limit				24		

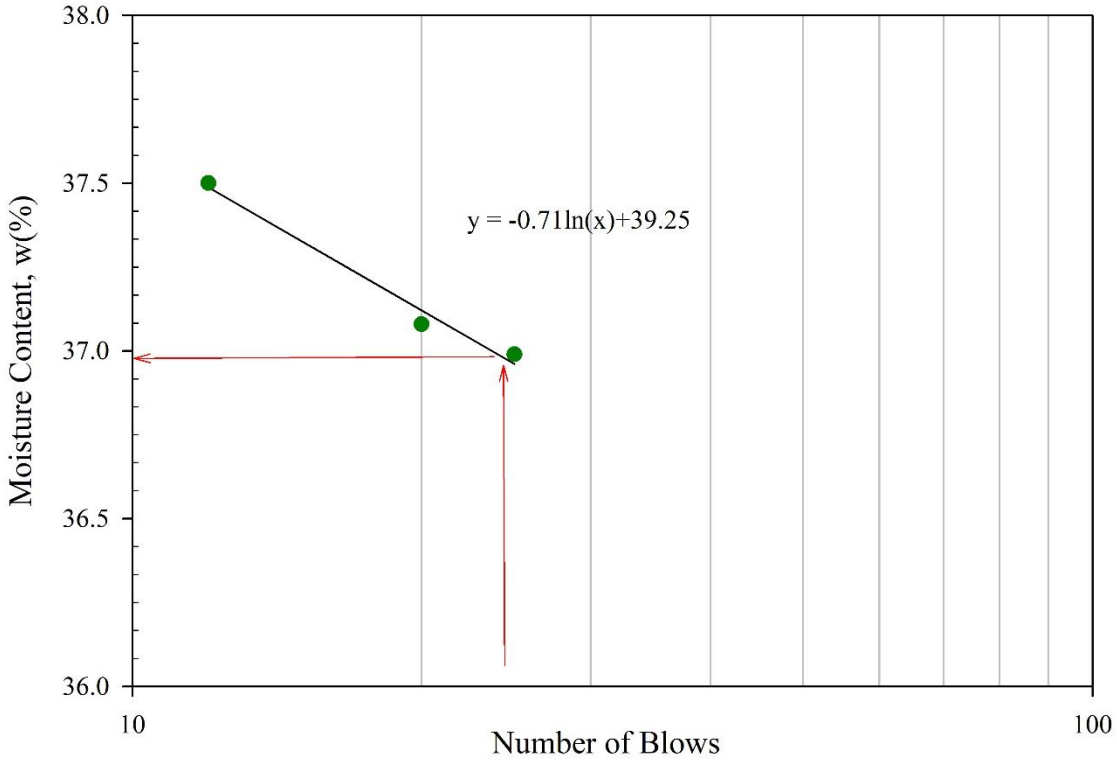

Figure H.4. Moisture Content versus Number of Blows for K30Q70.

Table H.9. Measurement of LL for K10Q90

Liquid Limit Test						
Test No.		1	2	3	4	5
Mass of Can	W_1 (g)	21.5	14.4	14.5	14.2	14.1
Mass of Can + Moist Soil	W_2 (g)	27.2	20.5	20.1	20.4	19.7
Mass of Can + Dry Soil	W_3 (g)	26.1	19.2	18.9	19.1	18.5
Moisture Content	w%	26.4	26.7	26.6	27.3*	27.3
Number of Blows	N	34	28	24	17	14

Table H.10. Measurement of PL for K10Q90

Plastic Limit Test						
Test No.		1	2	3	4	5
Mass of Can	W_1 (g)	21.3	14.2	14.8	13.9	14.4
Mass of Can + Moist Soil	W_2 (g)	22.3	15.1	15.5	15.6	16.2
Mass of Can + Dry Soil	W_3 (g)	22.1	14.9	15.4	15.3	15.9
Moisture Content	w%	23.9	23.2	26.8	23.8	20.7
Average Plastic Limit				23		

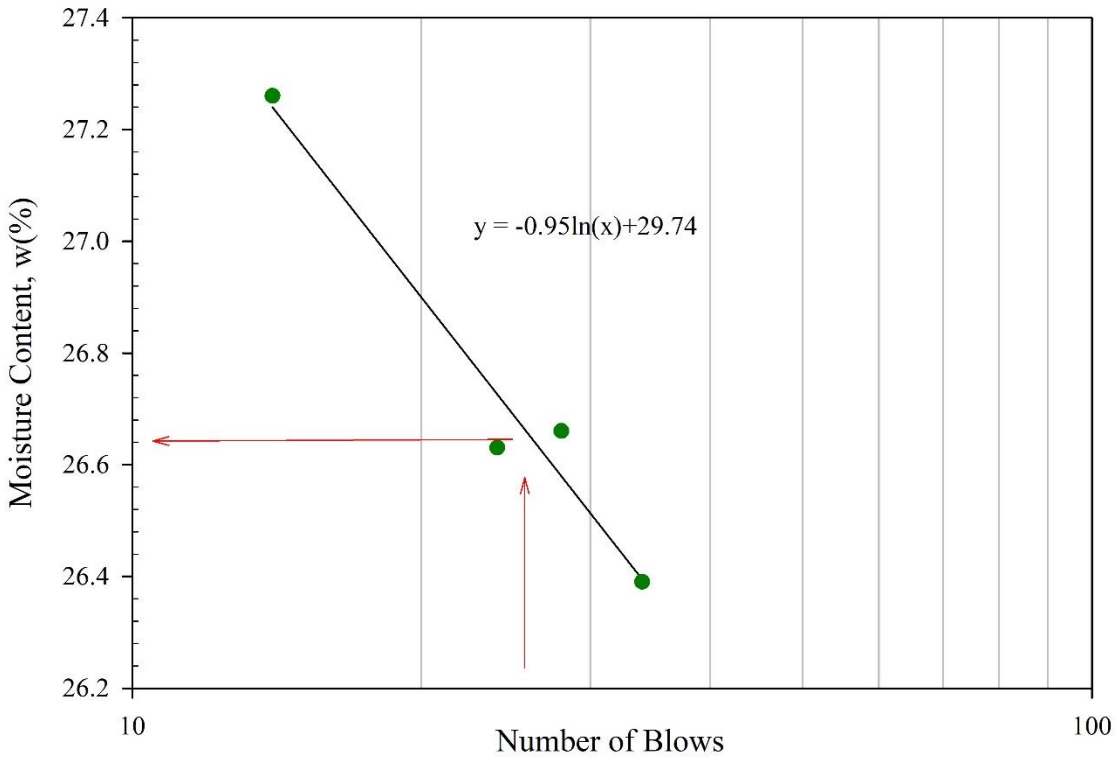

Figure H.5. Moisture Content versus Number of Blows for K10Q90.

Table H.11. Measurement of LL for M100

Plastic Limit Test						
Test No.		1	2	3	4	5
Mass of Can	W_1 (g)	13.9	21.5	14.0	14.1	21.7
Mass of Can + Moist Soil	W_2 (g)	23.1	31.1	23.6	23.9	31.7
Mass of Can + Dry Soil	W_3 (g)	15.2	22.7	15.3	15.3	22.9
Moisture Content	w%	629.0	658.0*	661.6*	682.4	723.4
Number of Blows	N	33	29	22	20	14

Table H.12. Measurement of PL for M100

Plastic Limit Test						
Test No.		1	2	3	4	5
Mass of Can	W_1 (g)	14.4	14.1	14.3	14.3	13.8
Mass of Can + Moist Soil	W_2 (g)	15.4	15.5	15.9	16.3	15.6
Mass of Can + Dry Soil	W_3 (g)	15.1	15.0	15.3	15.5	15.0
Moisture Content	w%	54.5	61.9	56.1	60.5	52.8
Average Plastic Limit				57		

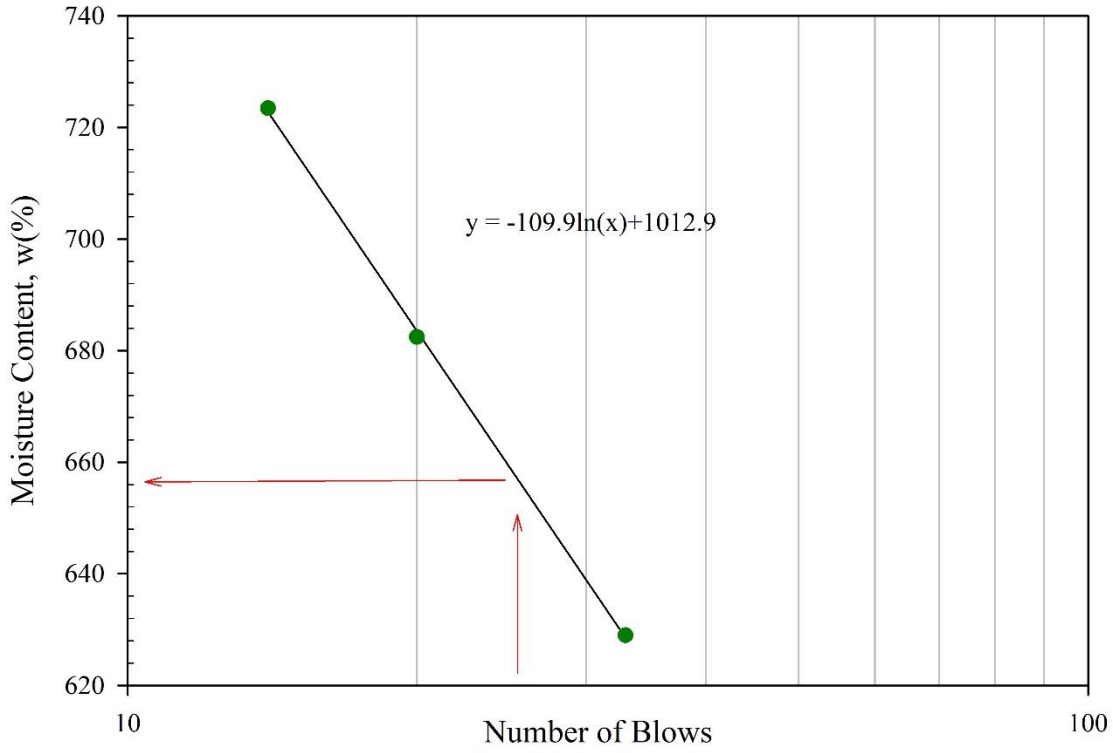

Figure H.6. Moisture Content versus Number of Blows for M100.

Table H.13. Measurement of LL for M70Q30

Liquid Limit Test						
Test No.		1	2	3	4	5
Mass of Can	W_1 (g)	13.9	13.7	14.1	14.1	21.7
Mass of Can + Moist Soil	W_2 (g)	20.3	21.8	21.3	22.1	28.2
Mass of Can + Dry Soil	W_3 (g)	15.2	15.2	15.5	15.6	22.8
Moisture Content	w%	401.5	415.2	424.7	433.3*	456.0
Number of Blows	N	33	28	24	18	16

Table H.14. Measurement of PL for M70Q30

Plastic Limit Test						
Test No.		1	2	3	4	5
Mass of Can	W_1 (g)	14.4	21.1	21.4	14.6	21.8
Mass of Can + Moist Soil	W_2 (g)	15.2	22.0	22.6	16.1	22.9
Mass of Can + Dry Soil	W_3 (g)	15.0	21.8	22.3	15.7	22.7
Moisture Content	w%	36.8	33.3	33.3	31.2	33.1
Average Plastic Limit				33		

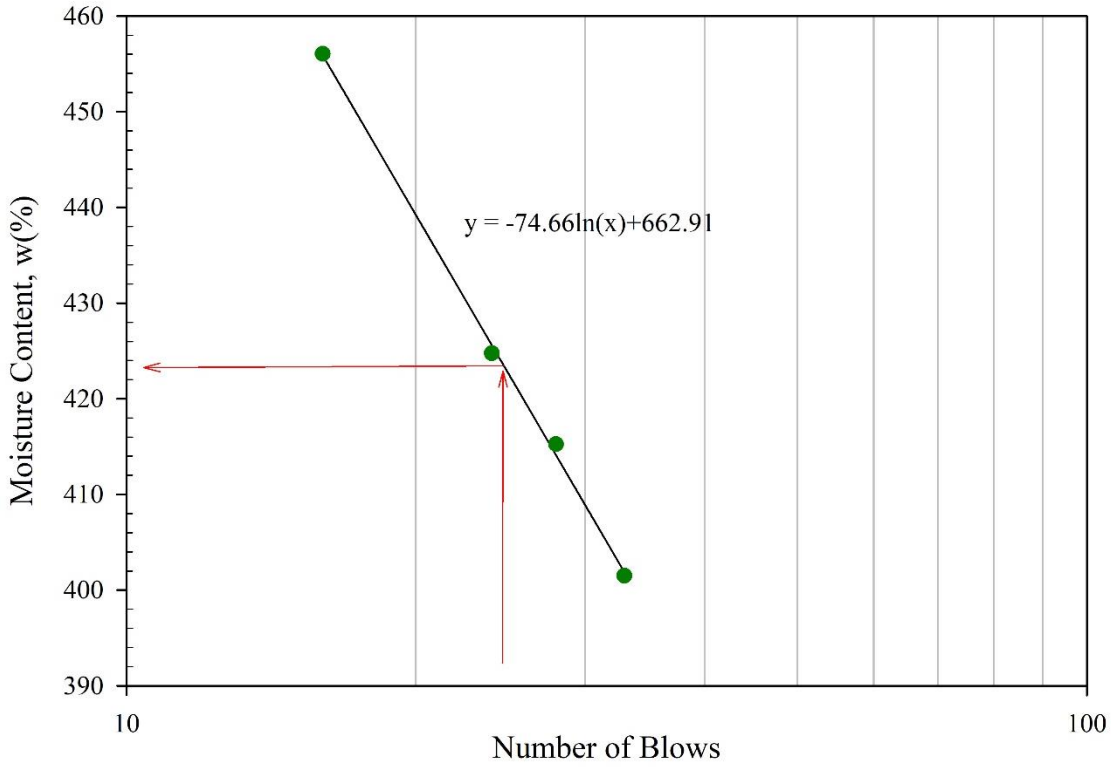

Figure H.7. Moisture Content versus Number of Blows for M70Q30.

Table H.15. Measurement of LL for M50Q50

Liquid Limit Test						
Test No.		1	2	3	4	5
Mass of Can	W_1 (g)	13.9	21.5	14.0	14.4	14.2
Mass of Can + Moist Soil	W_2 (g)	23.3	29.6	24.2	25.9	21.9
Mass of Can + Dry Soil	W_3 (g)	16.4	23.5	16.6	17.3	16.2
Moisture Content	w%	282.1	292.6*	290.6	295.8	297.6
Number of Blows	N	32	28	23	18	14

Table H.16. Measurement of PL for M50Q50

Plastic Limit Test						
Test No.		1	2	3	4	5
Mass of Can	W_1 (g)	21.4	14.1	14.2	14.3	13.8
Mass of Can + Moist Soil	W_2 (g)	22.7	15.0	15.2	15.3	14.9
Mass of Can + Dry Soil	W_3 (g)	22.5	14.8	15.0	15.0	14.7
Moisture Content	w%	27.3	27.6	25.0	28.9	25.8
Average Plastic Limit				26		

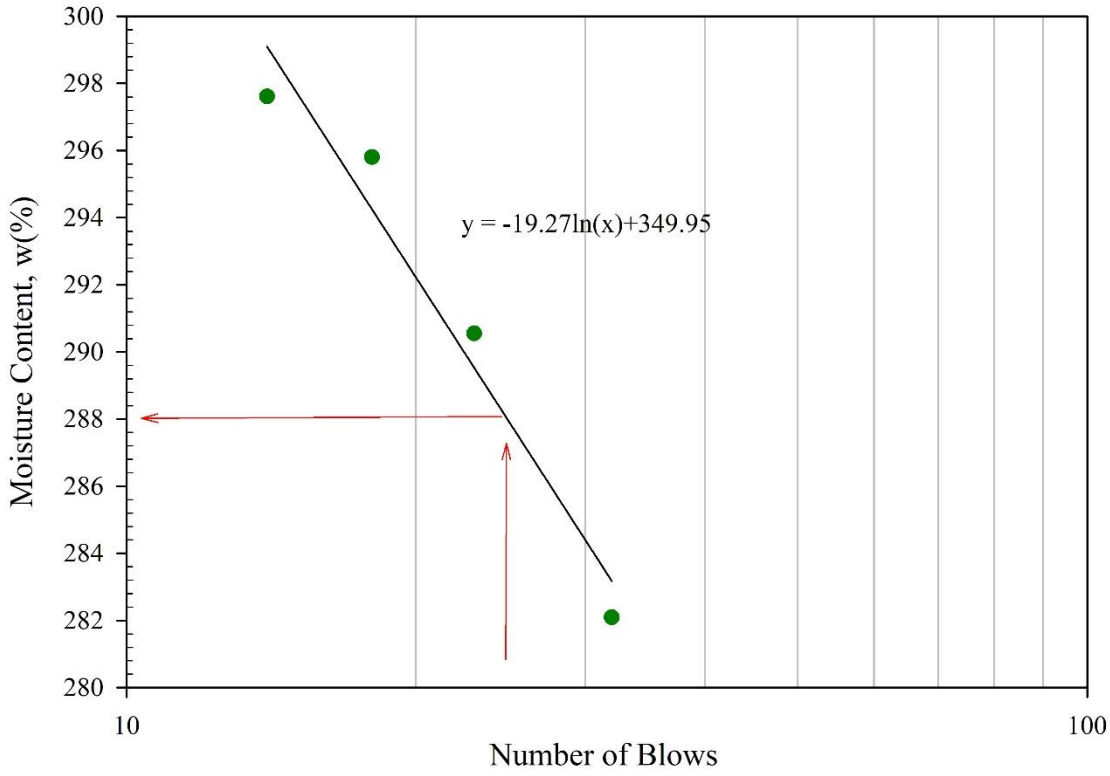

Figure H.8. Moisture Content versus Number of Blows for M50Q50.

Table H.17. Measurement of LL for M30Q70

Liquid Limit Test						
Test No.		1	2	3	4	5
Mass of Can	W_1 (g)	21.5	21.5	14.0	14.3	14.2
Mass of Can + Moist Soil	W_2 (g)	32.1	30.2	22.3	24.5	23.7
Mass of Can + Dry Soil	W_3 (g)	25.5	24.6	17.0	18.0	17.6
Moisture Content	w%	166.5*	176.9	177.6	180.8	180.1*
Number of Blows	N	35	26	23	18	15

Table H.18. Measurement of PL for M30Q70

Plastic Limit Test						
Test No.		1	2	3	4	5
Mass of Can	W_1 (g)	14.4	21.1	21.4	14.6	21.8
Mass of Can + Moist Soil	W_2 (g)	15.8	22.6	22.8	16.2	23.5
Mass of Can + Dry Soil	W_3 (g)	15.5	22.3	22.5	15.9	23.1
Moisture Content	w%	24.0	21.0*	25.8	22.4	24.2
Average Plastic Limit				23		

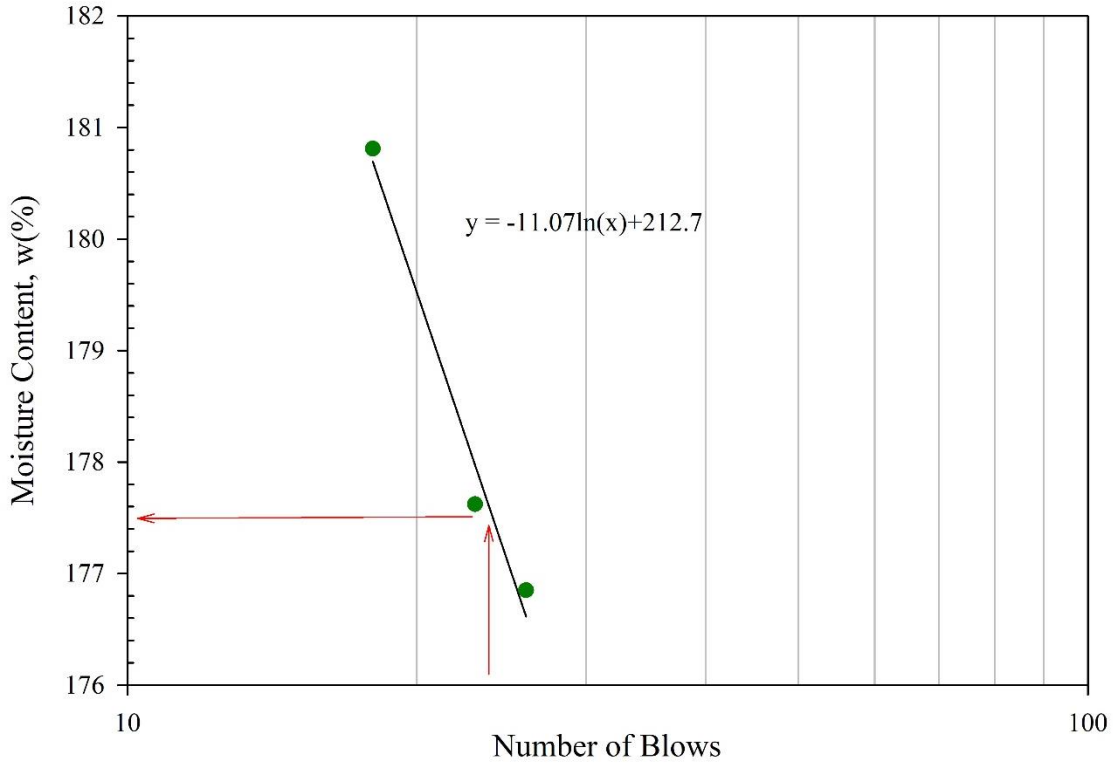

Figure H.9. Moisture Content versus Number of Blows for M30Q70.

Table H.19. Measurement of LL for M10Q90

Liquid Limit Test						
Test No.		1	2	3	4	5
Mass of Can	W_1 (g)	21.6	14.4	14.6	14.2	14.3
Mass of Can + Moist Soil	W_2 (g)	28.2	21.1	23.4	20.5	22.4
Mass of Can + Dry Soil	W_3 (g)	25.7	18.5	20.1	18.1	19.2
Moisture Content	w%	58.9	61.3*	60.9	62.7	63.2
Number of Blows	N	34	29	24	16	14

Table H.20. Measurement of PL for M10Q90

Plastic Limit Test						
Test No.		1	2	3	4	5
Mass of Can	W_1 (g)	14.6	21.1	14.4	21.4	14.3
Mass of Can + Moist Soil	W_2 (g)	15.8	22.0	15.4	22.8	15.2
Mass of Can + Dry Soil	W_3 (g)	15.6	21.8	15.3	22.5	15.1
Moisture Content	w%	24.1	22.4	23.9	25.0*	22.9
Average Plastic Limit				23		

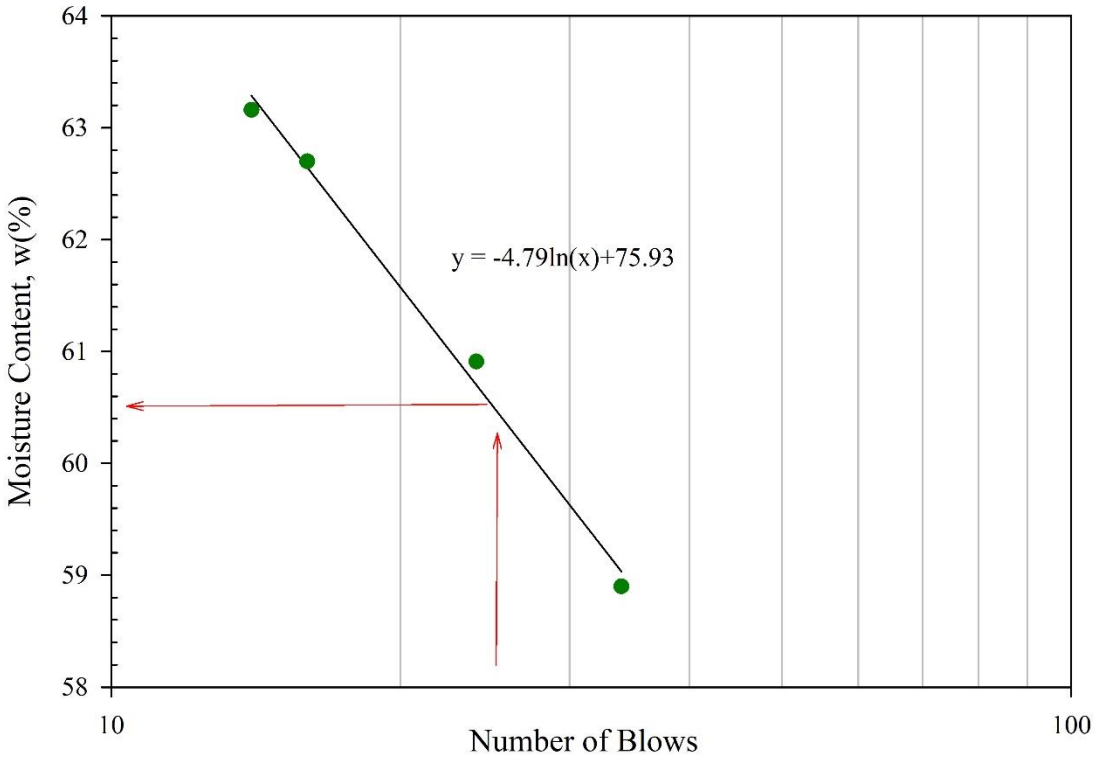

Figure H.10. Moisture Content versus Number of Blows for M10Q90.